An investigation into the characteristics of the phospholipid transfer protein RdgBβ and the phospholipid biosynthetic enzyme Cds1 in the mammalian heart.

Evelyn Fernanda Gomez Espinosa

A thesis submitted to University College London for the degree of Doctor of Philosophy

January 2017

Department of Neuroscience, Physiology and Pharmacology, University College London

I, Evelyn Fernanda Gomez Espinosa, confirm that the work presented in this thesis is my own. Where information has been derived from other sources, I confirm that this has been indicated in the thesis.

_____
  Evelyn Gomez Espinosa

DEDICATION

To my wonderful and loving husband William, for his never ending support and encouragement. To my beloved mother Maricarmen, brother Alejandro and sister Marithe for always believing this was possible.

Abstract

The conversion of phosphatidic acid (PA) to cytidine diphosphate-diacylglycerol (CDP-DAG) by CDP-DAG synthase (Cds) is the rate-limiting step for the biosynthesis of the mitochondrial lipid, cardiolipin (CL) and phosphatidylinositol (PI), the precursor for many signalling phosphoinositides. There are two Cds isoforms in mammals, Cds1 and Cds2. During cardiomyocyte growth and development, mitochondrial biogenesis is increased under the control of the transcription factor, PGC-1α which also regulates Cds1 expression. Mitochondria have limited capacity to synthesise their own lipids and are dependent on the endo/sarcoplasmic reticulum for many of their lipids, including PI and PA. RdgBβ (Retinal degeneration B beta) is a phosphatidylinositol transfer protein (PITP), recently found to be enriched in cardiac tissue, able to transfer both PI and PA. This investigation attempts to identify the residues within the PITP domain that are required for PA transfer and it focuses on the characterisation of the expression and distribution of RdgBβ and Cds1 in rat hearts and H9c2 cells which are derived from embryonic rat ventricles. Withdrawal of serum and the addition of retinoic acid induces differentiation of H9c2 cells towards a cardiomyocyte-like phenotype. At the protein level, proliferating H9c2 cells have low RdgBβ expression which increases dramatically following differentiation with retinoic acid. The increase in RdgBβ expression occurred in parallel with an elevation in mitochondrial content. In addition to the cytosol, RdgBβ was also located at membrane fractions, suggesting that RdgBβ may facilitate PI and PA transport between the ER and the mitochondria. The regulation of mRNA expression of Cds1 was not associated with cellular differentiation but with vasopressin stimulation of H9c2 cells. Both myoblasts and differentiated H9c2 cells showed an increase of Cds1 mRNA suggesting that Cds1 is involved in the PI cycle.

Acknowledgements

Contents

List of Tables

Abbreviations

aa	Amino acids
ANP	Atrial natriuretic protein
APS	Ammonium persulphate
AT1R	Angiotensin II type 1 receptor
ATP	Adenosine triphosphate
ATRAP	Angiotensin II receptor-associated protein
AVP	Arginine vasopressin
AVPR1	Arginine vasopressin receptor 1
BCA	Bicinchoninic acid
BNP	Brain natriuretic protein
bp	Base pairs
BSA	Bovine serum albumin
cDNA	Complementary deoxyribonucleic acid
CDP	Cytidine diphosphate
Cds	CDP-DAG synthase
CL	Cardiolipin
CLS	Cardiolipin synthase
Cos7	CV-1 (simian) in origin carrying the SV40 genetic material, cell line
COX4	Cytochrome C oxidase subunit 4
CTP	Cytidine triphosphate
DAG	Diacylglycerol
DDK	Protein tag composed of aspartic acid and lysine residues (FLAG)
DGK	Diacylglycerol kinase
Dm	Drosophila melanogaster
DMEM	Dulbecco's modified Eagle's medium
DMSO	Dimethyl sulfoxide

dpm	Disintegrations per minute
EC	Enzyme Commission number
ECL	Enhanced chemo-luminescence
EDTA	Ethylenediaminetetraacetic acid
ER	Endoplasmic reticulum
FCS	Foetal calf serum
FLAG	Protein tag composed of aspartic acid and lysine residues (DDK)
G3P	Glycerol 3 phosphate
GPAT	G3P acyl-transferase
GPCR	G protein-coupled receptor
GTPγS	guanosine 5'-O-[gamma-thio]triphosphate
H9c2	Emryonic rat heart myoblast cell line
HeLA	Human cervical cancer cell line
HL60	Human promyelocytic leukemia cell line
HEPES	4-(2-hydroxyethyl)-1-piperazine-ethanesulfonic acid
HRP	Horseradish peroxidase
Hu	Human
IGF-I	Insulin-like growth factor
IP3	Inositol trisphosphate; I(1,4,5)P3
IP3R	IP3 receptor
IPTG	Isopropyl β-D-1-thiogalactopyranoside
kDa	Kilo daltons
LPAAT	Lyso-PA acyl-transferase
LB	Luria broth
Lyso-PA	Lysophosphatidic acid
MAM	Mitochondria-associated membranes
Mdm35	Mitochondrial distribution and morphology protein
MNCL	Mono-lyso CL

mRNA	Messenger ribonucleic acid
Myc	Myelocytomatosis
MW	Molecular weight
NCBI	National Center for Biotechnology Information
Nir/RdgB	N-terminal domain-interacting receptor/Retinal degeneration B protein
NRC	Neonatal rat cardiomyocytes
PA	Phosphatidic acid
PBS(-T)	Phosphate-buffered saline(-tween)
PC	Phosphatidylcholine
pcDNA	Plasmid complementary deoxyribonucleic acid
PCR	Polymerase chain reaction
Pfam ID	Protein family identification code
PE	Phosphatidylethanolamine
PEST residues	Protein sequence rich in proline, glutamic acid, serine and threonine
PG	Phosphatidylglycerol
PGC1	Peroxisome proliferator-activated receptor coactivator-1
PGP	PG phosphate
PI	Phosphatidylinositol
PI3K	Phosphatidylinositol 3-kinase
PI4K	Phosphatidylinositol 4-kinase
PI4P-5-K	Phosphatidylinositol-4-phosphate 5-kinase
PIP	Phosphatidylinositol phosphate; PI(3)P, PI(4)P, PI(4)P
PIP2	Phosphatidylinositol bisphosphate; PI(4,5)P2, PI(3,5)P2, PI(3,4)P2
PIP3	Phosphatidylinositol trisphosphate; PI(3,4,5)P3
PIPES	1,4-Piperazine-di-ethanesulfonic acid
PIS	Phosphatidylinositol synthase
PITP	Phosphatidylinositol transfer protein

PKC	Protein kinase C
PLA1	Phospholipase A1
PLC(β)	Phospholipase C (type beta)
PLD	Phospholipase D
PMA	Phorbol myristate acetate
PS	Phosphatidylserine
PRELI	Protein of relevant evolutionary and lymphoid interest (mitochondrial mammalian homolog of Ups1)
qRT-PCR	Quantitative real time PCR
SR	Sarcoplasmic reticulum
TAE	Tris-acetate-EDTA
TAG	Triacylglycerol
Tam41	Mitochondrial translocator assembly and maintenance homolog [Homo sapiens]
TEMED	N,N,N',N'-tetramethylethylenediamine
Tm	Melting temperature
TRIAP1	TP53 regulated inhibitor of apoptosis 1
VAP	(Vesicle-associated membrane protein) VAMP-associated protein
WB	Western blot
WT	Wild-type

CHAPTER 1: Introduction

Biological membranes are fundamental cellular constituents that rely on the diversity of their structures and biophysical properties given by the mixture of their specific lipid and protein composition to function. Phospholipids are the major component of cellular membranes and each cellular organelle presents a specific lipid composition. For instance, although phosphatidylcholine (PC) and phosphatidylethanolamine (PE) are the most abundant cellular phospholipids, mitochondria are enriched in cardiolipin (CL) and the plasma membranes are enriched in phosphatidylserine (PS). Structurally phospholipids are composed of a molecule of glycerol connected to two fatty acids that may differ in length (Figure 1.1.). Phosphatidic acid (PA) is a key intermediate for phospholipid synthesis via its consecutive modification including the dephosphorylation to diacylglycerol (DAG) or the conversion into cytidine-diphosphate diacylglycerol (CDP-DAG). [34,111,112]

The endoplasmic reticulum (sarcoplasmic reticulum in muscle and cardiac cells) is the main site of phospholipid synthesis, but other organelles such as the Golgi apparatus and the mitochondria are capable of producing limited quantities of lipids. Mitochondria have the capacity to synthesise PE, PG and cardiolipin but not PC, PI and PS. The mechanisms of intracellular transport of lipids include general vesicular traffic or the use of specific transporters[111]. Mitochondria do not interact with vesicles and depend entirely on alternative routes to obtain many of their lipids[55]. Generally, mitochondria co-purify experimentally with a sub-region of the SR known as mitochondria-associated endoplasmic reticulum membranes (MAM). This fraction has being shown to possess PS, PE and PC synthesis capability[52,111].
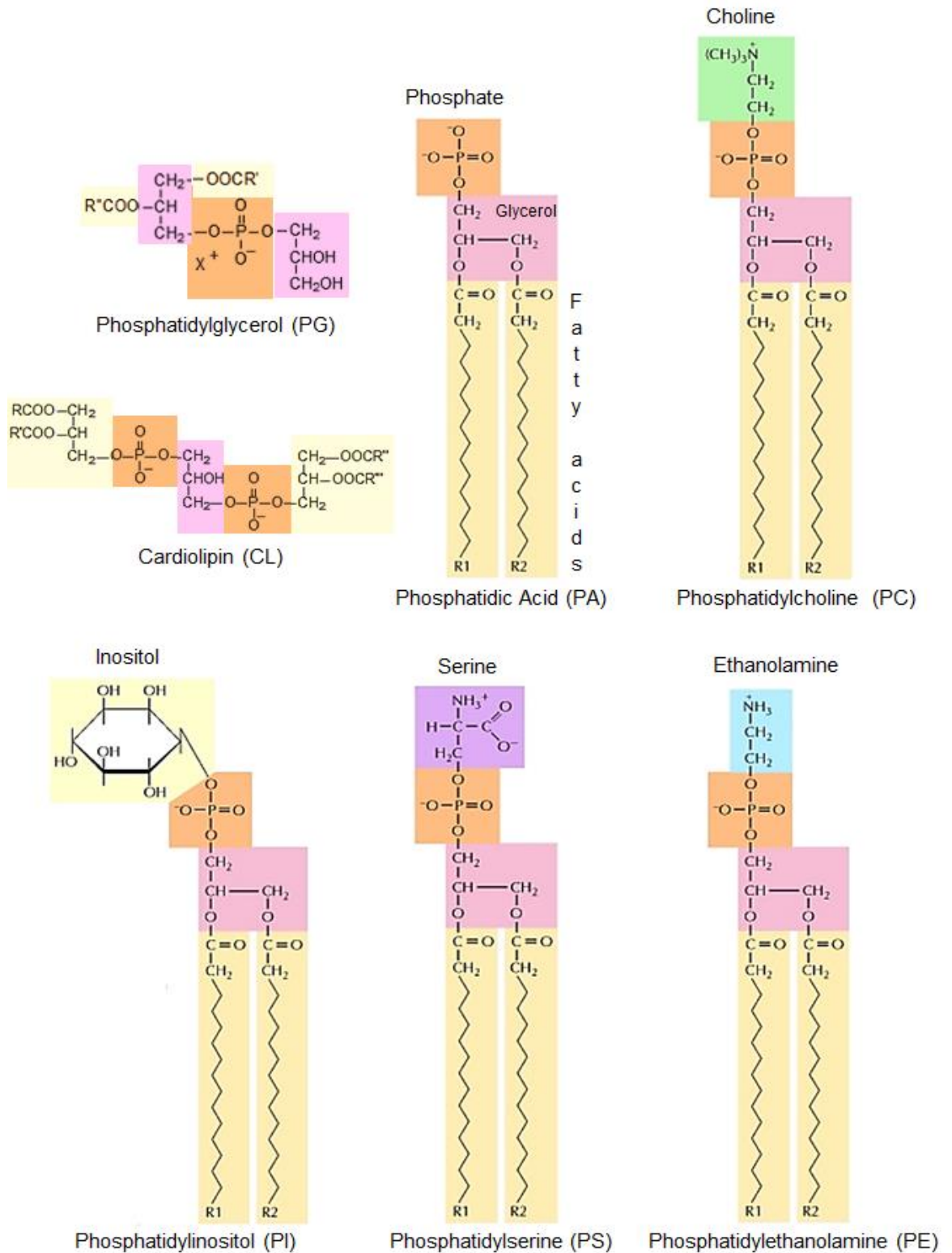
Figure 1.1: Structure of Phospholipids

Membrane phospholipids are made of two fatty acids (R1 and R2), which may differ in length, linked to glycerol (CH_2-CHO^- -CH_2O^-). The third carbon of glycerol is joined to a phosphate group (PO_4^{2-}) to form PA, the precursor of other phospholipids including PC, PS, PE, PI, or PG, the precursor of cardiolipin (CL).

1.1: Phosphatidic Acid (PA).

1.1.1: PA biosynthesis.

PA can be generated through different mechanisms: firstly, the *de novo* synthesis pathway consist of sequential acylations from glycerol-3-phosphate (G3P) by distinctive G3P and lyso-PA acyltransferases localised to both endoplasmic reticulum (ER) and mitochondrial membranes within mammalian cells. G3P acyltransferases (GPAT enzymes, EC 2.3.1.15) catalyse the conversion of G3P and acyl-CoA into lyso-PA. In mammals, there are four isoforms of GPAT enzymes that have been identified to date. GPAT1 and GPAT2 are found in the outer mitochondrial membranes while GPAT3 and GPAT4 are associated with the ER. PA is finally produced by the action of the lyso-PA acyltransferases (LPAAT, EC 2.3.1.51), which convert lyso-PA and acyl-CoA into phosphatidic acid (Figure 1.2.A). There are eleven LPAAT family members in mouse and human reported in the literature but only four isoforms of LPAAT display acyl donor specificity for PA (LPAAT 1-4) which in mammalian cells localise to the ER.[105,126] To date is still unclear whether PA is synthesised in mitochondria.

In addition to the G3P pathway, PA is also generated during cellular signalling during activation of G-protein coupled receptors as well as receptor tyrosine kinases. Hydrolysis of phosphatidylcholine (PC) by phospholipase PLD activity results in PA formation whilst hydrolysis of phosphatidylinositol bisphosphate (PIP2) results in DAG formation which is converted into PA by the action of DAG kinases., [116,130] (Figure 1.2.B-C)

Phosphatidic Acid Synthesis
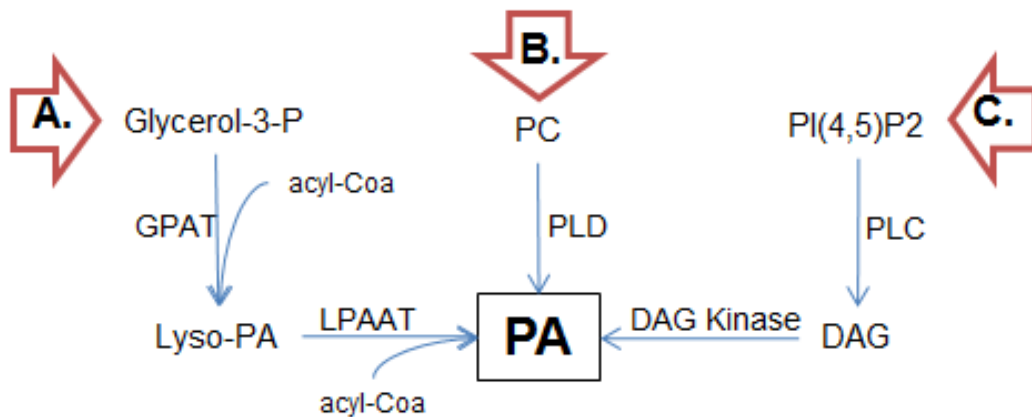
Figure 1.2: Phosphatidic acid biosynthesis.

[A]: PA is synthesised by the addition of an acyl group to Glycerol-3-Phosphate by a G3P acyltransferase (GPAT) to form Lyso-PA, followed by acylation of Lyso-PA by LPAAT.

[B]: PA is formed from PC hydrolysis by phospholipase D.

[C]: PA generation results from phosphorylation of DAG produced from the phospholipase C signalling pathway.

1.1.2: PA is the key intermediate of phospholipid biosynthesis.

The metabolic outcomes of synthesised PA include its deacylation back to lyso-PA by phospholipase PLA1 (EC 3.1.1.32). Newly synthesised PA is also rapidly dephosphorylated by members of the Lipin family (EC 3.1.3.4) to produce diacylglycerol (DAG) which can be involved in either cell signalling or the synthesis of triacylglycerol (TAG) and the phospholipids PC, PE, and PS (Figure 1.3.A). Alternatively, PA can react with CTP to produce CDP-DAG catalysed by Cds enzymes. CDP-DAG is the precursor for PI biosynthesis in the ER by PI synthase (PIS, EC 2.7.8.11) [74]. There is a single gene for PIS in mammalian cells and it does not exhibit acyl chain specificity[28]. Sequential phosphorylation of PI at the plasma

membrane produces phosphoinositides which are central for signalling and membrane traffic[8]. In mammals, the fatty acid chains of the phosphoinositides are enriched with 1-stearoyl-2-arachidonoyl species[33] (Figure 1.3.B and Figure 1.6).

Phosphatidylglycerol phosphate (PGP) is synthesised from glycerol-3-P and CDP-DG by PGP synthase, an enzyme located in the inner mitochondria membrane.[112] PG is formed through PGP dephosphorylation by PG phosphatase[79,112] (Figure 1.3.C).

a: Cardiolipin biosynthesis

Biosynthesis of cardiolipin, also known as diphosphatidylglycerol, takes place in the inner mitochondrial membrane. Cardiolipin (CL) is formed from the condensation of PG and CDP-DAG catalysed by cardiolipin synthase (CLS, EC 2.7.8.41.) in eukaryotic cells (Figure 1.2). Nascent CL in the mitochondrial membranes requires acyl chain remodelling which occurs either by deacylation–reacylation or by transacylation. The deacylation–reacylation reaction forms a monolyso-CL (MNCL) intermediate catalysed by several acyl-CoA dependent phospholipases, while CoA-independent transacylation of CL occurs by the transfer of an acyl chain from PC by the enzyme to form a functional mature CL molecule rich in linoleic acid[127]. For CL synthesis to occur, PA is required to be transferred from the outer mitochondrial membrane to the inner mitochondrial membrane. This is achieved by the PA transporter Ups1/Mdm35 complex in yeast,[26] and their homologues in humans, the TRIAP1/PRELI complex.[91]

Phospholipid Synthesis
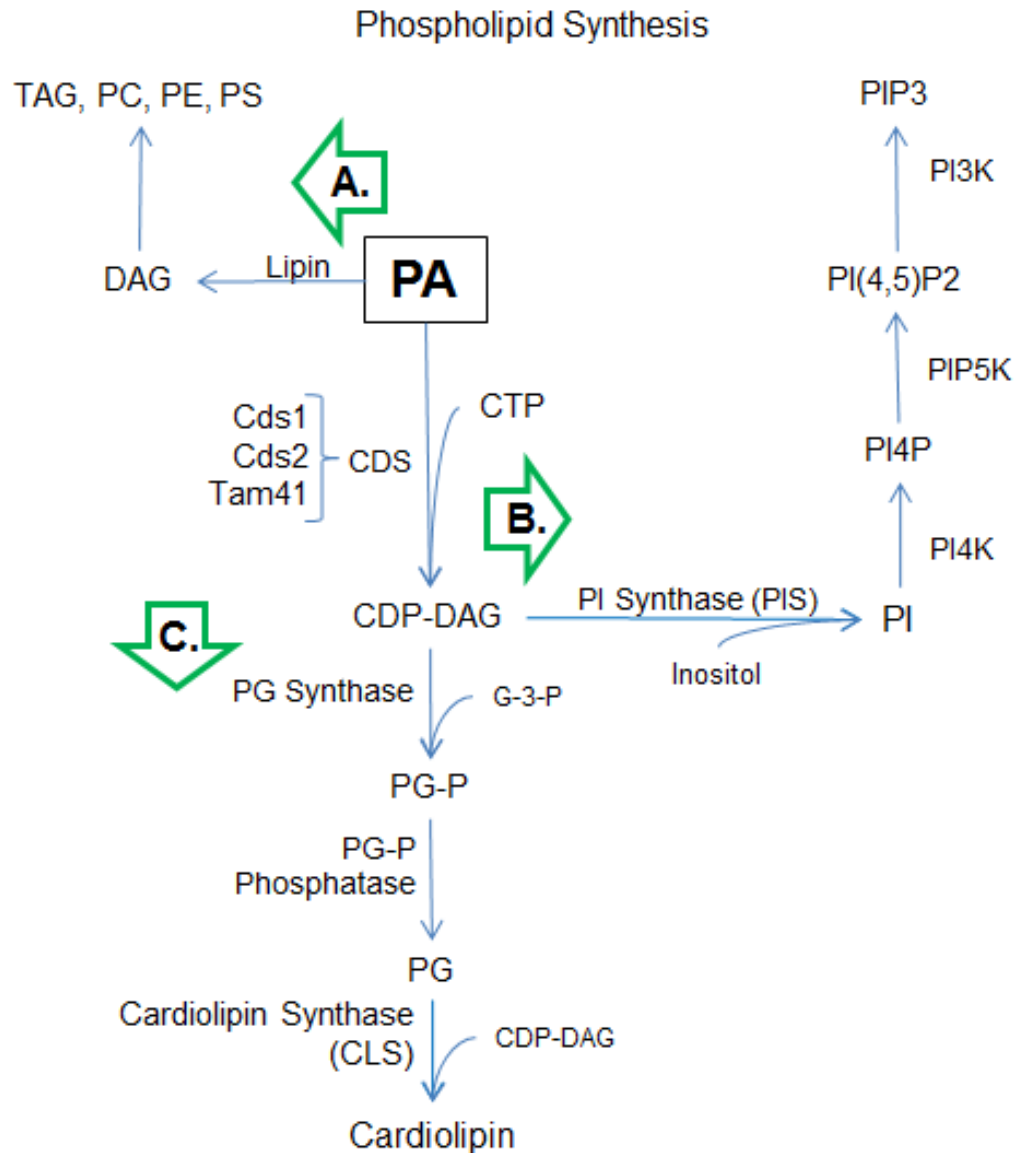
Figure 1.3: PA is the key intermediate on phospholipid biosynthesis.

[A]: Synthesis of triglycerides (TAG), PC, PS and PE via DAG following PA dephosphorylation by members of the Lipin family.

[B]: Synthesis of PI by PI synthase action on CDP-DAG formed by CDS enzymes from PA. PI is sequentially phosphorylated by kinases to produce phosphoinositides (PI4P, PI $(4,5)P_2$ and PI$(3,4,5)P_3$).

[C]: Cardiolipin synthesis results from the condensation of CDP-DAG and PG by Cardiolipin synthase.

1.1.3: CDP-DAG synthases (Cds)

The activity of the Cds enzymes is the rate limiting step for PI and Cardiolipin biosynthesis in the ER and the mitochondria respectively.[46,50,119] The Cds enzyme was first cloned from *E.Coli* [57] followed by *S. cerevisae* Cds, [99] and later in *Drosophila melanogaster* [124]. These species present one Cds gene. In mammals, cloning of human Cds enzymes was achieved, [46] and studies in mice [58] were able to characterise two Cds homologues Cds1 and Cds2. Early studies using rat liver reported that Cds was responsible to produce the CDP-DAG precursor of PI in the ER and CL in mitochondria [81]. However, studies in yeast (*Saccharomyces cerevisae*) revealed that Tam41 is the mitochondrial Cds while endogenous Cds1 was present in both ER and crude mitochondria but absent from purified mitochondrial fractions, [106] suggesting that Cds1 could be present in mitochondrial associated ER membranes known as MAMs.

The genes of mouse and human Cds1 encode a 461 a.a. protein (52.9 kDa) while Cds2 encode a 444a.a./445a.a. (51 kDa). The sequences of murine Cds1 and Cds2 are 56% and 57% identical, respectively, to the Drosophila Cds sequence[58]. Alignment of the amino acid sequences encoded by *Rattus Norvegicus* Cds1 and Cds2 showed that they are 69.5% identical and 81% similar (Figure 1.4). It was recently suggested that Cds2 provides CDP-DAG for the PI-cycle due to its selectivity for the acyl chains 1-stearoyl, 2-arachidonoyl species of the precursor PA. Cds1 showed no particular substrate specificity [29].

Initially, it was predicted that Cds were tightly membrane-bound enzymes with different number of trans-membrane domains between Cds1 and Cds2, with nine trans-membrane segments in Cds1 and eight in Cds2[58]. Indeed, the crystal structure of the Cds enzyme from the thermophilic bacterium *Thermotoga maritima* revealed the existence of a homodimer and each monomer is composed of nine transmembrane helices (Figure 1.5.A), exhibiting a funnel-shaped structural feature which enables Cds to simultaneously interact with membrane-associated PA and cytosolic CTP molecules to catalyse their condensation to form CDP-DAG with a hetero-di-metal centre for the cofactors Mg^{2+} and K^{1+}. The proposed catalytic mechanism of Cds is that the Mg^{2+} ion might serve as the metal responsible for activating the phosphate group of PA molecule, whereas K^{1+} promotes binding to the β- and γ-phosphates of CTP and facilitates the dissociation of pyrophosphate from the active site. (Figure 1.5.B).[71] Structurally, Cds1 and Cds2 differ mainly in their cytosolic N-terminal (residues 1-99; Figure 1.4).

Expression studies indicated that Cds1 and Cds2 mRNA exhibit different tissue specificity. In mouse, Cds2 is ubiquitously expressed whilst Cds1 has an expression pattern restricted to the brain, eye, smooth muscle and testis [46].

```
Rattus norvegicus CDP-diacylglycerol synthase
Cds1: NM_031242Cds2: NM_053643
Length: 462
Identity:      321/462 (69.5%)
Similarity:    374/462 (81.0%)

Cds1      1 MLELRHRGGCPGPGGAGTPPPREGEAAGGDHETESTSDKETDIDDRYGDL    50
            |.|||.|       ......||.:.|:      |:|:..|.||      ..|.
Cds2      1 MTELRQR------AVREDAPPEDKES-----ESEAKLDGET-----ASDS    34

Cds1     51 DARGDSDVPEVPPSSDRTPEILKKALSGLSSRWKNWWIRGILTLTMISLF   100
            ::|.::..|   |.|.|.|||:|.:|||.||||||||:|||||:.||:.|
Cds2     35 ESRAETAPP--PTSIDDTPEVLNRALSNLSSRWKNWWVRGILTMAMIAFF    82

Cds1    101 FLIIYMGSFMLMLLVLGIQVKCFQEIITIGYRVYHSYDLPWFRTLSWYFL   150
            |:|||:|..:||::|:..:|:|||.||||||||.||||||||||||||||
Cds2     83 FIIIYLGPMVLMMIVMCVQIKCFHEIITIGYNVYHSYDLPWFRTLSWYFL   132

Cds1    151 LCVNYFFYGETVADYFATFVQREEQLQFLIRYHRFISFALYLAGFCMFVL   200
            |||||||||||.|||.|.|||||.|:-.|.:|||||||.|||.||||||||
Cds2    133 LCVNYFFYGETVTDYFFTLVQREEPLRILSKYHRFISFTLYLTGFCMFVL   182

Cds1    201 SLVKKHYRLQFYMFAWTHVTLLITVTQSHLVIQNLFEGMIWFLVPISSVI   250
            |||||||||||||||.|||||||.|||||||.|||||||||:||||.||
Cds2    183 SLVKKHYRLQFYMFGWTHVTLLIVVTQSHLVIHNLFEGMIWFIVPISCVI   232

Cds1    251 CNDITAYLFGFFFGRTPLIKLSPKKTWEGFIGGFFSTVIFGFIAAYVLSK   300
            ||||.||:||||||||||||||||||||||||||||:||:||.::.||:.
Cds2    233 CNDIMAYMFGFFFGRTPLIKLSPKKTWEGFIGGFFATVVFGLLLSYVMSG   282

Cds1    301 YQYFVCPVEYRSDVNSFVTECEPSELFQLQNYSLPPFLQAVLSRETVSLY   350
            |:.||||||||.:|.|||..:||||:||:||.|::|..:|:::..:|:.:|
Cds2    283 YRCFVCPVEYNNDTNSFTVDCEPSDLFRLQEYNIPGVIQSLVGWKTMRMY   332

Cds1    351 PFQIHSIALSTFASLIGPFGGFFASGFKRAFKIKDFANTIPGHGGIMDRF   400
            |||||| |||||||||||||||||||||||||||||||||||||||||||
Cds2    333 PFQIHS-ALSTFASLIGPFGGFFASGFKRAFKIKDFANTIPGHGGIMDRF   381

Cds1    401 DCQYLMATFVHVYITSFIRGPNPSKVLQQLLVLQPEQQLNIYRTLKIHLT   450
            |||||||||:|||.|||||||||||:||.|.|.|:|:|||:|::.|||.|||
Cds2    382 DCQYLMATFVNVYIASFIRGPNPSKLIQQFLTLRPDQQLHIFNTLKSHLT   431

Cds1    451 EKGILQPTWKV-    461
            :||||....:.
Cds2    432 DKGILMSALEEE    443
```

Figure 1.4: Sequence alignment of Rat Cds1 and Cds2.

Figure 1.5 Structure and mechanism of *Thermotoga maritime* CdsA.

[A.] Overall structure of *Thermotoga maritime* CdsA homodimer location along the membrane in the substrate free form.

[B.] Proposed model for the catalytic mechanism of CDP-DAG synthesis. (Taken from Liu, et al. 2014)

1.1.4: PA is involved in cell signalling

In addition to its critical role as a metabolite at the heart of membrane phospholipid biosynthesis, PA has also been involved in cell signalling as a lipid second messenger that regulates several proteins implicated in the control of cell cycle progression and cell growth. While the LPAAT pathway is integral to de novo membrane PA biosynthesis, the activation of the signalling pathways of phospholipase C and phospholipase D (PLC and PLD) in response to growth factors and stress also produce PA. Both pathways are stimulated by the activation of their respective receptors at the plasma membrane. The PLD pathway produces PA from phosphatidylcholine (PC) hydrolysis and it is also responsive to nutrients. Two mammalian PLDs, PLD1 and PLD2 have been characterised and are regulated by small GTPases as well as protein kinase C [83]. The PA produced from this pathway mainly contains mono-unsaturated fatty acids and is readily distinguished from the PA generated from the PLC pathway.[116]

PA has been studied as a key target for the lipid second messenger of mTOR signalling, which integrates both nutrient and growth factor stimulation to control cell growth and proliferation. PLD-generated PA has been widely implicated in mTOR activation, however PA generated via the LPAAT and PLC pathways has also been described as playing a role in the regulation of mTOR specially in period of stress.[37]

The mammalian PLC family consists of at least 13 separate isoforms in 6 sub-families (β, γ, δ, ε, ζ and η) that differ in their structural organisation, mode of activation, cellular and tissue distribution, membrane-binding and catalytic

properties.[44] Phospholipase C beta Cβ (PLCβ) hydrolyses PI(4,5)P$_2$ into DAG and inositol 1,4,5-trisphosphate (IP$_3$). IP$_3$ regulates intracellular Ca^{2+} release from intracellular stores by binding to the IP$_3$ receptor (IP$_3$R) localised in the ER (Figure 1.6). DAG is the physiological activator of some isoforms of protein kinase C (PKC) and is rapidly phosphorylated by DAG kinases to form PA[18]. The PA which derives from the PLC pathway has a distinctive fatty acid composition in most mammalian cells. It is highly enriched in stearic acid (C18:0) and arachidonic acid (C20:4).[116]
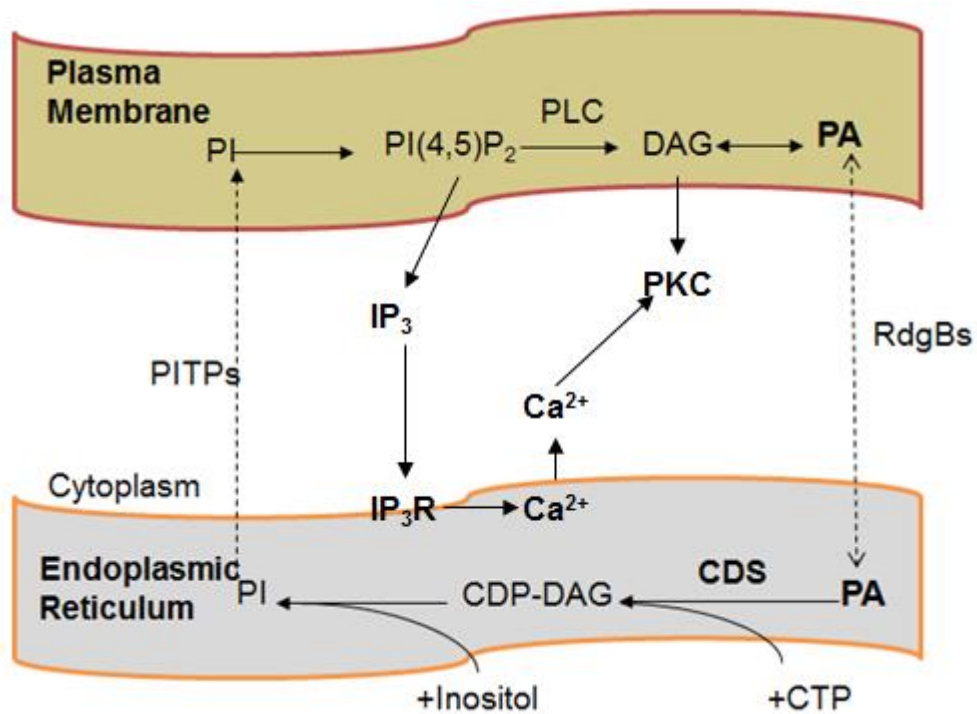
Figure 1.6: Phospholipase C signalling and PITPs involvement in PI and PA transport across cellular compartments.

The PLC pathway starts when agonists stimulate specific isoforms of PLC through their receptors. PLCβ catalyses the hydrolysis of phosphatidylinositol bisphosphate [PI(4,5)P$_2$] into the second messengers diacylglycerol (DAG) and inositol triphosphate (IP$_3$). PA is converted to DAG at the plasma membrane. All the members of the phosphatidylinositol transfer protein (PITPs) family function as non-vesicular transporters of phosphatidylinositol (PI). Class II PITPs (RdgBs) exclusively transfer PI and PA.

The limiting factor for PLC signalling is the amount of substrate available. $PI(4,5)P_2$ levels are maintained through the sequential phosphorylation of PI by lipid kinases present at the plasma membrane. However, PI and its precursor PA are synthesised at the ER and the mechanisms of PI and PA transfer between organelles has not been elucidated. In fact all organelles contain some lipids that were synthesised elsewhere. Lipid transport can occur by various mechanisms including diffusion, vesicular traffic and the recruitment of transport proteins.

a. Diffusion

Cellular lipids can diffuse laterally through membrane continuities, such as those that exist between the ER and the outer and inner nuclear membrane. Tubular connections have been observed between Golgi cisternae. The major membrane transport pathway between cellular organelles in the secretory and endocytic pathways is through the budding and fusion of membrane vesicles. In contrast, organelles such as mitochondria and peroxisomes are not connected to the vesicular transport system and lipids are most likely to enter and leave these organelles as monomers, assisted by both soluble and membrane proteins.

b. Vesicular trafficking of membrane components

Secretory and endocytic organelles are connected by bidirectional vesicular transport. The lipid raft hypothesis proposes that preferential interactions between lipids generate domains of specific lipid compositions to drive the sorting of membrane proteins[8,58]. Vesicle-independent movement has been demonstrated for PC, PE and PS between the ER, mitochondria, Golgi and the plasma membrane[57,64–69]

c. Recruitment of cytosolic proteins

Recruitment of cytosolic proteins by membrane phospholipid has also been found to facilitate lipid transfer. The lipid components include PI, PC and PA while the protein components include various domains including START and PITP. The phosphatidylinositol transfer proteins (PITP) family was identified and characterised by the ability of binding and transferring PI between different membrane compartments in vitro [23] Recently, it was reported that a subclass of the PITPs was able to bind and transfer PA in vitro[40,125].(Figure 1.6 and Figure 1.8).

1.2: Phosphatidylinositol Transfer Proteins (PITPs).

The PITP family has five members in the mammalian genome subdivided into two classes based on sequence analysis. The PITP domain is ~260 amino acids whose sequence is highly conserved in all species. The sequences can be found in electronic databases under the Pfam IDs PF02121.[23] There are several reports studying the suppression or downregulation of specific isoforms *in vivo* have implicating PITPs in a diverse range of effects such as defects in signal transduction via phospholipase C and phosphoinositide 3-kinase, membrane trafficking, stem cell viability, neurite outgrowth, and cytokinesis (Reviewed in Cockcroft and Garner 2011; Figure 1.8.B)[21]
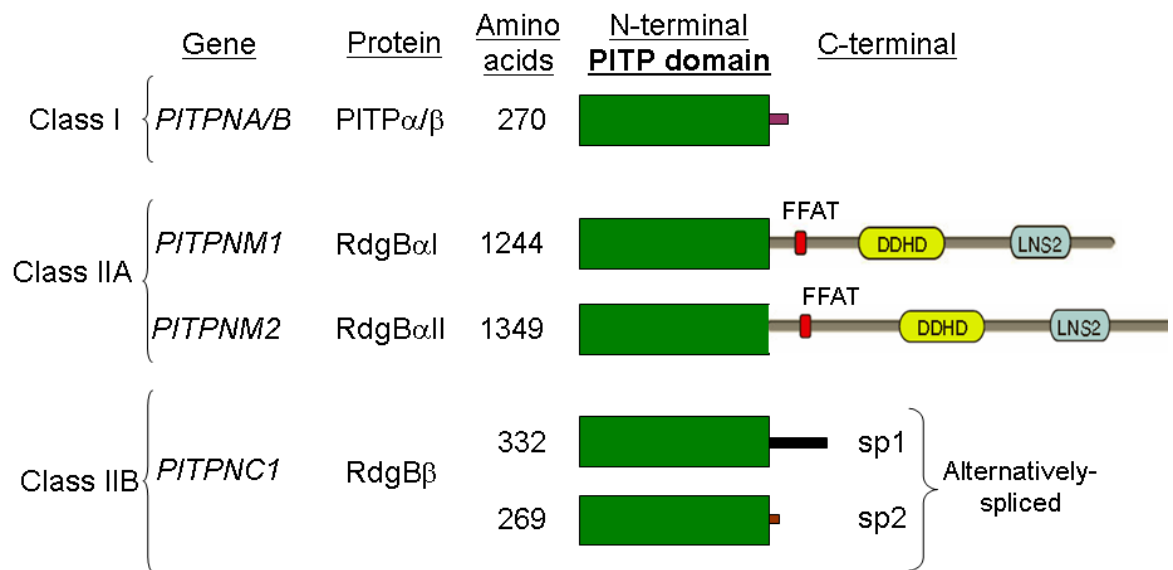
Figure 1.7. Structural organisation of the human PITP family.

Human PITP proteins are divided into Class I and II. Class II is subdivided into IIA and IIB. The splice variants of RdgBβ are shown. The number of amino acids of the entire protein is indicated. The different C-terminal tails are indicated by different colours. The domains are colour-coded: green, PITP domain; red, FFAT motif; yellow, DDHD domain; blue, LNS2 domain

1.2.1: Class I PITPs.

The class I PITPs includes the two highly homologous PITPα and PITPβ proteins of approximately 35kDa [23]. Based on the crystal structure of PITPα and PITPβ, the N- terminal PITP domain forms a hydrophobic cavity where a single molecule of either PI or PC binds; while their C-terminal extension forms the 'lid' that regulates the entry and exit of lipids to and from the cavity. Four amino acid residues (T59, K61, E86 and N90 using mouse PITPα numbering) were found to be

essential for binding to the inositol ring [109] (Figure 3.7). Conversely, the residues responsible for PC binding have not been identified. However, it has been reported that the mutation C95T which localises in the binding pocket, causes loss of PC transfer in PITPβ [15]. The residues within the PITP domain that make contact with both PI and PC are those in proximity to the phosphate group and the acyl chains (T97, K195, E218 and Y63)[109].The PI and PC molecular species bound by PITPα have been examined using tandem electrospray ionisation mass spectrometry (ESI-MS/MS), and compared with the profile of PI and PC molecular species in HL60 cells. PITPα showed selectivity towards two mono-unsaturated PC species in particular, 16:0/16:1 and 16:1/18:1. [56]

Several studies have shown that the PI transfer activity of PITPα and PITPβ can reconstitute PLC signalling in cytosol depleted cells[23]. For instance, PLC signalling gets disrupted when PITPα is phosphorylated at residues S166 and T59 in cells treated with the PKC activator phorbol myristate acetate (PMA)[82]. Mice lacking a functional copy or expressing a mutant PITPα unable to bind PI showed neurological defects.[47] On the other hand, PITPβ is required for retrograde traffic from the Golgi to the ER and for maintenance of the nuclear morphology of HeLa cells.[15] PITPβ deficiency is lethal in mice.[3] (Figure 1.8.B)

1.2.2: Class II PITPs.

Unlike Class I PITPs, all members of Class II PITPs bind and transfer PI and PA [40,125] (Figure 1.8). Class II PITPs (also known as RdgBs) are subdivided into IIA and IIB (Figure 1.7). The founding member of Class IIA is the *Drosophila melanogaster* Retinal Degeneration protein (Dm-RdgBα). In photoreceptor cells, Dm-RdgBα is considered to transfer the PI required to replenish the PLC pathway which generates electrical responses to light.[115] RdgBα are multi-domain membrane-associated proteins. They contain the PITP domain, a FFAT motif that binds to VAMP-associated proteins (VAP), where VAMP stands for vesicle-associated membrane proteins, and two additional domains, DDHD and LNS2. The DDHD domain is 195 amino acids and is also present in proteins with PA-PLA1 activity. The LNS2 domain is 130 amino acids also found in lipins and has been shown to bind PA. There are two RdgBα isoforms, RdgBαI (alt. name: PITPNM1, Nir2) and RdgBαII (alt. name: PITPNM2, Nir3) (Figure 1.7). [4,21-24]Recently, it was reported that Hu-RdgbαI translocates from the Golgi complex to the plasma membrane in response to growth factor stimulation in HeLa cells where it binds PA at its C-terminal region.[61] On the other hand, the N-terminal PITP domain of Hu-Rdgbαl and Dm-Rdgbα bound mostly PI and some PA which increased upon GTPγS stimulation in HL60 cells[40]. Most recently, it was proposed that RdgBα proteins facilitate the reciprocal transport of PA and PI at ER-PM membrane contact sites to maintain $PI(4,5)P_2$ metabolism after PLC activation[24]. The Class IIB PITP RdgBβ, consists of the PITP domain followed by an unstructured eighty amino acid N-terminal tail which is phosphorylated at two sites to form a 14-3-3 binding site. [41]
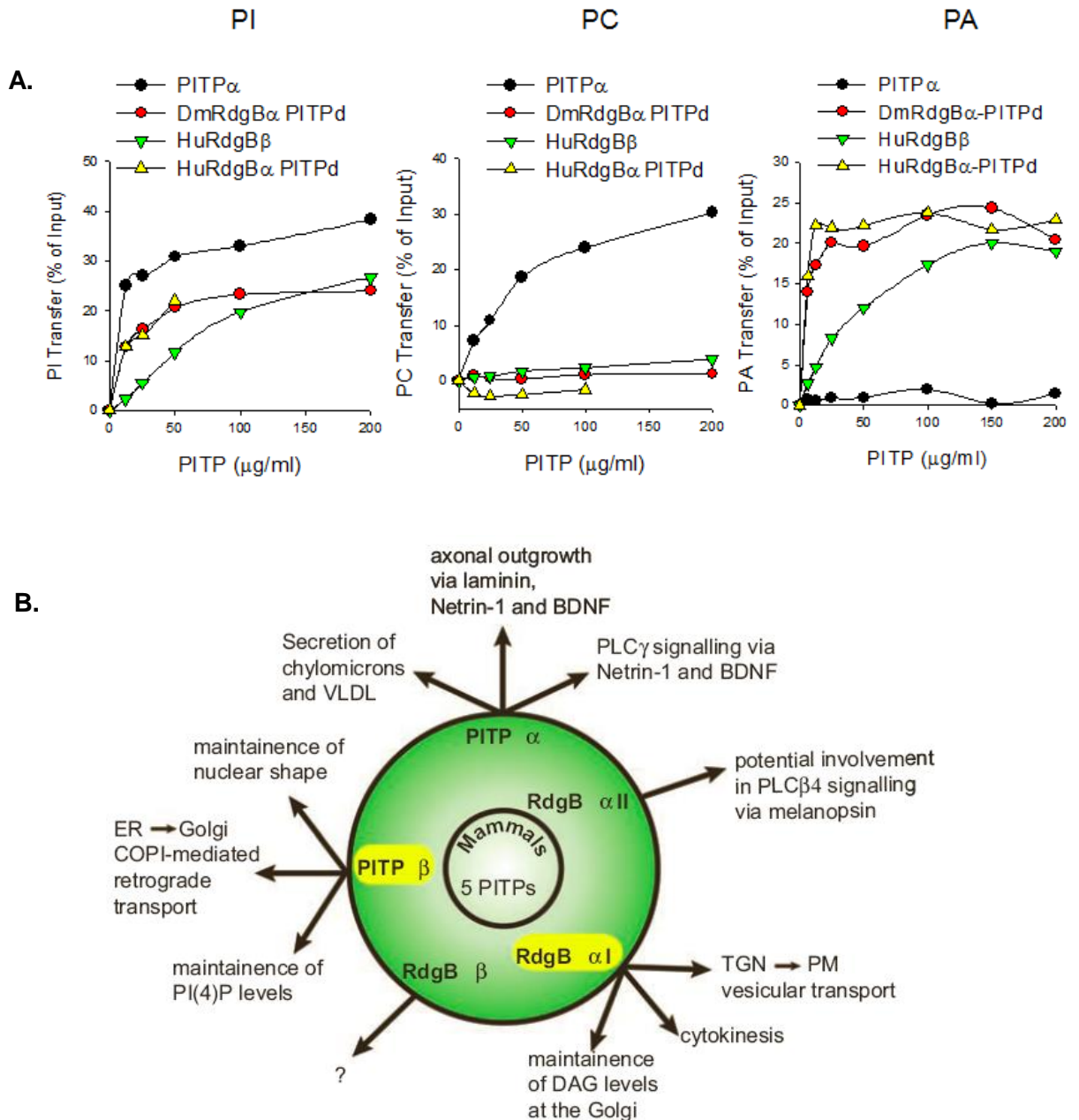
Figure 1.8: PI, PC and PA transfer activity and known functions of PITPs. [A.] The PI, PC and PA transfer activities of the PITP domains of class I and class II were measured by the amount of labelled lipid transferred to an acceptor compartment as a percentage of the total input present in the donor compartment. PITPα transfers PI and PC whereas RdgB proteins transfer PI and PA. The figure was taken from Cockcroft et al 2016[24]. [B.] PITPs reported functions in mammalian cells. The function of the individual PITPs in mammals is indicated. The PITPs that are highlighted in yellow are those which absence causes embryonic lethality. Figure taken from Cockcroft and Garner 2011[21]

1.2.3: RdgBβ

RdgBβ is also known as Cytoplasmic phosphatidylinositol transfer protein 1 (PITPNC1). Although it was identified in 1999, [39] studies of its characteristics have only been reported recently [40,41]. There are two splice variants of RdgBβ, sp1 and sp2, which differ at their carboxyl-terminal[104] (Figure 1.7). RdgBβ sp1 (38kDa) contains an amino terminal PITP domain and a specific 80 amino acid long C-terminal disordered (unstructured) region with two PEST sequences [41] (Figure 1.7). Disordered regions are found in proteins with signalling and regulatory functions frequently subject to tight regulation [6]. PEST sequences are often found in proteins subject to rapid turnover in cells [92].

The endogenous protein expression of RdgBβ has been investigated in a previous study.[41] Fractionation of concentrated rat heart cytosol by gel filtration showed immunoreactivity for a protein of the expected size suggesting that rat heart does contain endogenous RdgBβ. Its elution on gel filtration partially overlapped with 14-3-3 proteins which suggested that cytosolic RdgBβ is likely to be associated with 14-3-3. Indeed, transfection of Cos7 cells with FLAG-RdgBβ was found to directly bind to 14-3-3 proteins at the phosphorylated residues S274 and S299 which are located at the C-terminal (Figure 1.9). The phosphorylation was studied with the use of inhibitors of protein kinases (PK) A, B and C and it was suggested that RdgBβ phosphorylation is probably mediated by PKC.[41] The treatment of COS-7 cells with phorbol 12-myristate 13-acetate (PMA), increased the expression of FLAG-RdgBβ and mildly increased binding to 14-3-3 [41]. PMA is an analogue of DAG and a potent activator of PKC. In addition, independent from 14-3-3 binding, FLAG-

RdgBβ binds HA-tagged ATRAP in Cos-7 cells. This was found only after treatment with PMA for 16 hours. The binding site is located at the N-terminal PITP domain of RdgBβ, possibly at the regulatory loop (Figure 1.9).

RdgBβ mRNA expression has been found in different tissues, but it was found enriched in the heart [23;24]. The expression regulation of RdgBβ mRNA has not been directly studied but it was recently associated with the microRNA miR-126 in a cell-type specific manner. For instance, loss of miR-126 expression was related to an increased expression of RdgBβ in breast cancer cells, [90] whilst overexpression of miR-126 in leukaemic cells did not reduce the expression levels of RdgBβ.[2]

The lipid binding properties of RdgBβ have also been investigated. RdgBβ binds and transfers a specific species of PI, one enriched in stearic ($C_{18:0}$) and arachidonic ($C_{20:4}$) acids. It was the first protein to be reported to bind and transfer PA species derived from phosphatidylcholine (PC) hydrolysis by phospholipase D (PLD) which are rich in palmitic ($C_{16:0}$), palmitoleic ($C_{16:1}$) and oleic ($C_{18:1}$) acids. RdgBβ binds either PI or PA in similar proportions although with higher affinity for PA [40]. However, the normal levels of cellular PA are very low (<1% of all lipids), due to its rapid conversion into other metabolites [101]. This specific interaction could potentially be the clue to the functional role of RdgBβ. For instance, the transfer activity of RdgBβ could facilitate the reciprocal transfer of PI and PA between the ER and the plasma membrane and therefore maintain the $PI(4,5)P_2$ recycling pathway (Figure 1.3). Very recently, RdgBβ was found to bind the phosphoinositide PI4P in order to recruit the RAB1B to the Golgi in order to promote secretion of malignant pro-metastatic factors in human cells[45]
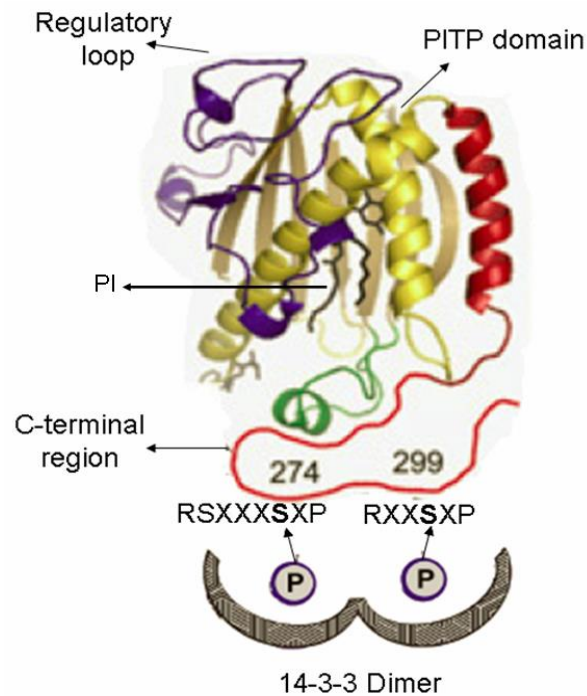
Figure 1.9. Predicted structure of RdgBβ.

Modelled structure of RdgBβ bound to 14-3-3. In the cytosol, RdgBβ directly binds with 14-3-3 dimer proteins at the phosphorylated sites indicated in the 80 amino acid C-terminal region (red). RSXXXSXP and RXXSXP are the phosphorylated motif sequences where 'X' is any amino acid and 'p→S' represents the phosphorylated serine residue. The PITP domain (yellow) of RdgBβ binds and transfers PI and PA and also interacts with ATRAP possibly at the regulatory loop (blue). Figure taken from Cockcroft and Garner, 2012[22].

1.3: Cardiac function, growth and development in health and disease

The mammalian heart is a complex organ whose function is to pump blood through the circulatory system to carry essential molecules across the body. This is achieved by a highly coordinated series of events within cardiomyocytes. For instance, the excitation-contraction coupling of cardiomyocytes is regulated by intracellular calcium ions (Ca^{2+}) levels. The prompt release of Ca^{2+} is facilitated by the close physical proximity between mitochondria, endoplasmic (sarcoplasmic) reticulum (ER; SR), and plasma membrane (sarcolemma). All of these cellular compartments play a role in calcium homeostasis.[114]

Following cell growth and terminal differentiation, mature cardiomyocytes can undergo an adaptive hypertrophic response as a result of pressure or volume overload, damage, or genetic factors. Cellular hypertrophy is accompanied by expression of several foetal genes, abnormal Ca^{2+} homeostasis, oxidative stress, increased protein synthesis, and mitochondrial DNA damage. Physiological heart enlargement is beneficial in order to increase cardiac output to compensate for the demands of normal development and growth but also transient stress. However, in the case of hypertension, valvular insufficiency, ischemia, infections, or genetic mutations, when the stress to the heart persists, pathological cardiac hypertrophy occurs. Pathological hypertrophy is characterised by reduced contractile function and plays a significant role in the development of heart failure. Cardiac hypertrophy is caused by a complex interaction of signal transduction pathways. The insulin-like growth factor (IGF-I) signalling (IGF-I–PI3K–AKT/PKB–mTOR) regulates physiological cardiac hypertrophy, whereas G-protein coupled signalling is a necessary event in the induction of pathological cardiac hypertrophy.[94]

1.3.1 Cardiac mitochondria

Mitochondria comprise approximately 30% of cardiac mass, where they are essential for providing the ATP that is required to meet the high energy demand for cardiac function [60,95]. The highly dense mitochondria in cardiomyocytes are arranged in a regular pattern around the nucleus, between the myofibrils and beneath the sarcolemma and occupy nearly a third of a volume of a cardiomyocyte.[54] In the adult cardiomyocyte, there are three distinct populations of mitochondria with unique spatial organisation: peri-nuclear mitochondria which are arranged in an area adjacent to the nucleus; interfibrillar mitochondria which are arranged along the myofibrils alongside the sarcomere; and subsarcolemmal mitochondria which are present in an area located just beneath the subsarcolemma as seen in Figure 1.10.
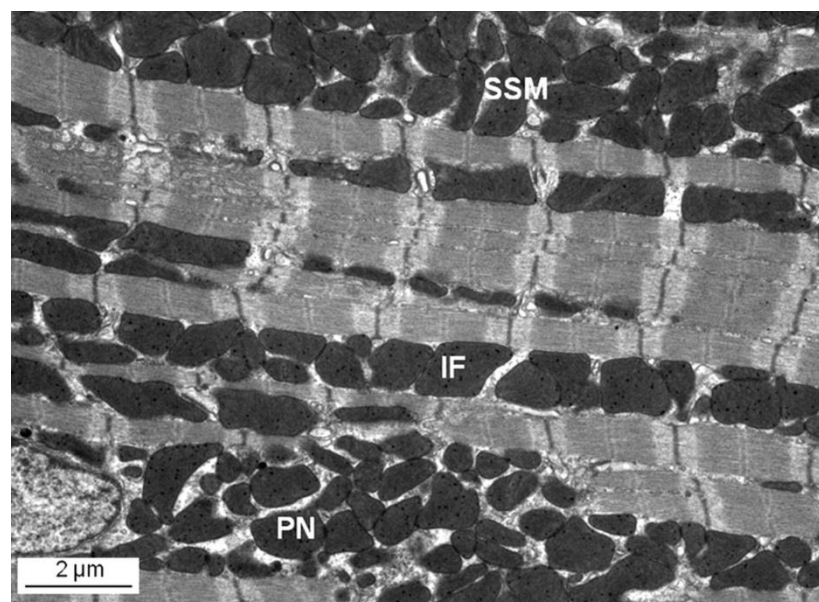
Figure 1.10: Distribution of mitochondria in the adult heart. Electron micrograph of adult murine heart indicating the subpopulations of cardiac mitochondria: perinuclear (PN), interfibrillar (IF) and subsarcolemmal mitochondria (SSM). Image taken from Ong and Hausenloy (2010)[85]

Cellular growth and development is associated with an increase in protein, lipid and mitochondrial biosynthesis. For instance the peroxisome proliferator-activated receptor _ coactivator-1 (PGC-1) family of proteins play a critical role in cardiac mitochondrial biogenesis[69,114] and PGC-1β transcript and protein were increased as a result of differentiation of H9c2 myoblasts[11]. In the adult heart, PGC-1 maintains high-level, coordinated expression of nuclear and mitochondrial genes encoding mitochondrial machinery. Mitochondrial function and energy production is compromised in the failing heart alongside decreased estrogen-related receptor (ERR)/PPAR/PGC-1 signalling[114]. Limited myocardial mitochondrial biogenesis occurs early in response to pathological stimuli and dilated cardiomyopathy but ultimately proliferation of mitochondria contributes to the eventual heart failure[1] The dynamic changes in cardiac mitochondrial number, structure, and function during developmental stages and in the failing heart are depicted in Figure 1.11.
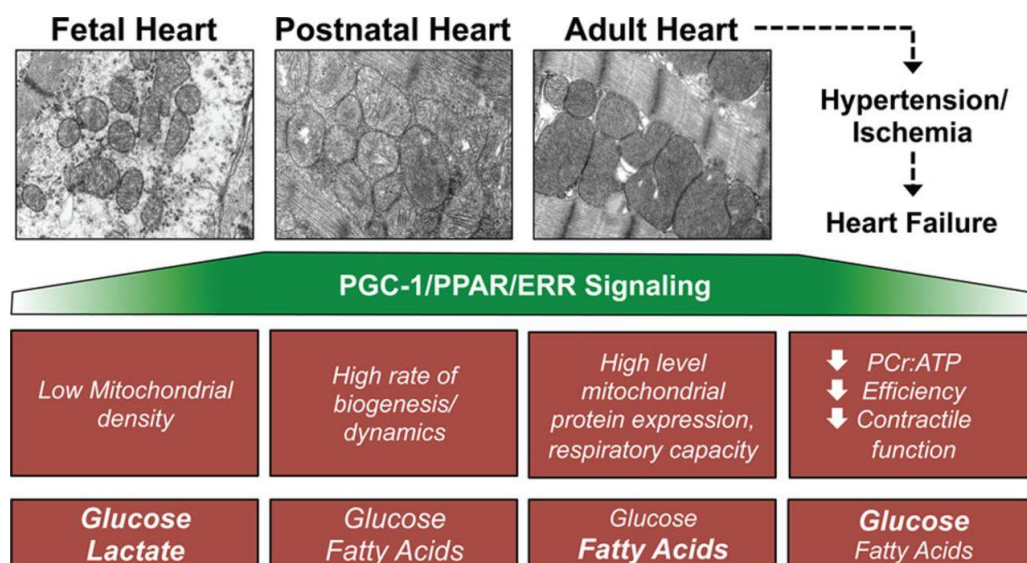
Figure 1.11: Cellular dynamics of cardiac hypertrophy. These electron micrographs of cardiac myocytes show the increase in mitochondrial number and organisation during the transition from the foetal period to the adult. In addition the cellular changes observed during the development of cardiac hypertrophy as a result of PGC-1/PPPAR/ERR signalling are paired with the corresponding mitochondrial alterations. Image taken from the review of Vega, Horton and Kelly (2015)[114]

1.3.2: Phospholipid metabolism in cardiac physiology and pathology.

In addition to their role in sarcolemma formation and structure, phospholipids are involved in the modulation of membrane bound enzymes and are functional components of cardiomyocyte membranes. The enzymology of the biosynthesis and the characteristics of the phospholipids related to this thesis (PA and CL) were described in section 1.1. This section will highlight some of the evidence of phospholipid metabolism associated with cardiac health and disease.

a. Phospholipid biosynthesis - CDP-DAG synthase (Cds)

Cds are key enzymes involved in the production of PI and CL from PA through CDP-DAG (Section 1.1.3). Loss of Cds function in *Drosophila* caused significant accumulation of neutral lipids in many tissues along with reduced cellular size. In addition there were reduced PI levels which generated low PIP_3, a regulator of the insulin pathway[72]. Mammalian Cds1 has been shown to be highly expressed in the heart [51] and in spontaneously hypertensive rats (SHHF), an increase in Cds1 mRNA was observed with increasing age whilst Cds2 mRNA decreased during heart failure development.[93]. Interestingly, Cds1 mRNA transcription was found to be directly regulated by the PGC-1 in adult mice however no other enzymes in the CL biosynthesis pathway were regulated by PGC-1. Gene expression profiling of PGC-1α^-/β^- hearts revealed a mitochondrial phenotype similar to the one found in Barth syndrome associated with reduced levels of CL, PC, and PE[68].

b. Phospholipid remodelling – Phospholipases

Pressure overload during early heart development influences postnatal growth and other physiological characteristics including the remodelling of membrane phospholipids. Neonatal rats subjected to abdominal aorta constriction showed changes in ventricular mass concomitant to a reduction in the concentrations of PC, PE, CL and PI.[84]

The fatty acid distribution of membrane phospholipids in the heart is continually in flux producing continuous degradation and remodelling through the action of phospholipases. For instance, there are several forms of phospholipase A2 identified in the mammalian heart playing critical roles in the maintenance of membrane structure and function. PLAs differ in primary structure, subcellular localisation, and requirement for Ca^{+2} for activity[16]. Calcium independent PLA2 modulates PLD activity in the heart under physiological and pathological conditions via hormonal stimulation of the plasma membrane.[70] Phospholipase A2b (iPLA2b) is the primary mediator of arachidonic acid release from cellular phospholipids during ischaemia.[59] In addition to PLA, both *in vivo* and *in vitro* studies have demonstrated that prolonged stimulation of PLC and PLD by agonists such as Ang II can induce cardiac pathologies including hypertrophy[78,131].

c. Phosphatidylinositol (PI)

Phosphatidylinositol constitutes 4-6 % of total myocardial phospholipids and during rat heart development, maximum PI concentration was found early in

neonatal stages.[84] Although a minor component, PI plays important roles as a glycolipid (glycoPI) anchoring proteins to membrane but especially as the precursor of phosphoinositides. The metabolism of phosphatidylinositol-4,5-bisphosphate (PIP_2), which is hydrolysed by PLC to the second messengers IP_3 and DAG following G-protein-coupled receptor stimulation (Figure 1.6) has been studied extensively in many types of tissues including the heart. For example, PIP_2 homeostasis may regulate arrhythmias caused by electrophysiological imbalance[123]. In isolated myocytes from stroke-prone spontaneously hypertensive rats (SHRSP), the Ca2+ influx as result of increased IP3 and DAG levels was higher than in normotensive WKY rats which correlated to increased protein synthesis suggesting a contribution to the development of pressure-overloaded cardiac hypertrophy[89]. In addition, cardiac ischaemia has been reported to cause a reduction of inositol phosphates, including IP_3 in both intact heart and cardiomyocyte models due to degradation. Nevertheless activation of the PI cycle can also aggravate myocardial damage upon re-oxygenation following an ischemic period after agonist stimulation.[123]

d. Phosphatidic acid (PA)

PA is a versatile phospholipid which is a key intermediate of phospholipid biosynthesis and signalling (Sections 1.1.2 and Section 1.1.4). As a result, the levels of cellular PA are very low and represent a challenge for experimentation design. In addition, the literature directly linking PA levels and heart physiology or pathology is scarce and there are no studies published in the past 20 years (personal observation). The associations of PA with cardiac metabolism are described and discussed throughout this thesis.

e. Cardiolipin (CL).

CL is highly enriched in cardiac tissues making up 15–20% of the total phospholipid phosphorus mass of the heart. The concentration of CL increases markedly with cardiomyocyte development suggesting that mitochondrial membranes are predominant structures accounting for the growth of total phospholipids concentration during the first five weeks of rat postnatal life. In fact, the rate of CL biosynthesis is higher in mitochondria isolated from neonatal rat hearts than in those from adults. CL is known to be associated with several inner mitochondrial membrane proteins, the most characterised being cytochrome *c* oxidase activity in adult rat myocardium[79,84,100]

Detrimental metabolism or function of mitochondrial cardiolipin leads to several cardiomyopathies and it has been subject of various reviews. Barth syndrome is an X-linked genetic disorder of CL remodelling caused by tafazzin mutations (160 found to date). As a result of the mutation, the levels of CL decrease to about 80% in platelets and skeletal muscle and 20% in cardiac tissue. In addition to reduced CL levels, the fatty acyl composition is altered. Tetralinoleoyl-CL, the most abundant species in the heart and most tissues are absent. The clinical manifestations include cardiomyopathy, skeletal myopathy, neutropenia, and growth retardation. Diabetic cardiomyopathy is characterised by altered lipid composition and mitochondrial dysfunction in the diabetic myocardium. In the early stages of pathological development in the type II diabetic mouse model, a sharp decrease in total cardiac CL and a shift to longer and polyunsaturated fatty acid species is observed. During the development of myocardial ischemia, there is an increase in reactive oxygen species (ROS) and after ischemia-reperfusion, ROS is thought to trigger lipid peroxidation as well as damage to cellular macromolecules and the

electron transport chain which, together, lead to apoptosis, necrosis, and tissue damage. Unsaturated CL acyl species in the mitochondrial inner membrane are vulnerable to ROS oxidative damage. Study of ischemia-reperfusion in rat and rabbit hearts reported a significant decrease in CL in the subsarcolemmal mitochondria, whereas CL in the interfibrillar mitochondria was unchanged as well as the levels of all other phospholipids. Exogenously added cardiolipin and no other phospholipids rescued the phenotype to mitochondria from reperfused hearts[79,100,127].

f. Phospholipid associated proteins - RdgBβ

RdgBβ, a protein with the capability of interact with PA, PI[40] and PI4P[45], is expressed with particularly strong expression in the heart[39,41,104] RdgBβ also interacts with membrane associated proteins such as the GTPase RAB1B[45] which promotes cell growth of primary cultures of neonatal cardiomyocytes *in vitro* and induces cardiac hypertrophy in mouse hearts[35] and the angiotensin receptor associated protein ATRAP[41] which may facilitate cardiovascular pathologies including hypertrophy and hypertension[86,107] The functional significance of RdgBβ in the heart has not been elucidated but it is possible that RdgBβ functions thorugh its ability to link phospholipids and proteins.

1.3.3: Biological systems to study cardiac physiology

In order to study the heart, the models used include cultured neonatal/adult cardiomyocytes, mouse atrial HL-1 cells and rat ventricular H9c2 cells (myoblasts). Neonatal rat cardiomyocytes (NRC) can be considered as a very useful model for cardiac ventricular cells, in particular to study various adaptive mechanisms. This model represents a homogeneous population of cardiac cells offering numerous experiments to simulate cardiac pathologies. However, their use involves a high number of animals and their isolation, culture and maintenance are expensive and their usage time is limited.[89] H9c2 and HL-1 cell lines are immortalised cells with a cardiac origin and both are widely used for the analysis of cardiac hypertrophy, injury and ischemic preconditioning [67]. Currently, the experimental outcomes of studies using these cell lines and their interpretations suggest significant differences between them. H9c2 myoblasts demonstrate high ATP levels, mitochondrial mass and respiratory activity, as well as a higher vulnerability to hypoxia and oxidative stress than HL-1 cells.[67,89] Kuznetsov and colleagues[67] show that H9c2 cells are more similar to primary cardiomyocytes than HL-1 cells with regard to energy metabolism patterns, such as cellular ATP levels, bioenergetics, metabolism, function and morphology of mitochondria. In contrast to HL-1, H9c2 cells were significantly more sensitive to hypoxia-reoxygenation injury in terms of loss of cell viability and mitochondrial respiration, whereas HL-1 cells were more resistant to hypoxia as evidenced by their relative stability. H9c2 cells exhibit a higher phosphorylation of AMP-activated protein kinase, but lower PGC1 alpha levels, suggesting that each cell type is characterized by distinct regulation of mitochondrial biogenesis[67].

a. H9c2 cells

The H9c2 myoblast cell line, isolated from the ventricular part of a BDIX rat heart, is currently used for skeletal and cardiac muscle studies due its biochemical, morphological and electrical/hormonal signalling properties[25,53,80]. In the myoblast stage, cells are still not fully differentiated into adult cardiomyocytes. However they are programed to develop the appearance of several cardiomyocyte-specific markers from mono-nucleated myoblasts to myotubes. Differentiation is achieved after the cells are cultured in a low serum concentration media,[80] which produces mostly cells with a skeletal muscle phenotype.[53] Furthermore, providing constant addition of all-trans retinoic acid (RA) to a 1% serum media induces a predominant presence of cells presenting an adult cardiac muscle phenotype. Cardiomyocyte-like structural features are normally evident in the presence of retinoic acid only and require 7-14 days[25]. Although, H9c2 differentiated cells do not present contractile activity, they are characterised by the increased expression of cardiac markers and the alpha-1 subunit of L-type calcium channels[80].

Retinoic acid treatment of H9C2 cells leads to an increase in mitochondrial biogenesis; both increases in mitochondrial mass and in changes in mitochondrial morphology are observed[11,25]. Indeed the levels of the transcriptional coactivator PGC-1α levels also increase upon retinoic acid treatment.[25]. H9C2 cells can be stimulated with vasopressin to induce hypertrophy. Stimulation of AVP1 receptors at pM–nM concentrations of AVP promotes the accumulation of IP_3, mobilization of SR calcium stores, elevation of calcium, and activations of phospholipases, PKC and ERK2. AVP stimulation was found to protect H9c2 cells against hypoxia/re-oxygenation–induced cell death via a GRK2/b2 arrestin1/ERK1/2–dependent

mechanism that leads to decreased caspase 3/7 activity and enhanced survival under conditions of ischemic stress[132]. Translational up-regulation and protein accumulation in response to vasopressin was preserved after retinoic acid treatment to maintain the cardiac phenotype.[14,118] These observations were also demonstrated in transgenic mice with inducible cardiac-restricted overexpression of V1AR which led to the development of left ventricular hypertrophy, dilatation, diminished contractile performance, and reprogramming of the HF gene profile in a G couple receptor–dependent manner[132] Therefore H9c2 cells are an excellent model system in which to directly test the effects of V1AR signalling during *in vitro* stress. However H9c2 myocytes do not appear suitable for studying various other forms of cardiomyocyte hypertrophy induced by angiotensin II, phenylephrine, and endothelin-1.[14]

Some of the modifications reported for H9c2 cells differentiation are summarised in Table 1.1.[11,12,25,80,88] [13,43,65] H9c2 cells and isolated neonatal cardiomyocytes respond similarly to several stimuli, this includes the developing of hypertrophic responses[118]. Recently, a comprehensive characterisation of transcriptome alterations during H9c2 differentiation towards a cardiac-like phenotype was reported [11]. H9c2 cells appear to be a useful model to study cardiac phospholipid metabolism and physiology.

Table 1.1: Modifications upon H9c2 cells differentiation

Feature	Proliferating	Differentiated	Reference
Cell morphology	Isolated myoblasts	Fused myotubes	Menard et al 1999
Cell Proliferation	Increase	Decrease	Comelli et al 2011 Branco et al 2012 Branco et al 2015
Cell growth rate	Decrease	Increase	Comelli et al 2011 Branco et al 2012 Branco et al 2015
Mitochondrial size and normal function	Decrease	Increase	Comelli et al 2011 Branco et al 2015
Stress response **β adrenegic mediated**	Protected	Increased	Branco et al 2013
G subunit, **Endothelin A receptor**	n/a	Increase	Giusti et al 2004
Pro-survival proteins	Increase	Decrease	Branco et al 2015
Cardiotoxicity and Apoptosis	High Decrease	High Increase	Konorev et al 2008 Branco et al 2012 Branco et al 2012
Metabolism	Glycolysis	Oxidative respiration	Pereira et al 2011 Branco et al 2015

1.4: Hypothesis

The research hypothesis is that the physiological function of RdgBβ in cardiac tissue is to facilitate phospholipid signalling and metabolism during cell development due to its association with phosphatidic acid. The null hypothesis is that RdgBβ does not play any role in the metabolism of cardiomyocytes.

1.4.1: Aims of the Thesis

To test the hypothesis this study was designed with three strategies as follows:

Phosphatidic acid is involved in the synthesis of phospholipids and in cell signalling in different cellular organelles. Recently the Class II PITPs were found to bind and transfer PA *in vitro*[40,125]. The first aim of this study was to examine whether residues that are essential for PI transfer affected the PA transfer activity of RdgB proteins. In addition, I examined potential residues that were responsible for PA transfer. For this analysis, mutational analysis was carried using the PITP domain of *Drosophila* RdgBα. This work was part of a collaboration with Dr Raghu's Laboratory who analysed these mutants in *Drosophila* phototransduction[125].

RdgBβ is capable of binding and transferring PA,[40] but our understanding of its physiologic functions remain to be fully elucidated. RdgBβ transcripts are highly expressed in the heart[39,104] and RdgBβ protein has been identified exclusively in the heart.[41] The second aim of this thesis was to characterise the protein and mRNA

expression of RdgBβ using Immunoblotting and qRT-PCR respectively in the H9c2 cell line and primary neonatal rat cardiomyocytes in order to examine its biological function.

Finally, H9c2 cells have been used extensively as a cardiac model and their ability to differentiate into a cardiomyocyte-like cell line has also been studied (Table 1.1). The third aim of this thesis was to examine whether retinoic acid treatment of H9c2 cells leads to increased levels of the enzyme Cds1 due to its upregulation with cardiac mitochondrial biogenesis and its involvement in phospholipid metabolism.

CHAPTER 2: Materials and Methods

2.1:   Bioinformatics

Multiple sequence alignments of proteins and nucleic acids were carried out using the Clustal Omega online tool (http://www.ebi.ac.uk/Tools/msa/clustalo/) which generated alignments between **three or more** sequences. In addition, the EMBOSS Needle online tool (http://www.ebi.ac.uk/Tools/psa/) created alignment of two sequences. For primer design and sequence analysis, the Basic Local Alignment Search Tool (BLAST; http://www.ebi.ac.uk/Tools/sss/) was used for comparing primary biological sequence information with a database of sequences and identify library sequences that resemble the query sequence above a certain threshold. The ExPasy Translate tool (http://web.expasy.org/translate/) allowed the translation of a nucleotide (DNA/RNA) sequence to a protein sequence. Reverse complement of nucleotide sequences was obtained using the Translate tool. To obtain the reverse complement of sequences the tool at http://reverse-complement.com/ was used.

2.2:   Molecular biology

2.2.1: Plasmids

The plasmids used for expression of the recombinant PITP proteins in *E. coli* (Table 2.1.), and transfection of RdgBβ-sp1 and Cds proteins in mammalian cells have been previously described (Table 2.2)[40,41,62,98]. The human Cds1 and Cds2 plasmids were a gift from Dr. Tamas Balla (NICHD Bethesda, MD, USA)[62]. These plasmids were sent on filter paper and reconstituted by immersing them in Tris-EDTA Buffer.

Table 2.1: Plasmids for expression of the recombinant PITP proteins used in this study.

PITP Protein	Organism	Accession number	Expression Plasmid-Tag	Plasmid Ab resistance	Ref.
PITPα	*Homo sapiens*	P48739	pRSETC-His	Ampicillin	[40]
PITPβ	*Homo sapiens*	Q00169	pRSETC-His	Ampicillin	[98]
Hu-RdgBα (a.a. 1-277)	*Homo sapiens*	O00562	pET14b-His	Ampicillin	[40]
Hu-RdgBβ	*Homo sapiens*	Q9UKF7	pRSETC-His	Ampicillin	[40]
Dm-RdgBα (a.a. 1-281)	*Drosophila melanogaster*	NP_511149	pRSETC-His	Ampicillin	[40]

Table 2.2: Plasmids used in this study for mammalian expression of RdgBβ, Cds1 and Cds2.

Protein	Organism	Accession number	Expression Plasmid (Tag)	Plasmid Ab resistance	Ref.
RdgBβ-sp1	*Homo sapiens*	Q9UKF7	pcDNA3.1(FLAG)	Ampicillin	[41]
RdgBβ-sp1	*Homo sapiens*	Q9UKF7	pIRES2-EGFP	Kanamycin	[41]
Cds1	*Homo sapiens*	BC074881	pEGFP-N1 (GFP)	Kanamycin	[62]
Cds2	*Homo sapiens*	BC025751	pEGFP-N1 (GFP)	Kanamycin	[62]
Cds1	*Homo sapiens*	BC074881	pcDNA3.1 (Myc)	Ampicillin	[62]
Cds2	*Homo sapiens*	BC025751	pcDNA3.1 (Myc)	Ampicillin	[62]

2.2.2: Transformation and growth of bacterial cultures.

XL1-blue super-competent *E. coli* cells were transformed to obtain plasmid stocks for mammalian cell expression, whereas the bacteria BL21 (DE3) pLysS competent strain (Stratagene) was transformed for recombinant protein expression in *E. coli* with the appropriate plasmid. The BL21 strain carries a chloramphenicol resistance gene, allowing for their selection in culture. The process of transformation was the same for either type of bacterial cells. For each transformation, 10µL of reconstituted or 2µL of stored plasmid was placed into an Eppendorf tube containing 100µL of bacteria. The tubes were flicked briefly, to ensure the contents were properly mixed and incubated on ice for 30 minutes. The mixtures were then placed into a water bath at 42°C for 45 seconds to allow the plasmids to enter the bacterial walls ('heat shock'). The tubes were immediately returned to ice for 2 minutes after which 800µL of autoclaved Miller's Luria broth (LB) was added to each tube. To ensure adequate mixing, the tubes were inverted several times and then placed at 37°C for 1 hour in an incubator. The LB (25g/L) was prepared with sterile water in Duran bottles, autoclaved and stored at 4°C.

To prepare agar for bacterial inoculation on 10 cm-diameter Petri dishes, Luria agar (25g/L) was prepared with sterile water in Duran bottles, autoclaved and stored at room temperature. Antibiotics were added to melted Luria agar depending on the plasmid according to Tables 2.1 and Table 2.2. Final concentration of either Ampicillin or Kanamycyn in Luria agar was 100µg/mL. Approximately 10 mL of warm mixture of agar supplemented with antibiotic was poured into each dish and left to set at RT.

Under aseptic conditions (with a Bunsen flame close by), 200µL of transformed cells were transferred onto the agar plates (two per transformation) and spread using a sterilised glass cell spreader. Plates were left to dry for a few minutes then left overnight upside down in the incubator at 37°C. Next day, using a sterile tip, one bacterial colony was picked and dropped into a falcon tube containing 5mL of LB plus antibiotic (100µg/mL ampicillin for XL1-blues) and, in the case of BL21 colonies, four falcon tubes were set up for culture in LB plus antibiotics (100µg/mL ampicillin plus 40µg/ml chloramphenicol for BL21s). These starter cultures were used as described in the following sections.

2.2.3: Maxi/Miniprep and DNA sequencing

The PureLink HiPure Plasmid DNA Maxiprep or Miniprep Kits (Invitrogen) allowed the purification of plasmid DNA from the culture of transformed XL1-blue cells described above. The choice of kit (Mini or Maxiprep) was made depending on the amount of plasmid required. Under aseptic conditions, the falcon tubes containing the 5mL starter cultures described in Section 2.2.2 were grown for ~16 hours in an incubator shaker at 37°C for Mini preps. Alternatively the starter cultures were incubated for ~8 hours; and then transferred into 250mL of Luria Broth plus ampicillin (100 µg/mL) overnight in an incubator shaker at 37°C for Maxipreps. The cells were harvested by centrifuging the overnight LB cultures at 4000g for 10 minutes. The LB media was discarded and the kit's buffers were added following the manufacturer's instructions. The final elution was carried out in 50 µL molecular grade water. The DNA concentration and quality of the obtained DNA was measured using the Nanodrop spectrophotometer. 1.5 µg of each plasmid preparation at a concentration of100 ng/µL was sent to Eurofins MG Operon for sequencing when plasmids were obtained as gifts to verify their sequence; finally the plasmids were stored at -20°C.

2.2.4: Production of PITP Recombinant Proteins

Recombinant PITP proteins were produced by transforming BL21(DE3)pLysS competent cells with plasmids (pET14b or prSETC), all encoding His6-tagged PITP proteins (Table 2.1). Transformation and bacterial growth procedures are detailed on Section 2.2.2.

The starter cultures (Four Falcon tubes containing the transformed bacteria described in Section 2.2.2) were placed at 37°C in an incubator shaker at 200rpm for ~8 hours. One starter culture was then transferred into each of four 1L glass flasks containing 200mL LB including ampicillin (100 μg/mL) and chloramphenicol (40 μg/mL). The cultures were placed back into the incubator shaker overnight at 37°C. Next day, the 200mL cultures were transferred to each of four flasks containing 900 mL LB with 100 μg/mL ampicillin and 40 μg/mL chloramphenicol. These large flasks were then placed into the incubator shaker at 37°C for 2 hours. Bacterial synthesis of the recombinant protein was induced by the addition of 0.5mM IPTG (Isopropyl β-D-1-Thiogalactopyranoside) to each large culture flask. The flasks were returned to the incubator shaker at the lower temperature of 28°C for 6 hours.

Bacteria were harvested by centrifugation at 6000rpm for 10 minutes, in a Sorvall RC 5B Plus centrifuge using a GS-3 rotor. The supernatants were discarded, and the cell pellets were re-suspended in 20 mL Sonication buffer (50mM phosphate buffer pH 8.0 [11.65 mL 1M Na_2HPO_4, 0.85 mL 1M NaH_2PO_4], 300mM NaCl and 1%Triton X-100). When preparing recombinant RdgBβ, Triton-X was excluded from the buffer. Bacterial suspensions were then transferred into a single

labelled 50 mL falcon tube with 20µL DNase (Sigma-Aldrich). The tube was placed at -20°C overnight.

2.2.5: Purification of recombinant protein

The bacterial pellet frozen overnight was thawed at room temperature, divided into two equal parts in 20 mL ultracentrifuge tubes, and centrifuged at 100,000g for 30 minutes at 4°C in a Kontron ultracentrifuge. The recombinant protein in the supernatant was captured using its His tag on an equilibrated nickel column of HIS-Select Nickel Affinity Gel (P6611, Sigma) in a PD-10 column (Disposable Chromatography Column, Bio-Rad Laboratories). The column was equilibrated with sonication buffer at room temperature, then filled with the supernatant and placed into a rotating wheel for 60 minutes at 4°C so the beads could capture the recombinant protein by their His tag.

Following capture of the protein, all the liquid was drained from the column. The resin was first washed with Low Salt buffer (50 mM phosphate buffer pH 6.0 [23.3 mL 1 M Na_2HPO_4, 1.70 mL 1M NaH_2PO_4], 300 mM NaCl and 10% glycerol), followed by 25 mL High Salt buffer (50 mM phosphate buffer pH 6.0 [23.3 mL 1M Na_2HPO_4, 1.70 mL 1M NaH_2PO_4], 525 mM NaCl and 10% glycerol). The recombinant protein was eluted from the resin by adding 3mL Imidazole (250mM) in High Salt Buffer and transferred into a desalting column (PD10) previously equilibrated with PIPES buffer pH 6.8 (20 mM PIPES, 137 mM NaCl, 2.7 mM KCl). (PIPES, 1,4-Piperazinediethanesulfonic acid, P6757, Sigma-Aldrich.). This elution

was allowed to drain from the desalting column. The purified recombinant protein was finally eluted with 4mL of PIPES buffer.

The concentration of the purified recombinant protein was assessed initially using the bicinchoninic acid (BCA) assay (Section 2.2.6.). Subsequently 1.0, 2.0 and 4.0 μg of the protein were run on a SDS-PAGE gel alongside 1.0, 2.0 and 4.0 μg BSA (Bovine Serum Albumin) and stained with Coomassie dye to visualise and evaluate protein purity (Figure 2.1). Imaging was done using a LAS-3000 system (Fuji). The protein concentration was adjusted accordingly using AIDA software by quantification of the bands relative to 1, 2 and 4μg BSA. The purity and yield of the recombinant proteins varied between plasmids and batches.

2.2.6: BCA assay for protein concentration

The Bicinchoninic Acid (BCA) kit was used to assess protein concentration. The BCA assay relies on the detection of a Cu^{2+}-protein complex which, under an alkaline environment, reduces Cu^{2+} to Cu^{1+} and turns the mixture from green/blue to purple/blue. The intensity of the colouration is proportional to the amount of protein present (BCA1, Sigma-Aldrich). As controls, BSA protein standard solutions of 0.05, 0.1, 0.2, 0.3, 0.4, 0.5, 0.6, 0.8 and 1 mg/mL were made up in distilled water and stored at -20°C. The assay was performed in a 96-well plate. 10μL of each standard was pipetted into plate wells in duplicate including a negative control. Purified recombinant protein or lysates of unknown concentration were diluted (regularly two dilutions, 1:10 and 1:20), and 10μL of the diluted sample pipetted also in duplicate into the wells alongside the standards.

A BCA/Copper (II) sulphate solution was made in a 50:1 ratio. 200µL of this mixture was pipetted into each well of the 96-well plate containing diluted sample or protein standard. The plate was then covered with cling film and placed into the incubator for 30 min at 37°Cto allow the colour to develop. The relative intensity of the coloured mixtures was read using a plate reader at λ=540nm. Only readings of the standards with regression coefficient of >0.95 were considered for calculations. The final concentration was an average of the two dilutions of the unknown samples concentration.

2.3: *In vitro* Phospholipid transfer activity assays

2.3.1: PI transfer activity.

PI transfer was assessed for all recombinant protein preparations to verify the activity status of each batch following a procedure reported previously[108]. Labelled [^{3}H]-Inositol rat liver microsomes were the donors and unlabelled liposomes made of PC and PI from egg yolk (98:2 molar ratio) were the acceptors. The buffer used for all preparations was SET buffer (0.25M sucrose, 1mM EDTA, and 10mM Tris-HCl pH 7.4). The total volume per assay was 250µL from which 100µL were the recombinant protein sample at different concentrations; 100µL of liposomes and 50µL of [^{3}H] microsomes.

The mixtures were incubated in a 25°C water-bath for 20minutes after which the reactions were quenched with 50µL ice cold STOP buffer (0.2M Sodium acetate, 0.25M Sucrose pH 5.0). Each tube was capped and vortex followed by centrifugation at 9500g for 15 minutes at 4°C to pellet the microsomes. 150µL of the supernatant were then transferred into scintillation vials for radioactivity counting in a Packard Tri-carb liquid scintillation analyser (TR2500). PI transfer was calculated by taking the amount of radioactivity measured per sample (x2), as a percentage of the total radioactivity input after subtraction of background activity. Each protein concentration was monitored in duplicate samples.

2.3.2: PA transfer assay

PA transfer activity of recombinant PITPs was assayed using an adaptation of a previously published protocol[20]. The donor compartment were liposomes made from egg PC and PA at a molar ratio of 98:2 plus radiolabelled PA (L-a-dipalmitoyl [2-palmitoyl-9, 10-$_3$H] Phosphatidic acid, Cat # 2063, ARC UK), and the acceptors were rat liver mitochondria at a concentration of 8mg/mL. SET buffer (0.25M sucrose, 1mM EDTA and 10mM Tris-HCl pH 7.4) was used for all dilutions.

Different concentrations of protein were mixed with donor and acceptor in a final volume of 200µL and then incubated at 37°C for 30 minutes. The mitochondria were pelleted by centrifugation at 9500g for 10 minutes at 4°C. The supernatant was discarded and the pellets resuspended in 500µL of SET buffer then transferred to a new tube containing 500µL of ice cold Sucrose buffer (14.33% w/v sucrose in

ddH2O) and pelleted again by centrifugation. The mitochondria were resuspended in 50µL of 10% SDS and boiled at 95°C for 5 minutes. The entire content of each tube was transferred to scintillation vials, Ultima-GOLD was added and radioactivity was counted using a liquid scintillation analyser (TR2500). Samples were analysed in duplicate. PA transfer was calculated as an average percentage of the total radioactivity input after subtraction of background activity.

2.3:   Quantification of mRNA by polymerase chain reaction (PCR)

2.3.1: RNA extraction

RNA extraction of H9c2 cell lysates and rat heart tissue was achieved using the RNA Miniprep Kit (NBS Biologicals) first by lysing and homogenising the samples in 350µL guanidine thiocyanate and 2-mercaptoethanol to release RNA and inactivate RNases. Lysates were centrifuged through the filtration column to remove cellular debris and DNA. The filtrate is then applied to a Spin Column to bind total RNA, followed by washing and elution as per manufacturer instructions. Elution volume was 30µL in RNase free water. RNA concentration and quality was measured using Nanodrop. Samples with concentrations over 100ng/μl and 260/280 and 260/230 ratios close to 2.00 were used for all experiments.

2.3.2: cDNA Synthesis

One microgram of RNA from each sample was used to produce cDNA by Reverse Transcription (RT)-PCR following the First-Strand cDNA Synthesis protocol given by the manufacturer using SuperScript III Reverse Transcriptase (Invitrogen). In every experiment a sample containing no reverse transcriptase (-RT) was

included to use as negative control. A volume of 20µL of concentrated cDNA was obtained per sample which was diluted 1:5 in molecular grade water.

2.3.3: Design and validation of primers for PCR

Specific *Rattus norvegicus* primers were designed using the website Primer 3 (http://bioinfo.ut.ee/primer3/) based on the NCBI sequence references on Table 2.3. The requirements included:

1. CG (guanine and cytosine nucleotides) content of minimum 50%, with an even distribution of all four bases along the length of the primer.
2. Maximum size of 20 base pairs.
3. Difference of annealing temperatures (Tm) between forward and reverse primers of below 1 degree Celsius.

Primers were manufactured by Sigma-Aldrich Custom Oligos service and sent in tubes to be reconstituted with TE buffer at 100µM. Once the set of primers was validated, 25µL aliquots at 10µM were made and stored at -20**°C.**

Table 2.3: Validated primers used for PCR experiments. *Housekeeping genes.

Protein NCBI Reference	Name	Forward primer	Reverse primer	Product Size (bp)
ANP **X00665.1**	Atrial natriuretic factor	ATACAGTGCGGTGT CCAACA	CGAGAGCACCTCCAT CTCTC	209
BNP **NM_031545**	Natriuretic peptide B	GGAAATGGCTCAGA GACAGC	CGATCCGGTCTATCTT CTGC	164
Cds1 **NM_031242**	CDP-diacylglycerol synthase 1	TACGACCTCCCGTG GTTTAG	CTCAGGACGAACATG CAGAA	194
Cds2 **NM_053643**	CDP-diacylglycerol synthase 2	GAGCCTTTGCGCAT TCTCAG	ACATGGGTCCAGCCA AACAT	137
CLS **NM_001014258**	Cardiolipin synthase (CLS)	CGGTGTTGGGCTAT CTGATT	CAGCAAGTGGATCAA GAGCA	153
PIS **NM_138899.2**	CDP-diacylglycerol-inositol 3-phosphatidyltransfer ase (Cdipt)	AGTGTCATCCACCT CGTCAC	AGACATGACACTGGG ACCTC	164
GAPDH * **NM_017008.4**	Glyceraldehyde-3-phosphate dehydrogenase	AGACAGCCGCATCT TCTTGT	CTTGCCGTGGGTAGA GTCAT	207
PGK1 * **NM_0532913**	Phosphoglycerate kinase 1	GAAGGGAAGGGAA AAGATGC	AAATCCACCAGCCTT CTGTG	180
RdgBβ **XM_573213**	Phosphatidylinositol transfer protein cytoplasmic 1	GAAGCGCGTGTATC TCAACA	TCGAGGTCTTTGGCT TCACT	219
RdgBα **NM_001008369**	Phosphatidylinositol transfer protein, membrane-associated 1 (Pitpnm1)	TGTTGGCAGGATGA GTGGAT	CAAAGCTGGCATCTG GTGAG	235
Tam41 **NM_001108642**	Mitochondrial translocator assembly and maintenance protein	CATGTGAAGCCCAA CGTAG	GCTGCTGTAACGTTC TAGGC	136

2.3.4: Polymerase Chain Reaction (PCR)

To validate the designed primers (Table 2.4), 5µL diluted cDNA prepared from H9c2 cells and rat heart tissue was used as a template for amplification in PCR using the enzyme Platinum Taq Polymerase (Invitrogen). The protocol given in the kit was followed with the difference that only 0.2µL of Taq was added per sample. The thermocycler program used for all primers is shown on Table 2.5.

Table 2.4: Overview of thermal cycler program for PCR.

Activity	Temperature	Time	Programme
Enzyme activation	94°	2min	
Denaturation	94°	30sec	
Annealing	60°	30sec	30 cycles
Extension	72°	1min	
Final extension	72°	5min	

2.3.5: DNA gel electrophoresis

To test the specificity of all the designed primers, their PCR products were analysed by electrophoresis in agarose NA gels in triplicate alongside a negative control (Figure 2.1.). DNA gel electrophoresis separates the PCR products based on their size and charge (the expected product sizes for each set of primers are given

in Table 2.4). A 1.6% agarose gel was prepared in a microwave by dissolving 0.65 g Agarose NA in 65mL Tris-acetate-EDTA buffer (0.8 mM Tris-HCl pH 8.0, 0.4 mM acetic acid, 0.02 mM EDTA). 5µL ethidium bromide (10 mg/mL) was added to the warm agarose solution and mixed by swirling. The mixture was then poured into a Bio-Rad gel caster tray and a comb was placed into the designated slots at one end of the gel. Setting was achieved at room temperature for ~30 minutes.

The set gel was transferred from the caster tray to the Bio-Rad Mini-Sub Cell GT Cell for submerged horizontal electrophoresis with the comb end (sample wells) placed at the black (negative electrode) end. The comb was then removed and TAE buffer was poured into the apparatus allowing buffer to fill the wells. 5 µL ethidium bromide (10 mg/mL) was pipetted directly onto the buffer at the positive electrode end of the apparatus to prevent the ethidium bromide travelling faster than the DNA sample which could have affected the visibility under UV light. Each well was loaded with a mixture of 5µL PCR product + 1µL 6X DNA loading dye (Blue #R0611, Fermentas) including a negative control (-RT), alongside 3µL Fermentas GeneRuler 1 kb DNA ladder (0.1 µg/µL, #SM0313, Fermentas). The lid was then placed onto the apparatus in the correct orientation, and electrical leads plugged into the Bio-Rad Power-Pac 3000. Agarose NA gels were run at 100 V for ~40 mins or until the dye front had travelled ⅔ along the gel.

The result was checked under UV light and imaged using a LAS-3000 system. If any set of primers produced more than one clear band; primer dimer (band of 100bp or lower) or no visible band, the primers were discarded and a new set was designed and tested.
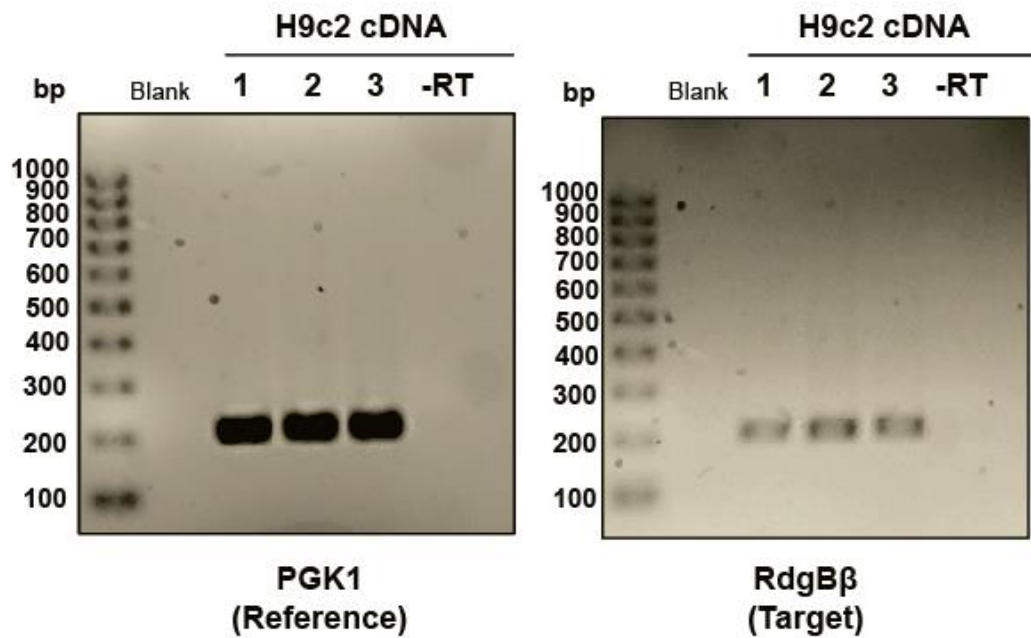
Figure 2.1: DNA gel electrophoresis testing PGK1 and RdgBβ primer specificity.

H9c2 cells were harvested in RNA lysis buffer and 1µg of extracted RNA was used to make cDNA by Reverse transcription PCR. 5µL of H9c2 cDNA was used to amplify the expression of the reference gene Phosphoglycerate kinase 1 (PGK1) and RdgBβ to test the specificity of designed primers. Three separate preparations (1, 2 and 3) of cells alongside a negative sample made without reverse transcriptase (-RT), and a DNA 1Kb ladder (bp) were separated by DNA gel electrophoresis (1.6% agarose NA gel). The images were taken on a LAS3000 imaging system. All primers were analysed in a similar manner.

2.3.6: PCR product purification and sequencing

Further primer validation for quantitative PCR included purification and sequencing of the positive PCR products. 30µL of purified DNA was obtained by using the QIAquick PCR Purification Kit (QIAGEN) and following the manufacturer instructions. The concentration of purified DNA was measured using Nanodrop.

For sequencing, the purified PCR products (~10ng) were cloned into pGEM-T easy vector (Promega) following the manufacturer protocol. Ligation mixtures were incubated overnight at 4°C. Transformation of XL1-blue cells was performed as described in Section 2.2.2. Duplicate LB plates containing 0.5mM IPTG, 80µg/mL X-Gal and 100µg/mL ampicillin were inoculated with the transformed bacteria. A positive bacterial colony (blue) was cultured in LB media overnight and the plasmid DNA was purified using the QIAprep Spin Miniprep Kit (QIAGEN). Final concentration was measured with Nanodrop and quality was evaluated by DNA gel electrophoresis in 1% Agarose NA gel. 15µL of purified DNA plasmid (100ng/µL) were then sent to Eurofins MWG Operon for sequencing. Sequences were confirmed by sequence alignment.

2.3.7: Real Time Quantitative PCR (qRT-PCR)

To quantitate mRNA from cDNA samples, qRT-PCR was performed in one step using a KAPA SYBR FAST qPCR Universal Master Mix (KAPA Biosystems) containing all components for qPCR except primers and template. Individual 15µL reactions (5µL cDNA +10µL Master mix with primers included) were set up on a 96 well plate. Housekeeping gene (PGK1) was added at a final concentration of 200nM

while all other primers were added at 300nM. In addition each set of primer included a No Template Control (NTC) and No RT Control (NRT) reactions. The NTC enabled detection of contamination in the reaction components, while the NRT enabled detection of contaminating gDNA. The plate was sealed, shaken and centrifuged briefly before it was placed in the BIORAD CFX96 machine following the protocol on Table 2.5. Reaction optimisation was achieved by testing different annealing temperatures and primer concentrations.

qPCR data obtained from the CFX96 machine was analysed in triplicate using the comparative ΔΔCT method[73] which compares the Ct value of one target against the reference target 'Housekeeping gene' (PGK1). Primers efficiency and sensitivity was analysed by producing qPCR standard curves testing H9c2 cDNA serial dilutions with 200nM PGK1 (Figure 2.2: A) and 300nM RdgBβ (2.3: B) primer sets. Optimal values obtained from the standard curves data were considered as: Efficiency (E): 90-110%; Slope: -3.6 to -3.1; and Regression (R^2) >0.98 which is an indication of reproducibility (Figure 2.2).

Table 2.5: Overview of BIORAD CFX96 program for qRT-PCR experiments.

Activity	Temperature	Time	Programme
Initial denaturation	95°	3min	
Denaturation	95°	15sec	
Annealing	60°	30sec	39 cycles
Extension	72°	30sec	
Melt curve	65°**to 95°**		

A.

PGK1
E=93.9%
R^2 = 0.99
Slope=3.1
Sensitivity: 0.06ng

B.

RdgBβ
E=106.1%
R^2 = 0.984
Slope=3.1
Sensitivity: 0.12ng
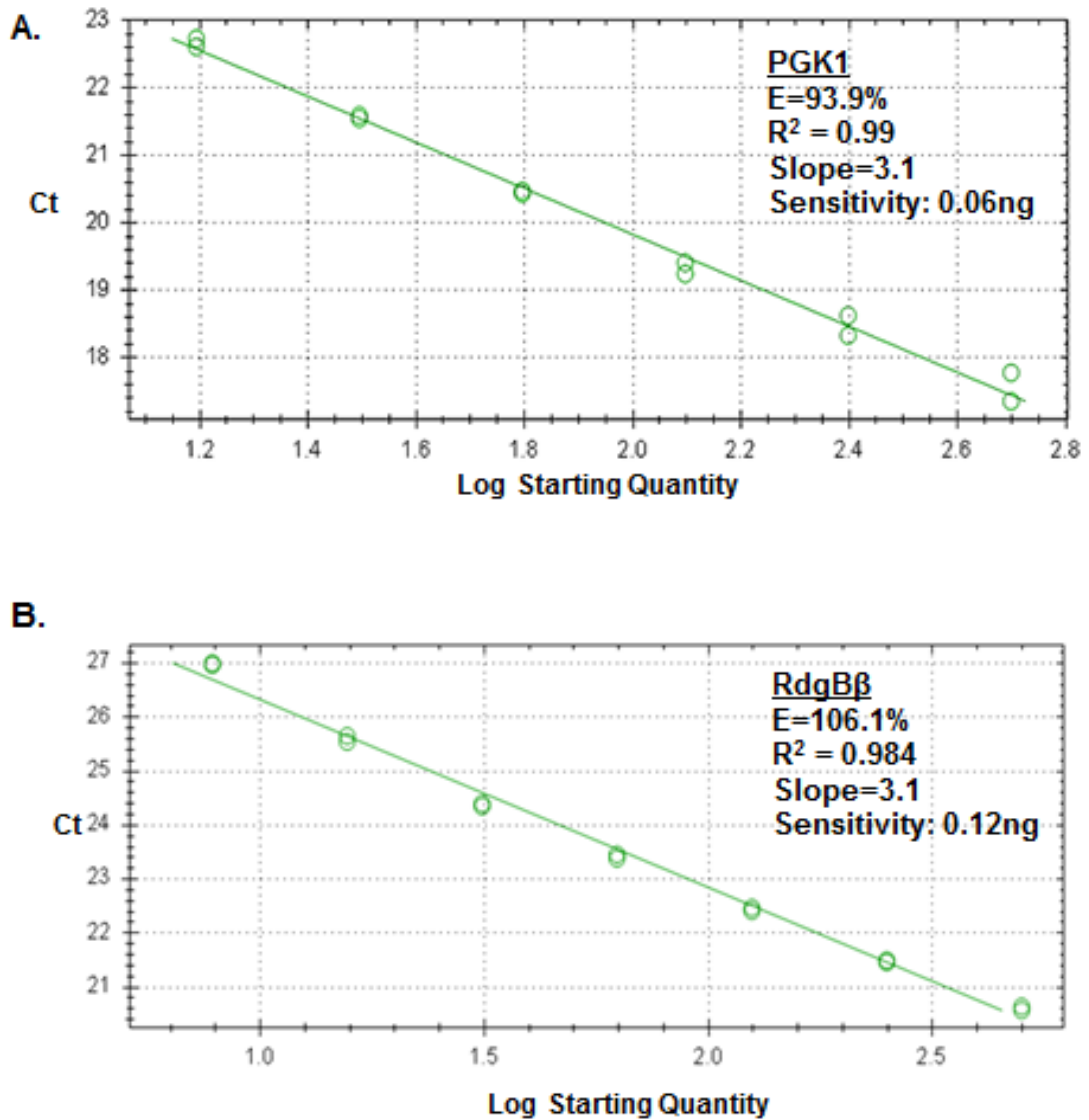
Figure 2.2: qPCR Standard Curves testing of PGK1 and RdgBβ primers efficiency and sensitivity.

Real Time Quantitative PCR (qRT-PCR) of H9c2 cDNA serial dilutions with 200nM PGK1 [A] and 300nM RdgBβ [B] designed primers using a KAPA SYBR FAST qPCR Universal Master Mix at 60°**C** annealing temperature on a BIORAD CFX machine. Sensitivity was the lowest concentration of H9c2 cDNA that produced amplification at these conditions. Print screen images from CFX96 report.

2.4: Cell-based assays

2.4.1: Cos-7 cells

Cos-7 cells (derived from African green monkey kidney cells), were used to confirm previous observations[41] and as controls for validating RdgBβ and Cds1 antibodies.

a. Cell culture

Cos-7 cells were grown in Dulbecco's Modified Eagle Medium (DMEM) cell culture medium supplemented with 10% heat-inactivated Foetal Calf Serum (FCS), 4 mM L-glutamine, 0.5 iu/mL penicillin and 50μg/mL streptomycin, in a T75 cell culture flask. Heat-inactivation of FCS was carried out by placing the unopened 500mL bottle in a water bath at 56°C for 1 hour. Cells were passaged 1:3 every 48 hours or 1:5 when left for 72 hours, in a class II laminar flow cabinet.

b. Transient transfection of DNA plasmids by electroporation

Cos-7 cells were seeded onto 10 cm cell culture plates (one per condition, 10 mL media per plate), at a concentration of 1.0-2.0 x 10^5 cells/mL, 24 hours prior to transfection to allow the cells to adhere to the plastic and reach a 70-80% confluency. On the day of the transfection, cell harvest was achieved by incubating cells for 5 min with Trypsin-EDTA Phenol red (0.25%; Gibco). The mixture was placed in a falcon tube and centrifuged at 12000 rpm for 5 minutes, then washed once in PBS.

71

Transfection was carried out by electroporation using a Bio-Rad Gene Pulser. Sterile 0.4cm electroporation cuvettes were prepared in the flow cabinet as follows: 10µg of plasmid DNA was pipetted at the bottom of the cuvette followed by 400µL of Cos-7 cells suspended in DMEM. The covered cuvettes were flicked gently to mix the contents and left at room temperature for 5 minutes. The Gene Pulser was set up at a 0.220kV Voltage; 950 µF High Capacitance and the Resistor (Pulse Controller) in the infinity position (∞). Two pulses were given to each cuvette before transferring it onto ice for 10 minutes. The cells were removed and re-suspended in fresh growth medium at room temperature. Cells were transferred to a T175 cell culture flask and grown for 24 to 48 hours depending on confluency before harvesting.

2.4.2: H9c2 cells

Vials of H9C2 cells (ATCC number CRL-1446) derived from embryonic BD1X rat ventricular tissue [63] were a gift from Dr. Stuart Nicklin from the Institute of Cardiovascular and Medical Sciences, BHF, University of Glasgow, UK. H9c2 myoblasts are able to differentiate into skeletal or cardiac muscle cells depending on the culture media.

a. Cell culture

H9c2 cells were seeded at around 2×10^5 cells/mL and cultured in Dulbecco's modified Eagle's medium (DMEM) 1X w/GlutaMAX + High Glucose +NaPyr (Cat # 31966-021) supplemented with 10% heat inactivated foetal calf serum (FCS) and

1% Penicillin/Streptomycin (Pen/Strep) under standard culture conditions (37 °C, 5% CO_2). Before 70% confluence, cells were passaged at a ratio of 1:3. H9c2 cells took a few days (about 3 to 4) after thawing before they started replicating. Cells were not passaged until they reached confluency and the media was replaced every two days. Cultured cells were not used for experiments beyond passage 30.

b. Transient transfection of DNA plasmids using Lipofectamine 2000.

Transfection of Tagged RdgBβ DNA into H9c2 cells was achieved using lipofection. Cells were seeded at $2x10^5$ cells/mL in 6 well plates containing 2mL complete media and cultured to ~80% confluency. One day prior to transfection the media was replaced by culture media without antibiotics. FLAG-tagged pcDNA and pIRES-RdgBβ plasmids (1μg/ml) were transfected using Lipofectamine 2000 (Invitrogen) following the manufacturer's protocol. Optimum conditions of transfection were obtained at a ratio of 6:2 for 24 hours after which the media was replaced for 24hours further incubation. Optimisation of Lipofectamine 2000 and DNA together with period of incubation was evaluated by SDS-PAGE (Figure 2.3).
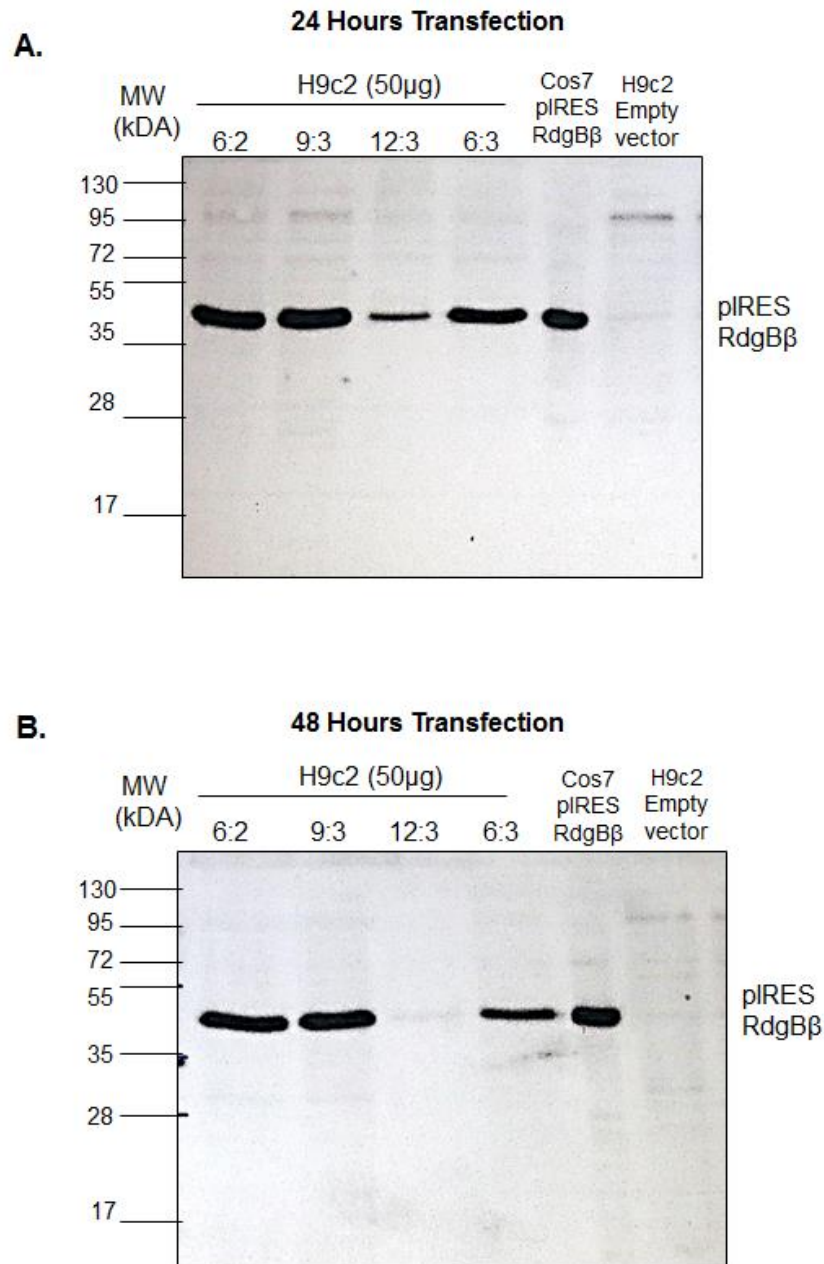
Figure 2.3: Optimisation of Lipofectamine 2000: DNA ratio.

H9c2 cells were cultured to ~80% confluency prior to transfection with Lipofectamine 2000 at different ratios (µL Lipofectamine: µg DNA) and left in culture with no antibiotics for 24 [A.] or 48 [B.] hours. 50µg of protein per sample separated by SDS-PAGE and probed with polyclonal Ab:Rb59 at a dilution of 1:200 for 2 hours in 5% milk in PBS as blocking buffer. Image obtained with LAS3000.

c. Preparation of lysates for SDS-PAGE

For SDS-PAGE analysis, the media was removed from the culture flask and cells were washed with PBS. To detach cells from the base of the culture vessel, 0.25% Trypsin-EDTA was added and left for 5 minutes at 37°C. Complete media was added to quench Trypsin action and cells were transferred to a falcon tube and centrifuged at 350g for 5 minutes at 4°C. Following a wash with PBS, H9c2 cells were pelleted and resuspended in RIPA buffer (50mM Tris-HCl pH 7.5, 150mM NaCl, 1% Triton X-100 (*v/v*), 0.5% sodium deoxycholate (*w/v*), 0.1% SDS (*w/v*), protease inhibitor cocktail) and either put on ice for 30 minutes or at -20°C for 5 minutes. The samples were sonicated and centrifuged at 12000g for 15 minutes at 4°C to pellet unbroken cells and debris. The supernatant was transferred to a fresh tube. The BCA assay was used to assess the protein concentration of the lysates. Typically, 50µg protein was mixed with enough 4X SDS-PAGE sample buffer and boiled at 95°C for 3 minutes before loading the gel wells.

d. Cell differentiation

H9c2 myoblasts cell line retain the ability to differentiate into skeletal muscle or cardiac cells depending on the culture media[80]. To differentiate cells into skeletal muscle in which myoblasts fuse to form mature multinucleated myotubes, H9c2 cells cultured in full media (10% FCS) were washed with PBS and the media was replaced for differentiation media (DMEM 1X w/GlutaMAX + NaPyr. (Cat # 31966-021) supplemented with heat inactivated 1% foetal calf serum and 1% pen/strep). Media was replaced every 48 hours and cells started to fuse after 6 days of culture.

To differentiate H9C2 myoblasts towards a cardiomyocyte-like phenotype, cells were cultured in differentiation media with the daily addition of 1µM All-trans Retinoic acid (RA; Sigma: Cat# R2625). RA was dissolved in DMSO at 1mM in 50µL aliquots at 1mM and kept at -20°C. Due to light sensitivity it was kept covered. Cardiomyocyte-like features were found after 8 days of differentiation and cells were viable up to 14 days of differentiation.

2.4.3: Neonatal rat cardiomyocytes

Primary culture of neonatal rat cardiomyocytes (NRVC) were used for comparison of the results obtained with the cell-line H9c2.

a. Isolation and culture.

The isolation of cardiomyocytes from Sprague-Dawley rat neonates (1-2 days old) was performed as described previously[76]. Heart dissection was achieved after euthanasia of the pups according to code of practice under Schedule 1 procedures approved by ASPA (Animals Scientific Procedures Act 1986) performed at the Biological Services Unit facilities. The hearts were finely minced and placed into warm (37°C) Digestion buffer (116mM NaCl, 20mM HEPES, 0.8mM Na_2HPO_4, 5.6mM glucose, 5.4mM KCl and 0.8mM $MgSO_4$, pH 7.35) containing 0.4 mg/ml collagenase type2 (Willington), 0.6 mg/ml pancreatin (Sigma), 100 units/ml penicillin and streptomycin and universal protease/phosphatase inhibitor (EZ block).

The first digestion occurred for 20 minutes at 37°C in a shaker (160 cycles/minute). The first supernatant was removed and discarded. Cell suspensions

from 7-8 subsequent digestions (15 minutes; 37°C; 136 cycles/minute) were recovered in FCS by centrifugation (5 minutes; 350g; RT). Cell viability was evaluated under the microscope with 10µl 0.5% Trypan blue after each digestion. The cell pellet was then either resuspended in RIPA or RNA lysis buffer for immediate analysis or resuspended in Plating Medium (Dulbecco's modified Eagle's medium (DMEM)/medium 199 [4:1 (v/v)], 15% (v/v) FCS, 100 units/ml penicillin and streptomycin) for culture. The cells were pre-plated on 60mm Primaria tissue culture dishes (30 minutes) to remove non-cardiomyocytes. *Non-* adherent cardiomyocytes were transferred to 60mm Primaria dishes pre-coated with sterile 1% (w/v) gelatine (Sigma-Aldrich UK) at a density of 4×10^6 cells/dish. After 24 hours, myocytes were confluent and beating spontaneously. Plating media was replaced for maintenance media (DMEM, 100 units/ml penicillin and streptomycin, 0%FCS). Viable cells were only seen for up to three days of culture.

2.4.4: Rat Heart cells treatments

a. Treatment with agonists

H9c2 cells were evaluated for G-coupled receptor stimulation using [Asn[1], Val[5]]-Angiotensin II (Sigma-Aldrich; A6402) and [Arg[8]]-Vasopressin (Sigma-Aldrich; V9879) at different concentrations. For treatment with chemical compounds, the cell culture media was aspirated and replaced with fresh media containing the compound at the appropriate time prior to cell harvest.

b. RNA interference by siRNA transfection

The down-regulation of the expression of RdgBβ and Cds1 mRNA in H9c2 differentiated cells and NRVC was achieved by siRNA transfection using 12nM siRNA oligonucleotides with HiPerFect Transfection Reagent following the manufacturer instructions. Rat specific siRNA oligos for mRNA downregulation of RdgBβ and Cds1 were purchased from QIAGEN (Table 2.6). Three siRNA Oligos were acquired for each protein and they were tested for mRNA reduction efficiency by qRT-PCR in combinations of pairs and all three together (Figure 2.4). For experiments in this study, RdgBβ mRNA was downregulated by transfection of Oligonucleotides 2+3 and Cds1 mRNA downregulation was achieved by transfection of Oligonucleotides 1+3.

The application of RNA interference (RNAi) was usually performed on the 8th day of differentiation with retinoic acid and incubated for further 72 hours. Alternatively, three rounds of siRNA transfection were performed every 72 hours for the duration of cell differentiation until day 9. Media was removed and cells were washed with PBS before detachment of the flask by Trypsin-EDTA action. After cells were pellet and washed with PBS, cell were divided into 70% for lysis in RIPA buffer for SDS-PAGE as described on Section 2.4.2.c, and 30% of the cells were harvested in RNA lysis buffer for RNA extraction as described on Section 2.3.1.

Table 2.6: siRNA Oligos purchased for RNA interference of H9c2 cells.

Name/ Gene Accession	QIAGEN Catalogue code	Sequences
Negative control	SI03650325	Sense: UUCUCCGAACGUGUCACGUdTdT Antisense: ACGUGACACGUUCGGAGAAdTdT
RdgBβ_1 **XM001081613,** **XM002724573,** **XM_573213**	SI05429753 Rn_Pitpnc1_1	Sense: 5'GACUGCAUGUGGUUAGAUATT-3' Antisense: 5' UAUCUAACCACAUGCAGUCTG-3'
RdgBβ_2 **XM001081613,** **XM002724573,** **XM_573213**	SI05429753 Rn_Pitpnc1_2	Sense: 5'GCAUGGAAUUAUUACCCAUTT-3' Antisense: 5' AUGGGUAAUAAUUCCAUGCCT-3'
RdgBβ_3 **XM001081613,** **XM002724573,** **XM_573213**	SI02937872 Rn_LOC498015_3	Sense: 5'CGAUAUCGCCUGUGACGAATT-3' Antisense: 5' UUCGUCACAGGCGAUAUCGAT-3'
Cds1_1 **NM 3142**	SI01497811 Rn_Cds1_1	Sense: 5'AGAUAUUGAUGACAGGUAUTT-3' Antisense: 5'AUACCUGUCAUCAAUAUCUGT-3'
Cds1_3 **NM 3142**	SI01497825 Rn_Cds1_3	Sense: 5'GGUUCGAUUGUCAGUAUUUTT3' Antisense: 5' AAAUACUGACAAUCGAACCTG-3'
Cds1_4 **NM 3142**	SI01497832 Rn_Cds1_4	Sense 5'CCCGUGGUUUAGAACACUATT-3' Antisense: 5'UAGUGUUCUAAACCACGGGAG3'

A.

B.
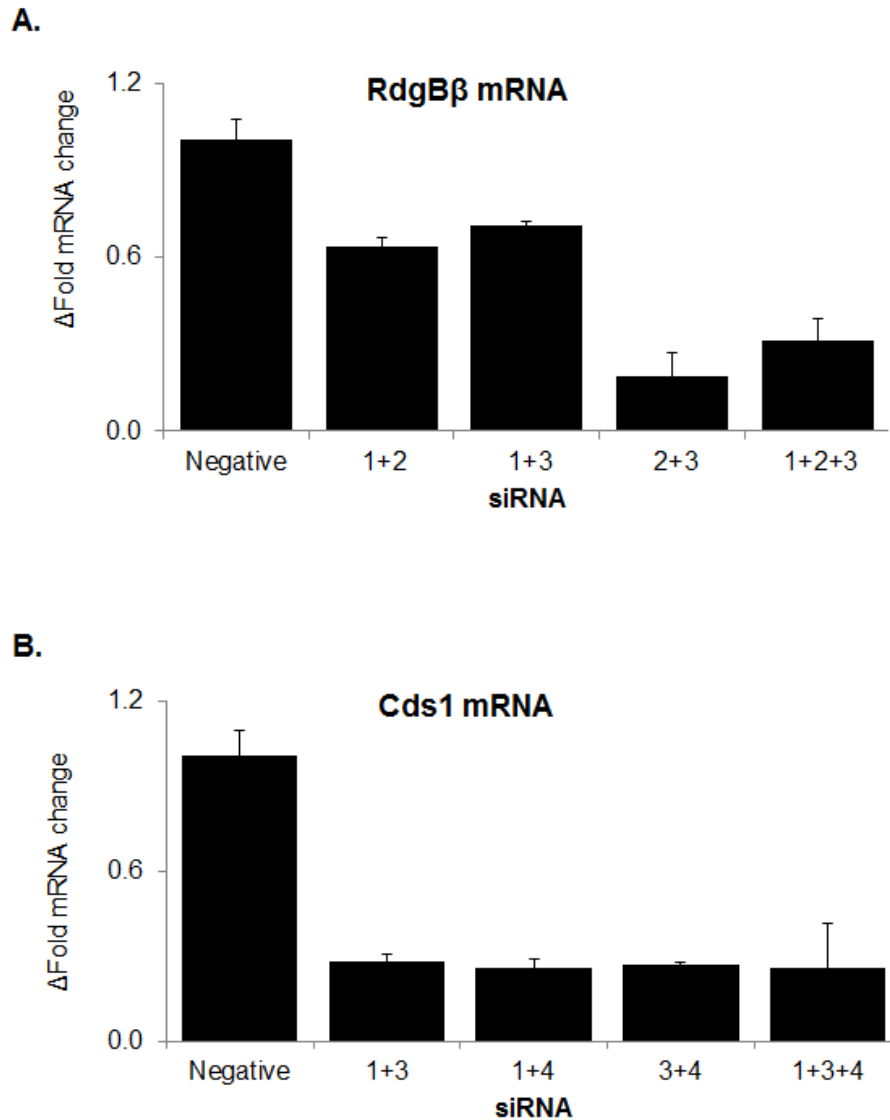
Figure 2.4: Test of efficiency of siRNA Oligonucleotides

H9c2 cells were differentiated for 8 days prior to transfection with 12nM total siRNA Negative control compared to combination of rat oligonucleotides RdgBβ (1,2,3) [A.] and siRNA oligonucleotides Cds1 (1,3,4) [B.] After 72 hours incubation, the cells were harvested in RNA lysis buffer and 1μg of extracted RNA was used to make cDNA by RT-PCR. 5μL of H9c2 cDNA was used to amplify the expression of the reference gene PGK1 and RdgBβ by qRT-PCR using SYBR I on a BioradCFX96. The graph shows the fold change of mRNA normalised to PGK1 using the Ct values from the CFX96 equipment applying the ΔΔCt formula. N=3 from one experiment.

c. Cell fractionation

To obtain the mitochondria, microsomes and cytosol from H9c2 cells, lysates in SET buffer (0.25M sucrose, 1mM EDTA, 10mM Tris-HCl pH 7.4) were sonicated on ice (50µm, 3×15 seconds) and centrifuged for 10 minutes (850g, 4°C) to pellet the nuclei and unbroken cells. Some of the homogenate was retained as whole cell extract (WCE). The homogenate was centrifuged for 15 minutes (9500rpm, 4°C) to sediment the mitochondria which were then washed with SET buffer twice. The supernatant containing the microsomes was centrifuged for 60 minutes (100,000 g, 4°C) to pellet the membranes. The membranes were resuspended in SET buffer and re-centrifuged twice. The supernatant (cytosolic fraction) was also retained.

2.5: Rat tissue isolation and differential fractionation

Animals of the species *Rattus norvegicus,* strain Sprague-Dawley were used for this study. Rats were bred and cared for at the UCL Biological Services Unit where rats were euthanised following the code of practice under Schedule 1 procedures approved by ASPA (Animals Scientific Procedures Act 1986).

2.5.1: Rat Heart

a. Neonatal rat hearts

The isolation of rat hearts was performed as follows: hearts of neonatal (1-3 days old) Sprague-Dawley rats were dissected and briefly washed in PBS. The hearts were finely minced and immediately transferred into either cold SET buffer (0.25M sucrose, 1mM EDTA, 10mM Tris-HCl pH 7.4) for differential fractionation, RIPA buffer [150mM NaCl, 1%(v/v) Triton X-100, 0.5% sodium deoxycholate,

0.1%SDS and 50mM Tris/HCl (pH 7.5)] for western blot analysis or RNA lysis buffer (NBS Biologicals) for RNA extraction.

b. Adult rat hearts

The procedure of differential fractionation of rat hearts was adapted from previous studies[77,121]. Adult rat hearts (~6 months old) were removed and placed onto a weighing boat with cold (4°C) isolation medium TSE buffer (220mM Mannitol, 70mM Sucrose, 5mM Tris-HCl pH7.4, 2mM EGTA) (+/-) subtisilin (0.4 mg/mL Sigma protease XXVII, P5380 previously referred to as nagarse) 10mL per gram of heart. Subtisilin is a protease which allows the release of the embedded mitochondria. Usually, each heart weighed about 1.25g. Using tweezers, hearts were squeezed gently to remove blood then perfused through the aorta briefly with x2 5mL of cold TSE to remove any residual blood. This was followed by perfusion with 5ml of TSE (+/-) subtilisin. Hearts were washed on weighing boats with clean TSE then dried by gentle pressing against filter paper. All non-ventricular tissue was trimmed off and clean hearts were transferred into a falcon tube filled with TSE and taken to the lab.

The ventricular pieces were homogenised thoroughly in TSE (0.4 mg/mL +/- 10mL/g subtilisin) in the motor driven pestle homogeniser. The homogenate was centrifuged at 850g for 5minutes at 4ºC. The supernatant was carefully decanted into a clean cold tube. This was the whole cell extract (WCE) (Figure 2.5.A). An aliquot (1-3 mL) of WCE was kept with the addition of protease inhibitors (1:100) at -80 ºC.The crude mitochondria were obtained by centrifugation of the WCE at 9500 g for 15 minutes at 4ºC. The supernatant (Microsomes + Cytosol) were kept aside on ice while the pellet was gently washed twice by swirling with 2 mL of TSE (+prot.

inh.) to remove a variable fluffy layer. The mitochondrial pellet was resuspended and homogenised in a glass tube diluted to 40mL of TSE and centrifuged again to obtain clean crude mitochondria (Figure 2.5.B).

The supernatant obtained after centrifugation of the WCE (Microsomes + Cytosol) was centrifuged once more on a separate tube to pellet any residual mitochondria. The supernatant was recovered and centrifuged at 100000g for 1hour at 4°C. The microsomal fraction composed mainly by endoplasmic reticulum (ER) was the pellet which was resuspended in TSE buffer while the cytosolic fraction was the supernatant (Figure 2.5.C).

To separate crude mitochondria into Pure Mitochondria and Membrane Associated Membranes (MAM), a Percol gradient was prepared following a previous study[121]. First, crude mitochondrial pellets were resuspended and homogenised in 12mL of TSE buffer. Two identical tubes were prepared with 8mL Percol buffer (11.2mL TSE and 4.8mL Percol) and slowly added 5 mL homogenised Crude Mitochondria. Tubes containing the Percol gradients were centrifuged at 95000g for 30 minutes in a swing out Kontron rotor TF41. The top fraction obtained after centrifugation corresponded to the MAM fractions which were removed first and transferred to a clean centrifugation tube followed by the bottom fraction corresponding to the pure mitochondrial fraction. Both fractions were centrifuged at 9500g for 15 minutes to pellet mitochondria. The MAM fraction was further centrifuged at 100000g for 1 hour (Figure 2.5.D). The protein content of all fractions was measured by BCA assay.
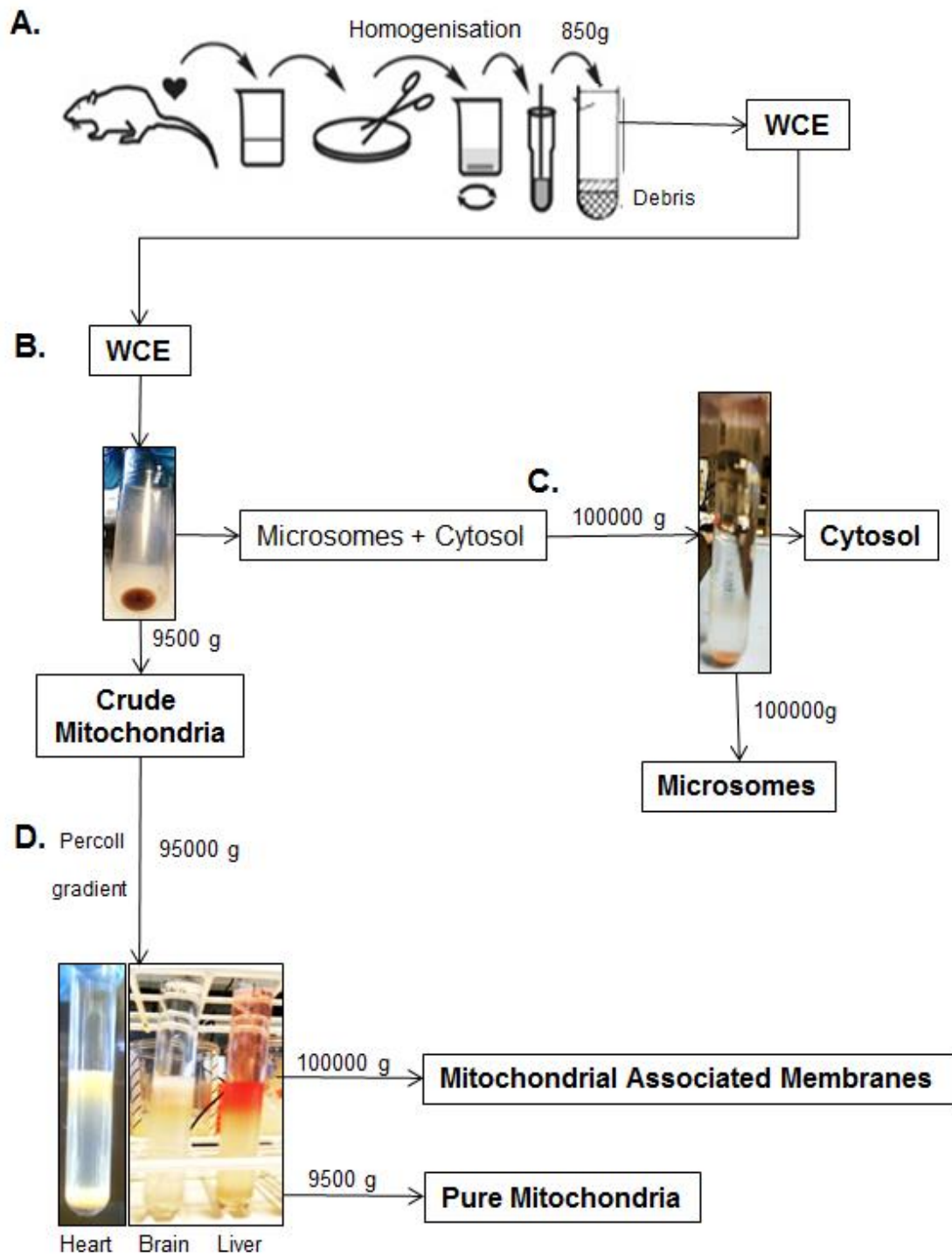
Figure 2.5: Flow chart of differential fractionation of rat tissue as described in Section 2.5.1.b.

2.5.2 Rat Brain and Liver

Rat Brain and Liver tissue was isolated alongside the heart dissection of rats and cellular fractions were obtained as exactly as described in section 2.5.1.b without any proteases in the isolation buffer (TSE).

2.6: SDS-PAGE Gel Electrophoresis and Western Blotting

2.6.1: Principle

The technique used for analysis of protein expression on the different samples was Sodium dodecyl sulphate polyacrylamide gel electrophoresis (SDS-PAGE) which separated proteins according to their molecular weight. Protein samples were boiled in SDS/PAGE sample buffer containing 10% (v/v) glycerol, 62.5 mM Tris-HCl pH 6.8, 2% SDS, 80 µg.mL-1 bromophenol blue and 5% β-mercaptoethanol to denature proteins. SDS binds tightly and evenly to the uncoiled polypeptide chain so that the charge-density along its length is approximately equal. The reducing agent β-mercaptoethanol breaks disulphide bonds, disrupting protein tertiary structure. SDS was also present throughout the acrylamide gel and running buffer, ensuring the proteins remain as denatured monomers. The negatively charged proteins travelled down the acrylamide gel towards the positive electrode induced by electric voltage.

Western blotting was the technique used for transferring the electrophoresed proteins by SDS-PAGE to a polyvinylidene difluoride (PDVF) membrane for immuno-detection and autoradiography.

2.6.2: Procedure overview

After cell harvesting (Section 2.4.2.d.) and tissue isolation (Section 2.4.), 50µg of sample mixed with SDS sample buffer was denatured at 95°C and loaded into 1.5mm Tris-glycine gels (12% acrylamide-bis) for electrophoresis at 130V for 90 min in Running buffer (25mM Tris, 0.2M Glycine, 0.1% SDS). Protein separation in the gel was wet transferred on to PVDF membranes overnight at 30V in Blotting buffer (25mM Tris, 0.2M Glycine, 1% Methanol). Non-specific protein binding was blocked with 5% milk in PBS-Tween for 1 hour at RT. PVDF membranes were then probed with specific antibodies diluted in blocking buffer (as indicated in the figure legends), for 3 hours at RT or at 4°C overnight. Chemiluminescent detection was accomplished with Western Blotting reagent ECL (GE Healthcare). Membranes were exposed using a LAS3000 Luminescent Image Analyser and the images were analysed using AIDA software.

a. **SDS-PAGE gels**

Most of the protein expression analysis was done using casted gels in a Bio-Rad mini-gel casting apparatuses. The percentage of acrylamide in the resolving gel depended on the size of protein that needed to be analysed. The larger the protein of interest, the lower the percentage of acrylamide in the resolving gel. In this study, 12% resolving gels were mostly used. However, gels with other acrylamide percentage were sometimes used and they are annotated in the figure legends. To make up resolving gels, a mixture of distilled water, 40% Acrylamide/Bis solution (BP14021, Fisher Scientific), 1.5M Tris pH 8.8 and 10% SDS was made in a glass

conical flask then, immediately prior to cast the gel, 10% w/v APS (Ammonium persulphate) and 1% TEMED (*N*,*N*,*N'*,*N'*- tetramethyl ethylenediamine) were added to the mixture to allow the gels to set. Using a disposable pastette, the gel mixture was poured between two glass plates (one smaller than the other) separated by 1.5mm to about 1cm below the edge of the smaller plate. The gel mixture was overlaid with 500µL water-saturated 1-isobutanol to exclude oxygen and allow acrylamide polymerisation.

Once the resolving gels set at room temperature or in an incubator, the isobutanol was removed from the apparatus, and the top of the gel dried by tapping with blotting paper. The stacking gel was a 4% Acrylamide mixture prepared alongside the resolving gel mixture (Distilled water, 40% Acrylamide/Bis solution (BP14021, Fisher Scientific), 1M Tris pH 6.8 and 10% SDS) and 10% w/v APS (Ammonium persulphate) and 1% TEMED were added just before pouring. Next, the stacking gel mixture was poured on top of the resolving gel. A 10 or 15-well comb was then positioned in the stacking gel and set at room temperature.

Gradient gels

NuPAGE Novex 4-12% Bis-Tris Gel 1.5mm, 10 well (Invitrogen, NP0335), were used in an XCell SureLock MiniCell for resolution of proteins of a range of molecular weights. The apparatus was assembled following the manufacturer's instructions. The gel was run at 200 V for 35 mins, in NuPAGE MES SDS Running Buffer (Invitrogen NP0002).

Samples were prepared using NuPAGE® LDS Sample Buffer (4X) (NP0007) was used to prepare protein samples for denaturing gel electrophoresis with NuPAGE® Novex® gels. NuPAGE® LDS Sample Buffer contains lithium dodecyl sulphate, pH 8.4, which allows for maximum activity of the reducing agent.

b. SDS-PAGE running conditions

Samples were loaded in the well of the acrylamide gels alongside 8µL molecular weight markers to allow the determination of protein molecular weight, PageRulerTM Plus Prestained Protein Ladder (SM1811 or SM1812, Fermentas).

After sample loading, the gel was run at 130 V for 90-95 mins or until the dye front reached the bottom edge of the gel. The apparatus was then dismantled and the stacking gel was carefully cut from the rest of the gel then placed into either distilled water for Coomassie staining or blotting buffer for western blotting.

c. Coomassie staining of gels

To visualise the purity of recombinant proteins or protein separation efficiency, electrophoresed gels were stained in Coomassie blue stain (0.1% (*w/v*) Coomassie blue R250, 40% methanol, 10% acetic acid, 50% distilled water) and destained with a mixture of 40% methanol, 10% acetic acid and 50% distilled water. Usually, the stain and destain mixtures were made up in 2 L amber bottles and stored at room temperature.

Prior to staining, the gel was washed briefly in distilled water in a small plastic box covered with cling film then the Coomassie stain was poured into the box to completely submerge the gel into it. There were two methods of staining: one

involved overnight incubation in the stain at room temperature on a rocker; the other one used a microwave to warm up the gel in stain for ~60 seconds to encourage the gel to take up the solution and then incubated in the stain at room temperature for 20 minutes on the rocker. For destaining, the gel was briefly washed in distilled water, then incubated in destaining mixture with a small piece of sponge which took up the excess stain. The destaining mixture was replaced several times until the protein bands were clearly visible.

Once the destaining was complete by either method, the gel was washed in distilled water and the protein bands imaged using a Fujifilm LAS-3000 imaging device, and quantified using AIDA software.

d. Western Blotting and antibody probing

PVDF membranes were prepared and equilibrated while electrophoresis was under way. To activate the membranes, they were soaked in 100% methanol until they turned translucent followed by a wash with distilled water. To equilibrate the PVDF membranes, they were left in blotting buffer at 4ºC until required together with pieces of blotting paper and filter sponges (2 per membrane).

The blotting sandwich was assembled in blotting buffer in the following order: sponge, blotting paper, gel, PVDF, blotting paper and sponge. The sandwich was placed inside the Bio-Rad Mini Protean tank. A small magnetic stirrer was placed into the tank, and an ice block placed alongside the blot transfer unit in the tank. The tank was then placed onto a magnetic stirring device and filled up with Blotting buffer. The lid was placed in the tank, with the electrodes appropriately aligned and

connected to the power pack. Blot transfer was carried out at 30 V overnight or 60 V for 4 hours.

e. PVDF Membrane Blocking

After the blot transfer had finished, the blotting apparatus was dismantled and the PVDF membrane was submerged in phosphate-buffered saline- tween (PBS-T; PBS: 20mM phosphate buffer pH 7.0 [10 mM Na_2HPO_4, 2mM KH_2PO_4], 300mM NaCl and 0.05% Tween20). The detergent Tween20 was added to the buffer to help remove non-specifically bound material. The membrane was then stained in Ponceau solution until the protein bands were visible to asses transfer efficiency and immediately washed in PBS-T. The blocking buffer (5% non-fat milk-PBS-T) was used to improve the sensitivity of the assay by reducing background interference and improving the signal to noise ratio. The membrane was then blocked by incubation at room temperature in for 1 hour.

f. Primary antibody incubation

Once blocking was completed, the appropriate primary antibody (Table 2.7 and Table 3.1) was diluted in blocking buffer and the membrane incubated in the mixture on a tube roller for 2 hours at room temperature or overnight at 4°C.

Table 2.7: Primary antibodies used for Western blotting.

Antigen (Name)	Function In the study	Manufacturer; Cat. No. or Reference	Species	Dilution for WB	Expected Molecular weight (kDA)
14-3-3 pan	Cytosolic marker	Santa Cruz Biotech; sc-629	Rabbit	1:1000	28
c-Myc-Cds1/2	Transfection efficiency	Santa Cruz Biotech; (C19) sc-788	Rabbit	1:1000	55
Calnexin	ER marker	ENZO; ADI-SPA-865-D	Rabbit	1:1000	90
Cds1	Protein expression	Novusbio; H0001040-M01	Mouse	1:100	55
COX IV	Mitochondrial marker	Cell Signalling; #4844	Rabbit	1:1000	17
Cytochrome C	Mitochondrial marker	Santa Cruz Biotech; (6H2) sc-13561	Mouse	1:1000	15
FLAG-RdgBβ (DDK)	Transfection efficiency	OriGene Tech; TA50011	Mouse	1:1000	50
GRP75	Mitochondrial marker	BioLegend; #818801	Mouse	1:1000	75
Mitofusin 2	Outer mitochondrial marker	Abcam; ab56889	Mouse	1:1000	75
PITPα (674)	Protein expression	Morgan et al., 2004	Rabbit	1:1000	36
PITPβ (1C1)	Protein expression	Morgan et al., 2006	Mouse	1:1000	36
Cardiac Troponin I	Cardiac marker	Santa Cruz Biotech; (H-170) sc15368	Rabbit	1:100	28

g. Primary antibody detection

The primary antibody recognised the target protein in a Western blot however it is not directly detectable. Therefore, tagged secondary antibodies were used depending upon the species of animal in which the primary antibody was raised. If the primary antibody was a mouse monoclonal antibody then the secondary antibody used was Anti-mouse IgG, peroxidase-linked whole antibody (from sheep) affinity purified general purpose reagent (ECL #NXA 931). All rabbit polyclonal antibodies were detected using Anti-Rabbit IgG (whole molecule)-Peroxidase produced in goat, affinity isolated antibody adsorbed with human IgG (Sigma-Aldrich; Catalogue Number A0545). Secondary antibody incubation was done after the membrane was washed with PBS-T three times for around 5 minutes each on the tube roller once the period of incubation with primary antibody had finished.

h. Blot exposure and imaging

Following secondary antibody incubation, the membrane was washed five times with PBS-T for 5 minutes each on the tube roller. For exposure, the membrane was placed into a plastic pocket cut to size and a 1:1 mixture of ECL or ECL Advance solutions (ECL Western Blotting Detection Reagents, GE Healthcare) was pipetted onto each membrane so that it was completely covered. The top leaflet of the plastic pocket was placed over the membrane avoiding bubble formation, and the membrane incubated in the solution for one to three minutes. Excess liquid was then wiped out from the pocket and from the membrane using absorbent paper. The chemoluminescence was measured using a LAS-3000 imaging system. Protein bands were quantified using AIDA software.

i. Stripping of western blots for re-probing

PVDF membranes could be stripped of the probed antibody and reused to look for other proteins. For re-probing, the western blotted membrane was rinsed with PBS-T, then it was heat-sealed into a polythene bag along with 10 mL stripping buffer (0.2 M glycine-HCl pH 2.5, 0.05 % tween-20, 100mM β-mercaptoethanol). The bag was immersed horizontally in a water bath pre-heated to 80°C for 20 mins. After incubation, the membrane was removed from the polythene bag and washed several times with PBS-T.

2.6.3: Production of RdgBβ sp1-specific polyclonal antibody

The custom-made antibodies against RdgBβ already available at the laboratory included the rabbit polyclonal antibodies Ab:101 and Ab:218. Ab:101 was made against two internal peptides of RdgBβ common to both rodent and human splice variants sp1 and sp2[41] while Ab:218 was made against the full length of the protein. Peptide synthesis and immunisations were performed by Eurogentec. In addition, the rabbit polyclonal anti-human RdgBβ (Rb59) was a gift from Dr. Tavazoie from the Rockefeller University, New York, USA[90].

Four additional anti-RdgBβ polyclonal Antibodies were commissioned. Antibodies Ab:R1 and Ab:R2 were produced in two rabbits by 4 immunisations one every 70 days with the peptide from Hu-RdgBβ sp1 (NCBI ref Q9UKF7.2). Peptide synthesis, immunisation and affinity purification was performed by Genosphere Biotechnologies. Antibodies Ab:522 and Ab:523 were manufactured by Eurogentec on their Rabbit- 3 months program.

a. Antibody affinity purification

The process of affinity purification of the sera Ab:101 and Ab:218 was divided into two stages. The first step involved the immobilisation of the antigen (8-10mg of Recombinant RdgBβ-sp1) to 2ml of AminoLink coupling gel (Thermo Scientific) in a 10ml column. The gel was equilibrated with coupling buffer (0.1M Na Phosphate buffer pH7 +0.05%NaN$_3$). A mixture of 5ml of antigen and 1ml of reductant buffer (1M NaCNBH$_3$ in 0.01M NaOH) was incubated with the gel on a rotating wheel overnight at 4°C. Later, the aqueous material was separated and the gel was quenched with 1M Tris-HCl and reductant buffers.

The second step, affinity purification, started with the equilibration of the antigen-coupled gel with PBS/Na$_3$. Then, 5ml of crude antibody serum diluted in PBS/Na$_3$ (1:1 ratio) was added to the gel and incubated on a rotating wheel overnight at 4°C. Following incubation, the column was centrifuged at 600rpm for 5 minutes to pellet the gel. The purified antibody was eluted from the gel twice, first with 5ml of 0.1M Glycine (pH 2.5) then with 5ml of 0.1M Triethylamine (TEA; pH 11.5). Both elutions were concentrated and their buffers exchanged to PIPES buffer separately by centrifugation at 3800 rpm for 90min at 4°C using Centriprep YM-10 (Millipore) until ~500µl of each elution was obtained. Finally both elutions were mixed together and 50µl aliquots were stored at -20°C. The bicinchoninic acid (BCA) assay was used to determine the purified antibodies concentration. Ab:101 at 1.1mg/ml and Ab:218 at 0.8mg/ml.

b. Dot blotting

Optimisation of RdgBβ antibodies, dilution ratios and blocking buffers for immunoblotting was performed by dot blotting. PVDF membranes were activated by methanol followed by ddH$_2$O washing and then placed on PBS wet filter paper. Each sample (2µl) was dotted on marked squares (1cm x1cm) on the membrane and then allowed to air dry. Analyses of different blocking buffers (3% and 5% milk, BSA and goat serum in PBS-Tween) and antibody concentrations (1:1000; 1:500; 1:100 and 1:50), were performed by incubation of membranes in blocking buffer for 1 hour at RT, followed by incubation in antibodies prepared in blocking buffer for 3 hours at RT. Secondary anti-rabbit antibody incubation followed several washes with PBS-Tween. Antibody reactivity was analysed by chemiluminescent detection (Figure 2.6). The optimal blocking buffer for most antibodies was found to be 5% milk in PBS-T.
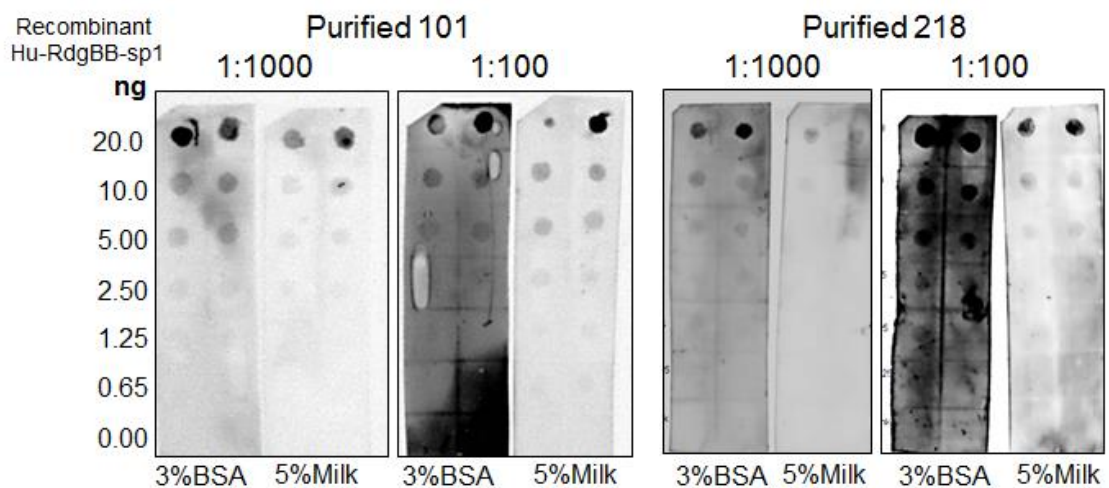
Figure 2.6: Dot blotting testing blocking buffer and antibody dilutions. Representative examples of affinity purified antibodies optimisation for immunoblotting.

2.7: Immunofluorescence microscopy

For visualisation and analysis of cell morphology, H9c2 cells were subjected to immunofluorescence microscopy. The cells were grown, treated and fixed directly in multi-well plates on coverslips. After washing the coverslip with PBS, the cells were fixed with 4%(w/v) paraformaldehyde in PBS for 15 minutes at room temperature.

The fixative mixture was removed followed by three washes with PBS for 5 minutes each. To permeabilise the cells, PBS- 100mM Glycine buffer (plus 0.2% TritonX-100) was applied for 10 min at RT followed by washing with PBS and incubation with the fluorescent conjugates DAPI (1:5000) and TRITC labelled Phalloidin (1:2000) for 30 minutes at RT in the dar to prevent fluorescence bleaching.

Subsequently, coverslips were washed in PBS and finally rinsed in water prior to mounting on a microscope slide with mowiol [13% (w/v) in 0.1 M Tris pH 8.5 with 33% glycerol (w/v)]. Fluorescence was recorded by excitation at 488 nm or 546 nm with a light source (Excite 120) using an Olympus IX80 microscope fitted with x20 and x40 air objectives. Images were acquired using a charge-coupled device camera (ORCA) controlled with CellF software (Olympus).

2.8: Cds activity assay

CDP diacylglycerol synthase (Cds) activity on isolated tissue and cellular samples was determined by measuring the level of incorporation of [^{3}H]-CTP into

CDP-DAG using external phosphatidic acid (PA). Assay conditions were assessed and optimised based on previous studies[29,119].

The isolated samples, source of Cds, were resuspended in CDS lysis buffer (50 mM Tris-HCl [pH 8.0]; 50 mM KCl; 0.2 mM EGTA, and 1/100 (v/v) protease inhibitor cocktail). If protease inhibitors were added, the buffer was kept at -20°C. All other components were diluted in CDS Assay buffer (50mM Tris-HCl [pH 8.0]; 100 mM KCl; 5.1mM Triton X-100; 2mg/mL BSA and 0.25mM DTT). The total volume per assay was 100µL which contained 50µg of the source of the enzyme, 200µM PA (Grade 1 Lipid Products Ltd, Table 2.8), 20mM $MgCl_2$ and 2µM CTP which was prepared as a mixture with 2.5µCi [^{3}H]-CTP (ARC #ART0343@1mCi/mL; Specific activity 20Ci/mmol).

The components of the assay were added in the following order: first the sample in triplicate including a sample containing BSA as negative control background, then immediately prior to PA addition, the $MgCl_2$ was mixed with the PA liposomes and later added to each sample, the reaction was initiated by the addition of CTP (radiolabelled +cold) to all samples. The sample mixtures were prepared on ice, once the CTP was added the samples were then incubated in a water bath at 30°C for 10min.

The reaction was terminated by transferring the samples to ice and adding 375µL $MeOH:CHCl_3:HCl$ (2:1:0.05) followed by the addition of 125µl $CHCl_3$ and 125µl dH_2O which separated the samples into two phases: the chloroform soluble (lower) and water soluble (top). The samples were centrifuged at room temperature

for 2 min and the lower phase was transferred to a new Eppendorf tube. To remove contaminating water-soluble radioactivity, 475µL of synthetic top phase solution made of a mixture of MeOH:H_2O (5:4.5) was added to the chloroform phase, vortexed and centrifuged. The lower chloroform phase was transferred onto scintillation vials then left in a fume cabinet for the solvent to evaporate overnight. Once the chloroform evaporated, 250µL MeOH was added to each vial, vortexed and scintillation fluid was added. Data was measured in disintegrations per minute (DPM) in a Packard Tricarb 2500 scintillation counter. Cds activity was expressed as an average of the triplicate DPM counts subtracted of the average background counts obtained from BSA samples.

2.8.1: Assay characterisation

The addition of 5.1mM (1.7%) Triton X-100 to the assay buffer in order to solubilise cellular membranes considerably increased the activity measurement (Figure 2.7.A). Furthermore, the requirement for specific species of exogenously added PA to the assay was considered (Figure 2.8.B). Egg PA (Lipid Products Ltd; Table 2.8) showed significantly higher Cds activity over di-palmitoyl PA in Cos7 cells transfected with human myc-Cds1 and Cds2.

In addition, endogenous Cds enzyme in rat heart pure mitochondria, obtained as described on Section 2.5.1.b, showed an increase in the level of incorporation of ^{3}H over time (0-11.5 minutes; Figure 2.8.A), as well as with increasing protein content per assay (0-200µg; Figure 2.8.B).

Table 2.8: Fatty acid composition of phosphatidic acid used in the Cds activity assay and PA transfer*

Fatty acid Name	*sn*-1 Notation	% in Phosphatidic acid (PA Grade1; Lipid Products)
Palmitic	16:0	32.1
Palmitoleic	16:1	2.1
Stearic	18:0	11.7
Oleic	18:1	36.2
Linoleic	18:2	12.5
Arachidonic	20:4	5.5
Molecular weight		650 g/mol

(*): As advised by the manufacturer.

A.

B.
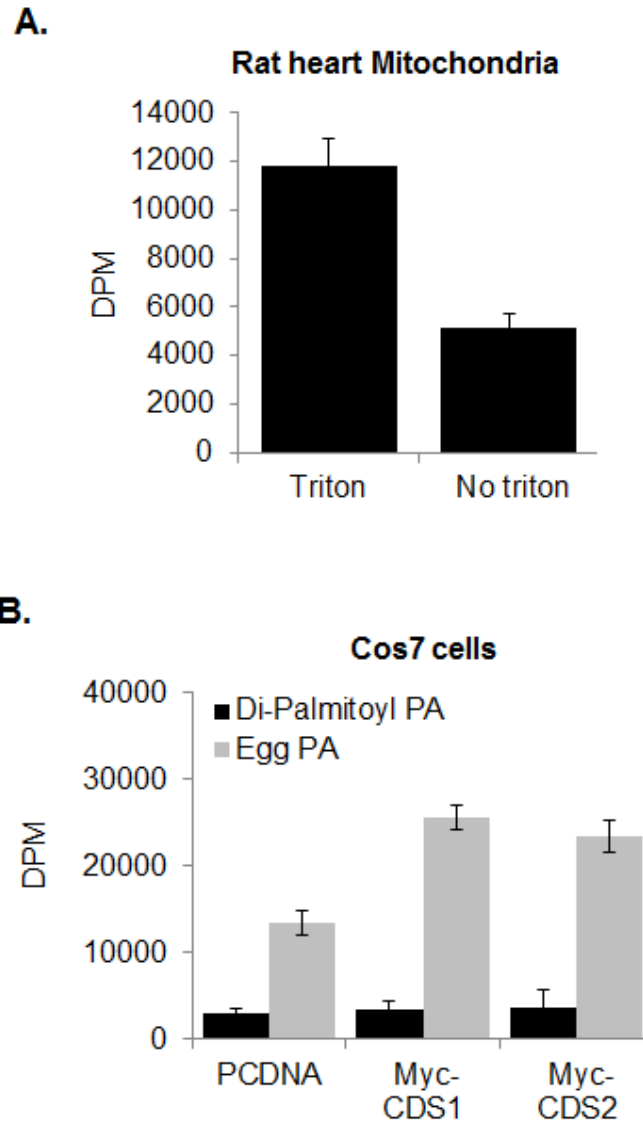
Figure 2.7: Cds activity assay characterisation – Triton X 100 and Source of PA.

[A.] Triton-X 100 requirement: 100µg of rat heart mitochondria obtained by differential centrifugation of rat hearts was incubated in Cds assay buffer ± 5.1mM (1.7%) Triton-X 100 for 15 minutes at 30°C. Bars show mean ± SEM from 2 experiments (N=4).

[B.] Source of exogenous PA: Cos7 cells were seeded at 1×10^6 cells/mL in T-75 flasks and after 16 hours culture, and transfected by electroporation with empty vector pcDNA, human Myc-Cds1 or Myc-Cds2 plasmids for 48 hours. Cells were harvested and 100µg of lysates were assessed for Cds activity in Cds assay buffer with 200µM Di-palmitoyl PA or Egg PA for 10 minutes at 30°C. Bars show mean ± SEM from 1 experiment (N=2).
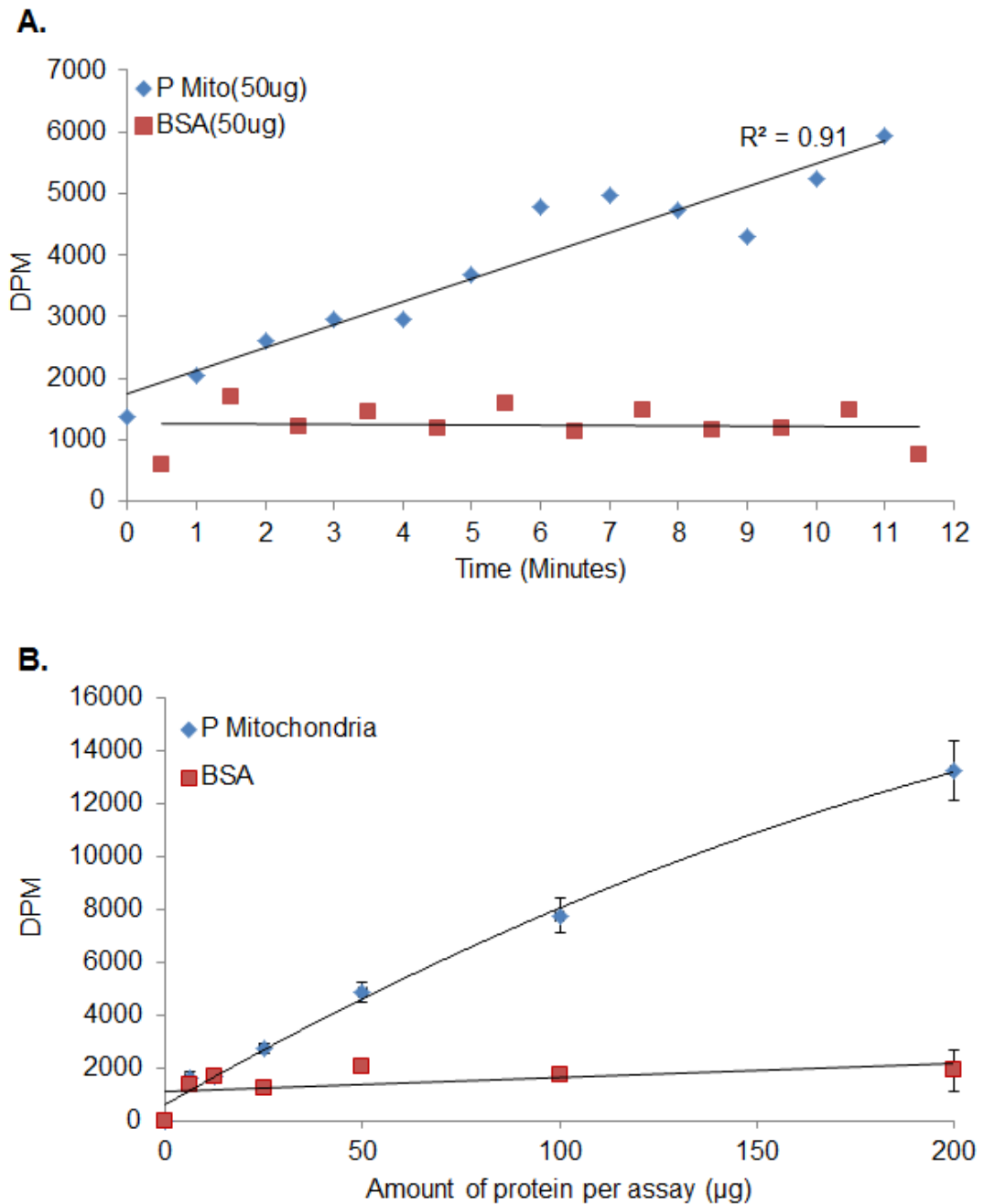
Figure 2.8: Cds activity assay characterisation – Time and Protein concentration dependency.

Cds activity of endogenous Rat Heart Pure Mitochondria compared to BSA.

[A.] Time-dependency: 10µL of sample was removed at 1 minute intervals from the incubation. Results from one experiment (n=1).

[B.] Protein concentration dependency: Assay was performed for 10 minutes at 30ºC. N=2 from one experiment.

2.9: PIS activity assay

The assay to determine Phosphatidylinositol Synthase activity on biological samples was an adaptation of the Cds activity assay described in Section 2.7. This assay measured the turnover of [^{3}H]-PI in cells as a consequence of PIS activity.

The PIS Assay buffer contained 50 mM Tris-HCl (pH 7.4) and 2 mM MnCl$_2$.The total volume per assay was 100μL which included 50μg of the source of the enzyme plus a mixture of 10μM Myo-Inositol+ 2.5μCi [^{3}H] Myo-Inositol diluted in PIS assay buffer.

The assay was then performed exactly as described on Section 2.7 with different incubation settings. PIS enzyme reactions were allowed for 15 minutes at 37°C.

2.10: PLC assay

The Phospholipase C (PLC) assay measured the amount of radiolabelled [^{3}H] Inositol phosphates as a result of PLC stimulation of radiolabelled cells as described previously[27]. The buffer used for the assay, HEPES buffer (137mM NaCl, 2.7mM KCl; 20mM HEPES; 2mM MgCl2; 1mM CaCl2; 5.6mM; 1mg/mL; 10mM LiCl; pH 7.2), was prepared fresh on the day of the experiment and was kept warm at 37°C. Cells were equilibrated in the buffer prior to incubation in the stimulant at 37°C for one hour. Each condition was set up in duplicate.

After stimulation, the cell plates were removed from the incubator and placed on ice. The buffer was replaced with 1000µl cold MeOH each well to stop the reaction. The cells were then scraped from each well using a cell scraper followed by a final wash with 900µl distilled water which was also transferred to the solvent tube. To separate the aqueous from the chloroform soluble components of the cells, 1mL chloroform was pipetted into each solvent tube following centrifugation at 1200rpm for 5mins.

The isolation of Inositol phosphates was achieved using glass Pasteur pipettes containing Dowex 1x8 anion exchange resin. After equilibration with 2 mL 2M ammonium formate / 0.1M formic acid, the columns were filed with 1.5mL of the aqueous top layer from each solvent tube. To elute unbound [^{3}H]-inositol the columns were washed with water followed by 5mM sodium tetra borate / 60mM sodium formate to elute GPI. These elutions were let to run through.

Finally, to elute total inositol phosphates from the columns, each Dowex was transferred to scintillation vials. Elution was achieved by the addition of 1M ammonium formate/0.1M formic acid. Ultima FLO scintillation fluid was added to each vial to cope with high salt content and radioactivity was counted on the liquid scintillation counter. Separately, the chloroform phase from each tube was transferred to scintillation vials and counted to obtain total lipid input. For data analysis, radioactive counts (dpm) of both top and bottom layers of each solvent tube was adjusted accordingly. A mean of the duplicate inositol phosphate values was calculated (dpm) and expressed as a proportion of the all the inositol phosphates produced in control-transfected cells treated with the same stimulation.

2.11. Data presentation and statistical analysis.

All data in this thesis is presented using descriptive statistics as the mean value of the measurements ± the standard error. Each figure indicates the sample size, the number of experiments and relevant details of calculations. The statistical significance of the observations between two samples was evaluated using the Student's t-Test (Paired Two Sample for Means) using Microsoft Excel software. P values below 0.05 were considered to be significant and were only included if data represented more than two experiments.

RESULTS AND DISCUSSION

CHAPTER 3: Analysis of the Phosphatidic Acid (PA) transfer activity of RdgB proteins.

3.1. Introduction

By studying the structure and biochemical properties of proteins, it is possible to find indications of their physiological function. Despite collaborative efforts from my research group, there are still no crystal structures available for any Class II PITP (RdgB) proteins to date. However, the structures of PITPα and PITPβ, with or without their lipid cargo, have been described.[96,109,122,129] Since the residues directly involved with the phosphate moiety and the inositol headgroup for PI binding are conserved in both Class I and RdgB proteins, multiple sequence alignment of the PITP domains allowed me to make predictions and comparisons between them (Figure 3.1). In addition, it was recently reported that RdgB proteins differ from PITPα and PITPβ in their phospholipid binding properties: Class I bind phosphatidylinositol (PI) and phosphatidylcholine (PC) whilst Class II bind PI and phosphatidic acid (PA)[40]. However, the biochemical basis of the PA transfer property of RdgB proteins remains to be fully elucidated.

RdgBβ was the first protein to be reported to transfer PA recently using a pyrene-labelled phospholipid quenching assay *in vitro* [40]. However, this assay was made in collaboration with another group and pyrene-labelled PA is not

commercially available. Therefore, I adapted another transfer assay to analyse [^{3}H]-PA transfer activity of recombinant proteins. The assay used rat liver mitochondria as acceptor compartments and [^{3}H]-PA labelled liposomes (PC: PA; 98:2) as donor compartments. This Chapter describes initially, an analysis of the PA transfer activity of the Wild Type (WT) PITP domains of Class II (RdgB) proteins compared to Class I PITPs using the new adapted assay to confirm previous observations with PITPα and Hu-RdgBβ; and further characterises the PA transfer activity of PITPβ and the PITP domain of RdgBα proteins[40].

In addition, a mutational analysis was performed in an attempt to identify the residues within the PITP domain that are essential for PA transfer. The recombinant mutants of the PITP domain of Dm-RdgBα tested include three of those that are unable to bind PI (Point mutations: T59A/E, K61A and N90F; numbers according to the mouse PITPα sequence; Figure 3.1 and Figure 3.2)[125]; followed by two mutants unable to contact the phosphate moiety of the phospholipid (Point mutations: Q22A and T97A). An analysis of the mutant that shows defective membrane binding (YW203/204AA) is also described, and the Chapter concludes with a discussion of the results and offers suggestions for future studies.

```
                              18 21/22              36                    59
O00562.4:RdgBa-Human      -MLIKEYHILLPMSLDEYQVAQLYMIQKKSRGESSGEGSGVEILANRPYTDGPGGSGQYT   59
Q00169.2:PITPa-Human      MVLLKEYRVILPVSVDEYQVGQLYSVAEASKNE-TGGGEGVEVLVNEPYEK-DGEKGQYT   58
P48739.2:PITPb-Human      MVLIKEFRVVLPCSVQEYQVGQLYSVAEASKNE-TGGGEGIEVLKNEPYEK-DGEKGQYT   58
NP511149.2:RdgBb-Drosophila  -MLIKEYRIPLPLTVEEYRIAQLYMIAKKSRGESHGEGSGVEIIINEPYKDGPGGNGQYT   59
Q9UKF7.3:RdgBb-Human      -MLLKEYRICMPLTVDEYKIGQLYMISKHSHEQ-SDRGEGVEVVQNEPFEDPHHGNGQFT   58
                          .*:**::.: :* :::**:: ** . :  :.*..  : . *.*:. *.*:. **.*

                          61                  86  90      97              113
O00562.4:RdgBa-Human      HKVYHVGSHIPGWFRALLPKAALQVEEESWNAYPYTRTYTCPFV-EKFSIEIETYYLPD  118
Q00169.2:PITPa-Human      HKIYHLQSKVPTFVRMLAPEGALNIHEKAWNAYPYCRTVITNEYMKEDFLIKIETWHKPD  118
P48739.2:PITPb-Human      HKIYHLKSKVPAFVRMIAPEGSLVFHEKAWNAYPYCRTIVTNEYMKDDFFIKIETWHKPD  118
NP511149.2:RdgBb-Drosophila  KKIYHVGNHLPGWIKSLLPKSALTVEEEAWNAYPYTRTYTCPFV-EKFSLDIETYYYPD  118
Q9UKF7.3:RdgBb-Human      EKRVYLNSKLPSWARAVVPKI-FYVTEKAWNYYPYTITEYTCSFL-PKFSIHIETKYEDN  116
                          .: :: .::* : : *: : . .*:.:** *** : * :: .* :.*.** **.*

O00562.4:RdgBa-Human      GGQQPNVFNLSGAERRQRILDTIDI-VRDAVAPGEYKAEEDPRLYHSVKTGRGPLSDDWA  177
Q00169.2:PITPa-Human      LGTQENVHKLEPEAWKHVEAVYIDIADRSQVLSKDYKAEEDPAKFKSIKTGRGPLGPNWK  178
P48739.2:PITPb-Human      LGTLENVHGLDPNTWKTVEIVHIDIADRSQVEPADYKADEDPALFQSVKTKRGPLGPNWK  178
NP511149.2:RdgBb-Drosophila  NGYQDNVFQLSGSDLRNRIVDVIDI-VKDQLWGGDYVKESEDPKHFVSDKTGRGPLAEDWL  177
Q9UKF7.3:RdgBb-Human      KGSNDTIFDNEAKDVER-EVCFIDI-ACDEIPERYYKESEDPKHFKSEKTGRGQLREGWR  174
                          *  .:: .  .        ***      .  :  *  *** : * ** **.*  *

                                               203/210  204/211
O00562.4:RdgBa-Human      RTAA-----------QTGPLMCAYKLCKVEFRYWGMQAKIEQFIHDVGLRRVMLRAHRQA  226
Q00169.2:PITPa-Human      QELVN---------QKDCPYMCAYKLVTVKFKWWGLQNKVENFIHKQE-RRLFTNFHRQL  228
P48739.2:PITPb-Human      KELAN---------SPDCPQMCAYKLVTIKFKWWGLQSKVENFIQKQE-KRIFTNFHRQL  228
NP511149.2:RdgBb-Drosophila  EEYWREVKGKKQPTPRNMSLMTAYKICRVEFRYWGMQTKLEKFIHDVALRKMMLRAHRQA  237
Q9UKF7.3:RdgBb-Human      DS-------------HQPIMCSYKLVTVKFEVWGLQTRVEQFVHKVV-RDILLIGHRQA  219
                          *  .:**:  ::*  :*.* :.*:*::.  : ::  ***

O00562.4:RdgBa-Human      WCWQDEWTELSMADIRALEEETARMLAQRMAKCNT-GSEGSEAQPPGKPSTE-A------  278
Q00169.2:PITPa-Human      FCWLDKWVDLTMDDIRRMEEETKRQLDEMRQKDPVKGMTADD----------------  270
P48739.2:PITPb-Human      FCWIDKWIDLTMEDIRRMEDETQKELETMRKRGSVRGTSAADV---------------  271
NP511149.2:RdgBb-Drosophila  WAWQDEWFGLTIEDIRELERQTQLALAKKMGGGEECSDDS--VSEPYVSTAATAASTTGS  295
Q9UKF7.3:RdgBb-Human      FAWVDEWYDMTMDEVREFERATQEATNKKIGIFPPAISIS---SIPLLPSSVRSAP----  272
                          ::.* *:.*  :::  ::*  :*  *
```

Figure 3.1: Multiple sequence alignment of PITPs and the PITP domain of Drosophila RdgBα.

The code on the left of each protein is the NCBI sequence reference number. The rectangles highlight the residues described in Section 3.3.1; inositol ring binding (T59, K61, E86 and N90; mouse PITPα numbering); Section 3.3.2 phosphate moiety binding (Q21/22, T97, T113 and K202); and Section 3.3.3 membrane association (WW/203 204; YW/210 211). The circle highlights the basic amino acids mentioned in Section 3.4. Sequence alignment obtained with Clustal Omega (1.2.1) online tool which colours the residues according to their physicochemical properties: Red (Small, hydrophobic); Blue (Acidic); Magenta (Basic); Green (Hydroxyl, sulfhydryl, amines). * (asterisk, fully conserved residue); : (colon, conservation between groups of strongly similar properties); and . (period, conservation between groups of weakly similar properties).

107
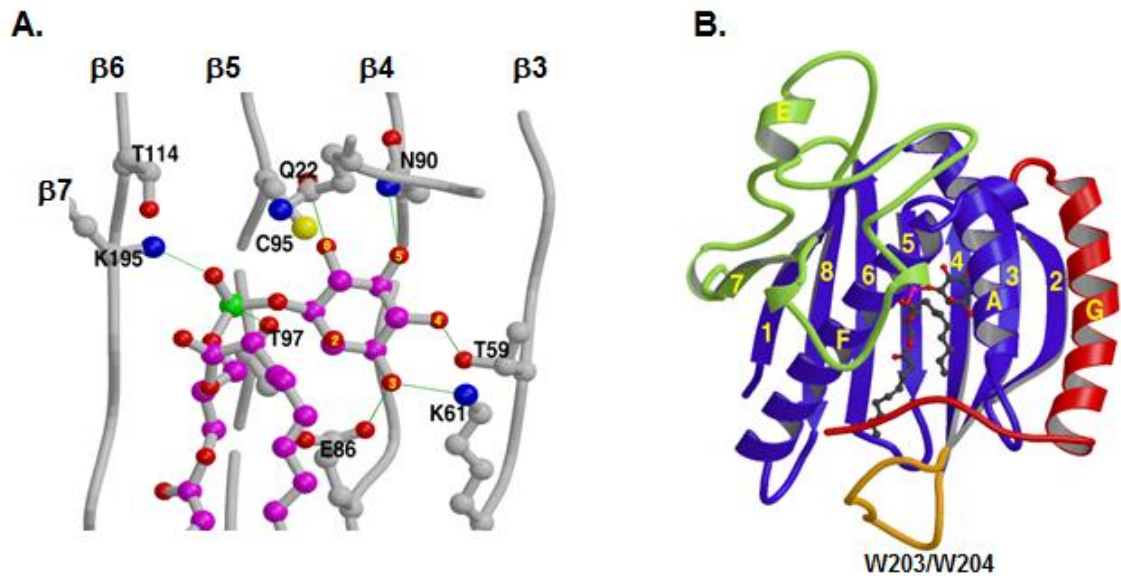
Figure 3.2: PITPα structure binding PI

[A.] Localisation of the residues responsible for the PI (magenta) interaction within the PITPα structure. The figure was taken from Cockcroft 2007.[19]

[B.] Overall fold structure of PITPα binding PI. Functional regions are lipid-binding core (blue), regulatory loop (green), C-terminal region (red), and lipid exchange loop (orange). The figure was taken from Tilley et al 2004.[109]

Table 3.1: List of the recombinant protein mutants analysed in this study.

Characteristic of the PITP domain	PITPα Mutants*	Ref.
Residues in contact with the inositol ring of PI	K61A N90F T59A & T59E	[125]
Associated with phosphate moiety binding.	Q21A T97A	N/A
Assist in membrane docking	YW203/204AA	[125]

* This study used mutants of the PITP domain of Dm-RdgBα which sequence numbers differ from PITPα but they were kept throughout to avoid confusion.

3.2. The PA transfer capability is exclusive of Class II PITPs

The ability of binding and transferring phosphatidylinositol (PI) and phosphatidylcholine (PC) is a characteristic of Class I PITPs (PITPα and PITPβ)[97,109]. On the other hand, Hu-RdgBβ, a Class II PITP, was recently reported to bind and transfer PI and phosphatidic acid (PA). The PA binding property was shared by other Class II PITPs including Human and *Drosophila melanogaster* RdgBα.[40] To analyse the PA transfer activity of Class II PITPs (Human RdgBα and RdgBβ and Drosophila RdgBα), wild type recombinant proteins were tested for PA transfer activity at serial dilutions ranging from 1.5 to 200µg/mL using an *in vitro* assay where the radioactivity transferred from di-palmitoyl-[^{3}H]-PA liposomes onto rat liver mitochondria was measured.

The results are presented as the % of radiolabelled PA transferred from the total input per nmol of PITP. The amount of protein was converted from µg/ml to nmol using the molecular weight of each recombinant protein tested (Figure 3.3). PITPα, PITPβ and the PITP domain of Hu-RdgBα (residues 1-277) were 36kDa (g/mol). The PITP domains of Dm proteins was calculated as 38kDa (g/mol) and Hu-RgdBβ as 45kDa (g/mol).

Hu-RdgBβ showed increased PA transfer activity according to a rise in content from 0.01 nmol of protein transferring 3.4±0.5% to 20±3% achieved by 0.3 nmol of protein and above. The other RdgB-PITP proteins (Dm-RdgBα and Hu-RdgBα) demonstrated higher activity than RdgBβ. As little as 4×10^{-3} nmol of protein showed PA transfer activity and saturation was reached by 0.06 nmol of RdgBα.

The highest percentage of PA transferred was 24.5±1% of the total input. In clear contrast, recombinant Class I proteins, PITPα and PITPβ did not transfer PA at any concentration (Figure 3.4.A).

To confirm the activity of the recombinant protein preparations, the PI transfer activity of two different batches of PITPα and Hu-RdgBβ was tested using a different *in vitro* essay which uses [^{3}H]-PI from rat liver microsomes as donor compartment and PC:PI liposomes as acceptor compartment. The PI transfer activity of PITPα was nearly twice the activity showed by Hu-RdgBβ (Figure 3.4.B). These data confirmed that all RdgB proteins can transfer both PI and PA[125].
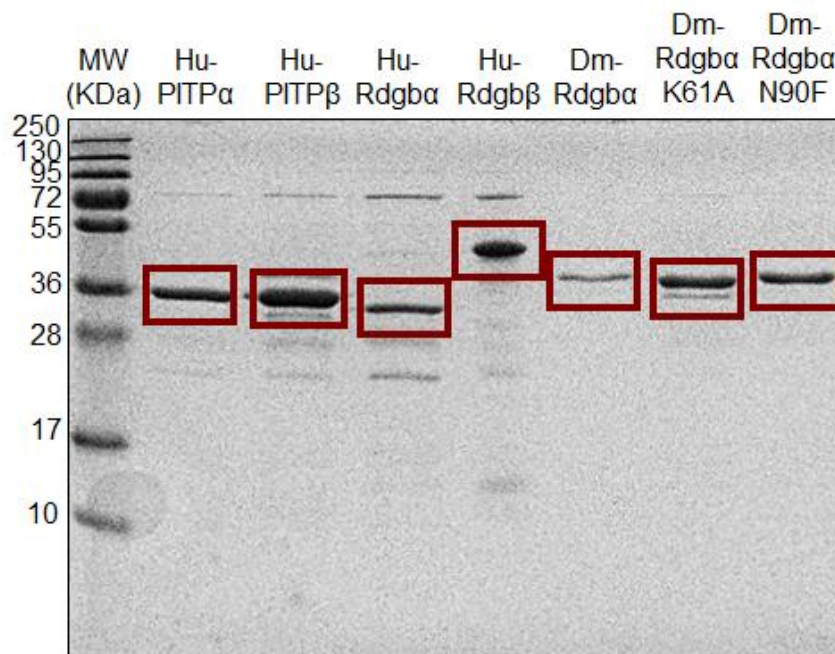
Figure 3.3: Recombinant proteins used in this study

Human PITPα, PITPβ, RdgBβ, the PITP domains of Human (Hu)-RdgBα (residues 1-277) and of Drosophila (Dm)-RdgBα (residues 1-281) including the mutants (Dm)-RdgBα K61A and N90F were separated by SDS-PAGE and stained with Coomassie blue to demonstrate their degree of purity. The red boxes indicate the band at the expected molecular weight for each protein.

Figure 3.4: Comparison of PA and PI Transfer by Class I and II PITPs.

[A.] PA transfer activity of recombinant wild type (WT) Class I proteins (PITPα and PITPβ) compared to the PITP domain of Class II [Human (Hu)-RdgBβ, Hu-RdgBα and Drosophila melanogaster (Dm)-RdgBα)] PITP proteins using [^{3}H]PA-labelled PC:PA (98:2) liposomes as donors and rat liver mitochondria as acceptors.

[B.] PI transfer of PITPα and RdgBβ. Two separate preparations [(1) and (2)] of recombinant proteins using [^{3}H]PI-labelled rat liver microsomes as donor and unlabelled PC:PI (98:2) liposomes as acceptors.

The transfer data (%) was calculated from the total input amount of radioactivity after substraction of the background radioactivity obtained when no recombinant protein was added. Data represents mean±standard errors of a minimum of 3 experiments for PA transfer and 2 experiments for PI transfer.
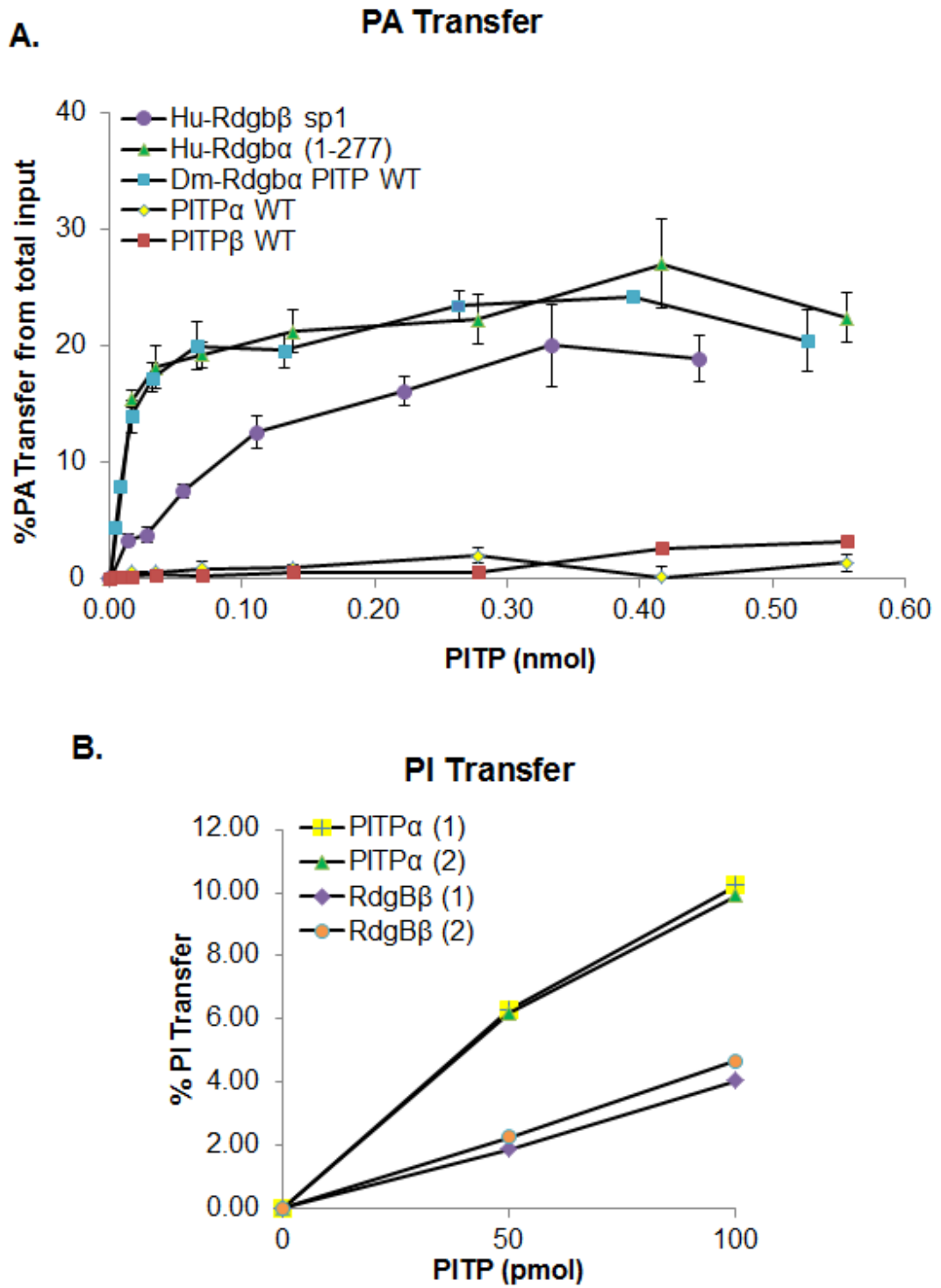
Figure 3.4: Comparison of PA and PI Transfer by Class I and II PITPs.

3.3: PITP domain residues that may affect PA transfer activity of RdgB proteins.

The difference in the phospholipid transfer properties of PITP proteins could lie within the PITP domain itself as RdgBs are only ~40% identical to the Class I PITPs. Based on the crystal structure of PITPα[109], some of the residues of the PITP domain responsible for binding to the inositol ring of PI, the phosphate group of PI and for membrane binding were mutated by site-directed mutagenesis then expressed in *E.coli* and purified, as described in Section 2.3, to determine whether they influence PA transfer activity in RdgB proteins.

For this mutational study I used *Drosophila melanogaster* (Dm) RdgBα mutants that were available in the laboratory excluding Dm-RdgBα Q21A and T97A which were mutated by Tim Ashlin. Hu-RdgBβ mutants did not purify in the quantities and quality seen for Dm-RdgBα mutants. However, the residues studied here are conserved in the PITP domain of RdgB protein which suggests that the results for Dm-RdgBα would be similar for all RdgB proteins (Figure 3.2.).

3.3.1: PA transfer activity is unaffected in mutants unable of binding PI.

A conserved property of the PITP domain of both Class I and Class II PITPs is the ability to bind and transfer PI *in vitro*. The crystal structure of PITPα identified the amino acid residues within the binding pocket that are in contact with the inositol ring of PI by hydrogen bonds and are essential for both *in vitro* and *in vivo* activity (T59, K61, E86 and N90; mouse PITPα numbering). [109] The Dm-RdgBα single point mutants K61A, N90F and, two versions of T59 (T59A and T59E) were analysed for PA transfer activity and compared to the wild type protein using the assay described in Section 2.3. As negative control, PITPα was included.

The PA transfer of the mutant proteins was unaffected at saturating quantities (0.06 nmol and above). However lower levels of the mutant proteins K61A, N90F and T59E showed reduced transfer activity. The activity of the T59A mutant was unaffected at all concentrations[125] (Figure 3.5). These results suggest that the residues of the PITP domain responsible for PI binding and transfer are not involved in PA transfer.

3.3.2: Effect of mutation in residues of the PITP domain associated with the phosphate moiety binding.

The PITP family of proteins conserve the residues Q21, T97, T113 and K202 which make contact with the phosphate moiety of phospholipids PI and PC as described previously[109] Residue Q21 in RdgB proteins occupies position Q22 in PITPα and PITPβ (Figure 3.4). To test whether these amino acids are required for PA transfer, two of the residues (Q21A and T97A) were mutated by site-directed mutagenesis of wild type Dm-RdgBα. After recombinant expression and purification of the proteins, the biochemical properties of these mutants were analysed. PI and PA transfer activity were assessed as described in Section 2.3.

The PI transfer of mutant Dm-RdgBα T97A showed reduced activity and its PA transfer activity was unaltered compared to wild type Dm-RdgBα at allquantities tested (. On the other hand, Dm-RdgBα Q21A affected both PI and PA transfer activity. PI transfer was abolished and PA transfer was severely reduced (Figure 3.5). These results suggest that the amino acid T97 is not involved in PA transfer; and Q21 although essential for PI transfer, it is important but not critical for the ability of the PITP domain of RdgB proteins to transfer PA *in vitro.*

Figure 3.5: PA Transfer activity of RdgB proteins does not require the residues that bind PI.

PA transfer activity of recombinant wild type Drosophila melanogaster (Dm-RdgBα WT) PITP domain compared to mutants unable to bind PI (N90F, K61A, T59E and T59A) using [^{3}H]PA-labelled PC:PA (98:2) liposomes as donors and rat liver mitochondria as acceptors. PITPα WT was used as negative control. Recombinant protein preparations were obtained by site directed mutagenesis followed by bacterial expression and purification.

The transfer (%) was calculated from the total input amount of radioactivity removed from the background values Data represents averages and standard errors of a minimum of 3 experiments with different recombinant protein preparations.

A.

B.
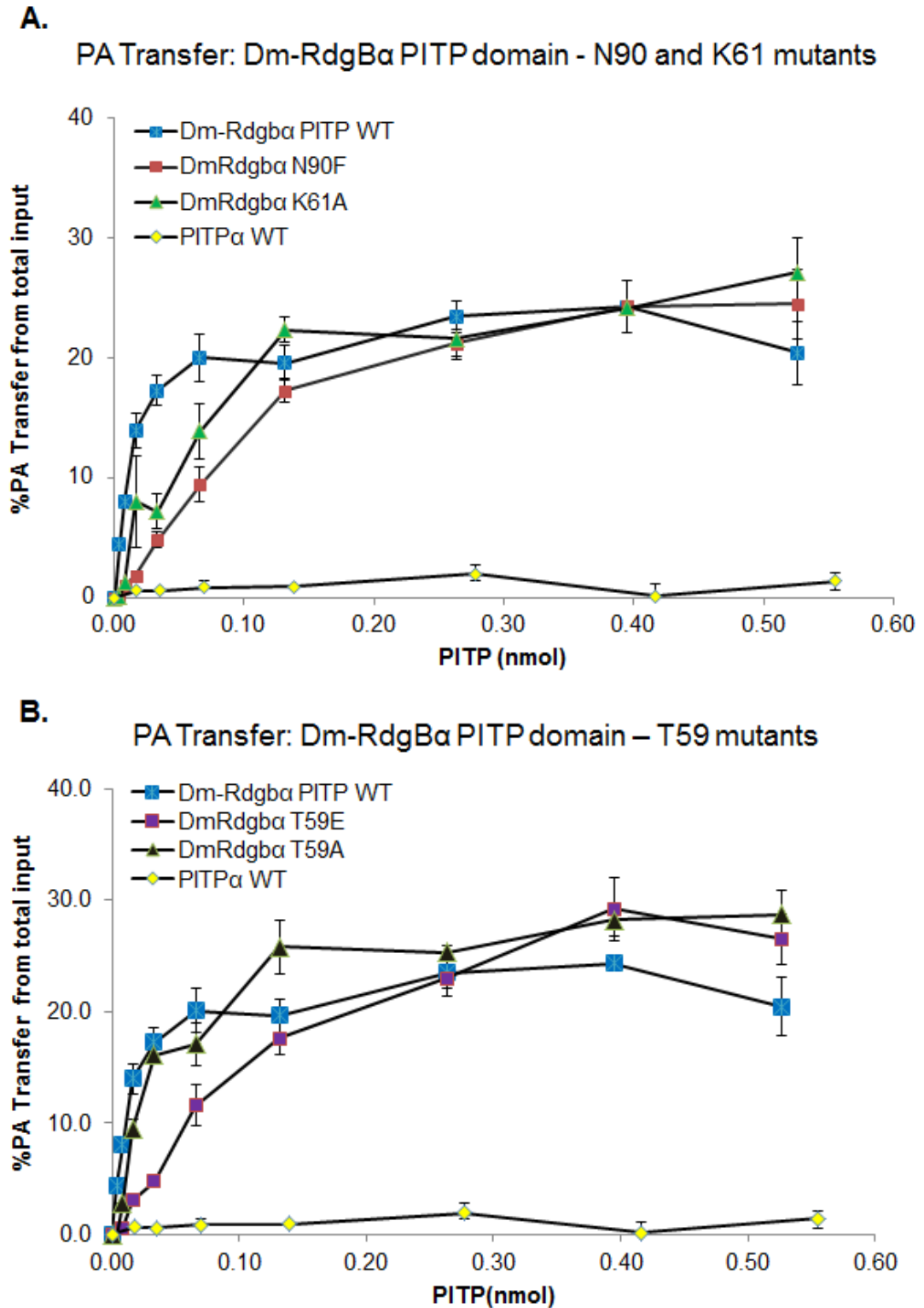
Figure 3.5: PA Transfer activity of RdgB proteins does not require the residues that bind PI.

Figure 3.6: PI and PA transfer activity of RdgB protein mutated to bind the phosphate moiety.

Phospholipid transfer activity of recombinant wild type Drosophila melanogaster (Dm-RdgBα WT) PITP domain compared to mutants unable to interact with the phosphate moiety (Q21A and T97A). Mutants obtained by site directed mutagenesis followed by bacterial expression and recombinant protein purification

[A.] PA transfer assay using [^{3}H]PA-labelled PC:PA (98:2) liposomes as donors and rat liver mitochondria as acceptors.

[B.] PI transfer using [^{3}H]PI-labelled rat liver microsomes as donor and unlabelled PC:PI (98:2) liposomes as acceptors.

The graphs show the averages (%) and standard errors of 2 experiments obtained from the total input amount of radioactivity following substraction of the background radioactivity.
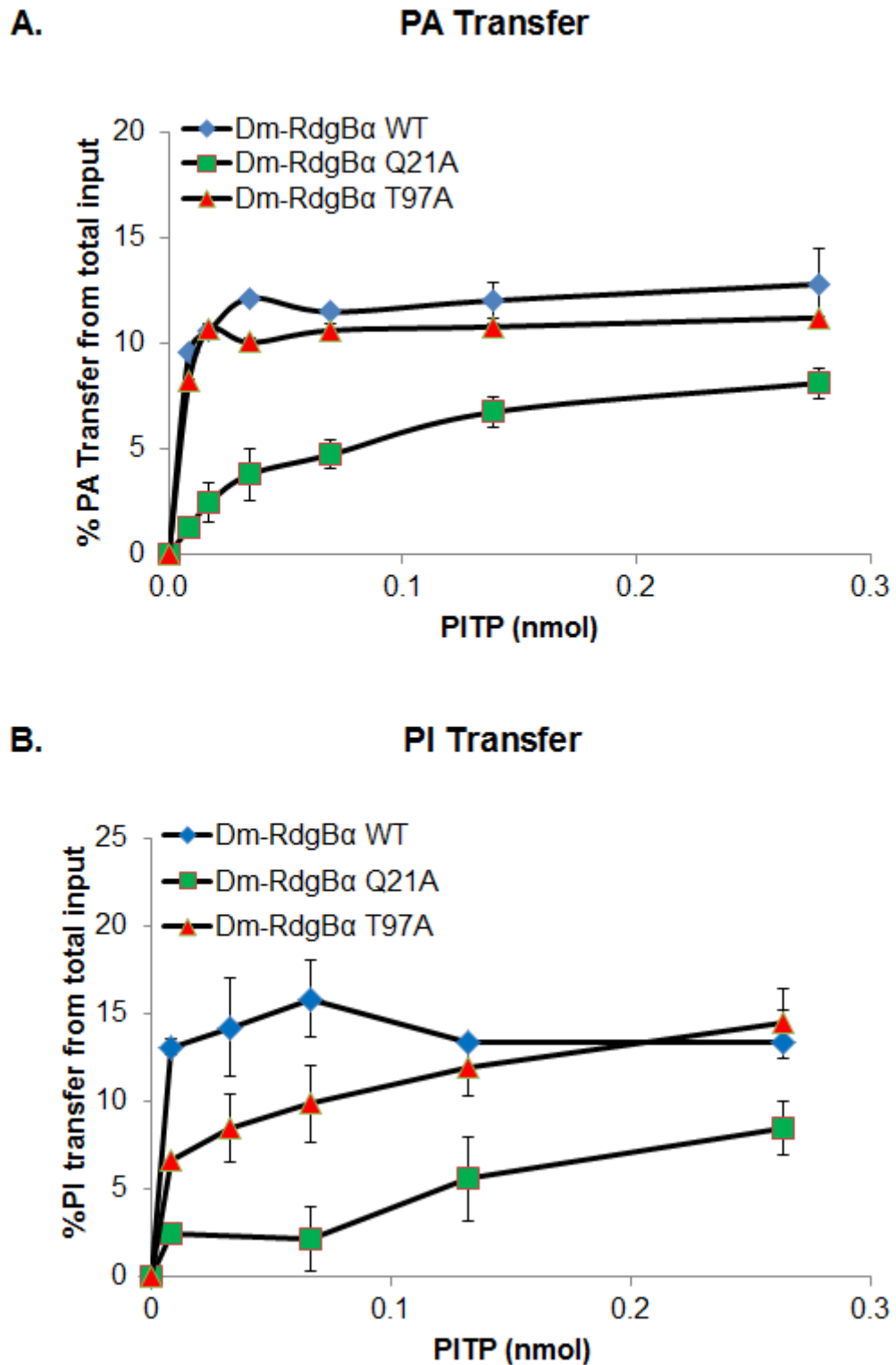
Figure 3.6: PI and PA transfer activity of RdgB protein mutated to bind the phosphate moiety.

3.3.3: Effect of the mutation affecting membrane interaction with the PITP domain.

Class I PITPs have been shown to dock to membranes via two tryptophan residues (W203 and W204) which are located at the lipid exchange loop of their structure (Figure 3.2). The WW203/204AA mutants failed to associate with the membranes and were inactive for PI transfer.[98,109] In RdgBα proteins, one of these residues is replaced by tyrosine (YW) and, in RdgBβ, by valine (VW). The equivalent residues in Dm-RdgBα are at positions 210 and 211 respectively (Figure 3.1). In this study, the PA transfer activity of Dm-RdgBα (YW/AA) was assessed using the assay described in Section 2.3.2 against the activity of the wild type protein and, as a negative control, PITPα was included.

The [^{3}H]-PA transfer activity by the YW/AA mutation protein was ~50% of the activity obtained with the wild type PITP domain of Dm-RdgBα protein regardless of the amount of protein in the assay (Figure 3.7). The results show an involvement of residues Y210/W211 in the PA transfer activity of RdgB proteins.

Finally, I compared the outcomes of all recombinant proteins at a specific amount (0.03nmol). This quantity of transfer protein was analysed based on the saturation of activity that was measured at higher values. It is evident that the RdgBα proteins (Hu and Dm) exhibit the highest activity and all mutants a reduced activity. This observation suggests that the mutant proteins transfer PA at a slower rate. (Table 3.2 and Figure 3.8).
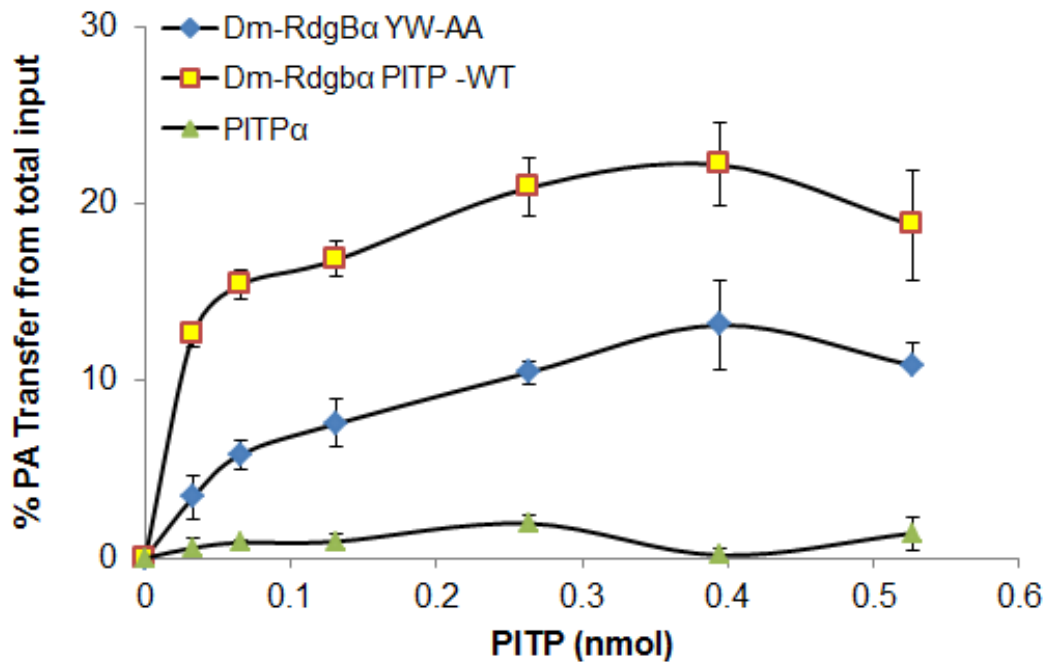
Figure 3.7: PA Transfer activity of the mutant YW210A / W211A.

The PA transfer activity of the recombinant Dm-RdgBα PITP domain mutation Y210A/W211A was compared to the wild type (WT) domain using [³H]PA-labelled PC:PA (98:2) liposomes as donors and rat liver mitochondria as acceptors. PITPα WT was used as negative control. The mutant was obtained by site directed mutagenesis followed by bacterial expression and recombinant protein purification. The data was obtained from 2 experiments and calculated as percentage of the total input amount of radioactivity which had the background radioactivity substracted.

Table 3.2: PA transfer from total input by 0.03 nmol PITP proteins

PITP	0.03 nmol	% PA transfer from total input
Human Class II	Rdgbβ sp1	3.8 ± 0.63
	Rdgbα (1-277)	18.1 ± 1.82
Dm-Rdgbα PITP	WT	17.2 ± 1.24
	N90F	4.8 ± 0.65
	K61A	7.2 ± 1.43
	T59E	4.7 ± 0.04
	T59A	16.0 ± 0.02
	Q21A	3.8 ± 0.21
	T97A	10.0 ± 1.23
	YW-AA	3.4 ± 0.63
Class I	PITPα WT	0.5 ± 0.13
	PITPβ WT	0.3 ± 0.05
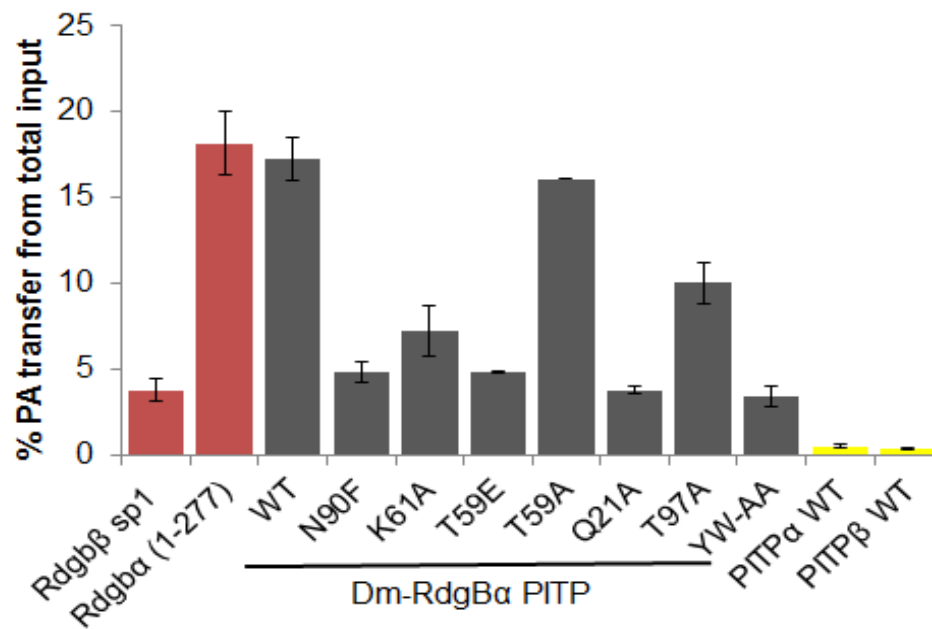
Figure 3.8: Comparison of PA transfer by PITP proteins (0.03 nmol)

3.4: Summary

It was demonstrated in this study that Class II proteins, Hu-RdgBβ and the PITP domain of Human and Drosophila RdgBα, are capable of transferring Phosphatidic acid (PA) *in vitro*; and this property is not shared with Class I PITPs, human PITPα and PITPβ. The PA transfer activity of the RdgBα PITP domains required much lower quantities compared to Hu-RdgBβ. Moreover the maximal activity achieved by RdgBα was greater than that achieved by RdgBβ (Figure 3.4.A). In contrast, PI transfer activity was observed for both classes of PITPs, as expected, since the residues that are essential for binding the inositol headgroup of PI are conserved in all PITPs (Figure 3.4). However, the PI transfer activity of PITPα was higher than the activity of Hu-RdgBβ (Figure 3.4.B) as reported previously[40,41].

On the mutational study of the PITP domain of Dm-RdgBα, I found that all the four mutated proteins (Dm-RdgBα T59A, T59E, K61A and N90F) showed PA transfer similar to the wild type protein up to saturation quantities. However the analysis of all proteins studied in this study at a specific low quantity (0.03nmol) showed the PA transfer activity was diminished for all mutants except T59A (Table 3.2 and Figure 3.8). Furthermore, the mutation of two of the residues studied within the PITP domain of Dm-RdgBα that are in contact with the phosphate moiety of PI showed that the T97A mutant displayed reduced PI transfer while Q21A showed no PI transfer activity (Figure 3.5.B). PA transfer was unaffected by the T97A mutation but the Q21A mutation severely reduced transfer activity (Figure 3.6.A). Since in PITPα the residues Q22 and T97 are involved in the recognition of both PI and PC,[109] the decreased PI transfer activity obtained in this study with the mutants was anticipated. The reduced PA transfer obtained with the mutant Q21A suggested that this residue is involved in PA transfer but not essential. The biochemical analyses of the other two residues that are in contact with the phosphate moiety of PI (T113 and K202) remain to be analysed. Finally, the PA transfer activity of the Y210A/W211A

mutant was compromised compared to the wild type PITP domain (Figure 3.7). This result suggested that association with membranes is not essential for PA transfer activity from RdgB proteins.
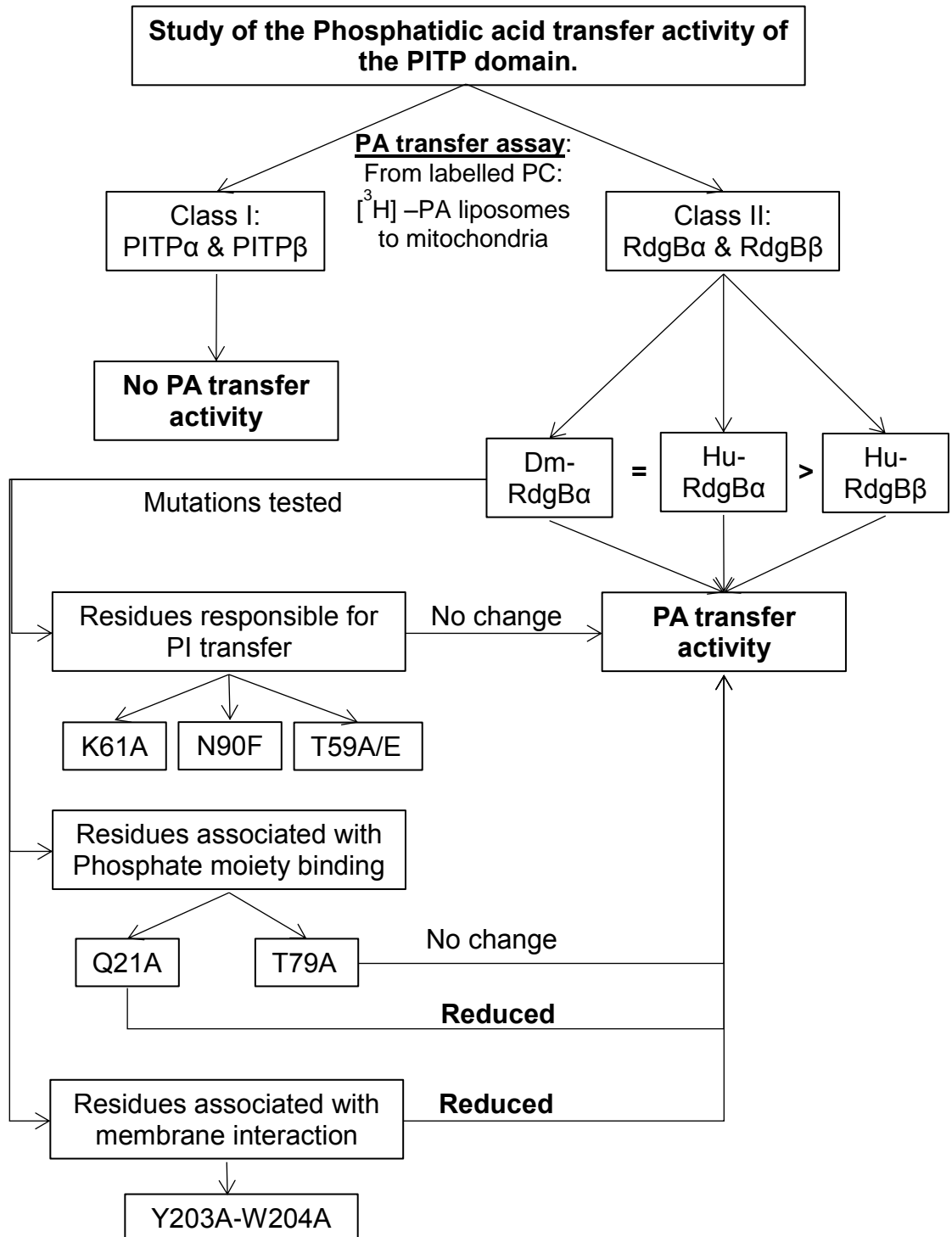
Figure 3.9: Flowchart summarising the results described in Chapter 3.

3.5: Discussion.

This study was unable to find the critical amino acids within the PITP domain of Dm-RdgBα that participate in PA transfer *in vitro*. In the literature, there are few studies of proteins capable of intracellular PA transfer activity. For instance, Hu-RdgBβ was the first protein to be described with PA transfer capability *in vitro*,[40] and we recently reported that Dm-RdgBα is also a PA transfer protein from the findings of this thesis[125]. Additionally, the complex of Ups1 and Mdm35 was reported to transfer PA across mitochondrial membranes in yeast.[26] Recently, the crystal structure of the Ups1-Mdm35 complex showed that the inner wall of the binding pocket is amphiphilic and consists of several conserved basic amino acids (R25, K61 and K155) which were demonstrated to play essential roles in the PA transfer activity between liposomes *in vitro*.[117]

Although no other proteins have been reported to transfer PA, sequence analysis of different PA binding proteins in mammalian cells has shown that they are diverse and share no apparent sequence homology but all contain at least one polybasic motif.[5] Furthermore, the head group of PA was found to be an effective docking site for basic amino acids. For instance, PA showed higher affinity for lysine (K) residues followed by arginine (R) and histidine (H).[66] Following this evidence while examining the sequence alignment of the PITP domain (Figure 3.1), I noticed that five of the residues in proximity to amino acid Q21 of the Hu-RdgBβ sequence are basic amino acids (K18, K28, H29, H31 and R36) and Hu-RdgBα contains three (K28, K29 R31). In contrast, positions 28 and 29 of PITPα andβ are occupied by glutamic acid (E) and alanine (A) and the only basic amino acid between residues 18 and 36 is K31 (Figure 3.1). Since the interaction between PA and the PITP

domain is specific to Class II PITPs (Figure 3.3.A), it is plausible that one or all of the basic residues around Q21 could be essential for PA transfer. I tested this argument by analysing the PA transfer activity of the recombinant mutant PITPα A29K alongside *Dictyostelium discoideum* Dd-PITP, which is homologous to PITPα[103], with lysine at position 29 (K29). However neither of these proteins was positive for PA transfer (Data not shown). Nevertheless, it is still possible that the double basic amino acid sequence (K28K29) and surrounding positively charged residues of RdgB proteins are crucial for their PA binding and transfer activity. Until the crystal structure of any RdgB protein is obtained, the observations into their sequence presented here could be taken into consideration for future biochemical studies.

.

CHAPTER 4: Characterisation of antibodies against RdgBβ in rat heart.

4.1: Introduction

RdgBβ transcripts are strongly expressed in the heart [39,104]. However the physiological function of RdgBβ in cardiac tissue has not been elucidated. By studying the expression pattern of a protein it is possible to identify some clues to understand its behaviour and function. Therefore I sought to describe the endogenous protein expression of RdgBβ in rat heart by immunoblotting. A previous study identified that RdgBβ could be detected in rat heart cytosol using a rabbit polyclonal antibody generated in-house named Ab:101 as well as with a commercial antibody[22]. Ab:101 was validated using recombinant RdgBβ and overexpressed protein expression in Cos7 cells by Western blot. However, the endogenous protein was detected only when rat heart cytosol was subjected to gel filtration to concentrate the antigen and both antibodies identified multiple cross-reactive bands. I began the investigation by confirming the previous observations of Ab:101 in Cos7 cells and recombinant RdgBβ followed by an assessment into the possibility of outcome improvement by affinity purification.

In addition, this study includes the characterisation of another six non-commercially available RdgBβ antibodies. Firstly, Ab:Rb59 is a polyclonal antibody reported in a recent study which identified RdgBβ as a gene targeted by the microRNA miR-126 in human breast cancer cells[90]. In addition, Ab:218 was another in-house made antibody available in the laboratory. Both antibodies (Ab:Rb59 and Ab:218) had not been characterised or validated for western blot analysis of rat

samples. The characterisation includes comparative evaluation of the sensitivity and specificity of antibodies Ab:Rb59, Ab:218 and Ab:101 detection on recombinant and overexpressed RdgBβ using Cos7 cells. The H9c2 cell line which derives from embryonic rat ventricles was also assessed for endogenous RdgBβ expression alongside rat heart samples.

Additionally, four polyclonal antibodies were further commissioned (Ab:R1, Ab:R2, Ab:522 and Ab:523). This Chapter presents a description of the characteristics and detection efficiency of these four RdgBβ antibodies. There is a summary of all the antibodies characterised in this Chapter in Figure 4.1.

Finally, Chapter 4 concludes with a discussion of the observations and highlights the importance of appropriate antibody characterisation and validation in biological experimentation.

Antibody Name	Hu-RdgBβ sp1 Sequence target (Residue numbers)	Reference
101	TKYEDNKGSNDTIFD (111–125) ACDETIPERYYK; (140–151)	Garner et al. 2011. Custom-made
Rb59	DPEKKATLNLPGMHSSDK (308–325)	Png, et al. 2012 Custom-made
218	Full length	Custom-made
R1 and R2	KATLNLPGMHSSDKPC (312-328)	Custom-made
522	DPEKKATLNLPGMHSSDK (308–325)	Custom-made
523	SSIPLLPSSVRSAPS (258-273)	Custom-made

Human: *Homo sapiens* (Q9UKF7.3)
Rat: *Rattus norvegicus* (P_002724619.1)

Length: 332
Identity: 320/332 (96.4%)
Similarity: 330/332 (99.4%)

```
Human     1 MLLKEYRICMPLTVDEYKIGQLYMISKHSHEQSDRGEGVEVVQNEPFEDP  50
            ||||||||||||||||||||||||||||||||||||||||||||||||||
Rat       1 MLLKEYRICMPLTVDEYKIGQLYMISKHSHEQSDRGEGVEVVQNEPFEDP  50

Human    51 HHGNGQFTEKRVYLNSKLPSWARAVVPKIFYVTEKAWNYYPYTITEYTCS 100
            ||||||||||||||||||||||||||||||||||||||||||||||||||
Rat      51 HHGNGQFTEKRVYLNSKLPSWARAVVPKIFYVTEKAWNYYPYTITEYTCS 100

Human   101 FLPKFSIHIETKYEDNKGSNDTIFDNEAKDVEREVCFIDIACDEIPERYY 150
            ||||||||||||||||||||||:|||:||||:||||||||||||||||||
Rat     101 FLPKFSIHIETKYEDNKGSNDSIFDSEAKDLEREVCFIDIACDEIPERYY 150

Human   151 KESEDPKHFKSEKTGRGQLREGWRDSHQPIMCSYKLVTVKFEVWGLQTRV 200
            |||||||||||||||||||||||||:|||||||||||||||||||||||
Rat     151 KESEDPKHFKSEKTGRGQLREGWRDNHQPIMCSYKLVTVKFEVWGLQTRV 200

Human   201 EQFVHKVVRDILLIGHRQAFAWVDEWYDMTMDEVREFERATQEATNKKIG 250
            ||||||||||||||||||||||||||||||||||||||||||||||||||
Rat     201 EQFVHKVVRDILLIGHRQAFAWVDEWYDMTMDEVREFERATQEATNKKIG 250

Human   251 IFPPAISISSIPLLPSSVRSAPSSAPSTPLSTDAPEFLSVPKDRPRKKSA 300
            :|||||||.|.|||||||||||||||||||||||||:|||||||||||
Rat     251 VFPPAISISGIALLPSSVRSAPSSAPSTPLSTDAPEFLSIPKDRPRKKSA 300

Human   301 PETLTLPDPEKKATLNLPGMHSSDKPCRPKSE 332
            ||||||||||||||||||||:::|:||||||||
Rat     301 PETLTLPDPEKKATLNLPGVYASEKPCRPKSE 332
```

Figure 4.1: Sequence alignment of Human and Rat RdgBβ highlighting the targets of the antibodies described in Chapter 4.

4.2: Polyclonal antibody Ab:Rb59 compared to Ab:101 and Ab:218.

The RdgBβ-specific rabbit polyclonal antisera Ab:101 was described previously as raised using two internal peptides common to both rodent and human RdgBβ[41] (Figure 4.1). Ab:101 detected recombinant protein of both RdgBβ splice variants, sp1 and sp2 as well as a C-terminal-truncated protein of the long splice variant (residues 1–263)[41]. In this thesis, the level of detection of antisera Ab:101 was analysed by immunoblotting of recombinant RdgBβ alongside Cos7 cells transfected with and without FLAG-Hu-RdgBβ (Figure 4.2.A). The sera of antibody Ab:101 detected 40ng recombinant Hu-RdgBβ and a strong band when overexpressed in Cos-7 cells corresponding to the expected molecular weight for RdgBβ. No band was seen in cells transfected with an empty vector (Figure 4.2: A; the red arrow indicates the expected molecular weight for RdgBβ). In addition, the antibody recognised an endogenous protein present as a double band at ~35 kDa and another band of ~70kDa. There was an evident background noise all over the PVDF membrane.

A recent study described another custom-made rabbit polyclonal RdgBβ antibody (Ab:Rb59) made against a sequence located at the C- terminal tail of the long isoform of human RdgBβ (Figure 4.1). Ab:Rb59 was used to show that a type of human breast cancer cells (MDA 231 cells) contained RdgBβ by showing a small region of the blot without including molecular weight markers or any other characterisation (Figure 4.2.C). Therefore, I sought to examine the sensitivity and specificity of Ab:Rb59 for RdgBβ protein recognition compared against other antibodies made in-house by my research group (Ab:101 and Ab:218).

Initially, Ab:Rb59 was assayed under the same conditions as serum Ab:101 (Figure 4.2: B). The level of detection by immunoblotting of Ab:Rb59 was ~5ng and above of recombinant RdgBβ. In addition, the level of background noise after the exposure of the PVDF membranes was significantly lower when probing with serum Ab:Rb59 than with Ab:101 and no additional bands were detected. The results also showed that transfected Cos-7 cells with an empty vector do not contain detectable levels of endogenous RdgBβ.

Figure 4.2: Sensitivity test of Ab:Rb59 compared to serum Ab:101

Cos-7 cells were seeded into 60 mm cell culture dishes at a concentration of 2 x10^5 cells/mL and transfected 24 hours later by electroporation with an empty vector [-] or pcDNA3.1-Flag-RdgBβ-sp1 [+]. Two days after transfection, cells were harvested in RIPA buffer. 50µg of each Cos-7 cell lysate alongside 5,10,20 and 40 ng of recombinant Hu-RdgBβ were subjected to western blotting using the RdgBβ antibodies Ab:101 at a 1:1000 dilution [A.] and Ab:Rb59 at a 1:100 dilution [B.] on separate membranes. The red arrow indicates the molecular weight (MW) expected for RdgBβ.

[C.] Figure of Western blot analysis presented as supplementary data taken from Png, et al 2012 showing RdgBβ detection in MDA 231 cells ± mIR-126 knock down.

A.

Cos 7 cells Flag-RdgBβ — Recombinant Hu-RdgBβ-sp1

MW: − + 5 10 20 40 ng

72, 55, 36, 25, 17

Serum Ab:101 1:1000

B.

Cos 7 cells Flag-RdgBβ — Recombinant Hu-RdgBβ-sp1

MW: − + 5 10 20 40 ng

72, 55, 36, 25, 17

Ab:Rb59 1:100

C.

control m126KD

PITPNC1

GAPDH

Signal Intensity: 2.0, 1.5, 1.0, 0.5, 0.0

control m126KD

*
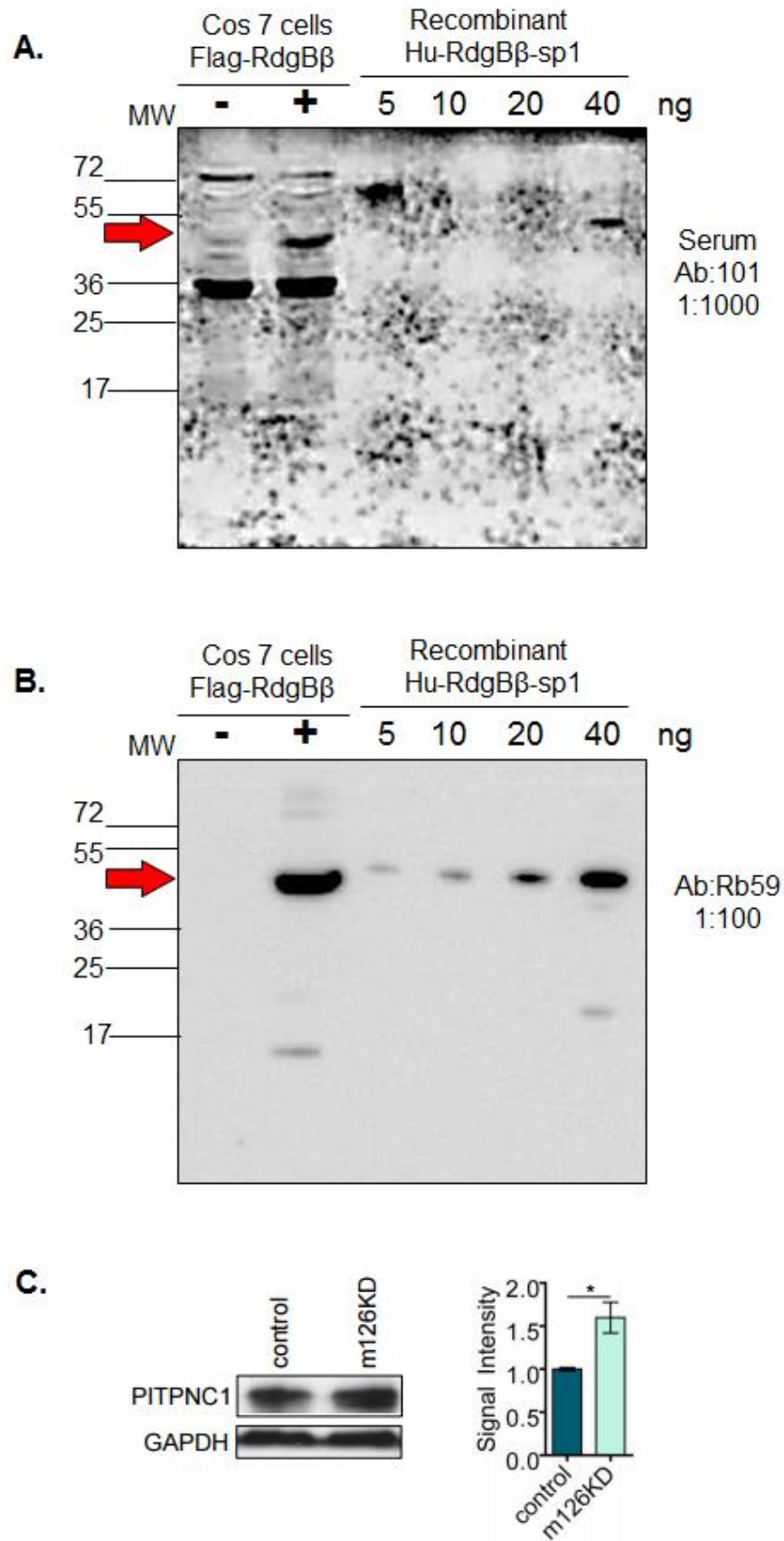
Figure 4.2: Sensitivity test of Ab:Rb59 compared to serum Ab:101.

4.2.1: Affinity purified polyclonal antibodies Ab:101 and Ab:218.

The polyclonal antibody Ab:101 has been used previously to analyse endogenous protein expression of RdgBβ on rat heart cytosol. In order to detect RdgBβ, it was required to concentrate the antigen by gel filtration and Ab:101 identified several additional cross-reactive bands.[41] Therefore I sought to improve antibody specificity by affinity purification of the crude antiserum of Ab:101 using recombinant RdgBβ sp1 covalently immobilised to agarose beads. Alongside Ab:101, I affinity purified the serum of polyclonal antibody Ab: 218 which was produced in-house against the full length sequence of RdgBβ.

Although both antibodies were raised using the human sequence of RdgBβ, the sequence alignment of rat and human showed that the identity of both proteins was high (Figure 4.1). Initially, to evaluate whether there was detectable RdgBβ protein levels in a heart-derived cell line, I performed western blot analysis of different quantities of H9c2 cell lysates. H9c2 cells are derived from embryonic rat ventricles[53]. As controls, I used overexpressed untagged pIRES-RdgBβ in Cos-7 cells and recombinant Hu-RdgBβ. Neither Ab:101 nor Ab:Rb59 were able to detect endogenous RdgBβ in up to 50μg of H9c2 cell lysates (Figure 4.3). This experiment also intended to test whether there was an improved immunoblotting outcome after affinity purification of Ab:101. Indeed the high background on the membrane was eliminated by using purified Ab:101 and the detection level of recombinant protein was also improved (Figure 4.3: A.). Purified Ab:101 detected 10ng and above of recombinant RdgBβ compared to the 40ng detection of the serum seen before (Figures 4.2.A and 4.5.B). However, it still detected cross-reactive bands and the band intensity was not as strong as the detected by Ab:Rb59. (Figure 4.3: B.).

Figure 4.3: H9c2 cells do not contain detectable levels of endogenous RdgBβ.

Cos-7 cells were seeded into 60mm cell culture dishes at a concentration of 2.0 x 10^5 cells/mL and transfected by electroporation one day later with pIRES-RdgBβ. Two days after transfection, cells were harvested in RIPA buffer on ice. H9c2 cells were seeded into a T-75 culture flask at a concentration of $2x10^5$ cells/mL and harvested in RIPA buffer on ice 48 hours later without any treatment. Western blot analysis of 50 μg the transfected Cos-7 cell lysate and 12,25 and 50 μg of non-treated H9c2 cell lysates using as positive controls 5 and 10 ng of recombinant Hu-RdgBβ. Two separate membranes were probed with the RdgBβ antibodies purified Ab:101 at a 1:1000 dilution [A.] and Ab:Rb59 at a 1:100 dilution [B.]

The red arrow indicates the molecular weight (MW) expected for RdgBβ.
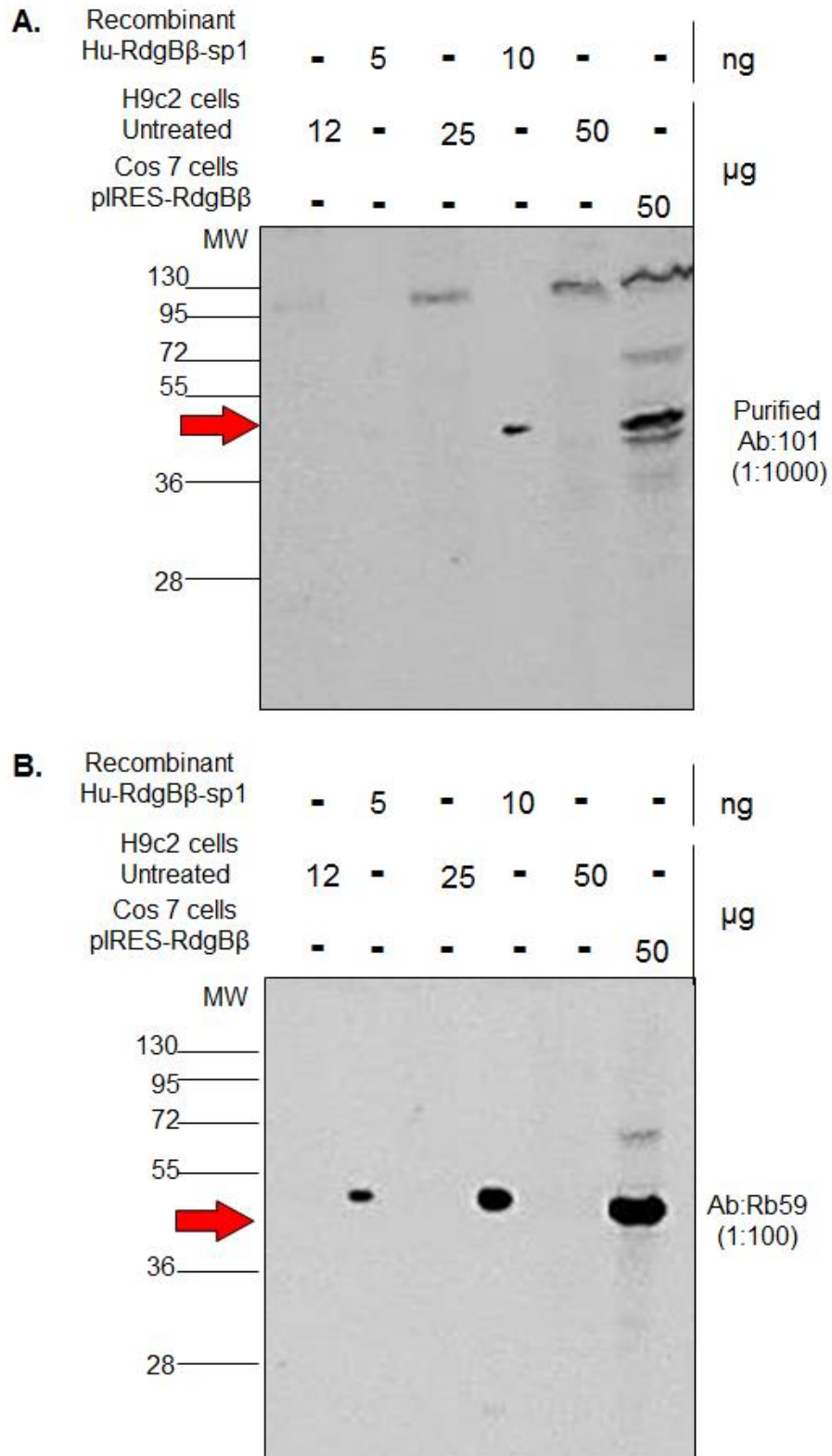
Figure 4.3: H9c2 cells do not contain detectable levels of endogenous RdgBβ.

4.2.2: Sensitivity test of affinity purified Ab:101 and Ab:218.

The sensitivity of the purified antibodies Ab:101 and Ab:218 was analysed by dot blotting. For comparison, the antibody Ab:Rb59 was used (Figure 4.4: A). At a dilution of 1:100, Ab:218 detected 5ng and above, Ab:101 detected 2.5ng and above and Ab:Rb59 detected 1.25ng and above of recombinant Hu-RdgBβ sp1 (Figure 4.4: A). The intensity of the dots obtained by probing with all the antibodies increased linearly with the amount of recombinant RdgBβ (R^2 > 93%) (Figure 4.4: B).

4.2.3: Specificity test of affinity purified Ab:101 and Ab:218.

To test the specificity of the affinity purified antibodies Ab:101 and Ab:218, lysates from whole rat hearts, cellular fractions from rat hearts and isolated adult cardiomyocytes were analysed by Western blot. Ab:R59 was used for comparison (Figure 4.5). Since H9c2 cells did not express detectable quantities of the RdgBβ protein (Figure 4.3), they were used as negative control. As positive controls, H9C2 cells overexpressing untagged pIRES-RdgBβ were expected to be detected at the correct molecular weight. However, pIRES-RdgBβ expression in cells was not as strong as the tagged FLAG-RdgBβ plasmid expression. Therefore, overexpressed FLAG-RdgBβ lysates were also included as positive controls. FLAG-RdgBβ and His-tagged recombinant RdgBβ-sp1 were expected to be detected at a higher molecular weight due to their tags (Figure 4.5; red arrows indicate the expected molecular weight of RdgBβ).

The specificity of Ab: 101 and Ab: 218 did not improve with affinity purification since several bands were detected when using both purified antibodies (Figure 4.5.B. and 4.5.C.). With Ab: 218, there was no a distinguishable band corresponding to RdgBβ (Figure 4.5.C). Purified Ab: 101 did detect bands of the expected size for the recombinant protein and FLAG- RdgBβ controls. However, these bands were not as strong as the cross-reactive bands and pIRES-RdgBβ did not show immunoreactivity to Ab: 101 (Figure 4.5.B).

In comparison, antibody Rb59 detected a single band at the expected molecular weight for all positive controls, while the whole and cytosolic rat heart fractions showed a stronger band at the expected molecular weight and two weak lower cross-reactive bands (Figure 4.5.A).
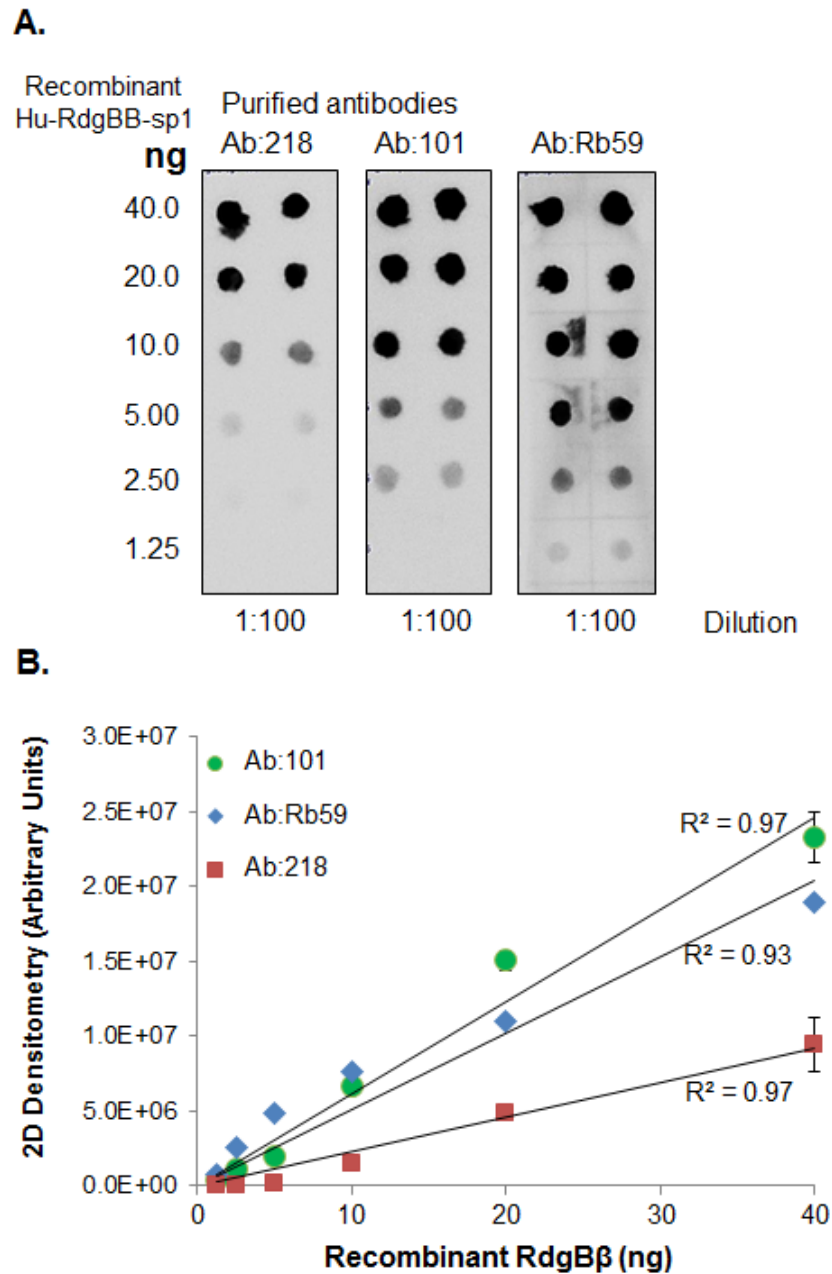
Figure 4.4: Sensitivity of affinity purified polyclonal antibodies 101 and 218 compared to polyclonal antibody Rb59.

[A.] Dot blotting of 2µl of serial dilutions from 40ng to 1.25ng of recombinant Hu-RdgBβ sp1 probed with polyclonal antibodies Ab:Rb59 (0.8mg/ml) and affinity purified antibodies Ab:101 and Ab:218 (1mg/ml). All antibodies diluted at 1:100.

[B.] The intensity of blotted dots was quantified using AIDA software. A single background value was subtracted from the intensity value for each dot. The data shown in the graph are the intensity of the dots in arbitrary units and the amount of recombinant Hu-RdgBβ in nanograms.

Figure 4.5: Specificity test of affinity purified antibodies Ab:101 and Ab:218 compared to antibody Ab:Rb59.

H9c2 cells were seeded into 60mm cell culture dishes at a concentration of 2.0×10^6 cells/mL and transfected 48 hours later with pcDNA3.1-FLAG-RdgBβ-sp1, pIRES-RdgBβ or not transfected [Ctrl]. Two days after transfection, cells were harvested in RIPA buffer on ice. In addition, two whole rat hearts (P21 days old) were isolated from which cytosolic cellular fractions were obtained by differential centrifugation. Western blot of 50 μg of each H9c2 cell and rat heart fraction and cell lysate alongside 10 or 20 ng of recombinant Hu-RdgBβ were subjected to western blotting using the RdgBβ antibodies Ab:Rb59 at a 1:100 dilution [A.] purified Ab:101 [B.] and purified Ab:218 at a 1:100 dilution at a dilution of 1:500 on separate PVDF membranes. The red arrow indicates the molecular weight expected for RdgBβ.
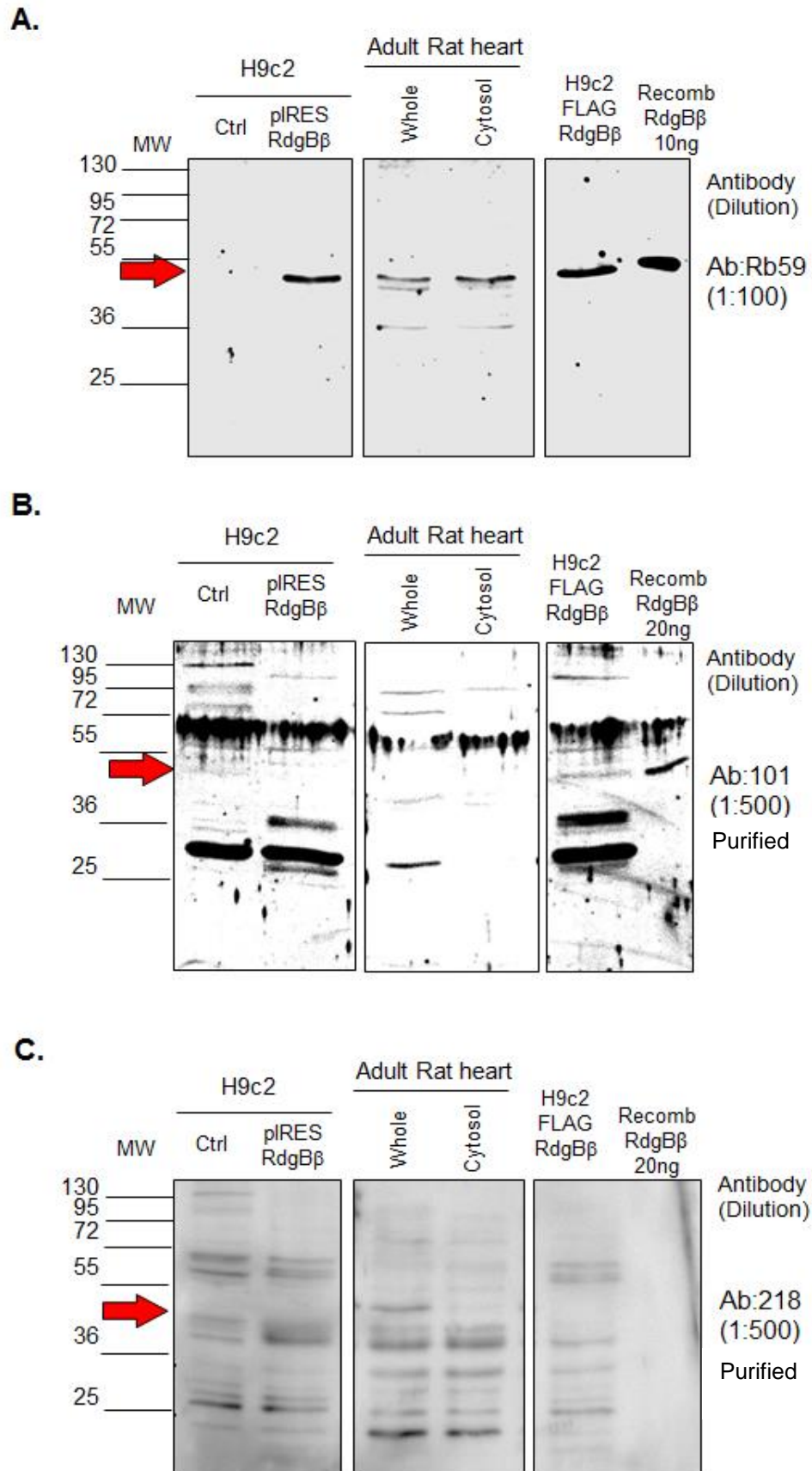
Figure 4.5: Specificity test of affinity purified antibodies Ab:101 and Ab:218 compared to antibody Ab:Rb59

140

4.3: Polyclonal Antibodies R1 and R2

The polyclonal antibody Ab:Rb59 showed better sensitivity and specificity when used in immunoblotting assays of rat heart cellular fractions and recombinant Hu-RdgBβ compared to antibodies Ab:101 and Ab:218 before and after affinity purification (Figures 4.2; 4.3; 4.4; and 4.5). Following these observations and due to the reduced availability of Ab:Rb59, it was decided to commission additional polyclonal RdgBβ antibodies to obtain sufficient antibody with similar effectiveness as Ab:Rb59. Antibodies Ab:R1 and Ab:R2 were raised against an amino acid sequence within the carboxyl extension of human RdgBβ sp1, similar to the sequence used to produce antibody Ab:Rb59. Antibodies Ab:R1 and Ab:R2 were affinity purified by the company who produced them (Eurogentech).

The sensitivity of antibodies Ab:R1 and Ab:R2 was analysed by dot blotting titration using recombinant Hu-RdgBβ (Figure 4.6: A.). Both antibodies Ab:R1 and Ab:R2 detected 0,65 ng and above of recombinant RdgBβ at a dilution of 1:100 as seen for Ab:Rb59 at a 1:200 dilution. However, Ab:R2 showed slightly stronger immunoreactivity than Ab:R1 as evidenced at a dilution of 1:1000 where Ab:R2 detected 0,65 ng and above while Ab:R1 detected 1.25 ng and above of recombinant Hu-RdgBβ (Figure 4.6: A.).

The investigation of the specificity of antibodies Ab:R1 and Ab:R2 was performed by western blotting Cos-7 cell lysates transfected with an empty vector or FLAG-RdgBβ alongside recombinant RdgBβ as control (Figure 4.6: B.; red arrows

indicate the expected molecular weight for RdgBβ). At a dilution of 1:100, Ab:R1 detected 10ng and Ab:R2 detected 5ng of recombinant RdgBβ. Both antibodies detected a band corresponding to FLAG-RdgBβ but there were also additional bands of slightly lower and higher molecular weights detected in both the transfected and the non-transfected cells. None of these bands are likely to be endogenous RdgBβ; they are cross-reactive bands. In addition, Ab:R1 and Ab:R2 showed several other cross-reactive bands of lower and higher molecular weights than the expected for RdgBβ (Figure 4.6: B.). The high cross-reactivity was observed in additional experiments with H9c2 cell lysates which makes both RdgBβ antibodies (Ab:R1 and Ab:R2) unsuitable for immunoblotting assays.

Figure 4.6: Characterisation of polyclonal antibodies Ab:R1 and Ab:R2

[A.] Sensitivity: evaluation by dot blotting of 2µl of serial dilutions from 20ng to 0.65ng of recombinant Hu-RdgBβ sp1 (in duplicate) probed with polyclonal antibodies Ab:R1 and Ab:R2. Ab:Rb59 was used as control. Two antibody dilutions were tested simultaneously 1:100 and 1:1000.

[B.] Specificity: Cos-7 cells were seeded into 60 mm cell culture dishes at a concentration of 2.0×10^5 cells/mL and 24 hours later transfected by electroporation with an empty vector [-] or FLAG-RdgBβ [+]. Two days after transfection, cells were harvested in RIPA buffer on ice. Western blot analysis of 50 µg of each Cos-7 cell lysate alongside 5 and 10ng of recombinant Hu-RdgBβ as controls. Two separate membranes were probed with the RdgBβ antibodies Ab:R1 and Ab:R2 at a 1:100 dilution. The red arrow indicates the molecular weight (MW) expected for RdgBβ.

A.

B.
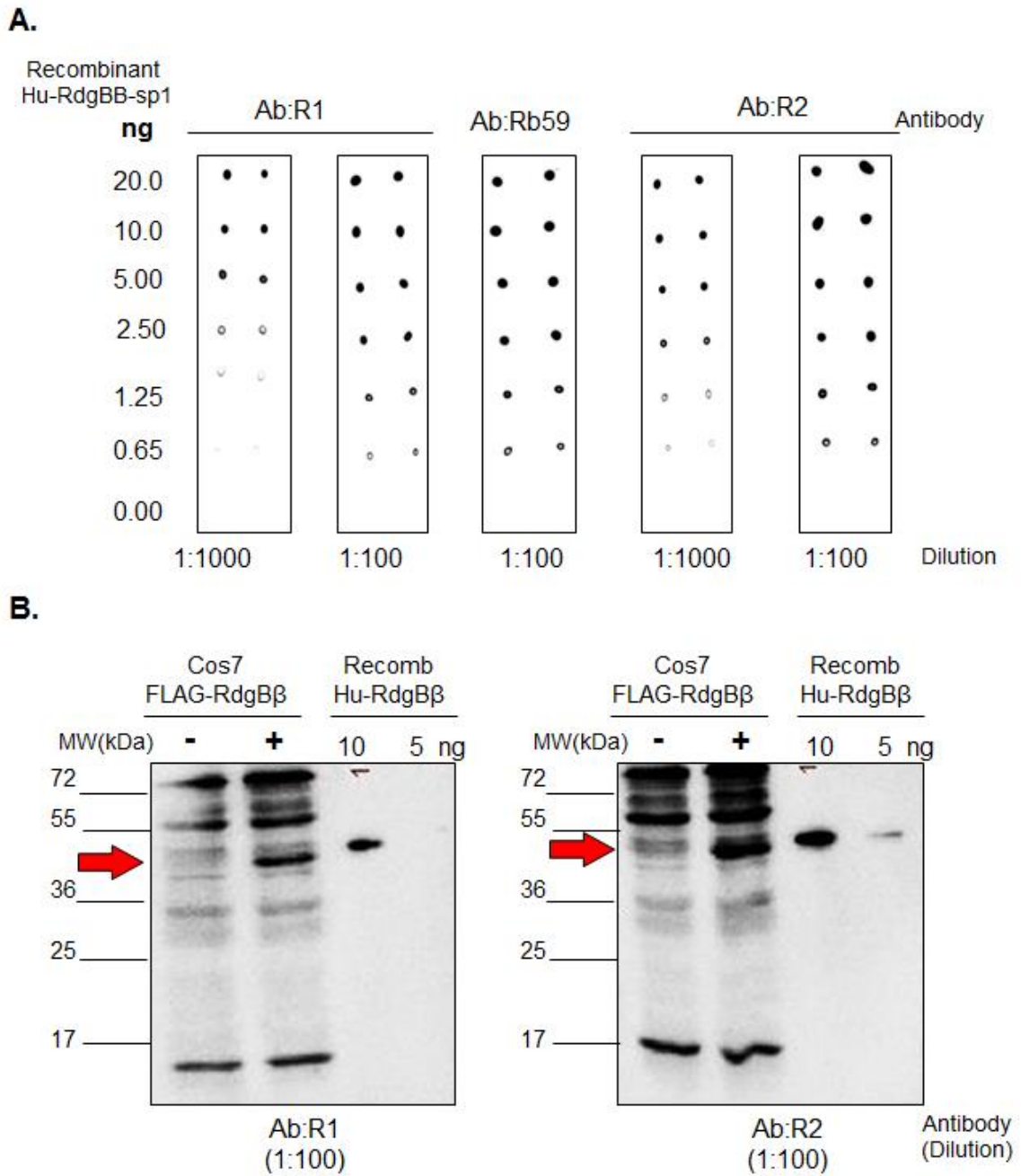
Figure 4.6: Characterisation of polyclonal antibodies Ab:R1 and Ab:R2

4.4: Polyclonal Antibodies Ab:522 and Ab:523

Previously in this chapter, I described Ab:Rb59 as an effective antibody for the detection of RdgBβ. However, the amount of Ab:Rb59 available in the laboratory was limited. The antibody Ab:101 was proven effective for recombinant and overexpressed RdgBβ detection but it was not specific when looking for endogenous protein. Moreover, Ab:218, Ab:R1 and Ab:R2 were also unsuitable for immunoblotting. The need to find another suitable antibody to study the endogenous expression of RdgBβ remained. Therefore two more antibodies were commissioned: Polyclonal antibody Ab:522 which was raised against an identical amino acid sequence as Ab:Rb59, and antibody Ab:523 made against a different peptide sequence to Ab:Rb59 but still within the carboxyl tail of human RdgBβ.

As with all the RdgBβ antibodies described so far, the sensitivity of both antibodies Ab:522 and Ab:523 were assessed by dot blotting titration using recombinant RdgBβ. For comparison, I used purified Ab:101 (Figure 4.7: A.). At a dilution of 1:500, Ab:101 detected 5ng and above, Ab:522 detected 10ng and above and Ab:523 only detected 20ng of the recombinant protein. At a 1:100 dilution, Ab:101 detected 2.5 ng and above, Ab:522 detected 2.5 ng and above and Ab:523 detected 5ng and above of recombinant RdgBβ (Figure 4.7:A).

The specificity for RdgBβ in western blot analysis was tested using Cos-7 cell lysates transfected with FLAG-RdgBβ alongside recombinant RdgBβ (Figure

4.7: B.). Both antibodies detected a strong band at the expected molecular weight corresponding to the transfected Cos-7 cells. However they also detected a band at the expected molecular weight on the non-transfected cells. Since Ab:522 detected only a weak band for the recombinant protein at 20 and 40ng this band is certainly a cross-reactive band. The use of siRNA (small interfering RNA) to silence RdgBβ expression in untreated cells confirmed that the protein being detected at~45 kDa was in fact an unspecific, cross- reactive band.

In addition, Ab:523 detected several other cross-reactive bands of lower and higher molecular weights (Figure 4.7: B.). The high cross-reactivity was observed in additional experiments with H9c2 cell lysates using Ab:523 (Figure 4.8.A). The antibody Ab:523 detected a band at the expected molecular weight for all samples regardless of the differentiation state of the cells. This band was not detected by Ab:Rb59 or Ab:101 (Figure 4.3). Therefore to test whether the band was indeed RdgBβ, undifferentiated H9c2 cells were transfected with rat RdgBβ siRNA for 72 hours to down-regulate mRNA expression which was confirmed by qPCR (Figure 4.8.C). The band observed at the molecular weight expected for RdgBβ was not affected by siRNA transfection (Figure 4.8.B), consequentially meaning that antibody Ab:523 was also not appropriate for detection of the RdgBβ protein using Western blotting.

Figure 4.7: Characterisation of polyclonal antibodies Ab:522 and Ab:523

[A.] Sensitivity: evaluation by dot blotting of 2μl of serial dilutions from 20ng to 0.65ng of recombinant Hu-RdgBβ sp1 (in duplicate) probed with polyclonal antibodies Ab:522 and Ab:523. Purified Ab:101 was used as control. Two antibody dilutions were tested simultaneously (1:100 and 1:500).

[B.] Specificity: Cos-7 cells were seeded into 60 mm cell culture dishes at a concentration of 2.0 x 10^5 cells/mL and 24 hours later transfected by electroporation with an empty vector [-] or FLAG-RdgBβ [+]. Two days after transfection, cells were harvested in RIPA buffer on ice. Western blot analysis of 50 μg of each Cos-7 cell lysate alongside 5, 10, 20 and 40ng of recombinant Hu-RdgBβ as controls. Two separate membranes were probed with the RdgBβ antibodies Ab:522 and Ab:523 at a 1:100 dilution. The red arrow indicates the molecular weight (MW) expected for RdgBβ.
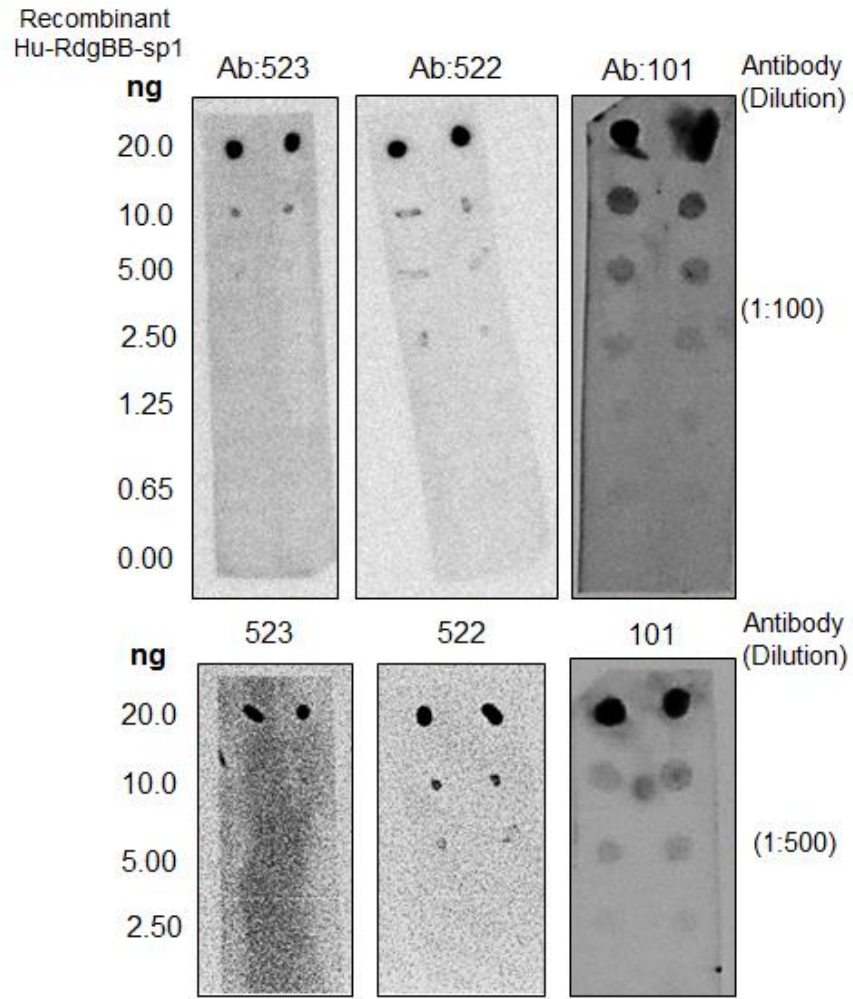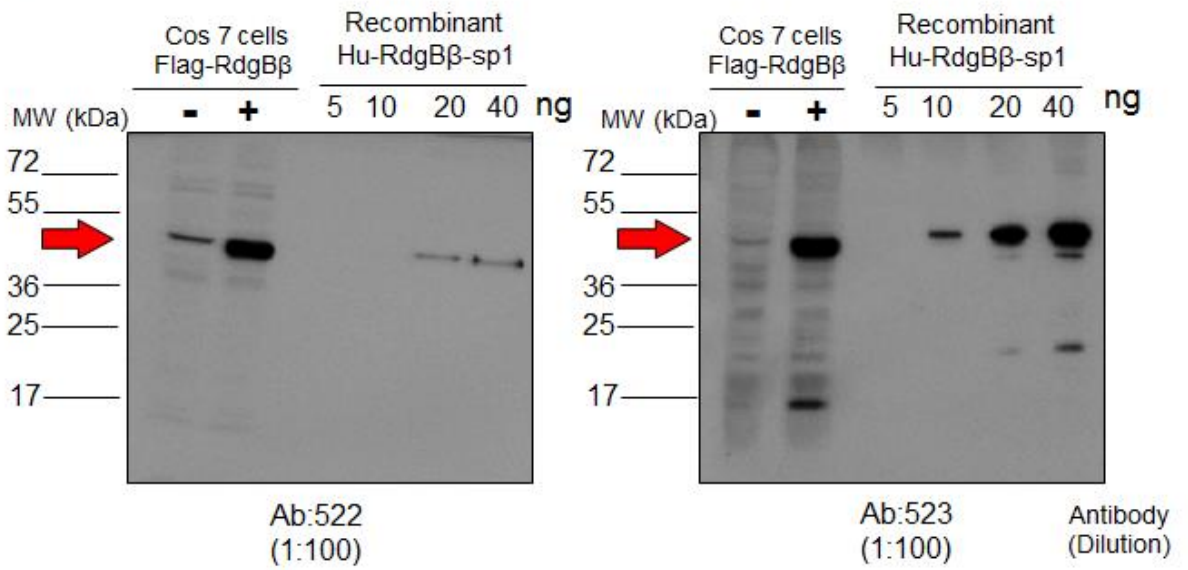
Figure 4.7: Characterisation of polyclonal antibodies Ab:522 and Ab:523

Figure 4.8: Immunoblotting detection of Ab:523 in H9c2 cells

H9c2 cells were seeded in 10 cm^3 cell culture dishes in complete media at a concentration of 2x10^{6}cells/mL and cultured for 48 hours before replacing the media for differentiation media containing 1% FCS in the absence or presence of daily 1µM retinoic acid for 8 days. Media was replaced every 48 hours.

[A.] Western blot analysis of expression levels of RdgBβ in H9C2 whole cell lysates (50µg and 75µg), run alongside varying amounts of Hu-RdgBβ recombinant protein (1-5ng). Ab:523 at 1:100 dilution and anti- Actin at 1:1000 dilution was used as a loading control.

 [B.] H9c2 cells growing in complete media (10%FCS) were transfected with rat - RdgBβ siRNA (12nM) for 72 hours and harvested in RIPA buffer and RNA lysis buffer. The Image shows immunoblotting of 50µg of lysate run alongside 1,5 and 10ng of recombinant RdgBβ probed with Ab:523 at a 1:100 dilution.

[C.] qPCR analysis of H9c2 mRNA of cells growing in complete media transfected with a negative control siRNA, or rat-RdgBβ siRNA normalised to PGK1. Bars represent the average of 3 measurements ± SEM from one experiment.

A.

B.

C.
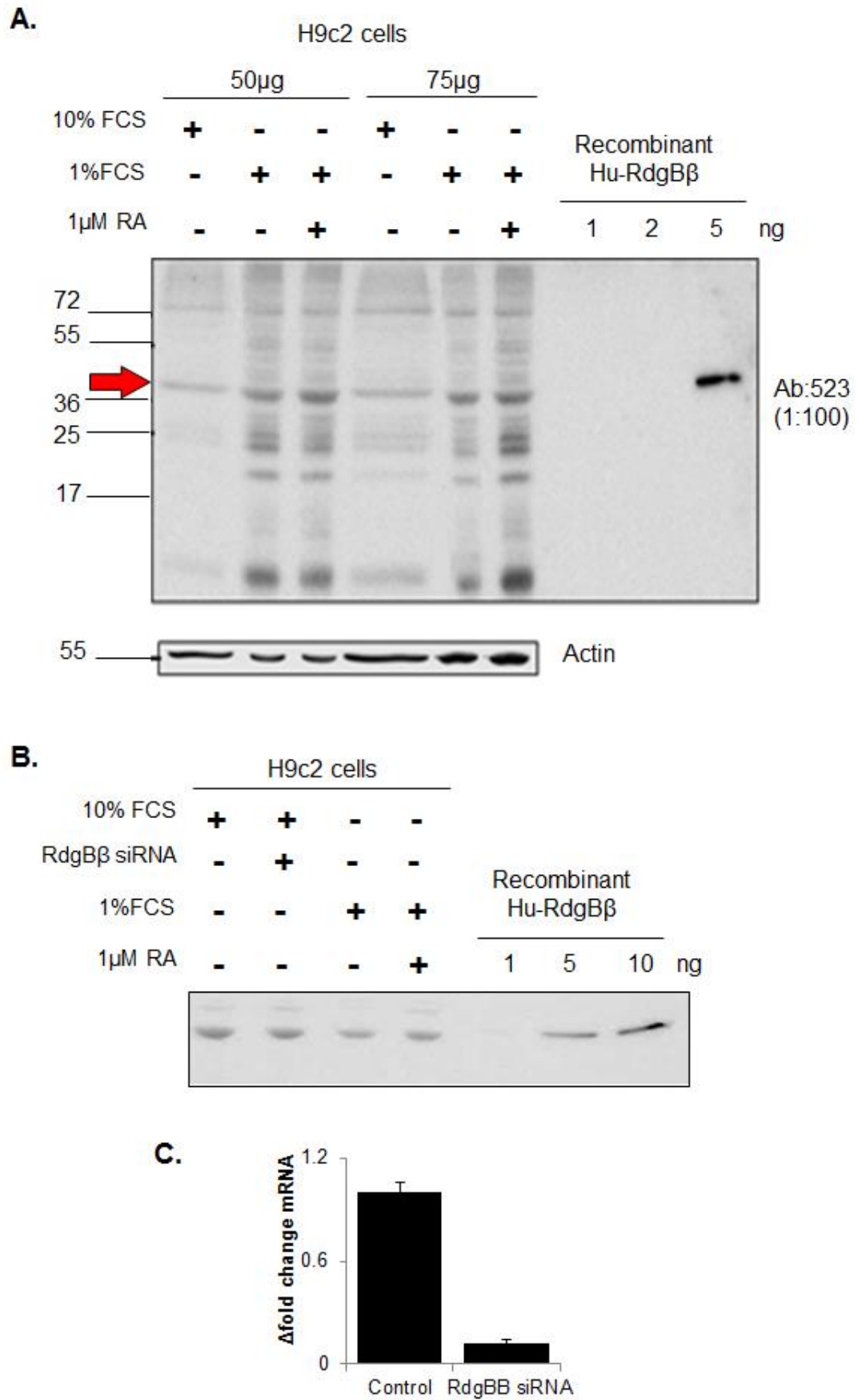
Figure 4.8: Immunoblotting detection of Ab:523 in H9c2 cells

4.5: Summary.

Is there a validated antibody capable of detecting endogenous expression of RdgBβ in rat heart?

Available antibodies

Commissioned antibodies

| 218 | 101 | Rb59 |

| R1 | R2 | 522 | 523 |

Polyclonal

Full length

a.a. 308-325

a.a. 312-328

a.a. 258-273

Peptide sequence antigen from Hu-RdgBβ*

a.a. 111-125

a.a. 308-325

Sensitivity test: Dot Blotting of recombinant protein

5ng 2.5n 0.6ng

0.6ng 0.6ng 2.5ng 5ng

Specificity test: Western Blotting of overexpressed & recombinant protein

Unspecific cross-reactivity

Unspecific cross-reactivity

No **Yes** **Yes**

Validated

No No No No

1:500 1:100

Optimal dilution

Figure 4.9: Flowchart summarising the results described in Chapter 4.

* Peptide sequence of Hu-RdgBβ sp1 (NCBI ref Q9UKF7.2). a.a.: amino acids.

4.6: Discussion

In this chapter, Ab:Rb59 was characterised and validated for the effective detection of RdgBβ by immunoblotting of recombinant and overexpressed protein in Cos7 and H9c2 cells, as well as in rat heart cells and tissue samples. Ab:Rb59 outperformed all other antibodies characterised in this thesis including Ab:101 and Ab:218 before and after affinity purification as well as antibodies Ab:R1, Ab:R2, Ab:522 and Ab:523 (Figures 4.2.B, 4.3.B, 4.4, 4.5 and 4.6).

Ab:101 was found to be effective at identifying recombinant and over-expressed RdgBβ, although it also detected additional cross reactive bands (Figure 4.2.A). These results correlated to the validation of Ab:101 on a previous study. Garner et al. (2011) reported that Ab:101 detected RdgBβ when overexpressed in Cos-7 cells and also no band corresponding to the expected molecular weight for RdgBβ was seen in non-transfected Cos-7 cell lysates. In addition, Ab:101 recognised an endogenous protein present as a double band at ~35 kDa. This doublet was identified as a cross-reactive band since it was not susceptible to RNA interference [41]. On the other hand, I found that the detection level obtained by titration of recombinant RdgBβ was significantly lower than the described before. The serum of the antibody Ab:101 was only able to detect 20ng and above of recombinant RdgBβ (Figures 4.2.A and 4.5.B) compared to the ~5 ng and above reported previously[41]. It has been reported that the functionality of antibodies varies over a period of time[120], it is possible that the antibody Ab:101 lost some detection ability with time.

The high background noise seen for western blot experiments using the sera Ab:101 was reduced with affinity purification and the sensitivity to the recombinant protein also improved (Figure 4.3.A). However, the specificity of the antibody Ab:101 did not improve with affinity purification (Figure 4.5.B), perhaps because it was not completely eluted from the purification gel due to high affinity of the antibody for the recombinant Hu-RdgBβ-sp1.

In addition, the antisera Ab:101 detected protein expression of RdgBβ in rat cytosol concentrated by gel filtration.[41] In this study I showed the endogenous expression of RdgBβ in rat heart samples using Ab:Rb59 without the need for concentrating the antigen (Figure 4.5.A). However, untreated H9c2 cells, which are myoblasts derived from embryonic rat heart, did not show detectable levels of the protein (Figures 4.3 and 4.5). Since the rat heart fractions used for these experiments did not discriminate the type of cells, it is plausible that RdgBβ is expressed in cells other than cardiomyocytes such as fibroblasts or endothelial cells. There is also the possibility that RdgBβ is expressed at later stages in cardiac development.

Antibodies Ab:218, Ab:R1, Ab:R2, Ab:522 and Ab:523 detected recombinant RdgBβ but none was specific at western blotting of H9c2 and Cos7 cells or rat tissue samples (Figures 4.5.C, 4.6.B , 4.7.B and 4.8). Therefore the need to obtain enough quantities of an antibody as effective as Ab:Rb59 still remains. Recently, another RdgBβ antibody was used in a study by the same group who provided us Ab:Rb59.[90] They used a commercial mouse polyclonal antibody raised against a full-length human RdgBβ (Locus AAH07905) for protein detection in human breast

cancer and normal epithelial mammary cells[45]. This antibody was not characterised with respect to its specificity.

Across the biological research literature, problems with cross-reactivity and variability of antibody-based assays have raised difficulties with the reproducibility of results. This has repeatedly put into question the use of non-validated antibodies with appropriate controls[7,120]. In this study, antibodies Ab:R1 and Ab:R2 were raised using an identical amino acid sequence in different animals and they showed dissimilar levels of detection of RdgBβ (Figure 4.6). The same scenario was seen with antibodies Ab:Rb59 and Ab:522 although they were made with the same antigen.

The problem of antibody based research reproducibility is compounded by a lack of consensus in standards and the extensive steps required for full validation. Initiatives such as the Antibody Registry (http://antibodyregistry.org/), intended to help with the identification of the antibodies [113] have been overwhelmed with commercial antibodies lacking characterisation. Nevertheless, it is my personal opinion that scientific journals and reviewers should encourage biological research, which relies on the quality of antibodies for their observations, to include a validation showing specificity, sensitivity, and reproducibility in the context for which the antibody is used or an appropriate citation. A suggested algorithm in Figure 4.10 offers a framework for antibody validation[9]. This information, including those experiments which failed to validate an antibody, could be gathered on a standard online database available to the scientific community. The entries of the database should include mandatory criteria of characterisation that could be used as a citation.
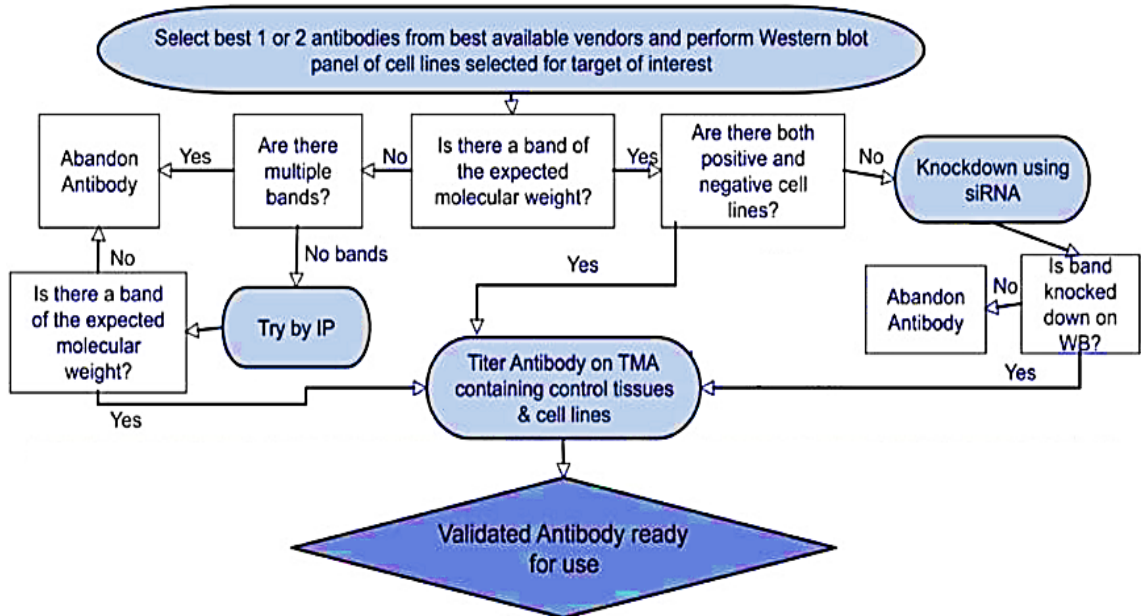
Figure 4.10: Algorithm for antibody validation

Framework of antibody validation for Western Blot (WB) using cell lines in vitro. Tissue microarray (TMA). Adapted from Bordeaux et al. 2010.

Considering the results and limitations described above, it was decided to use Ab:Rb59 for the expression analysis of RdgBβ in rat heart samples throughout this thesis.

CHAPTER 5: Study of RdgBβ expression in rat heart.

5.1: Introduction

Describing the expression pattern of RdgBβ in rat heart cells and tissue fractions could provide indications of its unknown physiological cardiac function. Previously, endogenous protein expression of RdgBβ was found in rat heart cytosol that was concentrated by gel filtration[41]. In addition, the mRNA transcripts of RdgBβ were also strongly expressed in heart samples[39,104]. In Chapter 4, it was described how I was able to directly detect endogenous protein expression of RdgBβ in adult rat heart fractions by immunoblotting using antibody Ab:Rb59 (Figure 4.5). However, it was unclear the type of cells that was expressing RdgBβ or whether protein expression was regulated with cell development since I also observed that the rat heart embryonic cell line H9c2 did not show detectable levels of RdgBβ protein (Figure 4.3). To address these questions and characterise the mRNA and protein expression of RdgBβ in rat heart further, I sought to evaluate the ability of H9c2 myoblast to differentiate into muscle cells or cardiomyocyte-like cells depending upon the composition of the culture media. The study also compares adult and neonatal rat heart samples and primary cardiomyocytes isolated from neonatal heart tissue.

This chapter first describes the endogenous expression of RdgBβ protein and mRNA after H9c2 myoblast differentiation to test whether RdgBβ is expressed in either skeletal or cardiac muscle and if this expression is regulated during muscle development. In addition, immuno-detection of RdgBβ by Ab:Rb59 was verified by

RNA interference transfection of H9c2 cardiomyocyte-like cells. The sub-cellular localisation of RdgBβ in differentiated H9c2 cells was also analysed.

Furthermore, RdgBβ expression was compared between neonatal and adult rat heart tissue to assess any changes related with cardiac maturity and this chapter also includes an analysis of isolated neonatal rat cardiomyocytes as a primary system for studying RdgBβ in rat heart. Finally, the cellular distribution of RdgBβ was explored in adult cardiac tissue in comparison to brain and liver cellular fractions. The chapter concludes with a discussion of the observations and recommendations for future studies.

5.2: Analysis of RdgBβ expression in H9c2 cells.

H9c2s cells conserve the ability to differentiate into muscle cells, either skeletal or cardiac-like[80], which have not been evaluated for endogenous RdgBβ protein expression. Proliferating myoblasts were cultured in media supplemented with 10% foetal calf serum (FCS). By reducing the FCS content to 1% for a minimum of 8 days, H9c2 myoblasts stopped cell cycling and started differentiation towards a skeletal muscle phenotype. When the serum reduction to the culture media was complemented with daily addition 1µM all-trans retinoic acid (RA) treatment, H9c2 cells differentiated into a cardiomyocyte-like cell line as indicated by the detection of cardiac troponin I (a cardiac marker) by immunoblotting (Figure 5.1).

Endogenous RdgBβ protein expression was examined by immunoblotting using antibody Ab:Rb59 (Figure 5.1). As expected, there was no band detected at

the expected molecular weight for RdgBβ in proliferating H9c2 cells (Figure 5.1; the red arrow indicates the expected molecular weight for RdgBβ). Similarly, H9c2 cells differentiated with 1% FCS alone showed no detectable protein expression. In differentiated H9C2 cells that were treated with retinoic acid, there was a strong band corresponding to the molecular weight of RdgBβ by immunoblotting. However Ab:Rb59 also identified an endogenous cross reactive band at ~55kDa in all samples. The increased expression of RdgBβ following differentiation was highly specific for this PITP family member. Class I PITP levels were unaltered by cellular differentiation of H9c2 cells (Figure 5.1 lower panel).

In addition, rat RdgBβ mRNA expression was assessed by end point polymerase chain reaction (PCR) with the expression of GAPDH used as loading control (Figure 5.2.A) followed by quantitative real time PCR (qRT-PCR) where RdgBα was used for comparison (Figure 5.2.B). RdgBβ mRNA expression was found in undifferentiated H9C2 cells by PCR and qRT-PCR, but RdgBβ mRNA analysis showed a stronger band with cellular differentiation detected by PCR and a 2.4±0.4 fold increase, obtained by qRT-PCR. A stronger band was also seen by PCR compared to cells cultured in 10%FCS and 1%FCS alone. Additionally, RdgBβ mRNA showed a 3.7±0.3 fold increase compared to proliferating H9c2 cells. In comparison, the other PITPs evaluated showed no variation in their expression (PITPβ protein and RdgBα mRNA) upon H9c2 differentiation.
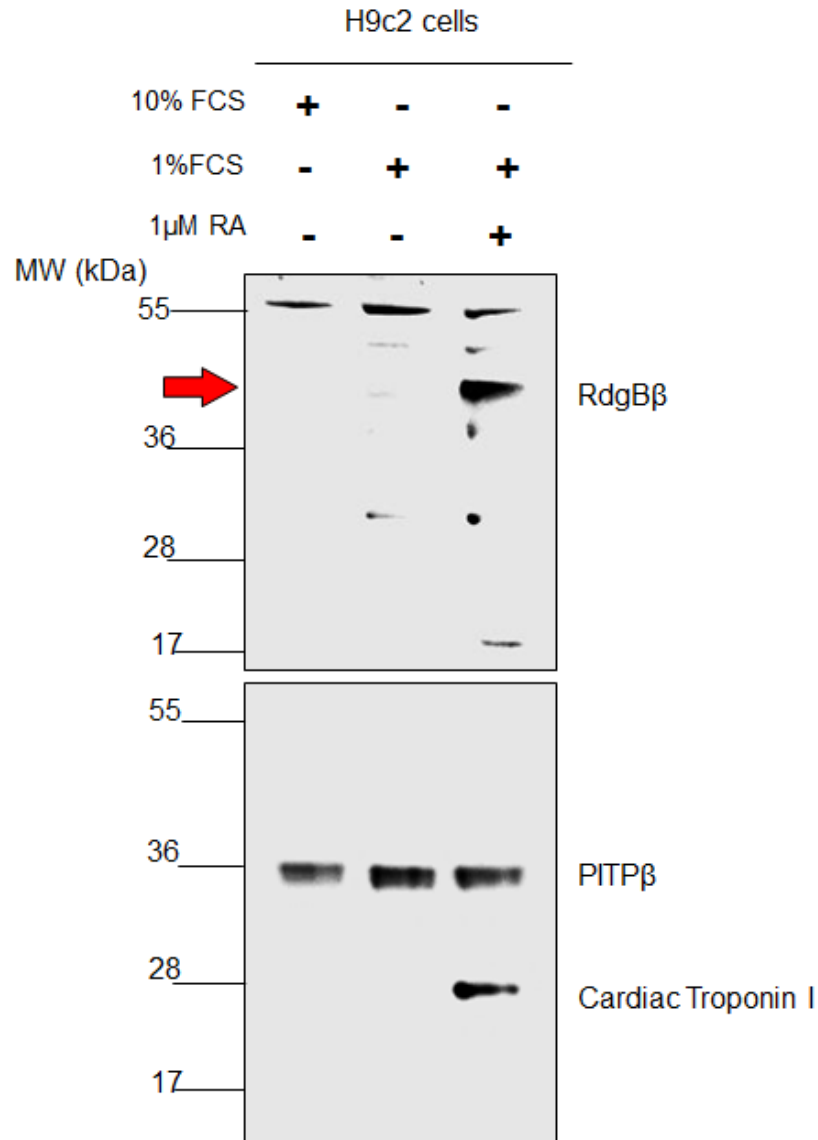
Figure 5.1: Endogenous RdgBβ protein expression in differentiated H9c2 cells

H9c2 cells were seeded into T75 culture flasks at a concentration of 2.0×10^6 cells/mL and cultured for 10 days in culture media supplemented with10% foetal calf serum (FCS) and passaged every two days; 1% FCS and the media replaced every two days; or 1% FCS media replenished every two days plus daily treatment with 1μM all-trans retinoic acid (RA). Cell lysates were harvested in RIPA buffer. 50μg of lysates were electrophoresed on a 4-12% NuPage gradient acrylamide gel. The Western blotting analysis used polyclonal antibody Ab:Rb:59 at a 1:100 dilution, and on a separate membrane, polyclonal anti-PITPβ (Ab:1C1) and anti-cardiac troponin I at a 1:1000 dilution were probed. Red arrow indicates the expected molecular weight for RdgBβ. MW: molecular weight.

A.

B.
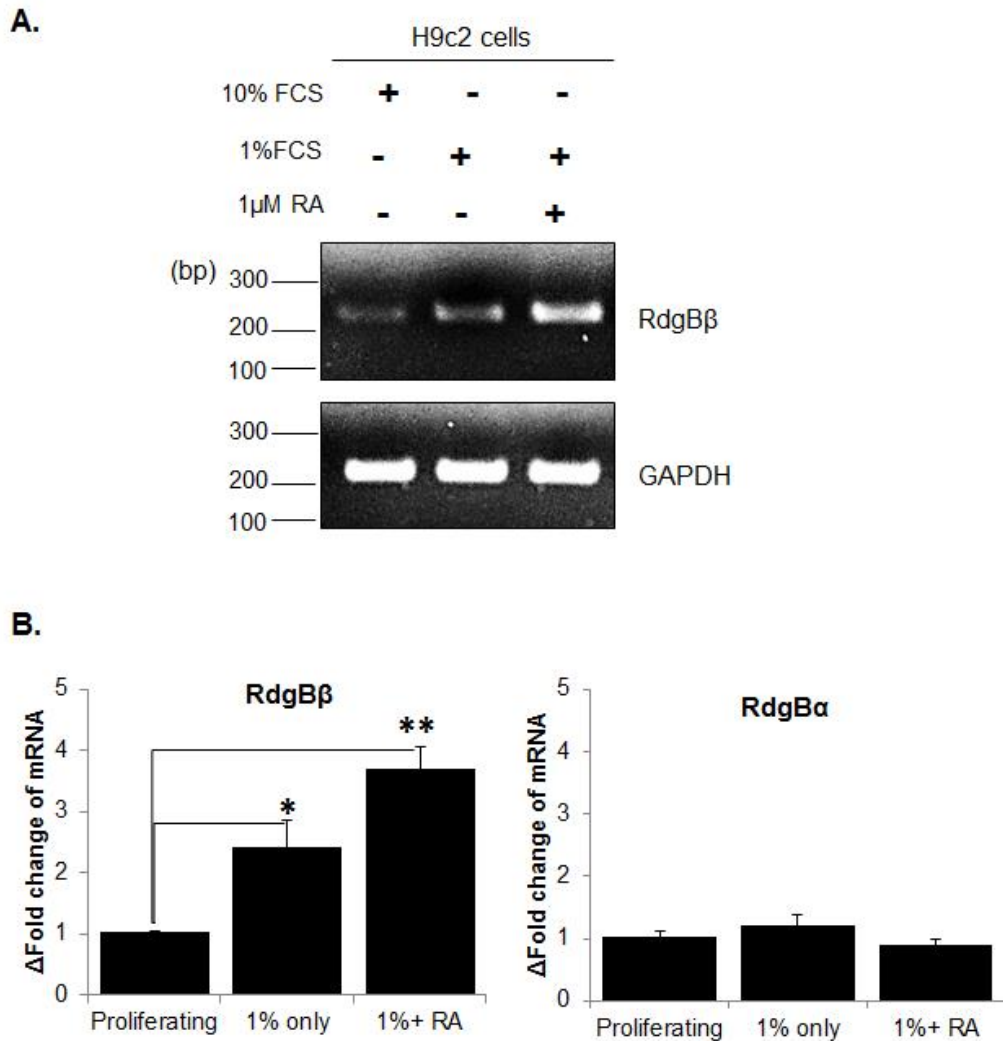
Figure 5.2: RdgBβ mRNA expression in differentiated H9c2 cells.

H9c2 cells were cultured for 8 days in culture media supplemented with 10% foetal calf serum (FCS); 1% FCS, or 1% FCS media plus daily treatment with 1µM all-trans retinoic acid (RA). RNA was extracted from cell lysates and 1µg RNA was used to obtain cDNA by reverse transcription.

[A.] End point PCR of 5µL cDNA using Taq polymerase and the indicated primers. Glyceraldehyde 3-phosphate dehydrogenase (GAPDH) was used as loading control.

[B.] qRT-PCR of 5µL cDNA using SYBR green. Fold change calculated using the ΔΔCt formula where Ct values were obtained in triplicate and normalised to the Ct values for PGK1. (*):p=0.002 (n=15 from 5 experiments) (**): p=1.7×10^{-9} (n=33 from 11 experiments).

5.2.1: Rat RdgBβ siRNA transfection.

To confirm that the band observed by Western blot upon H9c2 differentiation was indeed RdgBβ (Figure 5.3), the mRNA of RdgBβ was downregulated during the last three days of differentiation. The analysis was performed in duplicate by western blotting (Figure 5.3.A). The immunodetection experiment showed the loss of the ~44kDa bands corresponding to RdgBβ with rat RdgBβ siRNA transfection compared to the bands detected from differentiated cells transfected with a negative siRNA control. The rat RdgBβ siRNA transfection efficiency and specificity were evaluated by qRT-PCR. The RdgBβ mRNA expression of differentiated cells was reduced by 88% compared to the negative siRNA control whilst the mRNA of rat RdgBα was not altered (Figure 5.3.B).

5.2.2: Expression regulation during cardiomyocyte development.

Endogenous Rdgbβ was detected after differentiation of H9c2 with reduced serum and retinoic acid for 8 and 10 days (Figure 5.1 and Figure 5.2). In order to test the expression over time during differentiation, mRNA and protein were analysed by qRT-PCR and western blotting at 0, 4, 8, 10 and 12 days differentiation (Figure 5.4). Protein expression was not detected until day 8 of RA treatment and it increases on day 10 and remains until day 12 of the experiment (Figure 5.4.A). mRNA increased overtime from 0 to 8 days (2.7±0.3 fold increase) and remained at the same level until day 12 (Figure 5.4.B). The experiment was repeated three times with the same results. The difference of the mRNA and protein expression at day four suggest that translation of RdgBβ has not taken place or that the amount of RdgBβ was not detected by the antibody. However these observations indicate that RdgBβ expression increases with cardiomyocyte maturity.

Figure 5.3: Rat RdgBβ siRNA transfection in differentiated H9c2 cells

[A.] Protein expression was analysed by Western blot analysis of 75µg lysate of H9c2 cells differentiated in 1% FCS media plus daily treatment with 1µM all-trans retinoic acid (RA). On day 8 of culture, cells were transfected for 72 hours with 12nM Rat RdgBβ siRNA oligonucleotides 2+3 or a negative siRNA. Cell lysates were harvested in RIPA buffer and the protein separated using SDS-PAGE. Probing of the membrane was performed using polyclonal antibody Ab:Rb:59 at a 1:100 dilution. The red arrow indicates the expected molecular weight for RdgBβ. MW: molecular weight.

[B.] 1µg RNA of differentiated H9c2 cells transfected with rat RdgBβ or a negative siRNA was used to obtain cDNA by reverse transcription. qRT-PCR was performed using 5µL cDNA using SYBR green and the indicated rat primers (RdgBβ and RdgBα). The mRNA fold change expression was calculated using the ΔΔCt formula. Ct values were obtained in triplicate and normalised to the Ct values for Phosphoglycerate Kinase 1 (PGK1). Bars represent data of 2 separate experiments for RdgBβ plus 1 experiment in triplicate for RdgBβ and RdgBα. Error bars indicate SEM.

A.

Differentiated H9c2 cells

B.
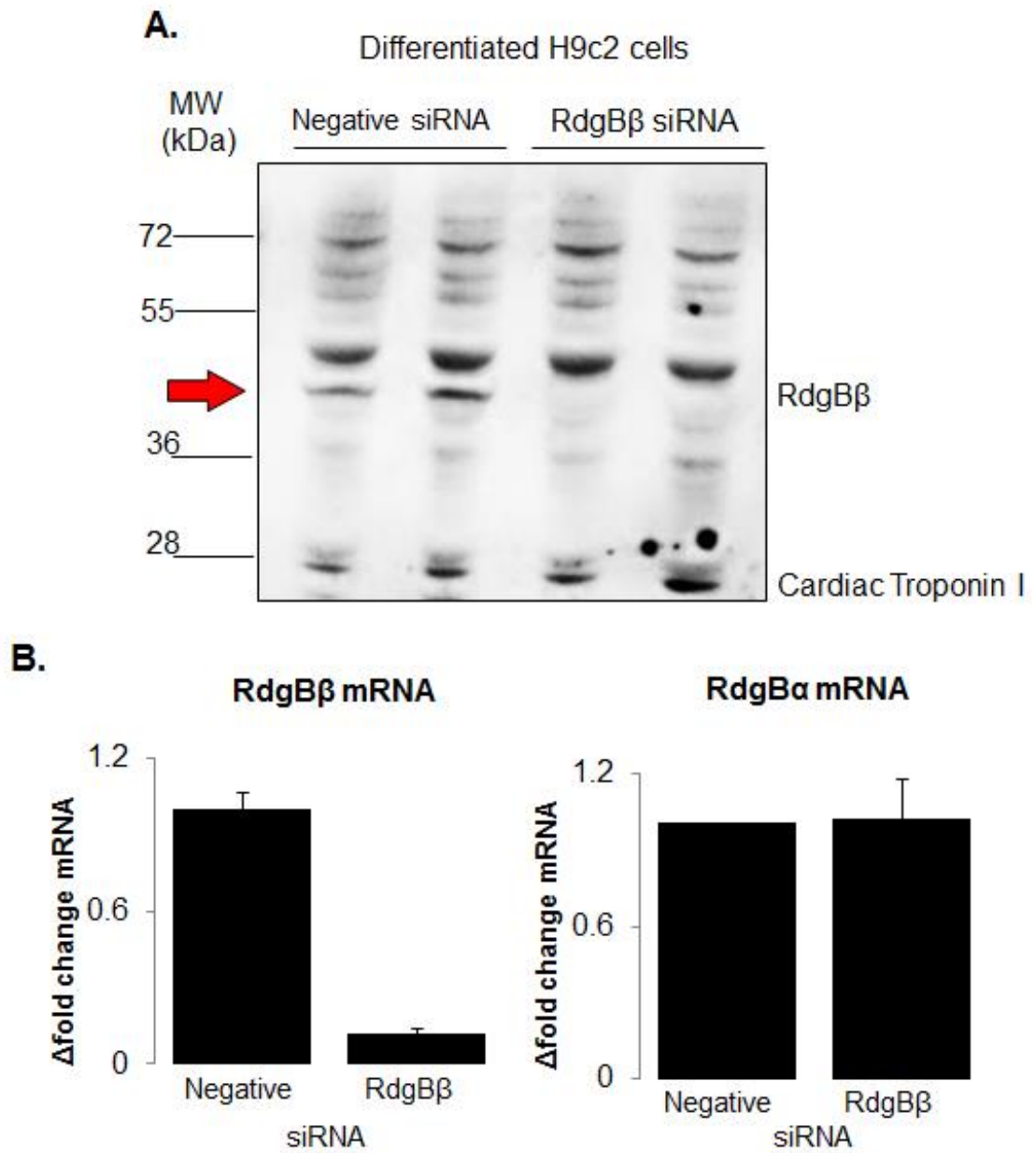
Figure 5.3: Rat RdgBβ siRNA transfection in differentiated H9c2 cells.
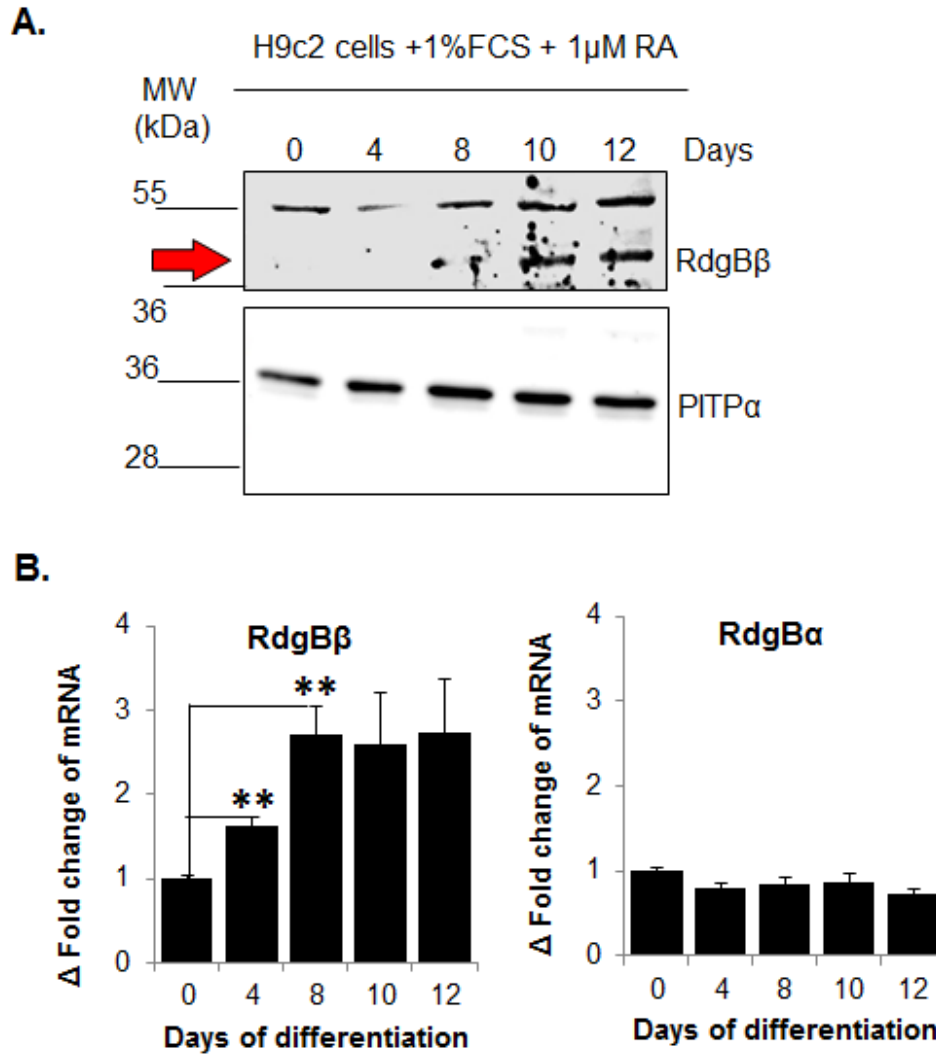
Figure 5.4: RdgBβ expression increases over time of differentiation of H9c2 cells. H9c2 undifferentiated cells were seeded into 6 well culture dishes at a concentration of 2.0 x 10⁶cells/mL and cultured for 2 days in media supplemented with 10% FCS which was then replaced for differentiation media and cultured for the number of days showing in the figure (0, 4, 8, 10 and 12). Cell lysates were harvested in RIPA buffer and RNA lysis buffer.

[A.] The protein content of the H9c2 cell lysates (75µg for RdgBβ and 50µg for PITPα) were separated in NuPage gradient gels (4-12%) and analysed by western blotting using polyclonal antibody Ab:Rb:59 at a 1:100 dilution, and anti-PITPα (Ab:674) at a 1:1000 dilution. Red arrow indicates the expected molecular weight for RdgBβ. MW: molecular weight.

[B.] 1µg RNA from cell lysates was used to obtain cDNA by reverse transcription. qRT-PCR was performed using 5µL cDNA, SYBR green and 300nM primers. The calculation of the change in mRNA expression was achieved using the $\Delta\Delta Ct$ formula where triplicate Ct values measured from each set of primers were normalised to the Ct values for PGK1. Bars show mean ± SEM of Ct measurements from 3 experiments (**): $p < 0.001$.

5.2.3: Subcellular localisation.

Overexpressed tagged RdgBβ was reported to be diffusely present throughout the cytoplasm. Human FLAG- RdgBβ in HEK293 cells[39] and Cos7 cells,[41] and mouse GFP-RdgBβ in PC12 cells.[104] In order to analyse the intracellular localisation of endogenous RdgBβ, cardiomyocyte-like H9c2 cell fractions were immunoblotted using antibody Ab:Rb59. The cellular fractions were obtained by differential centrifugation of cell lysates after 10 days of differentiation (1%FCS + 1μM RA). Fraction purity was assessed by immunoblotting using a mitochondrial marker (GRP75) and, PITPα, a soluble PITP located in the cytosol, was used for comparison. Ponceau staining of the membrane before probing was used as loading control (Figure 5.5).

Anti-GRP75 probing showed enrichment in crude mitochondrial fraction and no signal from microsomes indicating no mitochondrial contamination. The band corresponding to RdgBβ was enriched in the cytosolic fraction compared to whole cell extracts whereas very weak bands were seen at microsomes or crude mitochondria. In contrast, PITPα probing although it was enriched in the cytosol, it detected no bands on microsomes or crude mitochondria. These results localise RdgBβ primarily at the cytosolic fraction of differentiated H9c2 cells.
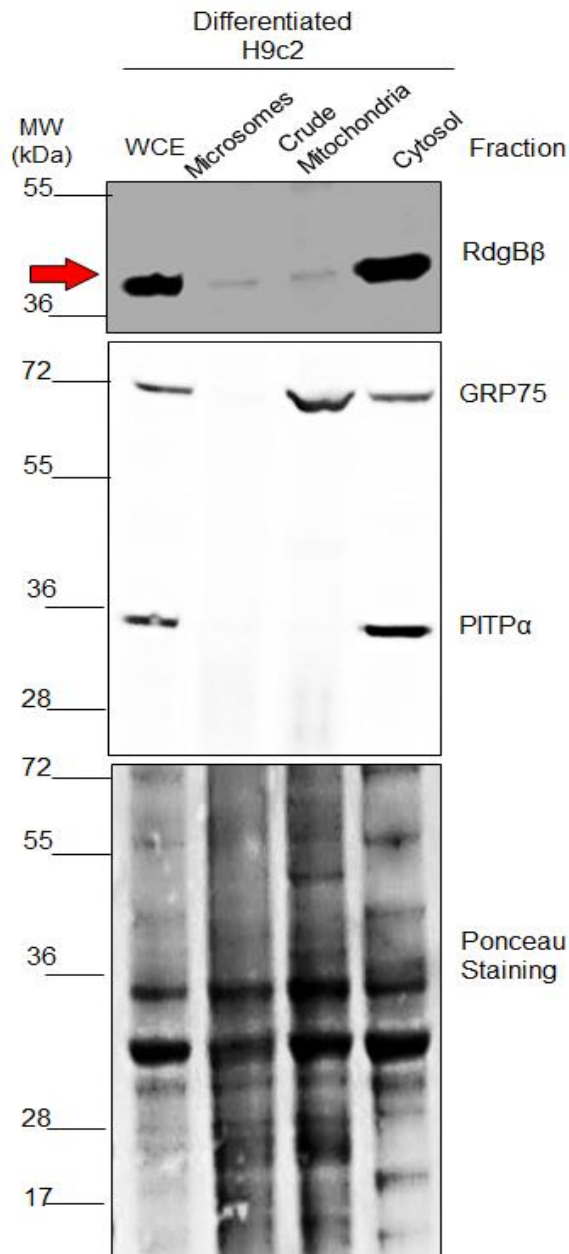
Figure 5.5: RdgB*β* is a cytosolic protein in differentiated H9c2 cells. H9c2 cells were cultured for 10 days in culture media supplemented with 1% FCS media plus daily treatment with 1µM all-trans retinoic acid (RA). Cell lysates were harvested in SET buffer and subjected to differential centrifugation fractionation. 50µg of each lysate was subjected to SDS-PAGE on NuPage 4-12% gradient acrylamide gel. PVDF membrane was imaged after Ponceau solution staining as loading control. Western blotting was performed using polyclonal Ab:Rb59 at a 1:100 dilution; and on a separate membrane using polyclonal antibodies anti-GRP75 (Ab:GRP75) as mitochondrial marker and anti-PITPα (Ab:674) at a 1:1000 dilution as comparator. Red arrow indicates the expected molecular weight for RdgBβ. MW: molecular weight.

5.3: Analysis of RdgBβ expression in rat heart.

The endogenous protein expression of RdgBβ was found in H9c2 cells that were differentiated towards a cardiomyocyte-like phenotype (Figure 5.1). In order to verify the presence of RdgBβ in primary samples, hearts from the *Rattus novergicus*, strain Sprague-Dawley were analysed for protein and mRNA expression of RdgBβ.

5.3.1: RdgBβ expression is stronger in adult than in neonatal rat heart.

To analyse whether the protein expression of RdgBβ changes with maturity, whole cell lysates from neonatal (1-2 days old) and adult (3 months old) rat hearts were obtained as described in Section 2.5; and immunoblotted using antibody Ab:Rb59 alongside proliferating H9c2 cells that were transfected with either an empty vector or untagged pIRES-RdgBβ as negative and positive controls respectively. Lysates were also blotted for 14-3-3 protein as loading control. I was able to demonstrate the presence of RdgBβ in both neonatal and adult rat heart whole cell lysates. Adult rat heart fractions showed a strong and specific immunoreactivity to Ab:Rb59 at the expected size for RdgBβ (Figure 5.6.A.). However hearts from neonatal rats (2 days old) showed much lower levels of the protein (Figure 5.6.B.). This result indicates that RdgBβ is upregulated upon maturation.
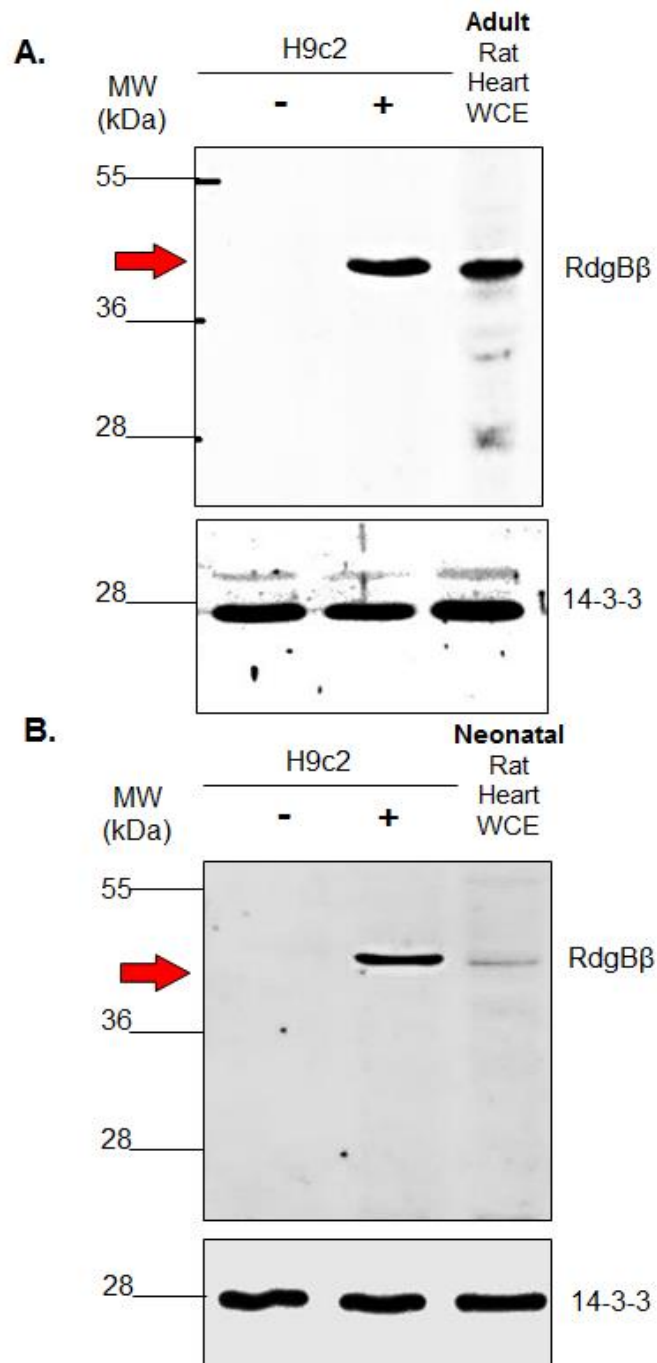
Figure 5.6: RdgBβ expression is stronger in adult than in neonatal rat heart.
H9c2 cells cultured in complete media (10% FCS) were transfected for 48 hours with either pcDNA3.1-FLAG-RdgBβ-sp1 [+] or an empty vector [-]. Cell lysates were harvested in RIPA buffer. In addition, Sprague-Dawley rat hearts were dissected and lysed in SET buffer. [A.] Two hearts from adult (3 months old) rats. [B.] Four hearts from neonate pups (2 days old) rats. The figure shows western blotting analysis of 50µg of each lysate using polyclonal Ab:Rb59 at a 1:100 dilution; and on separate membranes, probed with anti-14-3-3 (Ab:14-3-3) for comparison. Red arrows indicate the expected molecular weight for RdgBβ. MW: molecular weight.

5.3.2: RdgBβ expression in isolated neonatal rat cardiomyocytes

Cardiac tissue is comprised of cardiomyocytes and other constituent cell types including fibroblasts and endothelial cells. RdgBβ was detected in whole cell lysates from heart tissue which did not distinguish between cell types (Figure 5.6). Therefore whether the presence of RdgBβ in rat heart is due to cardiomyocyte content was tested by immunoblotting. Although RdgBβ expression was stronger in adult rat heart lysates, neonatal rat cardiomyocytes (NRC) were chosen as the primary system to study RdgBβ since their isolation, culture and transfection was more suitable to the laboratory set up than adult cells.

Cardiomyocytes were isolated by serial digestion of neonatal rat hearts, cell lysates were immunoblotted for a known cardiomyocyte marker (cardiac troponin I). There was a positive reaction of whole heart and isolated heart cells to the cardiac troponin I antibody. However, isolated heart cells that were cultured for 48 hours in maintenance media showed reduced reactivity to the cardiac troponin I antibody.   In addition, preparations of freshly isolated neonatal rat cells were positive to Ab:Rb59 immunoblotting similar to rat heart whole cell extracts (Figure 5.7.A). The mRNA expression of RdgBβ was also observed in neonatal rat hearts and isolated cells (Figure 5.7.B). Isolated neonatal rat cardiomyocytes showed a similar low intensity band as seen in proliferating H9c2 cells. These observations suggest that RdgBβ is expressed in cardiomyocytes, and that NRCs are an effective system to study RdgBβ. However, after cell culture RdgBβ expression is lost which was not investigated further.
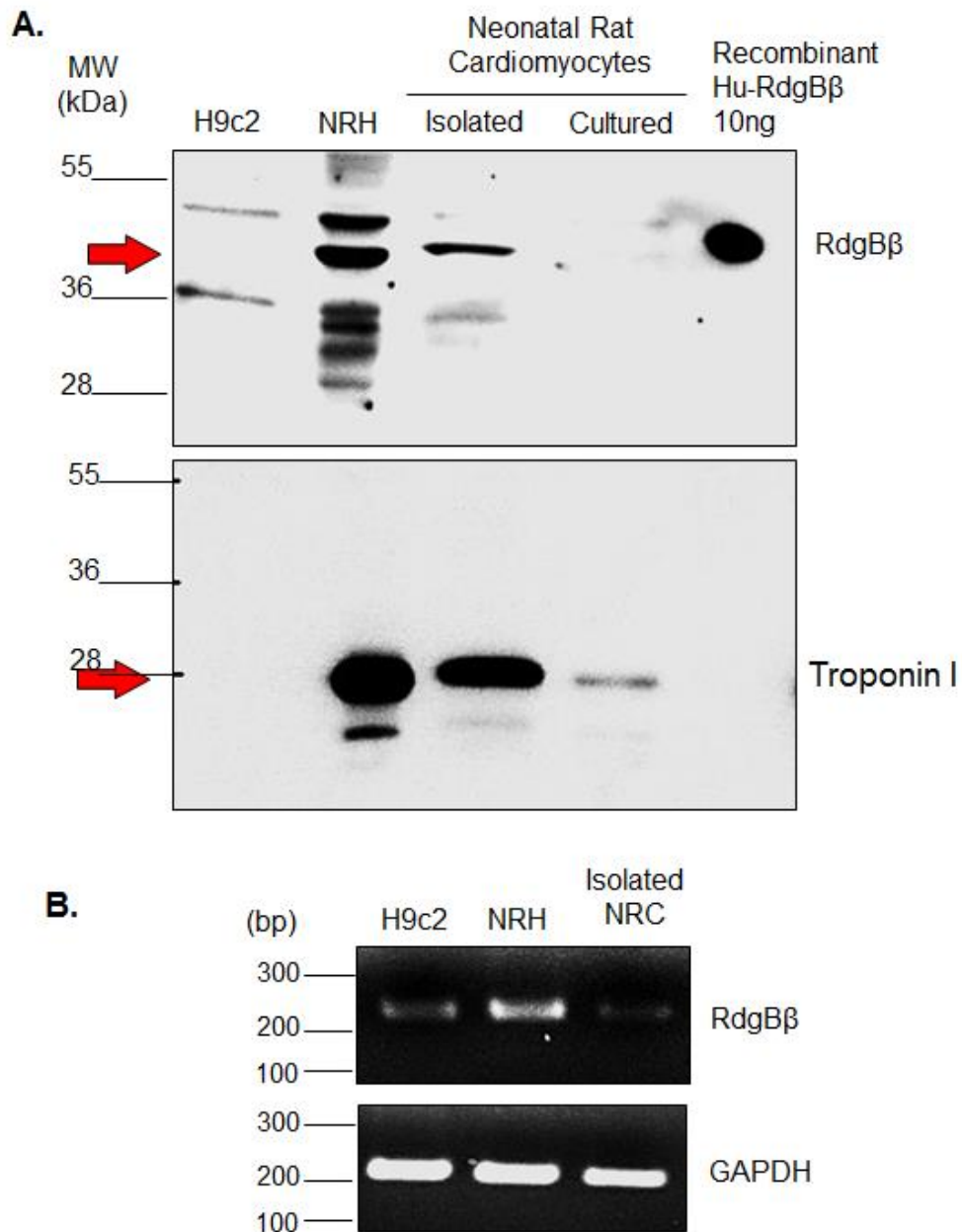
Figure 5.7: RdgBβ protein expression in isolated and cultured neonatal rat heart cells. Six neonatal (2 days old) Sprague-Dawley rat hearts were dissected; two of them were lysed in RIPA buffer. The other four hearts were serial digested to isolate cardiomyocytes, an aliquot was lysed in RIPA buffer and the rest was plated in Primaria 6 well dishes in maintenance media for 48 hours then lysed in RIPA buffer. The figure shows Western blot analysis of 50µg of lysates alongside undifferentiated H9c2 cells as negative control and 10ng recombinant Hu-RdgBβ as positive control. Using polyclonal Ab:Rb59 at a 1:100 dilution; and on a separated membrane, probed with anti-cardiac troponin I (Ab:Troponin I) as a cardiomyocyte marker. Red arrows indicate the expected (MW) molecular weight. NRH: Neonatal Rat Heart. NRC: Neonatal Rat Cardiomyocytes.

170

5.3.3: Subcellular localisation of RdgBβ in adult rat heart fractions

To study the subcellular expression of RdgBβ in primary cardiac tissue, adult rat hearts were fractionated by differential centrifugation and the fractions were immunoblotted for Ab:Rb59. RdgBβ was easily detectable in whole cell extracts (WCE), and upon fractionation, the protein was stronger in the cytosol compared to the other fractions. However, there was also positive immunoreactivity for microsomes, and a weak band was detected with mitochondrial associated membranes (MAM). Crude mitochondrial fractions showed a faint band, and pure mitochondria was negative for RdgBβ; Ab:Rb59 detected other cross-reactive proteins of higher and lower molecular weight than the expected band for RdgBβ (Figure 5.8).

In addition, the degree of purity of the fractions was examined by immunoblotting of the fractions using anti-calnexin antibody as microsomal marker and anti-Complex IV (COX IV) antibody as a mitochondrial marker. There was some mitochondrial contamination in the microsomes and a small microsomal contamination in the mitochondrial fractions whereas cytosolic fractions showed no contamination. This experiment was repeated several times with similar results. A fraction of RdgBβ seems to be associated with membranes in rat heart.
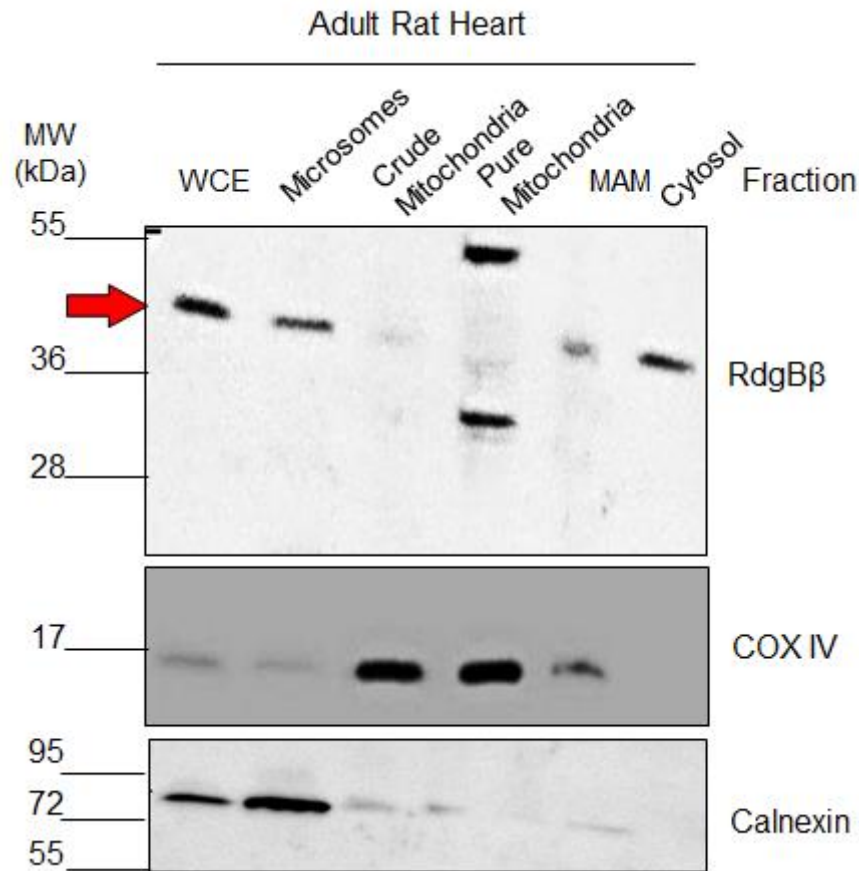
Figure 5.8: Subcellular localisation of RdgBβ protein expression in Adult Rat heart fractions.

Two female Sprague-Dawley rats (6 months old) were euthanised and their hearts dissected. Homogenised heart tissue was subjected to differential fractionation centrifugation and subjected to Western blot analysis. 50µg of each lysate was tested for RdgBβ expression using polyclonal Ab:Rb59 at a 1:100 dilution; and on separated membranes, probed with polyclonal anti-Complex IV (Ab:COX IV) at a 1:1000 dilution as a mitochondrial marker and anti-calnexin (Ab:calnexin) as microsomal marker at a 1:1000 dilution.

a. Comparison with rat brain and liver samples.

Along with the strong expression of RdgBβ in the heart, transcripts have also been found in brain, kidney, liver and testes [39,104]. To compare my observations in the heart with other tissue samples, immunoblotting of liver and brain tissue fractions, obtained in a similar manner to heart fractions, were tested for immunoreactivity with Ab:Rb59. Brain fractions showed endogenous RdgB expression following the same pattern of localisation as heart fractions. The immunoreactivity detected for the crude mitochondrial fractions accounted for the microsomal contamination as seen by the anti-calnexin antibody detection. In contrast, all liver fractions were negative for Ab:Rb59 (Figure 5.9).
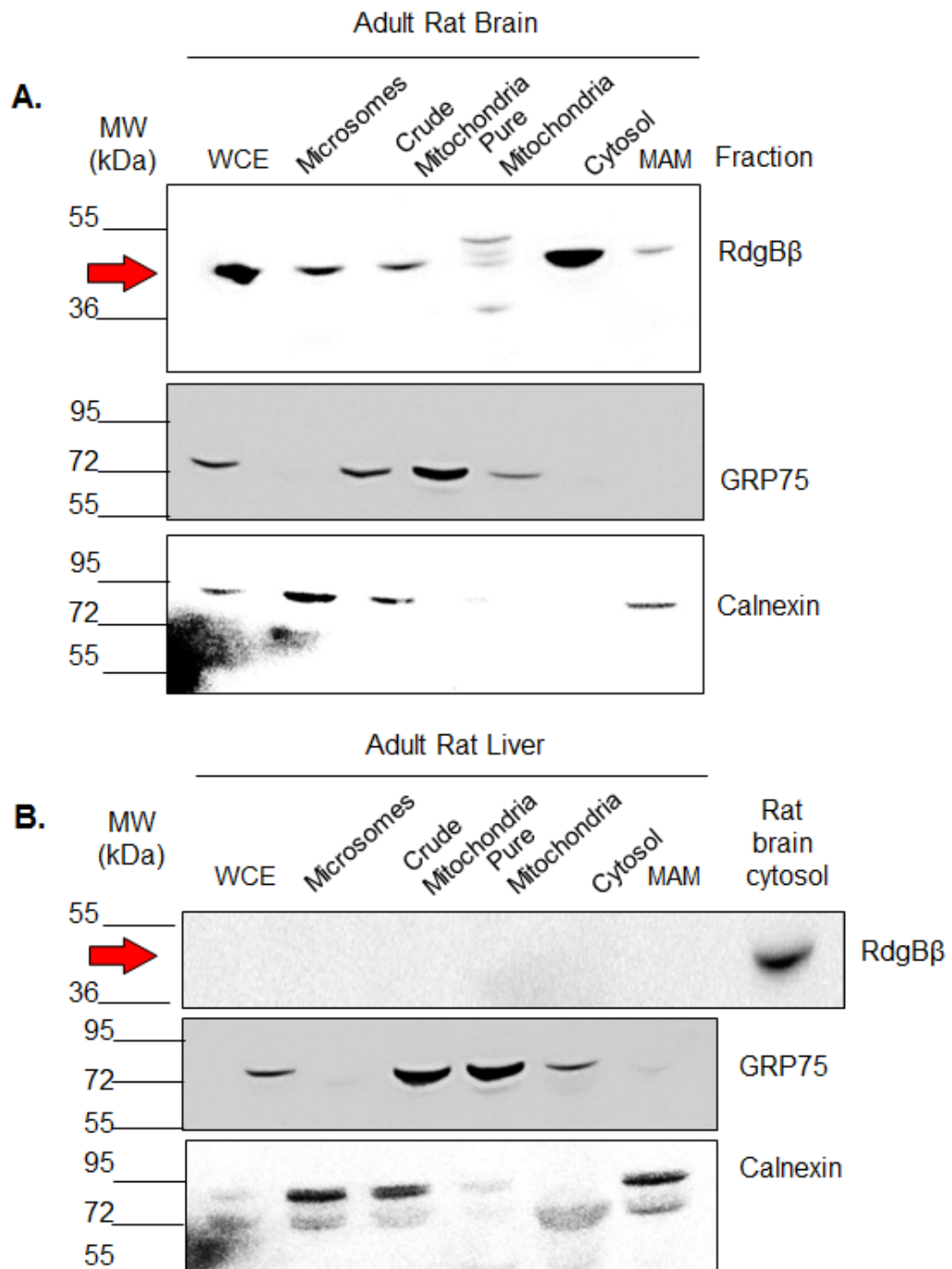
Figure 5.9: Subcellular localisation of RdgBβ protein expression in Adult Rat Brain [A.] and Liver [B.] fractions. Two female Sprague-Dawley rats (6 months old) were euthanised and their brains and livers dissected. Homogenised tissue was subjected to differential fractionation centrifugation and immunoblotted using polyclonal Ab:Rb59 at a 1:100 dilution for RdgBβ detection, and on separated membranes, probed with polyclonal anti-GRP75 (Ab:GRP75) at a 1:1000 dilution as a mitochondrial marker and anti-calnexin (Ab:calnexin) as microsomal marker at a 1:1000 dilution.

5.4: Summary and Discussion.

The present chapter describes the endogenous mRNA and protein expression of RdgBβ in rat heart tissue, both neonatal and adult, isolated cardiomyocytes and the differentiated H9c2 cell line. The findings are summarised in the flowchart presented in Figure 5.10.

There are no studies that have directly identified the expression pattern of native RdgBβ protein in H9c2 cells or in primary rat cardiomyocytes. The expression analysis of RdgBβ showed that protein and mRNA presence was increased over time in H9c2 cells differentiated for a minimum of 8 days and up to the 12 days evaluated (Figure 5.4). The siRNA transfection data verified that the protein detected by Ab:Rb59 was indeed RdgBβ (Figure 5.5). The cellular localisation study showed that RdgBβ is mainly cytosolic, but some immunoreactivity was observed in rat heart and brain microsomes (Figure 5.8 and Figure 5.9).

In addition, the increase in mRNA expression in muscle-like cells and H9c2 cells differentiated with RA at 4 days was dissimilar to the protein expression (Figure 5.1, Figure 5.2 and Figure 5.4), which suggests that RdgBβ translation might be regulated distinctly during cardiac cell growth and development. It is possible that RdgBβ expression could be detectable at a later stage in skeletal muscle differentiation since Northern blot of different human tissues also showed mRNA expression in the muscle.[39]
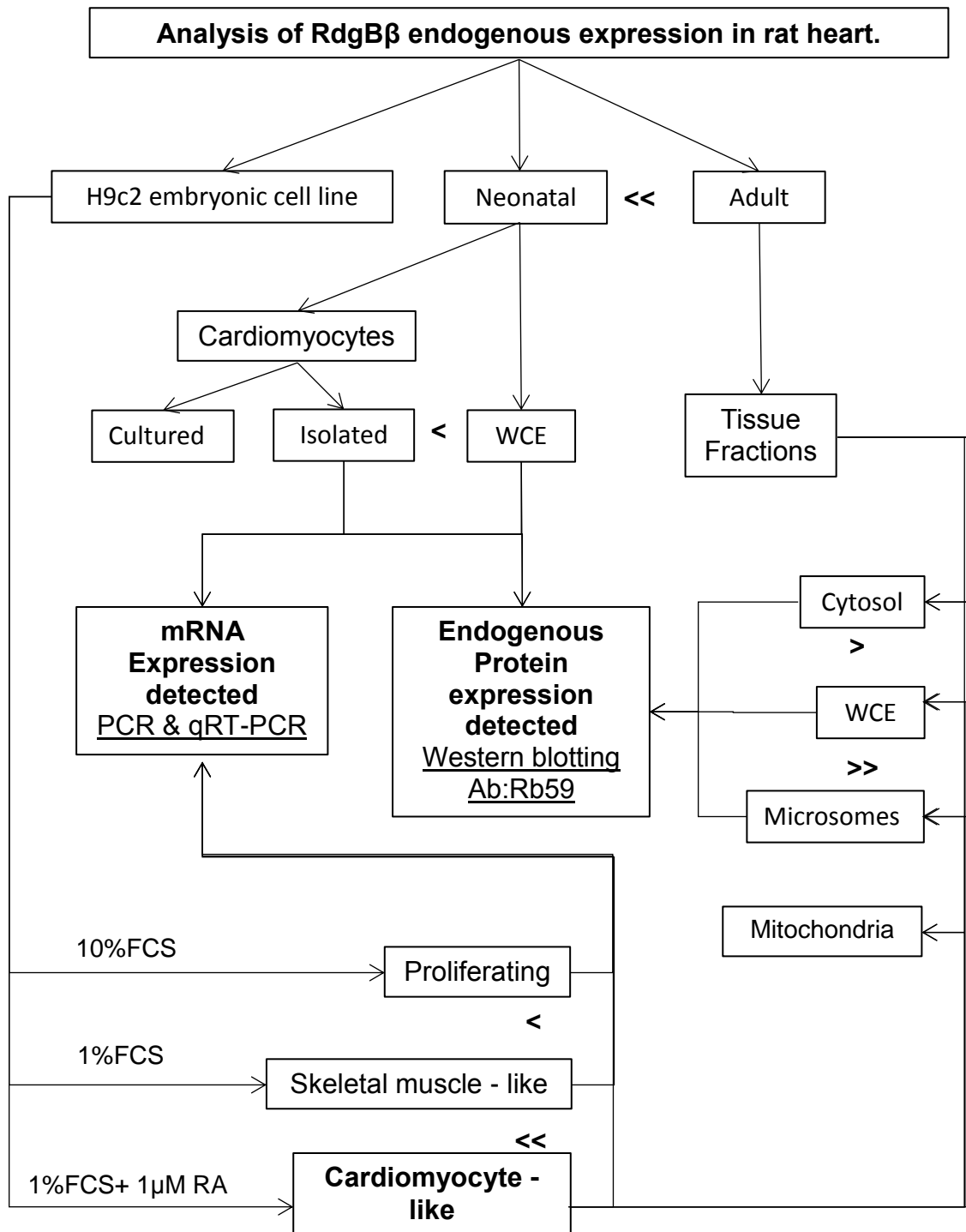
Figure 5.10: Flowchart summarising the results described in Chapter 5.

WCE: Whole cell extracts; FCS: Foetal calf serum; RA: Retinoic acid; qRT-PCR: Real time quantitative polymerase chain reaction.

The protein expression of RdgBβ was found to be stronger in the adult compared to neonatal rat heart lysates (Figure 5.6) and the RdgBβ signals detected by immunoblot on isolated neonatal rat heart cells were severely reduced or lost after 48 hours culture in maintenance media. The same samples of cultured neonatal rat cells showed a reduction or absence of immunoreactivity for cardiac troponin I (Figure 5.7) suggesting that the cultures of isolated neonatal rat cells were taken over by cells other than cardiomyocytes; for instance, cardiac fibroblasts. These results further support the idea that the expression of RdgBβ is related to development and maturity of cardiomyocytes and no other types of cells in the heart. This expression pattern has also been described in mouse brain where RdgBβ mRNA was mainly expressed in differentiating and mature neurons during both pre- and post-natal stages[104].

Earlier reports showed the intracellular localisation of RdgBβ throughout the cytoplasm of PC12 and HEK293 cell lines transfected with tagged RdgBβ; [39,41,104] and endogenous protein was previously detected in the cytosol of rat heart[41]. My results correlate with these findings directly in differentiated H9c2 cells and adult rat heart cellular fractions obtained by differential centrifugation; RdgBβ is mainly a cytosolic protein in rat heart and brain (Figures 5.10 and 5.11.A).

The regulation of protein translation of RdgBβ has not been explained to date. However it is known that micro RNAs represent one of several mechanisms of translational regulation[102] and miRNA 126 has been shown to regulate RdgBβ expression in breast cancer cells.[90] In the contrary, a recent study reported that

RdgBβ expression was not affected by over expression of mir126 in leukemic cells suggesting that miRNAs' function is highly tissue-dependent.[2]

Additionally a recent report showed that RdgBβ was able to translocate to the membranes of transfected Cos7 cells after PMA stimulation in order to bind a membrane protein (ATRAP)[41]; and recently a study revealed that RdgBβ associates with Golgi membranes in several cancer cells to bind the phospholipid PI4P and recruit another protein (RAB1B)[45]. In this thesis I found further evidence of the association of RdgBβ with cellular membranes (microsomes and mitochondrial associated membranes) in rat heart and brain (Figures 5.5, Figure 5.8 and Figure 5.9) which offers a good indication that the physiological function of RdgBβ in the heart could also be related to its ability to connect membrane protein and lipids .

For instance, considering the PA binding[40] and transfer (Figure 3.4) properties described for RdgBβ. Cellular PA is present in very small quantities mainly due to their rapid conversion into other phospholipids or its involvement in cellular signalling including for example the PLD-generated PA regulation in the effects of mTOR in several systems, cell types, and cellular phenotypes. (Reviewed in Foster, 2007)[36] and the increased the level of PA in cardiac sarcolemma as a result of inotropic agents stimulation known to stimulate cardiac hypertrophy.[31] However, as a lipid, PA is unable to move freely through the cytoplasm; therefore RdgBβ could directly facilitate PA-mediated processes especially in events where cells require extensive changes such as in stress conditions. Future studies will require a special design to address the physiological association of PA and RdgBβ in cardiac cells.

CHAPTER 6: Analysis of Cds1 expression in the rat heart.

6.1: Introduction.

RdgBβ protein expression was detected only when H9c2 cells were differentiated towards a cardiomyocyte-like phenotype and it was stronger in adult compared to neonatal rat hearts (Chapter 5). These results suggested that RdgBβ expression was regulated by development and maturation. Recently, it was reported that H9c2 cells differentiated with RA led to an increase in mitochondrial biogenesis regulated by the transcriptional coactivator peroxisome proliferator-activated receptor –γ coactivator-α (PGC-1α)[25]. In mice, PGC-1α deficient hearts showed reduced expression of the gene encoding CDP-DAG synthase 1 (*Cds1*)[68]. Cds enzymes catalyse the reaction between phosphatidic acid (PA) and CTP to form CDP-DAG, and RdgBβ is a PA binding protein. Therefore, I examined whether retinoic acid treatment of H9c2 cells also led to increased levels of Cds1.

This chapter starts with a description of the differentiation of H9c2 myoblasts by evaluating cell morphology and expression of markers of the cardiomyocyte phenotype. The analysis also includes microsomal and mitochondrial markers upon differentiation. The study also examines the mRNA and activity content of enzymes involved in phospholipid synthesis before and after differentiation.

The Cds1 expression analysis revealed a discrepancy between the mRNA and protein data. This prompted an investigation into the efficiency of the antibody used to detect Cds1 protein expression. This anti-Cds1 was used in recent

publications but it was not characterised[42,119]. Cds1 is an integral membrane protein known to be localised in the microsomal fraction[29,71,106,119]. Therefore the validation study of anti-Cds1 started with an analysis of the cellular localisation of the 55kDa band detected by the antibody in differentiated H9c2 cell fractions and adult rat heart fractions. The Ab:Cds1 characterisation also included the analysis of overexpressed human Cds1 in Cos7 cells and rat Cds1 siRNA transfection of H9c2 cells. The results found Ab:Cds1 to be unsuitable for the detection of endogenous Cds1 which affected the progress of the investigation. The chapter concludes with a discussion of the results, reinforcing the argument of chapter 4, regarding the damage that uncharacterised commercial antibodies are inflicting on biomedical research.

6.2: Characterisation of H9c2 cells differentiation.

6.2.1: Cell morphology comparison.

The cell morphology of H9c2 proliferating myoblasts compared to differentiated myocytes was studied visually from images taken by differential interference contrast microscopy (DIC) of cells in culture, and immunofluorescence microscopy of the nuclei with DAPI and actin filaments with Phalloidin staining of fixed H9c2 cells (Figure 6.1.). Proliferating myoblasts were observed as stellate or spindle-shaped single mono-nucleated cells. On the other hand, low serum media culture promoted cell fusion and elongation into fibres in the presence or absence of RA. However, H9c2 cells differentiated with RA showed a degree of multi-nucleation not evident in cells differentiated in 1% FCS alone. Morphological changes became noticeable after a minimum of 4 days culture in differentiation media.
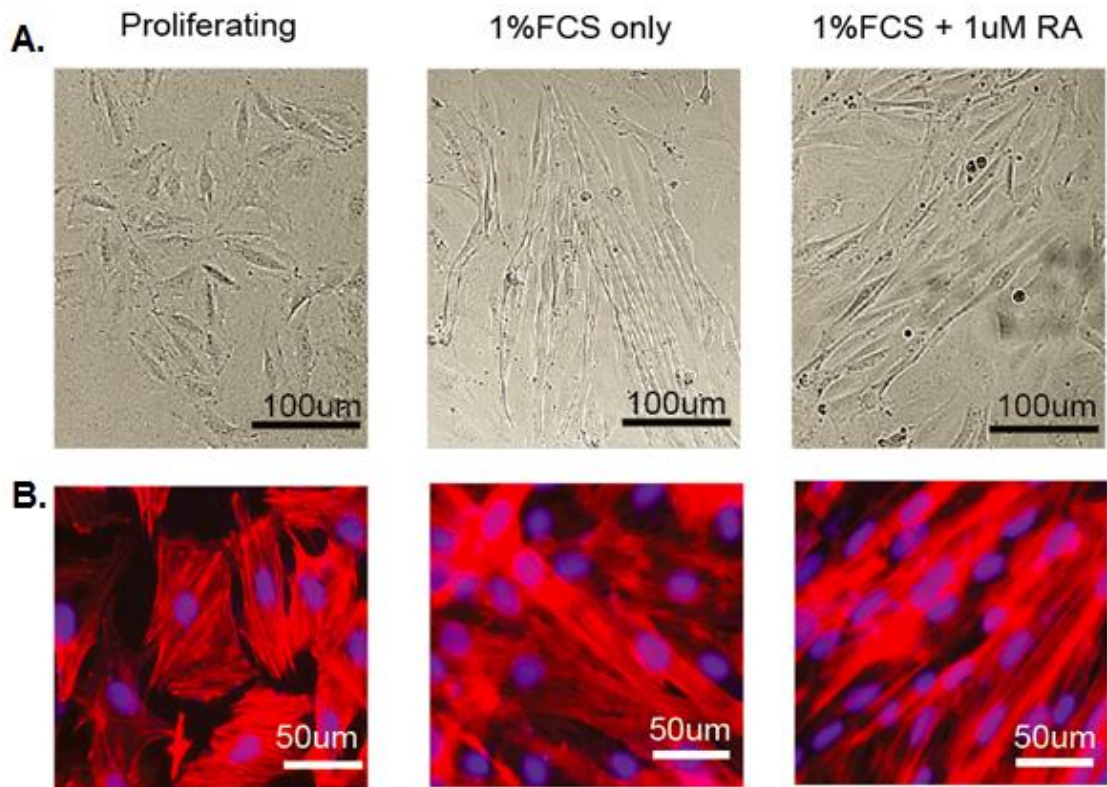
Figure 6.1: Morphological study of H9c2 cells after differentiation.

H9C2 myoblasts were seeded in 12 well plates with coverslips at 1×10^6 cells/mL and differentiated into myocytes with media containing reduced serum (1%FCS) ± daily supplement of all-trans retinoic acid (1μM RA) for eight days. Proliferating cells were passaged every two days.

[A.] Differential interference contrast (DIC) image of H9c2 cells in culture at 20x magnification.

[B.] H9c2 cells were fixed to the coverslips after media removal and washed with PBS. Immunofluorescence was achieved by nuclei staining with DAPI (blue) while actin filaments were stained with TRITC-Phalloidin (red). Images were taken at 40x magnification.

6.2.2: Retinoic acid-induced differentiation increases the expression of cardiac-specific markers.

Differentiation of H9c2 cells was achieved by culturing the myoblasts in 1% foetal calf serum (FCS) in the presence or absence of all-*trans*-retinoic acid (RA) for a minimum of 8 days. The cardiomyocyte-like phenotype was tested for specific cardiac markers by immunoblotting with cardiac troponin I (Figure 6.2.A.), and qPCR analysis of the mRNA expression of Atrial natriuretic protein (ANP) and Brain natriuretic protein (BNP) (Figure 6.2.B).

Protein expression of cardiac troponin I was only detected in H9c2 cells differentiated with RA. Ponceau staining was used as loading control and it showed no noticeable differences in the overall protein profiles of proliferating H9c2 myoblast and differentiated myocytes. Relative mRNA expression of ANP showed a small 3.04 ±0.6 fold increase in cells differentiated with low serum alone compared to proliferating H9c2s, whilst there was a substantial 39.3±17 fold increase in mRNA expression obtained by the addition of RA. In a similar fashion, the relative expression of BNP mRNA showed a 4.3±1.2 fold increase in cells cultured in 1% FCS only and 26.3±9.3 fold increase obtained from RA differentiated H9c2s compared to undifferentiated cells. Increased ANP or BNP mRNA expression also indicated cell hypertrophy. These results demonstrate that H9c2 cells differentiated with low serum and retinoic acid exhibit characteristics found specifically in cardiomyocytes.

Figure 6.2: Retinoic acid-induced differentiation increases the expression of cardiac-specific markers.

H9c2 cells were seeded into 6 well culture dishes at a concentration of 2×10^6 cells/mL in complete medium (10% FCS) for 48 hours. Proliferating cells were passaged every two days while serum media was reduced to 1%FCS and replenished every two days for 10 days in the presence or absence of daily treatment with 1µM all-trans retinoic acid (RA). Cell lysates were harvested in RIPA buffer and RNA was extracted from cells of which 1µg was used to obtain cDNA by reverse transcription.

[A.] SDS-PAGE was performed using 75µg of cell lysates on a gradient 4-12% acrylamide gel transferred to a PVDF membrane, stained with Ponceau solution and imaged to test transfer efficiency and as a loading control. Membranes were subjected to western blotting using polyclonal antibody anti-Troponin I at a 1:100 dilution. MW: molecular weight.

[B.] qRT-PCR of 5µL cDNA using SYBR green. Fold change calculated using the $\Delta\Delta Ct$ formula where Ct values were obtained in duplicate or triplicate and normalised to the Ct values for the housekeeping gene Phosphoglycerate Kinase 1 (PGK1). Error bars indicate SEM.

ANP: Atrial natriuretic protein, 1% only ($p=0.05$, $n=7$ from 3 experiments) and RA ($p=0.02$, $n=11$ from 4 experiments).

BNP: Brain natriuretic protein, 1% only ($p=0.1$, $n=4$ from 2 experiments) 1%+RA ($p=0.08$, $n=8$ from 3 experiments)
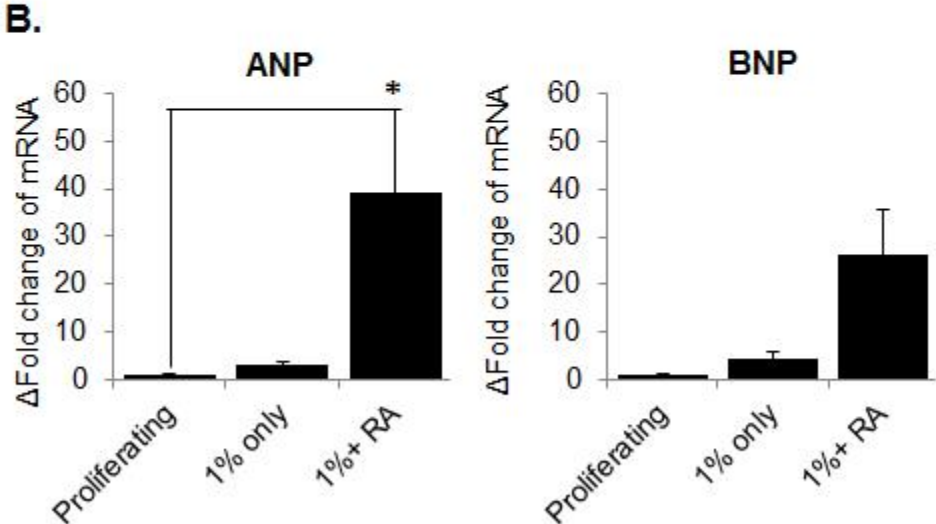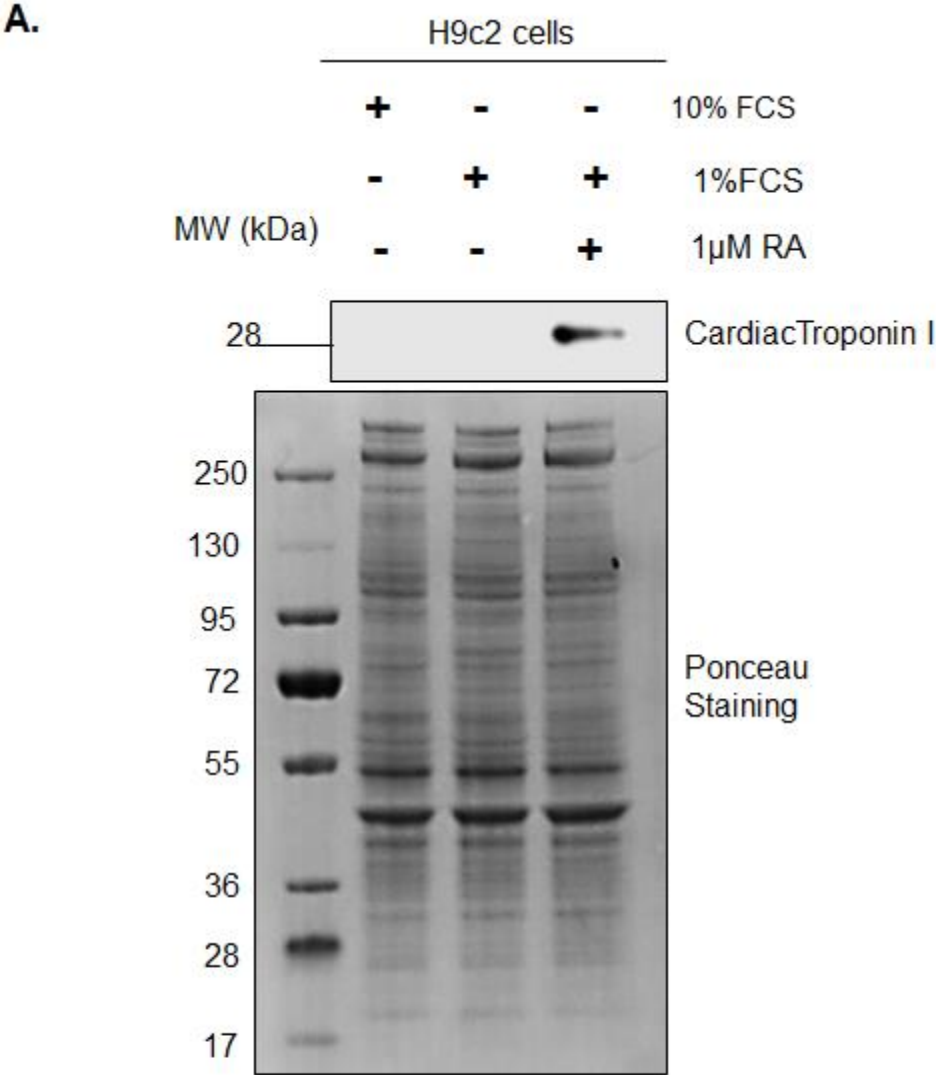
Figure 6.2: Retinoic acid-induced differentiation increases the expression of cardiac-specific markers.

6.2.3: Mitochondrial content increases with H9c2 myoblasts differentiation.

The expression pattern of representative mitochondrial proteins was assessed by immunoblotting to test whether biogenesis of these organelles increased with differentiation of H9c2 myoblasts as described previously[25]. The mitochondrial proteins analysed include, 75 kDa glucose-regulated protein (GRP75), Complex IV (COX IV) and cytochrome C. I also studied the protein expression of CDP-DAG synthase 1 (Cds1), a protein found to be regulated by transcriptional coactivator peroxisome proliferator-activated receptor –γ coactivator-α (PGC-1α) which is considered the master regulator of mitochondrial biogenesis[68]. As a comparison, the microsomal protein calnexin as well as the cytosolic protein PITPα were evaluated (Figure 6.3.A).

The expression of all three mitochondrial proteins was increased with differentiation regardless of the addition of retinoic acid whereas cytosolic PITPα was unaltered. The antibodies against these proteins detected a single band at the expected molecular weights. A semi-quantitative densitometry analysis of the bands obtained in separate experiments showed a significant increase in the protein expression of cytochrome C (3.1±0.7 fold increase) and GRP75 (3.93±1.5 fold increase) compared to the proliferating cells content (Figure 6.3.B.).

The microsomal content, tested by calnexin protein expression, was detected by a single band at the expected molecular weight and showed a slight reduction in muscle-like cells (1%FCS) while it was unaltered in cardiomyocyte-like

cells (1% FCS + RA). However the results of Cds1 were unclear; the antibody detected a band at the expected molecular weight (55kDa, Figure 6.3.A, blue arrow) that was stronger with RA differentiation but also several other bands of higher and lower molecular weights were observed. The intensity and presence of these bands varied in different experiments.

In addition, H9c2s cells were tested for time dependent expression of mitochondrial and microsomal proteins following daily treatment with retinoic acid. The cell lysates were harvested every 2 days for a total of 12 days (Figure 6.4.). The expression of the cardiomyocyte marker cardiac troponin I was detected only after 8 days of retinoic acid treatment, thus, that was the minimum period of treatment required to begin to see the cardiac-like phenotype. In parallel, mitochondrial content was increased over time as detected by the protein expression increase of GRP75 and cytochrome C. This pattern was also observed for the 55 kDa bands detected by the Ab:Cds1 antibody which showed a substantial increase by 10 days of treatment (Figure 6.4, blue arrow). In addition, the detection of calnexin and the cytosolic protein 14-3-3 remained unaltered during RA differentiation during all of the 12 days of experimentation. These results confirmed the increase in mitochondrial biogenesis that rises upon differentiation of H9c2 cells.

Figure 6.3: Mitochondrial content increases with differentiation of H9c2 cells.

H9c2 cells were cultured in complete media (10% FCS) for 48 hours. Proliferating cells were passaged every two days while serum media was reduced to 1%FCS and replenished every two days for 10 days in the presence or absence of daily treatment with 1μM all-trans retinoic acid (RA). Cell lysates were harvested in RIPA buffer every two days.

[A.] 50μg of protein content from cell lysates was separated on a NuPage gradient 4-12% acrylamide gel. Protein detection was achieved by western blotting using monoclonal anti-Cds1 at a 1:100 dilution (blue arrow shows the expected molecular weight for Cds1), polyclonal anti-calnexin at a 1:1000 dilution as a microsomal marker. GRP75, COX IV and cytochrome c antibodies at a 1:1000 dilution were used as mitochondrial markers. The cytosolic marker used was PITPα detected by antibody 674 at a 1:1000 dilution. MW: molecular weight.

[B.] Protein expression detected by immunoblotting was imaged and the bands obtained were subjected to semi-quantitative 2D densitometry using AIDA software. Graphs show the averages of 3 separated experiments and the error bars represent SEM. (*): $p < 0.05$. Cytochrome c: $p = 0.01$, $n = 3$. GRP75: $p = 0.03$, $n = 4$.
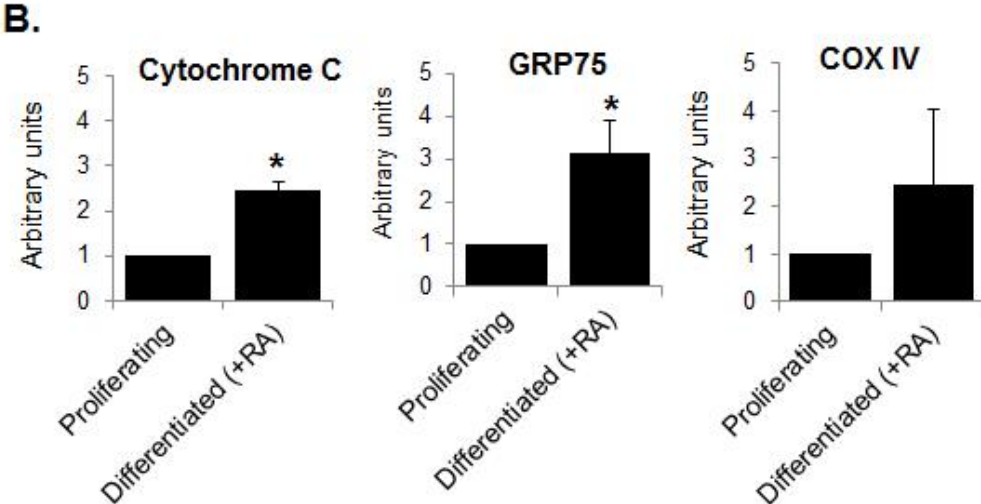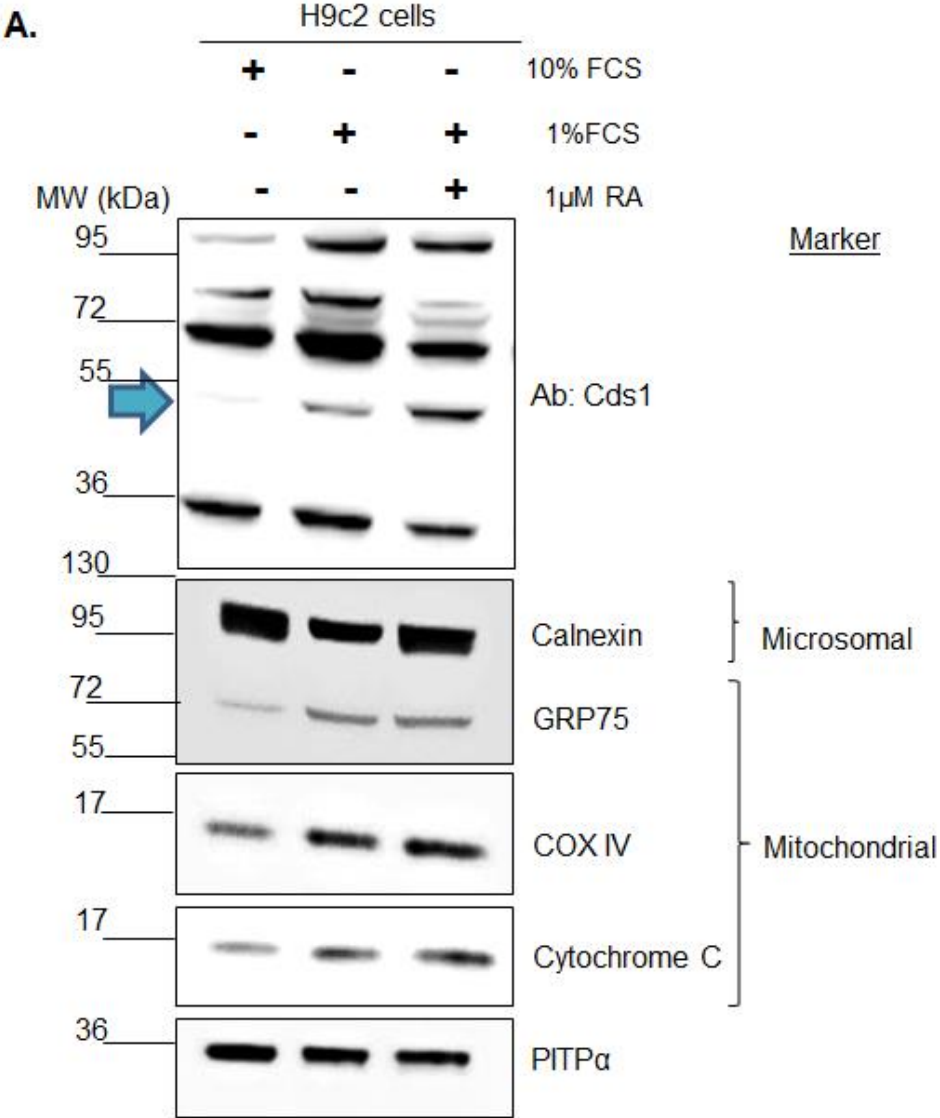
Figure 6.3: Mitochondrial content increases over time with differentiation of H9c2 cells.

Figure 6.4: Mitochondrial content increases over time with differentiation of H9c2 cells.

H9c2 cells were seeded into 6 well culture dishes at a concentration of $2x10^6$cells/mL in complete media (10% FCS) for 48 hours. All cells were cultured in reduced serum media (1%FCS) and replenished every two days for 12 days in the presence of daily treatment with 1µM all-trans retinoic acid (RA). Cell lysates were harvested in RIPA buffer.

Protein detection was achieved by western blotting using monoclonal anti-Cds1 at a 1:100 dilution (blue arrow corresponds to the expected molecular weight for Cds1). Anti-troponin I at a dilution of 1:100 was the cardiomyocyte marker while the polyclonal anti-calnexin at a 1:1000 dilution as a microsomal marker. GRP75 and cytochrome c antibodies at a 1:1000 dilution were used as mitochondrial markers and Anti-14-3-3 was used to detect the 14-3-3 as a cytosolic marker at a 1:1000 dilution. MW: molecular weight.
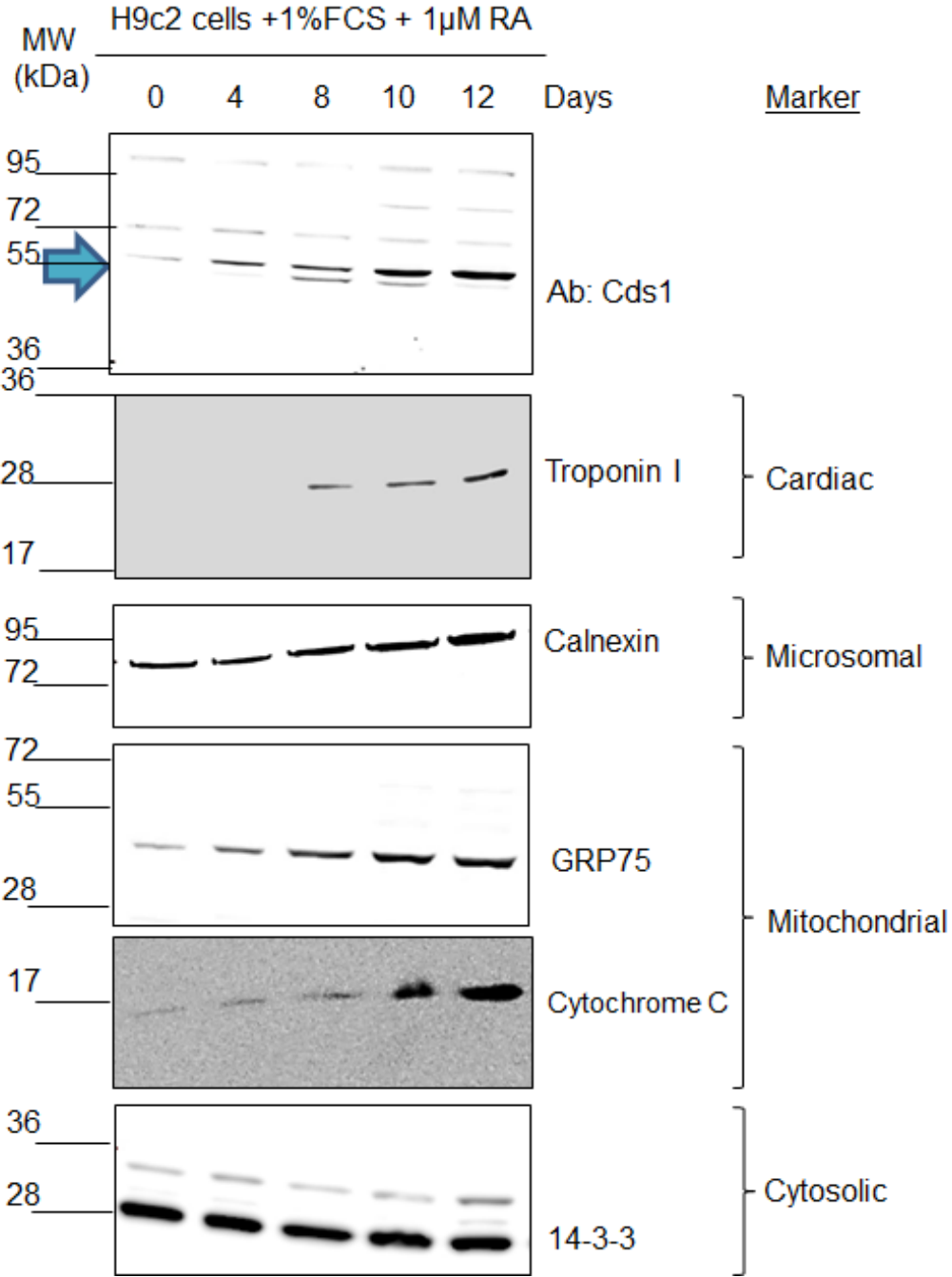
Figure 6.4: Mitochondrial content increases over time with differentiation of H9c2 cells.

6.2.4: Expression of phospholipid biosynthetic enzymes after H9c2 cells differentiation.

In order to evaluate whether the mRNA content of Cds1 also increased with cell differentiation, as suggested by immunoblotting using the antibody Ab:Cds1 (Figure 6.3 and Figure 6.4), qPCR analysis of cDNA obtained from H9c2 cells was performed in the presence or absence of cellular differentiation. For comparison, the mRNA expression of other Cds proteins (Cds2 and Tamm41) alongside phosphatidylinositol synthase (PIS) and cardiolipin synthase (CLS) was also evaluated (Figure 6.5).

Cds1 mRNA expression was significantly not altered by serum media reduction (1% FCS only), and the addition of retinoic acid increased relative mRNA expression (1.7±0.1 fold increase) compared to Cds1 mRNA in proliferating cells. mRNA expression of other mammalian Cds enzyme (Cds2), showed a reduction in mRNA upon H9c2 cells differentiation with low serum (0.65±0.003 fold decrease) and modest increase on the cardiomyocyte-like cells (1.56±0.14 fold increase), compared to undifferentiated cells. In addition, the mRNA expression of PI synthase was unaltered regardless of the differentiation method but cardiolipin synthase showed a small increase in mRNA expression in the absence (1.6±0.2 fold) and presence (1.4±0.1 fold) of retinoic acid (Figure 6.5.A).

To further test the mRNA expression increase observed for the Cds proteins, H9c2 cells were cultured in differentiation media containing RA for a total of 12 days. Cells were harvested every two days and the RNA was extracted for cDNA synthesis and qPCR analysis (Figure 6.5.B). The mRNA expression of all three enzymes with CDP-DAG synthesis capability was tested, Cds1, Cds2 and Tamm41. Cds1 and Cds2 showed a similar mRNA increase over time whilst Tamm41 mRNA was diminished. The strongly increased protein expression seen for the antibody Ab:Cds1 does not correlate with the relatively modest yet significant mRNA increase seen by qPCR. It is possible that Cds proteins translation is rapidly activated upon small increases in mRNA during cardiac differentiation. Alternatively, the sensitivity of the antibody is greater than expected or it is detecting a cross reactive band at the expected size for Cds1.

Figure 6.5: mRNA expression of phospholipid biosynthetic enzymes after H9c2 cells differentiation.

H9c2 cells were cultured ± differentiation media supplemented with 1%FCS± 1µM retinoic acid (RA). 1µg RNA of each lysate was used to make cDNA by reverse transcription. 5µL cDNA were assessed for mRNA expression by qPCR using SYBR green and the indicated primers. Bars represent the fold change of mRNA ± SEM calculated using the ΔΔCt formula where Ct values were normalised to the Ct values for the housekeeping gene Phosphoglycerate Kinase 1 (PGK1).

[A.] CDP-DAG synthases (Cds1 and Cds2), P(T<=t) two-tail analysis p<0.001 (**)

 Cds1 mRNA 1% +RA: p=0.00009, n=29 from 8 experiments.

Cds2 mRNA after 1%CS +RA: p=0.0009, n=18 from 6 experiments.

PI synthase (PIS) no statistically significant (NS)

Cardiolipin synthase (CLS) after 1%FCS +RA: p=0.0008, n=15 from 5 experiments.

[B.] Cds1, Cds2 and TAMM41mRNA expression of H9c2 cells over 12 days of differentiation. Mean from 2 experiments in duplicate (n=4). P(T<=t) two-tail analysis p<0.001 (**)

Cds1: (0-4 days) p=0.005; (0-8) p=0.4; (0-10) p=0.002; (0-12) p=0.02.

Cds2: (0-4 days) p=0.2; (0-8) p=0.1; (0-10) p=0.02; (0-12) p=0.001.

TAMM41: (0-4 days) p=0.1; (0-8) p=0.01; (0-10) p=0.001; (0-12) p=3.7×10^{-4}
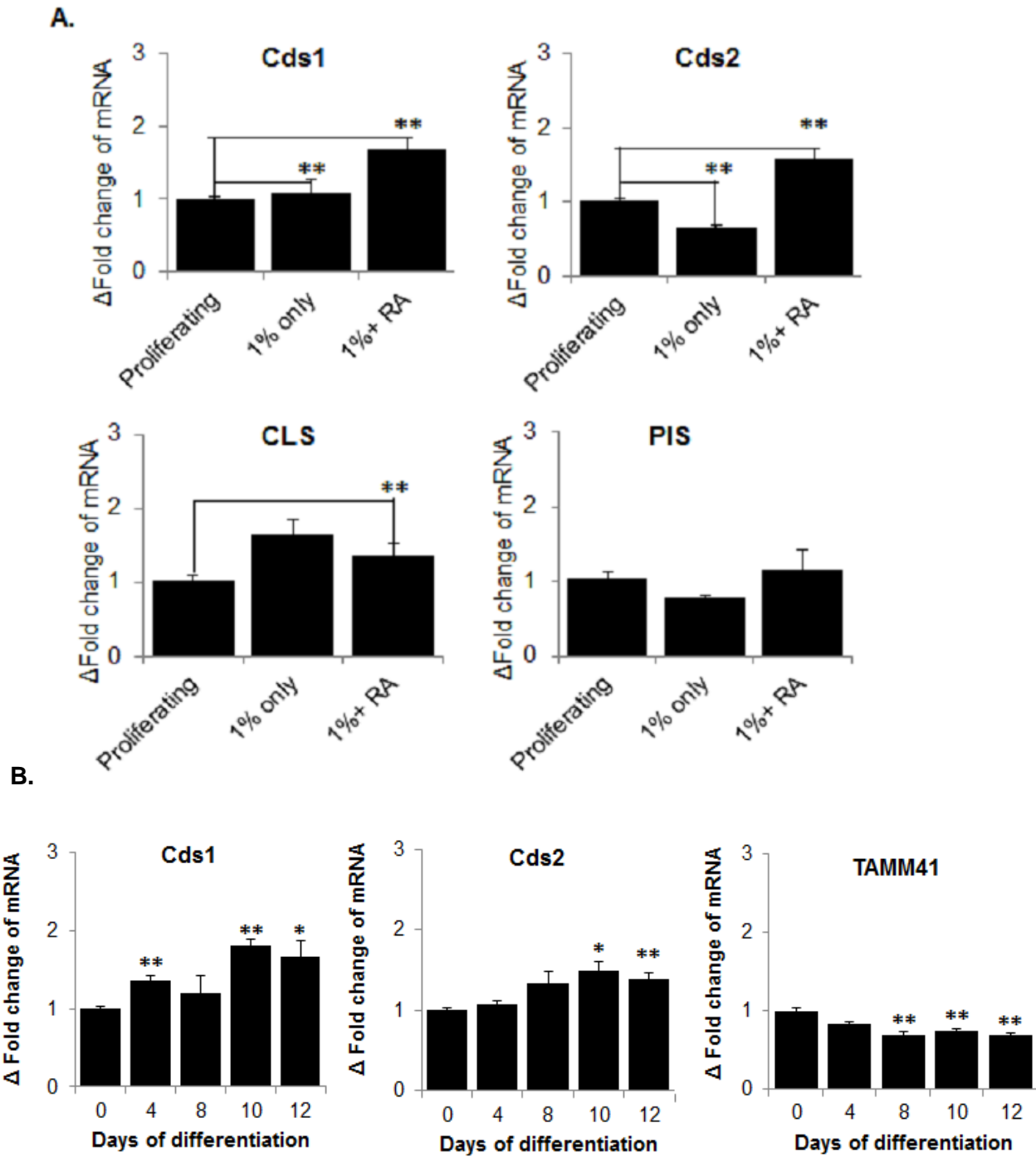
A.

B.

Figure 6.5: mRNA expression of phospholipid biosynthetic enzymes after H9c2 cells differentiation.

6.2.5: Cds1 and PIS Enzyme activity.

CDP-DAG synthase (Cds) activity of H9c2 cells was assayed to test whether the differentiation state of H9c2 cells influences stimulation of phospholipid synthesis via Cds catalysis of PA and CTP. The assay was an adapted procedure[29,119] which measured the level of incorporation of [^{3}H]-CTP into CDP-DAG using external phosphatidic acid in a pH8 buffer on H9c2 cell lysates of undifferentiated cells alongside cardiomyocyte-like cells (Figure 6.6.A). The Cds activity upon retinoic acid differentiation increased close to 2 fold (1.95±0.02, p=0.01, n=6) relative to untreated H9c2 myoblasts (Figure 6.6.A).

In addition, PI synthase (PIS) activity of H9c2 cells differentiation was measured by the incorporation of [^{3}H]-myo inositol into phosphatidylinositol (PI) in a pH 7.4 buffer containing 2mM $MnCl_2$ (Figure 6.6.B). The PIS activity increased close to 4 fold from 12203±1210 DPM counts in undifferentiated cells to 46484±1613 DPM counts in cardiomyocyte-like cells. These results suggested that phospholipid biosynthesis increases substantially when myoblasts differentiate into cardiomyocytes.
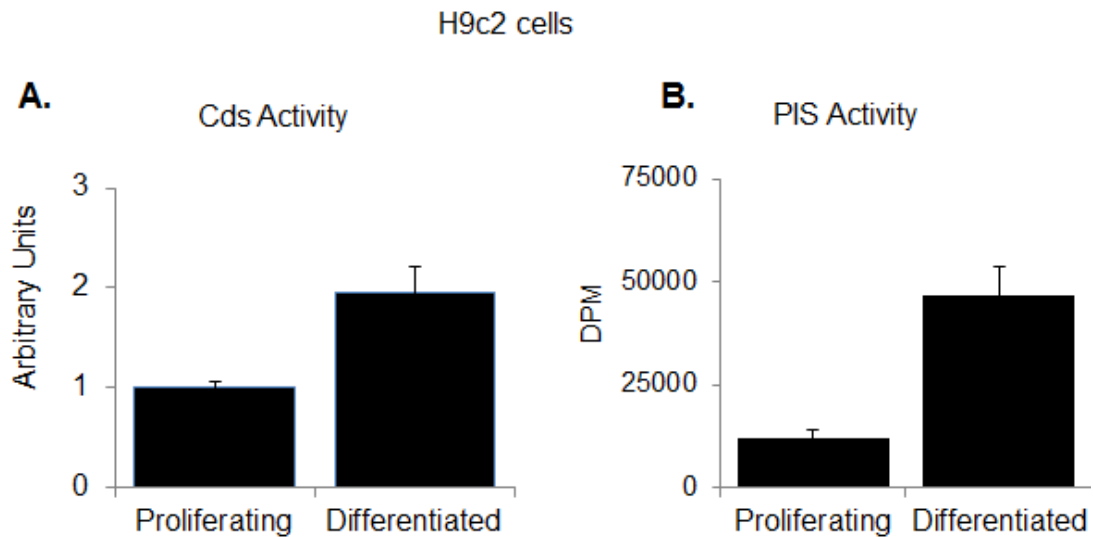
Figure 6.6: Cds and PIS activity in H9c2 cells.

[A.] 50µg of H9c2 cells cultured ± differentiation media for 8 days were used for Cds assay in a total volume of 100µL. Triplicate sample mixtures were incubated for 10 minutes at 30° C. The solvent soluble phase was separated and counted for radioactivity. Arbitrary units: The bars represent the average DPM counts subtracted from background values from 2 experiments normalised to 1 for proliferating cells ± SEM.

[B.] PIS assay of 50µg of H9c2 cell lysates. Triplicate sample mixtures were incubated for 15 minutes at 37° C. The bars represent DPM counts of the solvent soluble phase separated from the mixtures subtracted from background values ± SEM from 1 experiment.

6.3: Identification of the protein detected by Ab:Cds1.

There were conflicting results when studying the expression of Cds1 in H9c2 cells. The high intensity of the protein band detected by Ab:Cds1 at the expected molecular weight (55kDa) for Cds1 did not match the mRNA expression increased obtained by qPCR (Figure 6.3, Figure 6.4 and Figure 6.5). Since the use of rat Cds1 primers was fully validated, a characterisation of Ab:Cds1 was granted.

Ab:Cds1 (clone 2D10) is a monoclonal antibody raised in mouse using a sequence from human Cds1 (amino acids 1-99). To assess the likelihood of Ab:Cds1 to detect the rat Cds1, a sequence alignment analysis of the human protein compared to rat was performed (Figure 6.7). A comparison of the full length of the proteins showed a 95.4% identity and 97.2% similarity. However, the specific sequence of amino acids 1-99 showed that rat Cds1 shares 89% of identity with Human Cds1 suggesting that specificity for rat Cds1 might be compromised. The antibody Ab:Cds1 is available from different providers which have predicted for the antibody to work in mouse, rat, pig and orangutan. Antibody Ab:Cds1 has been used in the detection of human Cds1 in a recent publication using non-small cell carcinoma lung cells. [42]

Cds1 is an integral membrane protein known to be localised in the microsomal fraction.[58,71,106,119] Therefore to characterise Ab:Cds1 I first analysed the cellular localisation of the 55kDa band in H9c2 differentiated cells and adult rat heart cellular fractions, followed by analysis of Cds1 overexpression in Cos7 cells and down-regulation by siRNA transfection of differentiated H9c2 cells.

Phosphatidate cytidylyltransferase 1/CDP-DAG Synthase (Cds1)

Homo sapiens (Human) reference [NP_001254.2]
Rattus norvegicus (Rat) reference [NP_112521.2]
Length: 461
Identity: 440/461 (95.4%)
Similarity: 448/461 (97.2%)

```
Human      1 MLELRHRGSCPGPREAVSPPHREGEAAGGDHETESTSDKETDIDDRYGDL   50
             ||||||||| |||| . ||| . : ||| ||||||||||||||||||||||
Rat        1 MLELRHRGGCPGPGGAGTPPPREGEAAGGDHETESTSDKETDIDDRYGDL   50

Human     51 DSRTDSDIPEIPPSSDRTPEILKKALSGLSSRWKNWWIRGILTLTMISLF  100
             | : | | | | : | | ||||||||||||||||||||||||||||||||||
Rat       51 DARGDSDVPEVPPSSDRTPEILKKALSGLSSRWKNWWIRGILTLTMISLF  100

Human    101 FLIIYMGSFMLMLLVLGIQVKCFHEIITIGYRVYHSYDLPWFRTLSWYFL  150
             |||||||||||||||||||||||||.||||||||||||||||||||||||
Rat      101 FLIIYMGSFMLMLLVLGIQVKCFQEIITIGYRVYHSYDLPWFRTLSWYFL  150

Human    151 LCVNYFFYGETVADYFATFVQREEQLQFLIRYHRFISFALYLAGFCMFVL  200
             ||||||||||||||||||||||||||||||||||||||||||||||||||
Rat      151 LCVNYFFYGETVADYFATFVQREEQLQFLIRYHRFISFALYLAGFCMFVL  200

Human    201 SLVKKHYRLQFYMFAWTHVTLLITVTQSHLVIQNLFEGMIWFLVPISSVI  250
             ||||||||||||||||||||||||||||||||||||||||||||||||||
Rat      201 SLVKKHYRLQFYMFAWTHVTLLITVTQSHLVIQNLFEGMIWFLVPISSVI  250

Human    251 CNDITAYLFGFFFGRTPLIKLSPKKTWEGFIGGFFSTVVFGFIAAYVLSK  300
             |||||||||||||||||||||||||||||||||||||:||||||||||||
Rat      251 CNDITAYLFGFFFGRTPLIKLSPKKTWEGFIGGFFSTVIFGFIAAYVLSK  300

Human    301 YQYFVCPVEYRSDVNSFVTECEPSELFQLQTYSLPPFLKAVLRQERVSLY  350
             |||||||||||||||||||||||||||||.|||||||:|||.:|.||||
Rat      301 YQYFVCPVEYRSDVNSFVTECEPSELFQLQNYSLPPFLQAVLSRETVSLY  350

Human    351 PFQIHSIALSTFASLIGPFGGFFASGFKRAFKIKDFANTIPGHGGIMDRF  400
             ||||||||||||||||||||||||||||||||||||||||||||||||||
Rat      351 PFQIHSIALSTFASLIGPFGGFFASGFKRAFKIKDFANTIPGHGGIMDRF  400

Human    401 DCQYLMATFVHVYITSFIRGPNPSKVLQQLLVLQPEQQLNIYKTLKTHLI  450
             ||||||||||||||||||||||||||||||||||||||||:|||.||.
Rat      401 DCQYLMATFVHVYITSFIRGPNPSKVLQQLLVLQPEQQLNIYRTLKIHLT  450

Human    451 EKGILQPTLKV      461
             ||||||||.||
Rat      451 EKGILQPTWKV      461
```

Monoclonal antibody clone 2D10 immunogen (Grey)

Difference in sequence compared to rat Cds1 (Red)

Figure 6.7: Ab:Cds1 target in Human and rat Cds1 aligned sequences.

6.3.1: Differentiated H9c2 cell fractions

The expression pattern of the 55 kDa protein detected by Ab:Cds1 was analysed by immunoblotting of differentiated H9c2 cell fractions obtained by differential centrifugation. To assess the degree of purity of the fractions, specific organelle markers were studied. Calnexin was the microsomal marker whilst COX IV, GRP75 and cytochrome c were the mitochondrial markers (Figure 6.8.A).

Figure 6.8 shows the results from one experiment which was repeated twice with similar results. Ab:Cds1 detected the 55kDa protein enriched in the crude mitochondrial fraction and not in the microsomal fraction as expected (Figure 6.8.A, blue arrow). The immunoreactivity of the markers indicated a low level of contamination. However, crude mitochondrial fractions are known to contain associated membranes as detected by the microsomal marker. In addition, the highest Cds activity was found in the crude mitochondrial fractions (10262±1127 DPM), nearly twice the counts measured for the whole cells extract (5880.4±642). In contrast, microsomal Cds activity was not enriched in differentiated H9c2 cells as it was PIS activity (Figure 6.8.B).

Figure 6.8: Differentiated H9c2 cell fractions protein expression, Cds and PIS activity.

H9c2 cells were cultured in differentiating media for 8 days in the presence of daily 1µM all-trans retinoic acid (RA). Cells were harvested, lysed and subjected to differential centrifugation

[A.] Protein expression was analysed by western blotting of 50µg of each cell fraction using monoclonal antibodies anti-Cds1 at a 1:100 dilution and anti-cytochrome c at a 1:1000 dilution as a mitochondrial marker, and on separate membranes the polyclonal antibodies (1:1000 dilution) anti-calnexin as a microsomal marker, anti-GRP 75 as mitochondrial marker and anti-14-3-3 as a cytosolic marker. The blue arrow indicates the expected molecular weight for Cds1. MW: molecular weight.

[B.] Cds Activity: 50ug of cell fraction was incubated for 10 min at 30° C in Cds activity assay buffer. Bars represent the average of triplicate samples from 2 experiments ± SEM. PIS Activity: 50µg of cell fractions was incubated for 15 min at 37°C in PIS assay buffer. Bars represent the mean± SEM of three samples obtained from 1 experiment using the fractions described in A.
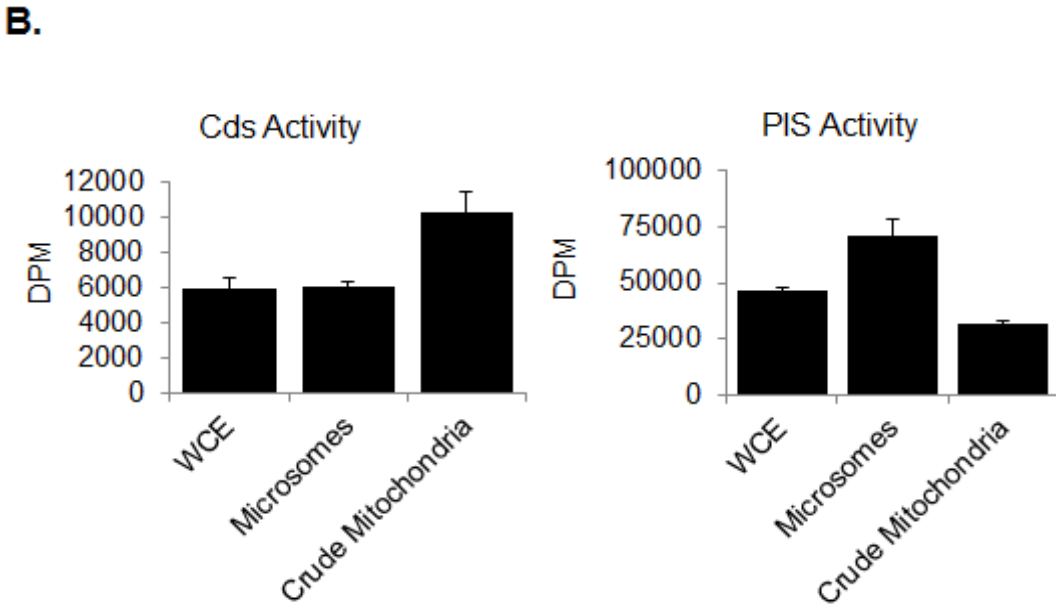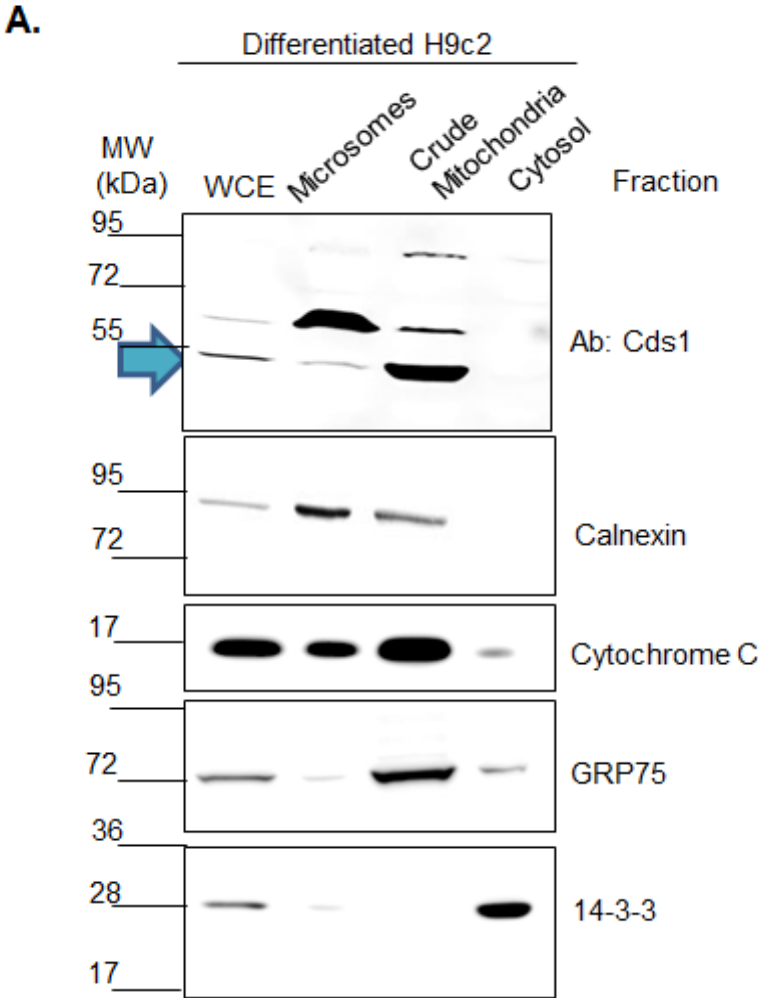
Figure 6.8: Differentiated H9c2 cell fractions.

6.3.2: Adult rat heart fractions

The results obtained with Ab:Cds1 together with Cds activity in differentiated H9c2 cell fractions showed that Ab:Cds1 was detecting a 55kDa protein enriched in crude mitochondria where Cds activity was also the highest compared to the other cellular fractions (Figure 6.8.). In order to compare these observations in primary tissue, the protein expression and enzyme activity assays were performed using cellular fractions from adult rat hearts.

The fractions were obtained by dissection followed by differential centrifugation of whole hearts by an adapted protocol from previous studies.[77,121] It is understood that the heart is a tissue enriched in highly dense mitochondrial content and so initially, tissue isolation and homogenisation was performed in the presence of the protease subtilisin, which was recommended to increase yield and purity of the mitochondria. The fractions were studied by immunoblotting (Figure 6.9.A). Cds and PIS activity assays were performed as described above (Figure 6.9.B). Figure 6.9 represents the results from one experiment which represents the observations of five other similar experiments.

The antibody Ab:Cds1 detected a single strong band at 55kDa in the crude mitochondrial fraction (Figure 6.9.A., blue arrow). The expression of mitochondrial markers (GRP75, COX IV and cytochrome c) was detected strongly in the mitochondria. However, although membranes were probed with anti-calnexin to test for purity of the microsomal fractions, no bands were detected (data not shown). It was noted that in the protein profile obtained by Ponceau staining of the PVDF membrane the proteins were only visible in the crude mitochondrial fraction. This result suggested that the presence of protease in the isolation buffer had broken

down non-mitochondrial proteins. Nevertheless the enzymes Cds and PIS showed the same pattern of activity seen in differentiated H9c2 cells. Cds activity was stronger in the crude mitochondrial fraction (Figure 6.9.B), while PIS activity was concentrated in the microsomes (Figure 6.9.C).

Figure 6.9: Adult rat heart cell fractions obtained in the presence of protease: protein expression, Cds and PIS activity.

Two females Sprague-Dawley rats (6 months old) were euthanised, the hearts were dissected and homogenised in a pH 7.4 buffer containing subtisilin (0.4 mg/mL) and subjected to differential centrifugation.

[A.] 50µg of each rat heart tissue fraction was analysed by western blotting using monoclonal antibodies anti-Cds1 at a 1:100 dilution and anti-cytochrome c at a 1:1000 dilution as a mitochondrial marker and on separate membranes the polyclonal antibodies (1:1000 dilution) anti-GRP 75 and anti-complex IV (COX IV) as mitochondrial markers. Prior to blotting, the membranes were stained temporarily with Ponceau solution and imaged. Blue arrow indicates the expected molecular weight for Cds1. MW: molecular weight.

[B.] Cds Activity: 50µg of cell fraction was used for Cds activity analysis for 10 minutes at 30° C. [C.] PIS Activity: 50µg of fractions was used for PIS assay for 15 minutes at 37° C. The bars for [B.] and [C.] represent the mean ±SEM of 3 measurements of radioactivity incorporated into the fractions analysed in [A.] in one experiment. Micro: Microsomes. C Mito: crude mitochondria. Cyto: cytosol.
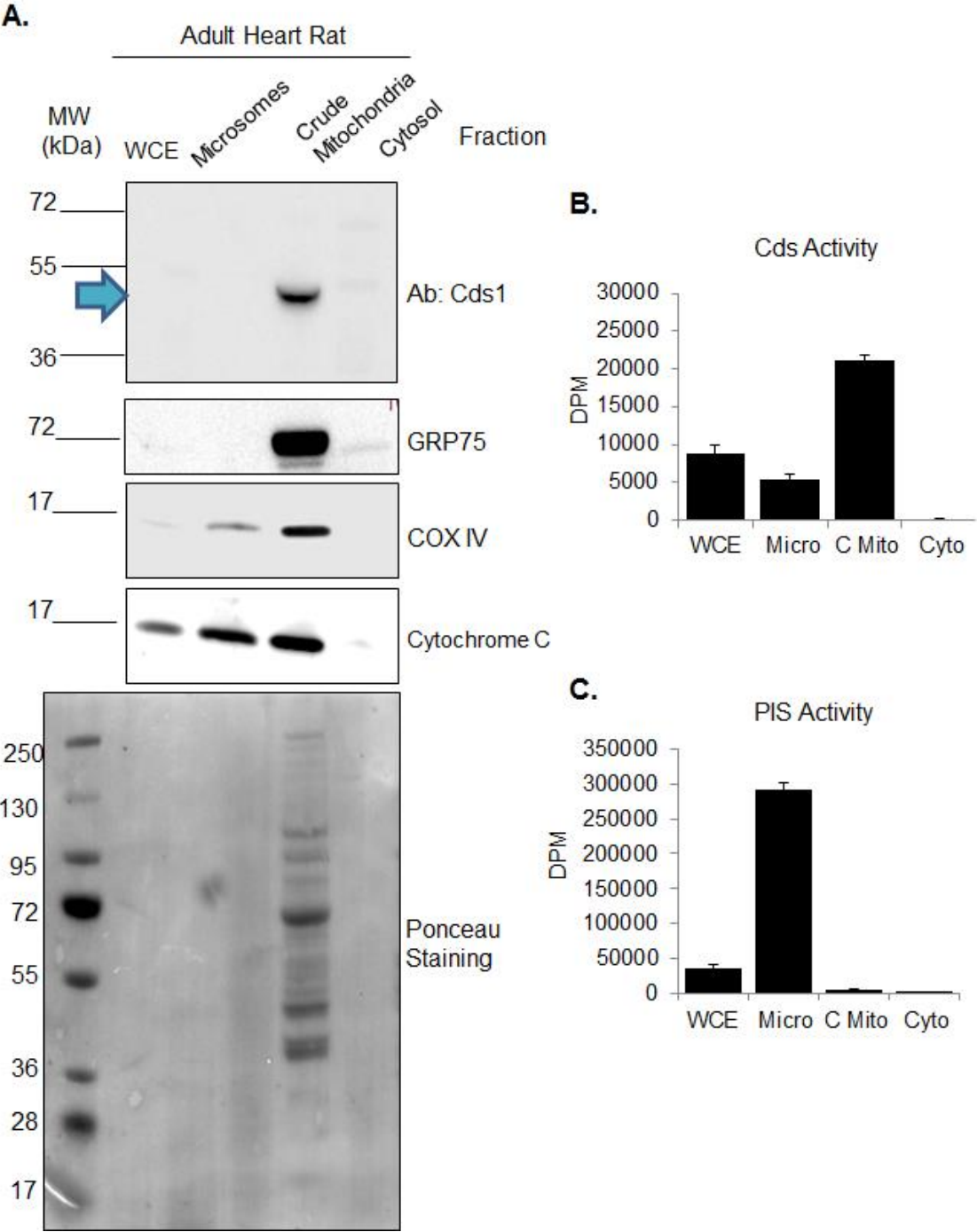
Figure 6.9: Adult rat heart cell fractions obtained in the presence of protease: protein expression, Cds and PIS activity.

a. Pure mitochondria and Mitochondrial Associated Membranes of rat hearts.

In order to further analyse the protein detected by Ab:Cds1 in adult rat heart crude mitochondrial fractions, crude mitochondria was fractioned into pure mitochondria and mitochondrial associated membranes (MAM) by Percol gradient centrifugation. No subtisilin was included in the isolation buffer to assess the effect of this protease in the results (Figure 6.9.). The purity of the fractions was assessed by immunoblotting using calnexin as a microsomal marker and GRP75 and mitofusin 2 as mitochondrial markers (Figure 6.10.A). In addition, the activity of Cds and PIS was analysed using the assays described above (Figure 6.10.B and Figure 6.10.C).

By isolating the fractions in the absence of the protease, the protein profiles were readily observed by Ponceau staining indicating that in order to compare different organelles alongside each other, the use of protease in mitochondrial isolation should be avoided. There was an enrichment in crude and pure mitochondrial fractions with a low level of mitochondrial contamination in microsomal fractions detected by anti-GRP75. A single band was detected by Ab:Cds1 at 55kDa by western blotting. Contrary to the observation in fractions isolated with the protease, all fractions were positive for Ab:Cds1. However, the band was stronger in crude mitochondria and the strongest signal was observed in pure mitochondrial fractions, which also showed no level of microsomal contamination. This observation indicates that the protein identified by Ab:Cds1 was a mitochondrial protein. In addition, the Cds activity measurements reflected the intensity of the protein bands obtained with Ab:Cds1 while PIS activity was concentrated in the microsomal fractions once more. This observation reinforces the notion that the highest Cds activity is found associated with mitochondria in the rat heart.

Figure 6.10: Adult rat heart cell fractions: protein expression, Cds and PIS activity.

Four females Sprague-Dawley rats (6months old) were euthanised, the hearts were dissected and homogenised in a pH 7.4 buffer and the lysates were separated by differential centrifugation.

[A.] On a 4-12% gradient acrylamide gel 50µg of adult rat heart fractions were subjected to SDS-PAGE. After transfer of protein profiles onto PVDF membranes, Ponceau staining was performed and imaged. Protein expression was analysed by western blotting using monoclonal antibodies anti-Cds1 at a 1:100 dilution, on separate membranes, the polyclonal antibodies (1:1000 dilution) calnexin as microsomal marker and anti-GRP 75, anti-mitofusin2 and anti-complex IV (COX IV) as mitochondrial markers. Blue arrow indicates the expected molecular weight for Cds1. MAM: Mitochondrial Associated Membranes. MW: molecular weight.

[B.] Cds Activity: Three measurements of the same sample mixtures containing 50µg of each cell fraction were used assay Cds activity during 10 minutes at 30° C. [C.] PIS Activity: 50µg of each fraction in triplicate were used to assay PIS activity for 15 minutes at 37° C. The bars in [B.] and [C.] represent the mean ± SEM DPM counts from one experiment where the background reading was subtracted the values obtained from the fractions tested in [A.]. Micro: microsomes. C Mito: crude mitochondria. P Mito: pure mitochondria.
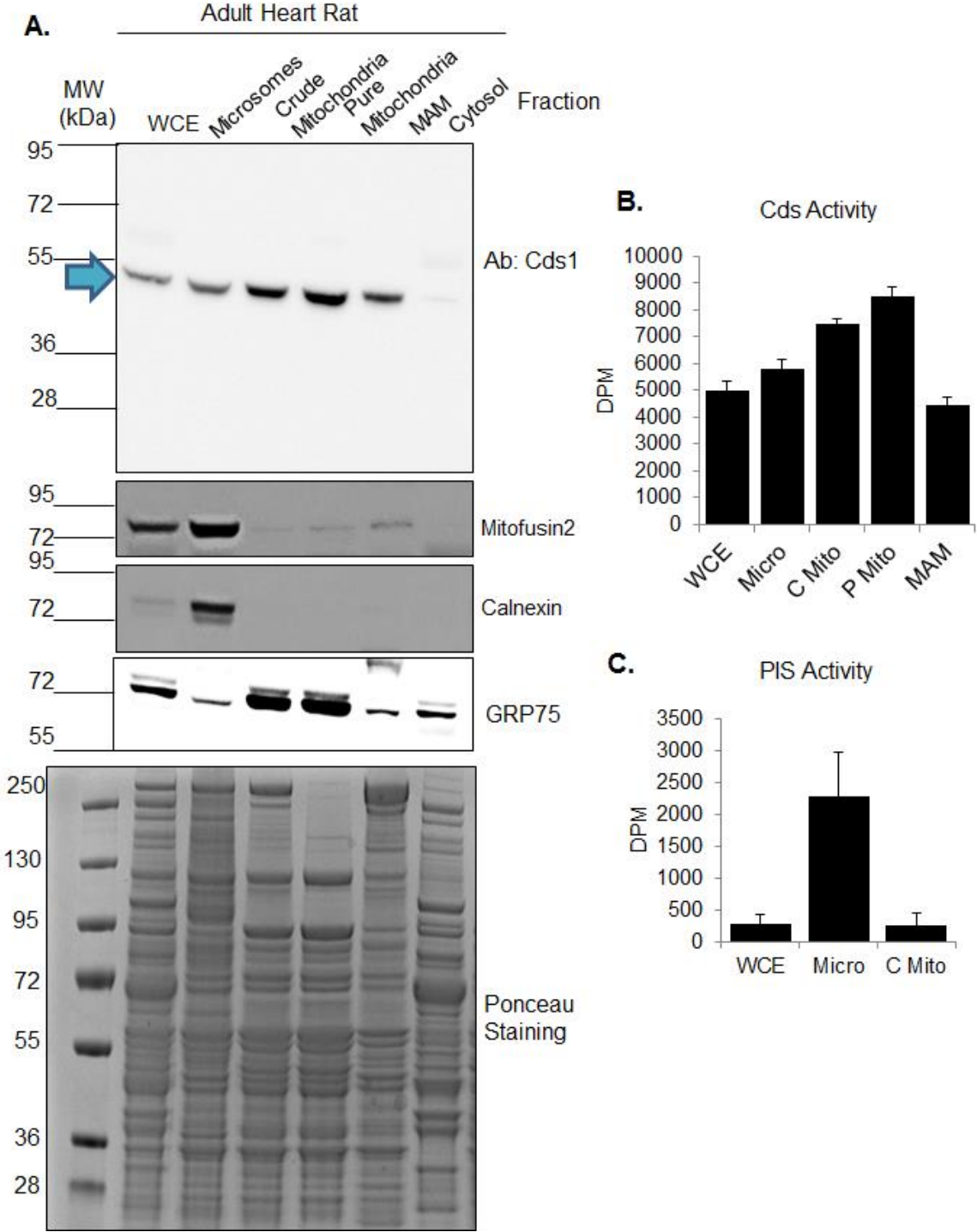
Figure 6.10: Adult rat heart fractions: protein expression, Cds and PIS activity.

6.3.3: Anti-Cds1 recognises overexpressed Cds1 and no Cds2.

To validate Ab:Cds1 for immunoblotting, Cos7 cells were transfected with human myc-Cds1. Furthermore, the specificity of the antibody was tested by comparing overexpressed myc-tagged human Cds1 and Cds2 by western blotting. The plasmids were transfected and analysed on a 7.5% acrylamide gel following the methods in the publication from the group that provided us with the plasmids.[29] Cos7 cells transfected with an empty pCDNA plasmid were used as negative control (Figure 6.11.). The Cds activity of the overexpressed cell lysates was also analysed to evaluate whether the protein expression pattern reflected the activity of the enzymes (Figure 6.11.C).

Ab:Cds1 detected a very strong signal at ~80kDa exclusively from Cos7 cell lysates transfected with human myc-Cds1, which indicated that the antibody is specific for human Cds1. In comparison, the anti-myc antibody detected stronger transfection of the human myc-Cds2 over myc-Cds1 in Cos7 cells with a detection pattern similar to the one seen with Ab:Cds1 (Figure 6.11.B). On the other hand, the analysis of Cds activity on the transfected cells showed a higher activity from the Cds1 over the Cds2 overexpressed samples (Figure 6.11.C).

In addition, the single band previously seen at 55kDa from pure mitochondrial rat heart (Figure 6.10) was detected at a much lower molecular weight compared to overexpressed Cds1 at ~36kDa (Figure 6.11.A) , suggesting that this endogenous protein is a mitochondrial protein of unknown identity with possibly higher expression in rat samples than Cds1.

Figure 6.11: Ab:Cds1 recognises overexpressed human Cds1.

Cos7 cells were transiently transfected with human myc-Cds1, myc-Cds2 or an empty pCDNA vector by lipofection for 24 hours and further cultured for 24 hours.

75µg of each Cos7 cell lysates were harvested in PBS and mixed with 2x Laemmili buffer and warmed at 60°C for 5 minutes alongside 50µg of pure mitochondrial fraction obtained from differential centrifugation of adult rat hearts. SDS-PAGE was performed using 7.5% acrylamide gel at 200 volts for 45 minutes. Proteins were analysed by western blot using monoclonal antibodies:

[A.] Anti Cds1, Ab:Cds1 at 1:100 dilution.

[B.] Anti-myc, Ab:Myc at 1:1000 dilution.

[C.] 50µg of each Cos7 cell lysates and cellular fractions of cells transfected with myc-Cds1 were tested for Cds activity for 10 minutes at 30°C. Samples were analysed in triplicate and the bars show mean ± SEM of one experiment.
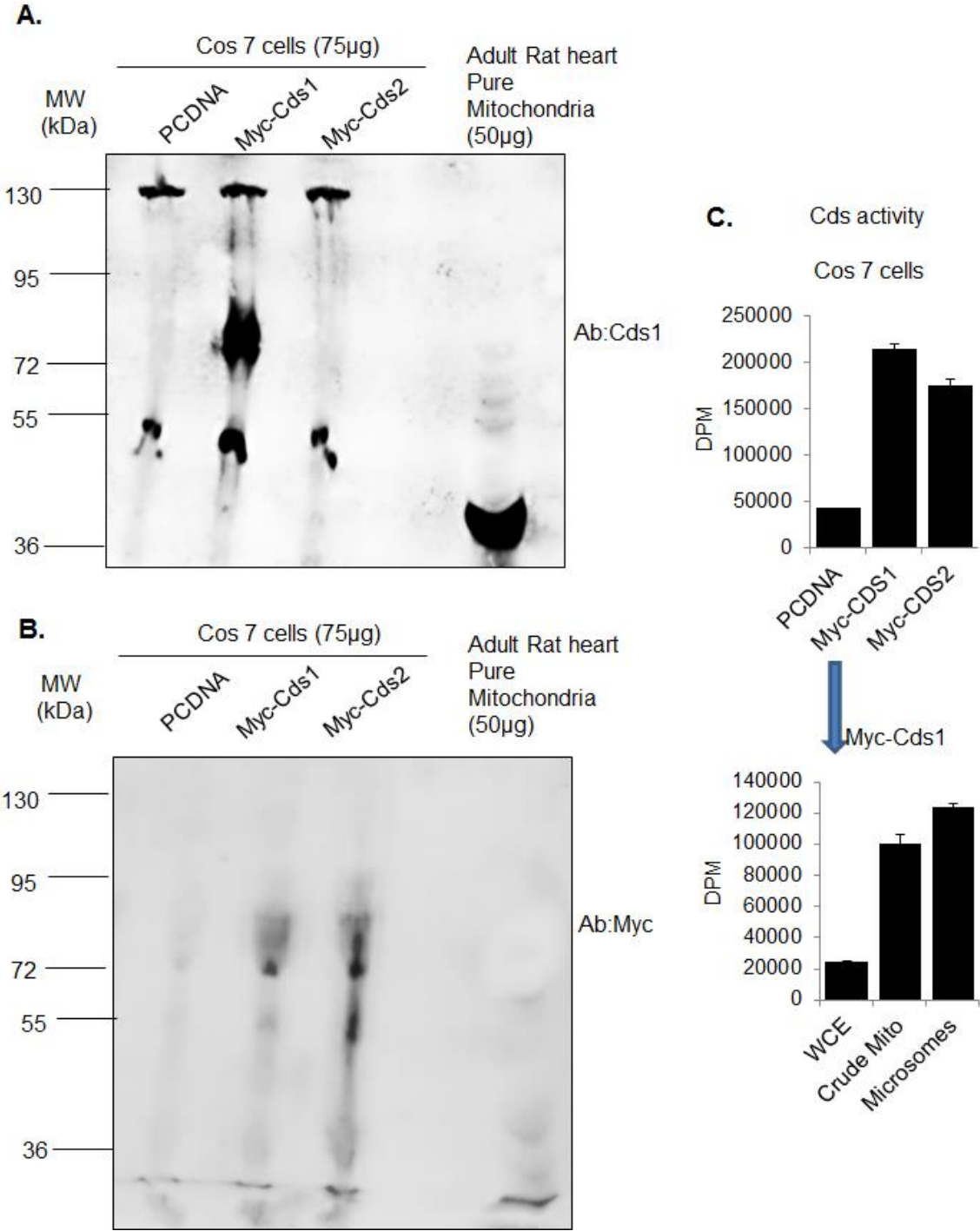
Figure 6.11: Ab:Cds1 recognises overexpressed human Cds1.

6.3.4: Transfection of siRNA Cds1 in differentiated H9c2 cells

Although Ab:Cds1 does recognise overexpressed Cds1 and not Cds2, the endogenous protein thought to be Cds1 did not co-migrate with the overexpressed Cds1 (Figure 6.11). Therefore the identity of the detected 55kDa protein was ultimately tested for Cds1 mRNA down-regulation by rat siRNA transfection of differentiated H9c2 cells. Due to the length of time required for differentiation (9 days), siRNA transfection was evaluated at consecutive 3 day intervals using a negative siRNA or a combination of two rat Cds1 siRNA oligonucleotides and analysed by immunoblotting (Figure 6.12.A). Down-regulation efficiency and specificity was tested by qPCR of Cds1 mRNA alongside Cds2 and Tamm41 mRNA (Figure 6.12.B).

Cds1 mRNA down-regulation was effective as seen by the 72±0.5% reduction in relative mRNA found by qPCR after one round (transfection on day 6) and 76±2% reduction after three rounds (transfections on days 0, 3 and 6) of siRNA transfection compared to cells transfected with a negative siRNA. This down-regulation was specific for Cds1 since Cds2 and Tamm41 mRNA was not affected by Cds1 siRNA transfection (Figure 6.16.B). However, none of the bands detected by Ab:Cds1 were visibly affected by rat Cds1 siRNA after any number of siRNA transfections including the signal of the 55kDa protein, which was the band presumed to be Cds1. The experiment was repeated several times and although some signal reduction was noted in 2 experiments, the majority of results determined that antibody Ab:Cds1 recognises another 55kDa protein in rat tissue possibly alongside Cds1. Therefore, Ab:Cds1 was not suitable for the study of the protein expression of endogenous Cds1 in rat heart by western blotting.

Figure 6.12: The 55kDa protein detected by Ab:Cds1 in H9c2 cells is not affected by rat Cds1 siRNA

H9c2 cells were cultured in media supplemented with 1% FCS media plus daily all-trans retinoic acid (1µM RA) for a total of 9 days. On day 0, 3 and/or 6 of differentiation, 12nM of two rat Cds1 siRNA oligonucleotides or a negative siRNA were introduced into the cells and incubated for 3 days. As control sample, no siRNA was transfected (untreated). Cell lysates were harvested in RIPA buffer and RNA lysis buffer on day 9 of differentiation.

[A.] 75µg of differentiated H9c2 cell lysates were analysed by western blotting on a PVDF membrane stained with Ponceau solution as a loading control. Membranes were probed with monoclonal antibody Ab:Cds1 at a 1:100 dilution.

[B.] 1µg RNA was used to obtain cDNA by reverse transcription qRT-PCR of 5µL cDNA using SYBR green and the indicated primers. Ct values were obtained in triplicate and the ΔΔCt formula was used to normalise to the Ct values from Phosphoglycerate Kinase 1 (PGK1). The bars represent average fold change in mRNA ± SEM using the samples in [A.]. (*): $p < 0.05$
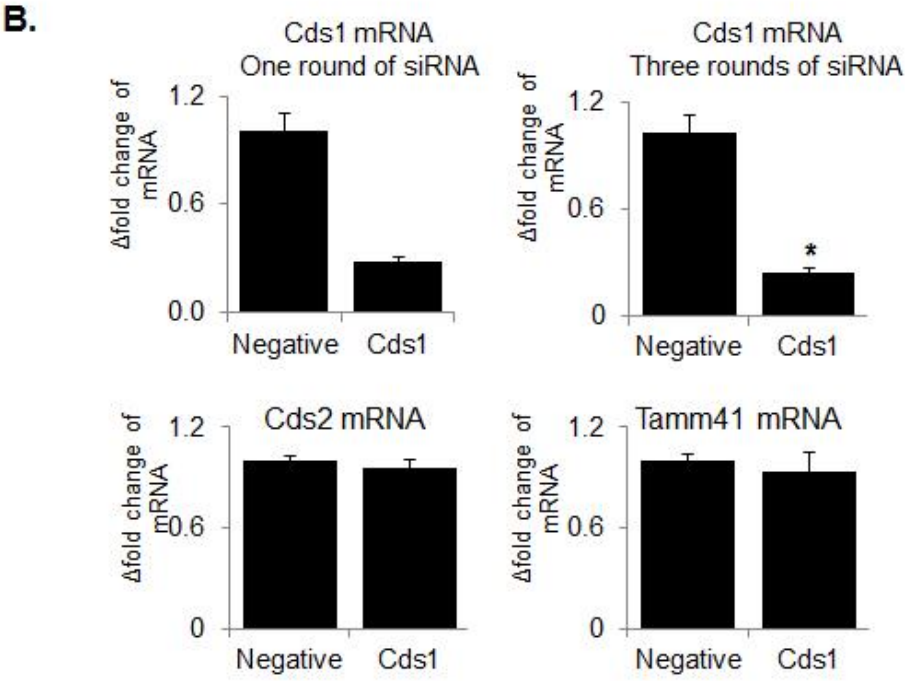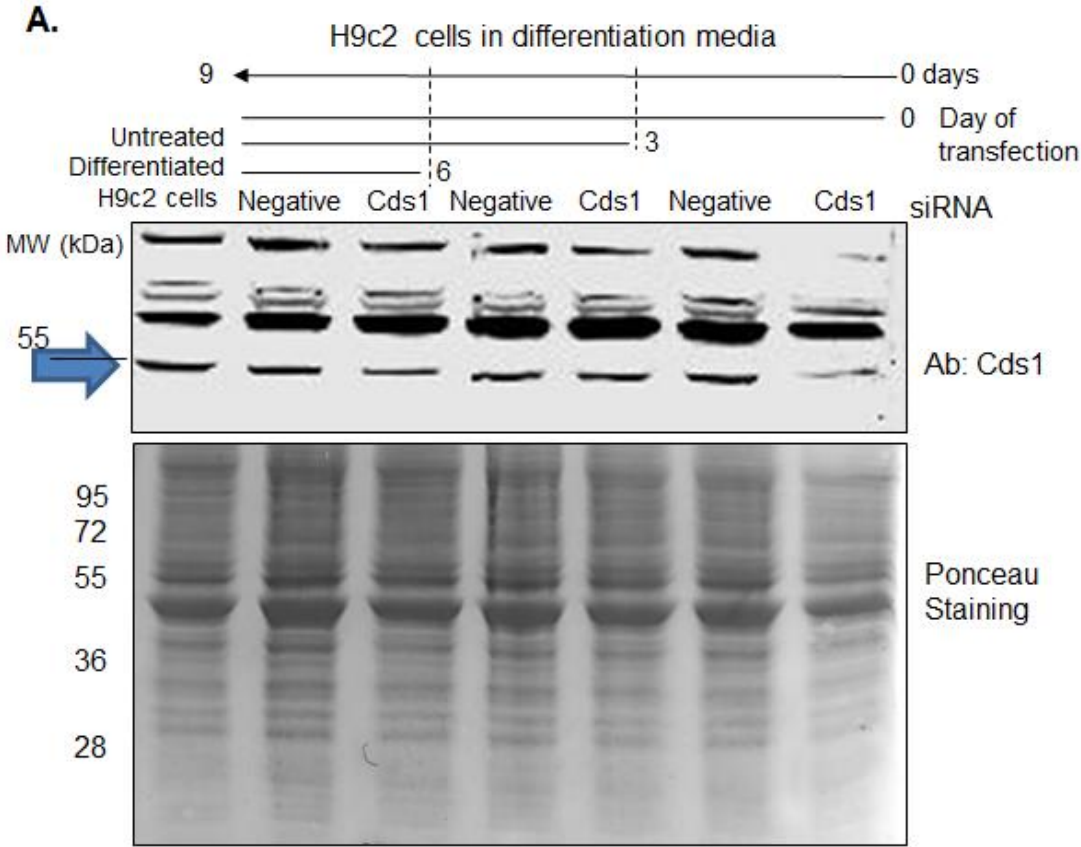
Figure 6.12: The 55kDa protein detected by Ab:Cds1 in H9c2 cells is not affected by rat Cds1 siRNA.

6.4: Summary and discussion.

In this chapter I investigated the expression pattern of proteins involved in phospholipid biosynthesis in H9c2 cells subjected to differentiation brought about by reducing the concentration of FCS from 10% to 1% and by adding all-trans-retinoic acid. Differentiated cells exhibited a cardiomyocyte-like phenotype confirmed on the basis of changes to morphological features as compared with the parental line (Figure 6.1). The changes in cell morphology were found to occur in concomitance with the expression of specific cardiac markers including cardiac troponin I, ANP and BNP (Figure 6.2), in agreement with previous reports investigating cardiomyocyte-like differentiation of H9c2 cells. [25,80,88]

During the course of myoblast differentiation there was an increase in the expression of the mitochondrial proteins COX IV, GRP75 and cytochrome C, which implied an increase in mitochondrial biogenesis (Figure 6.3 and Figure 6.4). Other recent studies had also reported up-regulation of proteins related with mitochondrial function, including PGC-1, ATP synthase and cytochrome c oxidase. [11,25] PGC-1 is known for acting as a master regulator of energy metabolism and mitochondrial biogenesis and it has been shown to regulate Cds1 expression in the adult heart by a mechanism which involves direct transcriptional activation[68]. Conversely, other mitochondrial enzymes known to assist in CL biosynthesis, such CLS, were not regulated by PGC-1.[68] Similarly in this study, although the immunoblotting analysis of differentiated H9c2 cells determined mitochondrial content increases (Figure 6.3 and Figure 6.4), the mRNA expression of the enzymes involved in phospholipid

synthesis was not up-regulated (Figure 6.5). Nevertheless, Cds and PIS activities did increase after differentiation (Figure 6.6) and CLS activity was not investigated.

Endogenous Cds1, together with PIS, were recently found restricted to a sub-fraction of the calnexin-positive ER fragment after membrane fractionation of epidermoid carcinoma human cells.[119] Cds1 was also localised exclusively to the ER in yeast (*Saccharomyces cerevisiae*); where the mitochondrial translocator assembly and maintenance protein, homolog (Tamm41) was found to be the mitochondrial Cds enzyme leading to cardiolipin biosynthesis.[68] In this study, when differentiated H9c2 cells and adult heart tissue were fractionated, Cds activity was constantly higher in the enriched mitochondrial fractions, rather than in microsomes or mitochondrial associated membranes as expected (Figure 6.8 and 6.10). However the degree of purity of the fractions requires further consideration and, established MAM marker antibodies such the sigma1 receptor or ACSL4 were not investigated in these experiments. Although mitofusin2 has been reported to be present tethering mitochondria to the ER allowing the communication of calcium between these two organelles,[30] it is considered as a mitochondrial rather than MAM marker protein based on its ability to promote mitochondrial fusion. In addition, the intention of including Cds activity measurements to cellular fractions was to compare activity with protein expression as measured by the Ab:Cds1 and therefore no attempt was made to find the statistical significance of those observations. Furthermore the Cds activity assay used here was not able to distinguish between Cds1, Cds2 or Tamm41 contribution towards the CDP-DAG synthesis measured and that could be subject of future studies.

Additionally, immunoblotting analysis showed a stronger content of overexpressed human myc-Cds2 than myc-Cds1 in transfected Cos7 cells. Cds

activity on the contrary, showed higher activity from Cds1 over Cds2 (Figure 6.11) which might be explained by the recent report on the specificity of Cds2 in the fatty acid species of the PA used as substrate in the assay. Cds2 preferred 1-stearoyl-2-arachidonoyl-phosphatidic acid (18:0/20:4) whilst Cds1 showed no particular substrate specificity.[29] The PA used for the Cds assay in this study contained low quantities of arachidonic and stearic acids (Table 2.10).

The study into the protein expression of Cds1 was put into question due to the characterisation of the antibody used. The localisation study in conjunction with the observation that the endogenous 55kDa protein detected by the antibody Ab:Cds1 was not down-regulated by rat Cds1 siRNA in H9c2 cells suggested that the band detected a mitochondrial associated protein of unknown identity with higher intensity than Cds1(Figure 6.13). However, since this observation relied on siRNA data, additional controls other than the negative siRNA and untreated transfection controls should have been included in the study for a definite answer. The absent controls include an endogenous positive control sample with no siRNA where all reagents other than the siRNA should be added to test for any effect from the transfection reagents such as cytotoxicity or other non-specific effects. In addition, a 'mock' control of a validated siRNA pool or individual siRNA targeting a well-characterized housekeeping gene, such as GAPDH which is well-expressed but non-essential could have been included to establish cellular viability.

The datasheet of Ab:Cds1, commercially known under catalogue number H00001040-M01, shows as positive control a western blot image of a single band detected at 55kDa in human liver without any further details. In addition, the publication citing the antibody used human lung cells and it did not include an antibody characterisation[42]. The same antibody has been sold by various companies

under different codes. For instance, the study reporting that Cds1 activity coincides with protein expression of calnexin enriched fractions used antibody MCA5324Z[119] which shows exactly the same details as H00001040-M01. Both studies used human cell lines as their model. In addition, the crystal structure of Cds1 showed that it forms a homodimer[71] and when Cos7 cells were overexpressed with Myc-Cds1 demonstrated that Ab:Cds1 does recognise a 80kDa protein which could be the dimer form of the protein (Figure 6.11); plus the sequence in rat corresponding to the human Cds1 sequence used as immunogen was 89% identical (Figure 6.7). It is possible that the antibody exclusively recognises human Cds1 and not rat Cds1. Further characterisation to test species specificity will be required. An alternative to this problem for future studies in rat heart could be using another antibody, for example, anti-Cds rabbit antibody (product No. ab84019, Abcam,). However, this antibody has not been characterised appropriately increasing the risk of spending time and resources which might end again in invalidation. In chapter 4, I already discussed the problems associated with the use of uncharacterised antibodies in research.

CHAPTER 7: Effects of Arginine Vasopressin stimulation on the expression of RdgBβ and Cds1 in H9c2 cells.

7.1. Introduction

This study attempted to describe the endogenous expression of RdgBβ and Cds1 in H9c2 cells and rat heart samples in order to identify clues leading to the elucidation of their physiological function in the heart. For protein expression of RdgBβ, the antibody Ab:Rb59 was validated for immunoblotting experiments (Chapter 4), which determined that RdgBβ is a cytosolic protein upregulated by differentiation of H9c2 cells, and its protein and mRNA expression increased with cardiac maturation (Chapter 5). On the other hand, protein expression of Cds1 was limited to mRNA results due to the invalidation of the antibody used for immunoblotting on rat samples. Contrary to RdgBβ, Cds1 mRNA was not affected by H9c2 differentiation (Chapter 6).

This chapter describes work into an approach that was pursued considering the limitations of this thesis. Since H9c2 cells present receptors for vasopressin (AVP V1) which are coupled to PLC signalling[132] and AVP stimulation was found to produce H9c2 cellular hypertrophy and increased protein synthesis,[14] the effect of AVP receptors stimulation in H9c2 cells was evaluated for possible changes in the expression of RdgBβ and Cds1.

7.2: Arginine Vasopressin stimulation in H9c2 cells.

To evaluate whether the changes observed in H9c2 cells upon differentiation resemble the effects of G-coupled receptor-mediated PLC signalling in H9c2 cells, the expression pattern of H9c2 cells was studied after chronic stimulation with the vasodilator Arginine Vasopressin (AVP).

7.2.1: AVP stimulation of PLC activity in H9c2 cells.

PLC activity was measured by an assay described previoulsly[48] which quantifies the [^{3}H]-inositol phosphates produced as a result of PIP_2 hydrolysis by phospholipase C stimulation in H9c2 cells. In brief, 1µM AVP or Ang II were added to the cells in culture and incubated for one hour. The addition of 10mM LiCl to the incubation buffer inhibited the hydrolysis of inositol phosphates back to inositol allowing the inositol phosphates to accumulate. Untreated cells provided the base level activity control of the assay (Figure 7.1).

The treatment with arginine vasopressin increased the proportion of labelled inositol phosphates from 9.7±4.6% to 43.9±3.5% in proliferating H9c2 cells. Similarly, RA differentiated cells showed an increase in PLC activity from 5.9±0.04% to 37.3±4.2% of labelled inositol phosphates. On the contrary, Angiotensin II did not stimulate PLC-mediated PIP_2 hydrolysis in H9c2 cells irrespective of the differentiation state, which suggested that AngII receptors are absent or not expressed in sufficient quantities to produce a measurable reaction.
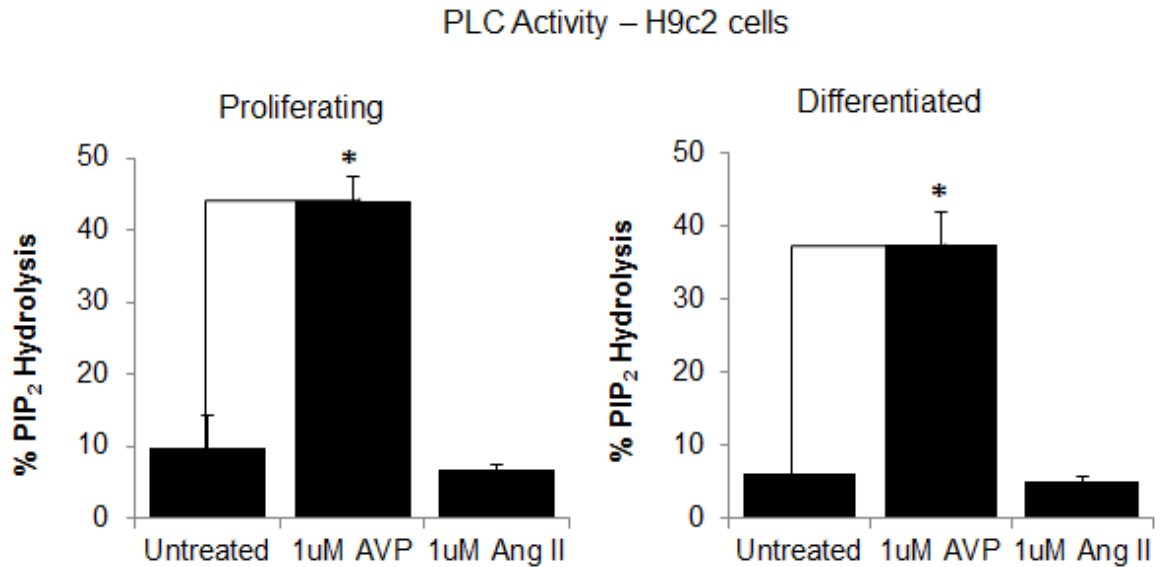
Figure 7.1: PLC-mediated PIP$_2$ hydrolysis in H9c2 cells.

H9c2 cells were seeded into 6 well culture dishes and cultured for 2 days (Proliferating) or 8 days (Differentiated) before [^{3}H]-Inositol was added for 16 hours. Radiolabelled media was removed and replaced by buffer containing LiCl in the absence or presence of the agonist in duplicate: 1µM Angiotensin II (Ang II) or 1µM Arginine Vasopressin (AVP). Cells were incubated for 1 hour at 37° C with the stimulants before harvesting. The samples were separated into aqueous or chloroform soluble phases and [^{3}H]-inositol phosphates formed were isolated from the aqueous phase using Dowex columns. For data analysis, the average of radioactive counts (dpm) was expressed as a proportion of the total radioactivity counted per sample. The bars show average of 2 experiments ± SEM. Proliferating (p=0.02), differentiated cells (p=0.003).

7.2.2: Arginine Vasopressin stimulation effect in the expression of RdgBβ in H9c2 cells.

The effect of AVP stimulation in the expression of RdgBβ in H9c2 cells was analysed by immunoblotting and qRT-PCR (Figure 7.2). After 3 days of 0.5µM AVP stimulation no change was observed in the protein expression of RdgBβ detected by antibody Ab:Rb59 compared to the expression of PITPα regardless of the differentiation state (Figure 7.2.A). Similarly treatment with 0.5µM AVP had no impact on RdgBβ mRNA expression of differentiated H9c2 cells and showed a non-significant increase of RdgBα relative mRNA expression. However, proliferating cells showed a reduction in RdgBβ mRNA content of around 40% decrease (Figure 7.2.B).

These results indicated that the expression of RdgBβ is not regulated by vasopressin stimulation in H9c2 differentiated cells. Since the experiment with proliferating cells was performed only twice, the significance of the decrease in RdgBβ mRNA is difficult to interpret.
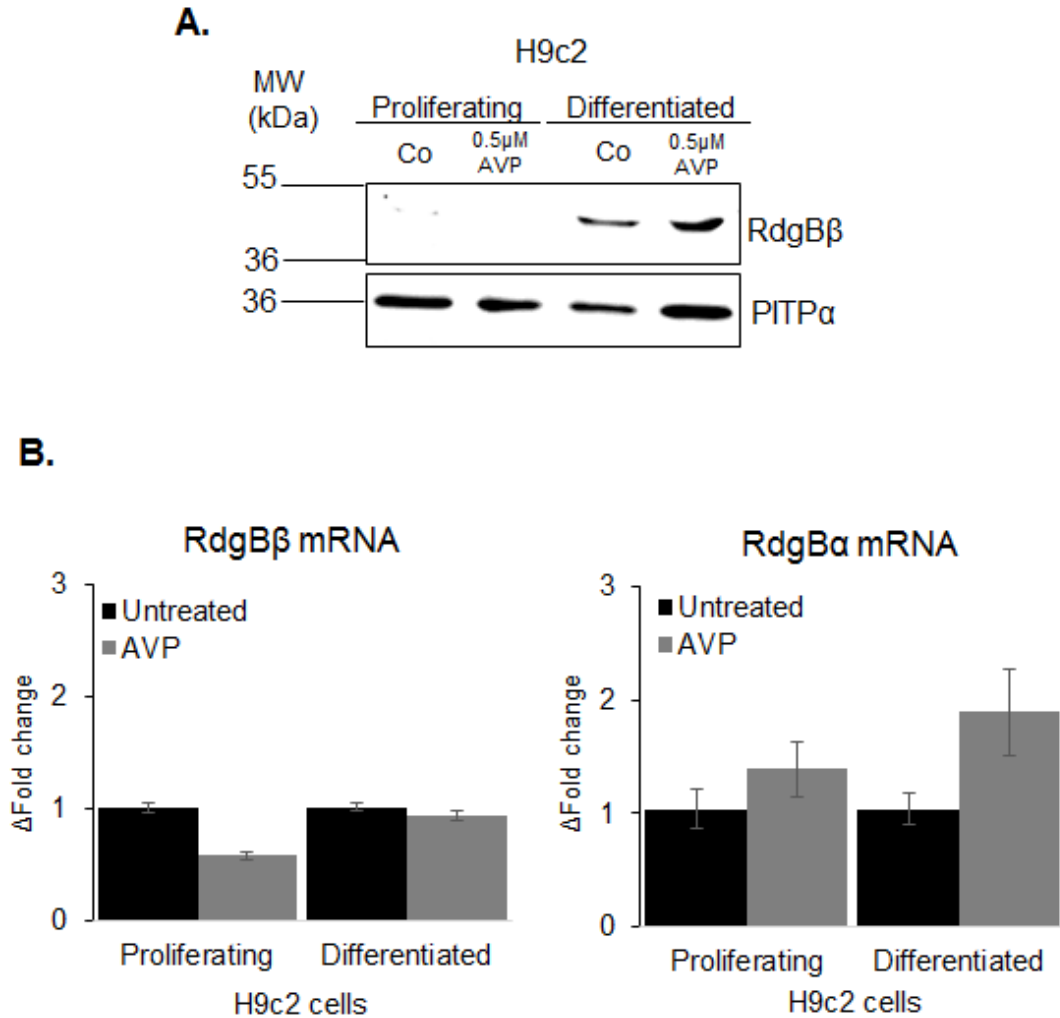
Figure 7.2: Expression of RdgBβ after stimulation of H9c2 cells with AVP.

H9c2 cells were cultured for 2 days (Proliferating) or 8 days (Differentiated) then 0.5 µM arginine vasopressin (AVP) or no stimulant (Untreated) were added to the media for 3 days.

[A.] 75µg of cell lysate was subjected to western blot analysis using polyclonal antibodies Ab:Rb59 for RdgBβ detection at a 1:100 dilution and Ab:674 for PITPα detection at a 1:1000 dilution.

[B.] 1µg of RNA for each sample was used to produce cDNA which was then used for qRT-PCR analysis using the primers indicated in triplicate samples. The bars represent the average fold change of relative Ct values normalised to PGK1 obtained with the ΔΔCt formula ± SEM of 7 experiments for RdgBβ (Differentiated) and 2 experiments for RdgBβ (Proliferating) and RdgBα mRNA.

7.2.3: AVP stimulation effect in Cds activity and Cds1 mRNA expression in H9c2 cells.

The Cds activity and mRNA expression of Cds1 were also analysed after chronic stimulation of Arginine Vasopressin of H9c2 cells prior and after differentiation (Figure 7.3). The Cds activity upon AVP treatment in proliferating cells resembled the activity observed upon retinoic acid differentiation with a close to two fold increase. On the other hand, Cds activity of differentiated H9c2 cells was minimally increased by AVP stimulation (Figure 7.3.A). These results suggest that AVP promotes Cds-mediated CDP-DAG synthesis in proliferating cells but not in terminally differentiated H9c2 cells.

Additionally, Cds1 mRNA expression was substantially increased with vasopressin stimulation in both myoblasts and differentiated H9c2 cells, although the increase in proliferating cells was higher (4.07±0.17 fold increase) than in differentiated cells (3.09±0.27 fold increase). In comparison, Cds2 mRNA expression was unaffected by AVP stimulation (Figure 7.3.B). The significance of the mRNA expression increase of Cds1 mRNA remains to be explored.

A.

B.
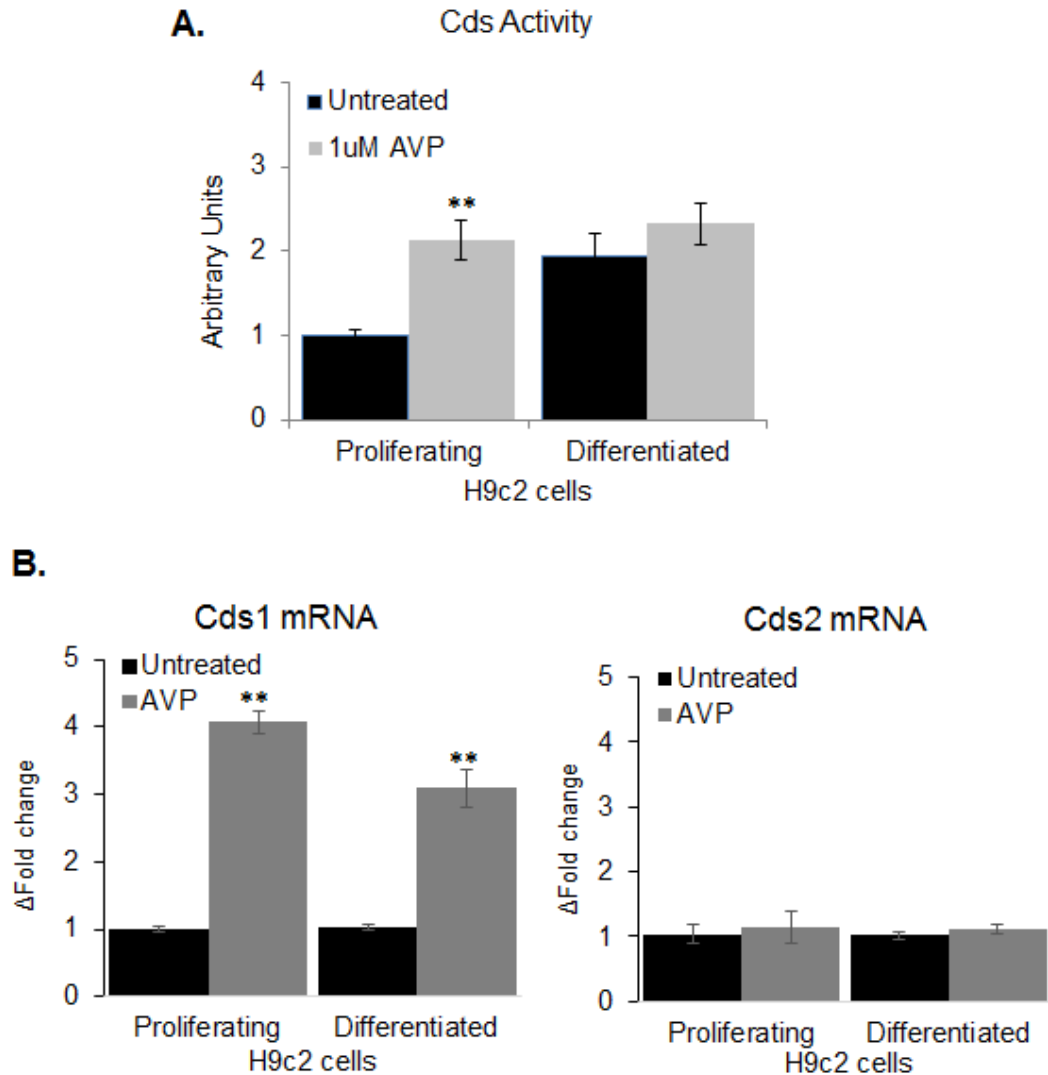
Figure 7.3: Cds activity in H9c2 cells.

H9c2 cells were cultured in complete media (10% FCS) for 16 hours (Proliferating), or cultured in serum media reduced to 1%FCS in the presence of daily 1μM all-trans retinoic acid. The cells were incubated ±1μM Arginine vasopressin (AVP) for 3 days.

[A.], 50μg of cell lysates was tested for Cds activity for 10 minutes at 30° C. The bars represent dpm counts relative to proliferating untreated cells counts ± SEM. (Proliferating: 2.13±0.2, p=0.009, n=6; Differentiated: 2.33±0.006, p=0.005, n=6)

[B.] 1μg mRNA was used to produce cDNA by reverse transcription. 5μl of cDNA was used in qRT-PCR analysis using SYBR-green and the indicated primers in triplicates. The bars represent the average of Ct values normalised to PGK1 using the ΔΔCt formula relative to the untreated samples. Proliferating Cds1 mRNA: (**) $p=3.3 \times 10^{-7}$ from 7 experiments (n=21). Cds2 mRNA: n=6 from 2 experiments.

7.3: Summary and discussion.

Chapter 7 described work into the effects of chronic AVP stimulation in H9c2 cells. Firstly it was observed that H9c2 cells responded to AVP but not to AngII stimulation (Figure 7.1). This result suggests that proliferating and differentiated H9c2 cells do not express Ang II receptors. Alternatively, these receptors might be inactive or present in very small quantities in this cell line. Similarly, a previous study identified Ang II stimulation on H9c2 cells to be ineffective and found an association between vasopressin stimulation of H9c2 myoblast and differentiated cells with the development of cardiac hyperthrophy.[14]

Furthermore, the expression analysis found that RdgBβ is not regulated by AVP stimulation (Figure 7.2), indicating that the increase in expression upon cellular differentiation observed in this thesis (Chapter 5) is not a result of G-coupled PLCβ signalling.

Finally, chronic AVP treatment substantially increased Cds activity in proliferating cells while the response in differentiated cells was much smaller (Figure 7.3.A). A previous study exploring vasopressin stimulation in H9c2 cells differentiation also noticed this difference by showing that AVP evoked a large PLC signalling-induced Ca^{2+} release in H9c2 myoblasts, whereas the response in differentiated cells was weaker.[128] This result was not reflected in the mRNA expression analysis where Cds1 was significantly increased upon AVP stimulation regardless of the differentiation state of the cells (Figure 7.3.B). Therefore it would appear that the increase of Cds1 mRNA upon AVP stimulation might influence the Cds activity of H9c2 cells distinctively on the state of differentiation.

CHAPTER 8: Effects of RdgBβ and Cds1 silencing by siRNA on cell morphology and Cds activity.

8.1: Introduction

In this thesis the endogenous expression of RdgBβ and Cds1 has been studied in H9c2 cells. Chapter 7 explored the influence of AVP stimulation on their expression and provided a small insight into Cds1 mRNA regulation. However, the physiological functions of these proteins remain unclear. This Chapter describes briefly two approaches taken to explore the possible contribution of Cds1 and RdgBβ towards CDP-DAG formation in the rat heart and shows the observations on the effects of rat RdgBβ and Cds1 mRNA downregulation in differentiated H9c2 cell morphology.

8.2: Potential involvement of Cds1 and RdgBβ in Cds activity in the rat heart.

8.2.1: Cds1 mRNA downregulation effect in total Cds activity.

The Cds assay used in this study did not distinguish the contribution of each Cds protein present in the lysates. Although the characterisation of the Ab:Cds1 demonstrated that this antibody is not suitable for the study of the protein expression of Cds1 in rat heart samples, the mRNA expression was effectively downregulated by siRNA transfection (Chapter 6). Therefore, the contribution of Cds1 towards total Cds activity in differentiated H9c2 cells was tested by comparing

Cds activity in cells transfected with rat Cds1 siRNA against a negative siRNA oligonucleotide during cellular differentiation (Figure 8.1).

After one Cds1 siRNA transfection at day 6 of differentiation (72 h), the total Cds activity was reduced by 30±4%. Similarly, three consecutive transfections at days 0, 3 and 6 of differentiation (72h x 3) showed the activity diminished by 25±6%. These results indicated that Cds1 is a minor contributor to the total Cds activity during H9c2 cells differentiation using this particular assay.

8.2.2: Effects of RdgBβ on Cds activity.

The most notable characteristic described for RdgBβ to date is its ability to transfer Phosphatidic acid (PA) between membranes *in vitro*,[40] and PA is the substrate of Cds enzymes which is converted into CDP-DAG. Therefore I tested whether RdgBβ influenced Cds activity in the rat heart firstly by comparing Cds activity of H9c2 cells where RdgBβ mRNA was downregulated (Figure 8.2.A), followed by the addition of recombinant RdgBβ to microsomal and crude mitochondrial fractions of adult rat hearts (Figure 8.2.B).

Rat RdgBβ siRNA transfection marginally reduced Cds activity of differentiated H9c2 cells, and the addition of recombinant protein did not alter Cds activity measurements of microsomes and crude mitochondrial fractions. These results indicated that is highly unlikely that RdgBβ directly influences CDP-DAG synthesis in the rat heart.

227
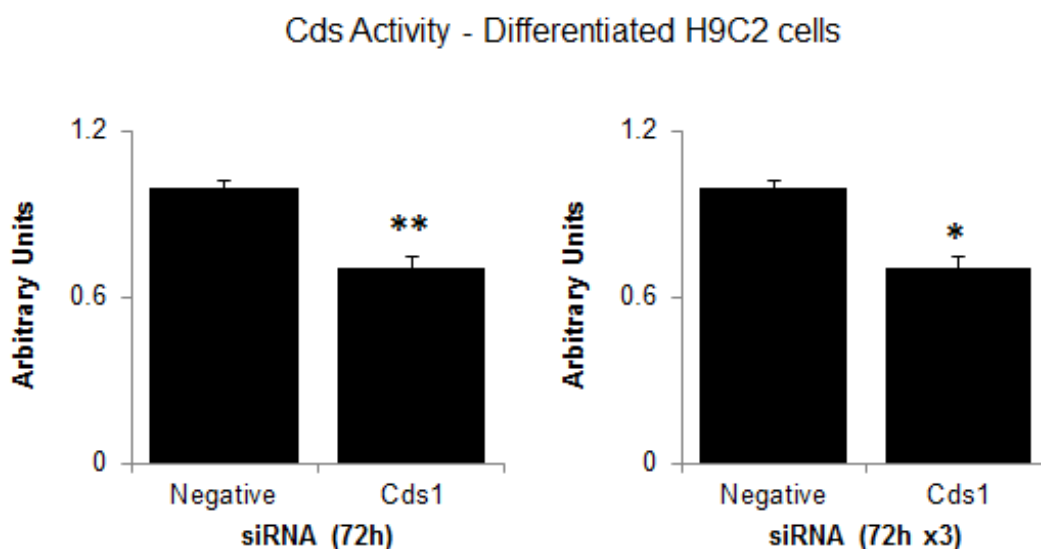
Figure 8.1: Cds1 mRNA downregulation effect in Cds activity in differentiated H9c2 cells.

The Cds activity assay was performed using 50µg of cell lysates from differentiated H9c2 cells which were transfected with two rat Cds1 siRNA oligonucleotides for the duration of the nine days differentiation (72h x 3), or transfected on the last 3 days (72h).

The graph shows the average normalised to the values obtained from negative siRNA cell lysates. 72h (**): p=0.0004, n=9 from 2 experiments. 72h x 3(*): p=0.03, n=9 from 3 experiments.

A.

B.
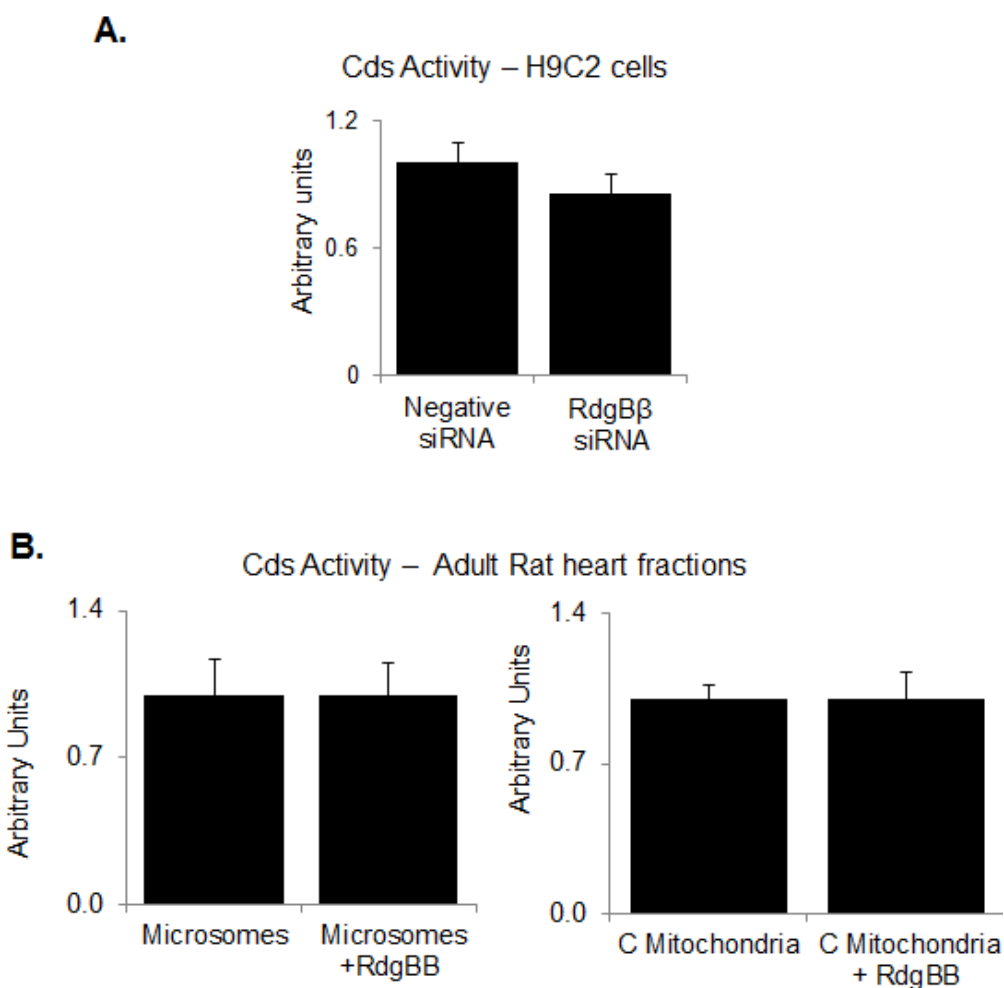
Figure 8.2: Effects of RdgBβ in the rat heart Cds activity.

[A.] Cds activity of 50μg of differentiated H9c2 cells transfected with a negative siRNA or two rat RdgBβ siRNA oligonucleotides for the duration of the 9 days differentiation (72h x 3).

[B.] 50 μg of microsomal and crude mitochondrial fractions obtained by differential centrifugation of adult rat hearts were tested for Cds activity ± 200μg/mL recombinant RdgBβ. p=0.002 (n=6 from 2 experiments)

8.2.3: Effects of RdgBβ and Cds1 mRNA downregulation in the morphology of differentiated H9c2 cells.

During the siRNA experiments described in previous chapters, I noticed that the cells in culture differed in their morphology when seen under the microscope depending on the type of siRNA oligonucleotides transfected into H9c2 cells. Consequently, the changes in cell morphology after rat RdgBβ and Cds1 siRNA transfection were analysed by immunofluorescence of the actin filaments by phalloidin staining of fixed cells. Untreated proliferating and differentiated cells were also analysed for comparison (Figure 8.3).

Differentiated H9c2 cells transfected with a negative siRNA showed the same multinucleated fused cells seen in non-transfected cells whilst cells where RdgBβ mRNA was downregulated showed a substantial increase in cell volume conserving multinucleation and actin filaments. In comparison, transfection of RdgBα siRNA was vastly detrimental to the cells whilst PITPβ mRNA downregulation did not show any change in cell morphology. This observation suggested that unlike other PITPs, RdgBβ may influence H9c2 cells hypertrophy.

In addition, Cds1 siRNA transfection of H9c2 cells showed a distinct abnormality in the shape of cells upon Cds1 siRNA transfection; the cells looked rounded with a loss of the bright actin filaments compared to cells transfected with negative siRNA suggesting that Cds1 is involved in actin filaments formation during differentiation of H9c2 cells.
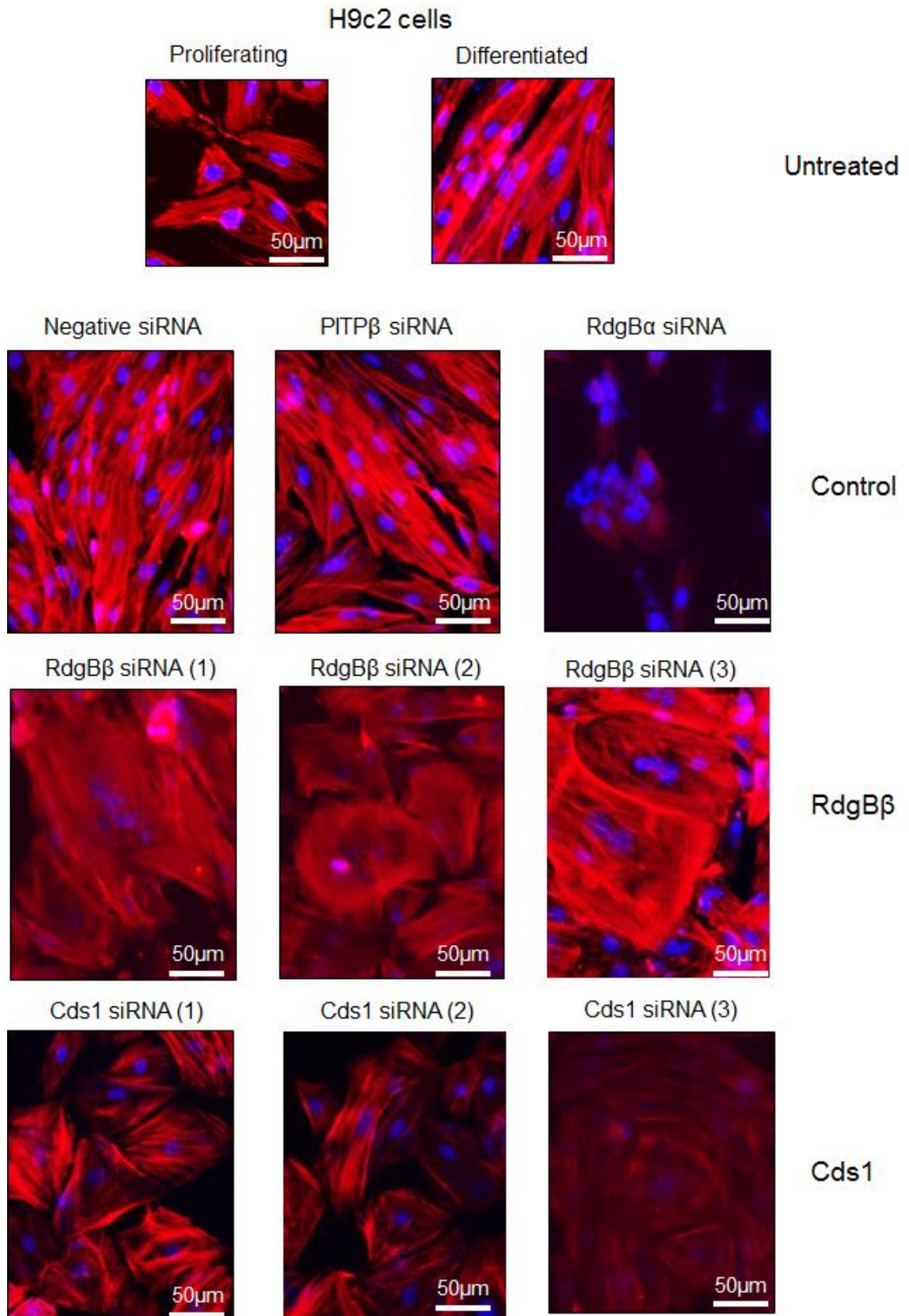
Figure 8.3: Effects of RdgBβ and Cds1 mRNA downregulation in differentiated H9c2s cell morphology.

Figure 8.3: Effects of RdgBβ and Cds1 in differentiated H9c2 cells morphology.

To study cell morphology, H9c2 cells were seeded at a concentration of 1×10^6cells/mL on 12-well plates containing coverslips. Proliferating cells were cultured in media supplemented with 10% FCS. Differentiated cells were cultured in 1% FCS+ daily 1µM retinoic acid for 9 days. Rat siRNA transfection of cells was performed on day 0, 3 and 6 during differentiation. After 9 days, cells were fixed with 4% formaldehyde and analysed by immunofluorescence. Nuclei were stained using DAPI at a 1:5000 dilution (blue) and actin filaments were stained with TRITC phalloidin at a 1:1000 dilution (red). Images were taken at a 40x magnification.

RdgBβ and Cds1 images (1) and (2) were taken from separate coverslips in one experiment while (3) were taken from a separate experiment.

8.3: Summary and discussion

The CDP-DAG synthesis in rat heart samples using the Cds activity assay described in this thesis was found not to be affected by RdgBβ (Figure 8.2) and Cds1 was a minor contributor (Figure 8.1). The source of PA used for the assay might have influenced those results. A recent report showed that the fatty acid species of the PA used as substrate in the assay was specific for Cds2 activity which preferred 1-stearoyl-2-arachidonoyl-phosphatidic acid (18:0/20:4). Cds1, conversely, showed no particular substrate specificity, although di-oleoyl PA (18:1/18:1) displayed less activity[29]. The PA used for the Cds assay in this study contained 5.5% of arachidonic acid, 11.7% of stearic acid and 36% of oleic acid (Table 2.10). Although the fatty acid preference of the mitochondrial Cds enzyme (Tamm41) has not been studied, these observations suggest that the Cds activity measured from H9c2 cells and rat heart fractions could be partly due Tamm41 catalytic action.

Finally, RdgBβ protein and mRNA expression was found not to be influenced by AVP stimulation (Figure 7.2) and it did not affected Cds activity in the rat heart (Figure 8.2). Nevertheless the specific upregulation of protein and mRNA expression upon H9c2 differentiation (Chapter 5) and the observation that RdgBβ mRNA downregulation lead to cellular hypertrophy (Figure 8.3), indicate that the cardiac function of RdgBβ is likely associated with physiological hypertrophy due to cell growth and development.

CHAPTER 9: Conclusions

9.1: Concluding remarks

9.1.1: Phosphatidic Acid (PA) transfer activity is a property exclusive of Class II PITP proteins.

Hu-RdgBβ was the first protein to be described with PA transfer capability *in vitro*.[40] Using a different assay, this thesis confirmed that PA transfer is a characteristic of human RdgBβ and the PITP domain of human and fly (Dm) RdgBα.[125] This property was not shared with Class I PITPs, PITPα and PITPβ (Figure 3.4.A), therefore establishing a clear difference between Class I and Class II PITPs. This observation suggested that the RdgB proteins function *in vivo* may facilitate PA metabolism by transferring PA between cellular compartments. Indeed, in a recently reported collaboration using *Drosophila* phototransduction as a model system, RdgBα mutants presented a delayed PIP_2 resynthesis and an increase on PA levels compared to wild-type flies following light-stimulated PLC activity.[125] This study demonstrated that RdgBα is required to facilitate PA metabolism during *Drosophila* phototransduction *in vivo*, Moreover it has been reported that human RdgBα can also bind PA *in vitro*,[40] and murine RdgBα was able to rescue the retinal degeneration and altered electrophysiological light response phenotype of RdgB – null mutant flies.[17]

In this thesis, there was an attempt to determine the residues within the PITP domain of RdgB proteins responsible for PA transfer between membranes *in vitro*.

The mutational analysis of the residues that are in contact with the inositol ring of PI showed that they are not involved for PA transfer (Figure 3.5). On the other hand, the PA transfer activity of the Y210A/W211A mutant was compromised compared to the wild type PITP domain (Figure 3.7) indicating a requirement for membrane docking for PA extraction from the membranes. In our recent report, the YW/AA mutant was also unable to transfer PI *in vitro* or to rescue the fly mutant phenotype, suggesting that PI transfer is another very important function of RdgB proteins *in vivo*[125].

9.1.2: The use of antibodies in biological research requires appropriate characterisation.

This study included a characterisation of seven polyclonal antibodies made by commission using different sequences of the human RdgBβ as antigens. The results showed that only one antibody (Ab:Rb59) was effective for the detection of endogenous RdgBβ by western blot (Chapter 4). The process of producing antibodies not only requires a considerable amount of time and resources but their efficiency and validity is never guaranteed. The raising concern for the misuse of antibodies in biological research was discussed in Section 4.6. Most recently, with the aim to reach a consensus to standardise antibody validation, the Global Biological Standards Institute (GBSI) is organising an event in conjunction with the Antibody Society, 'Antibody Validation: Standards, Policies and Practices.' This initiative brought together academic researchers, antibody producers, pharmaceutical companies, funders, and journals (https://www.gbsi.org/event/asilomar/#dialogue).

In addition to antibodies made in-house, commercial antibodies have also proven to be unreliable. For example, Ab:Cds1 (sold by different companies under different catalogue numbers (i.e. MCA5324Z and H00001040-M01**),** has not been characterised using an appropriate negative control by either the manufacturers or the research groups that have used it. For instance a recent study using NSCLC cell lines chose Ab:Cds1 based only on its availability.[42] The mRNA expression analysis on this study followed the downregulation of the transcription factor ZEB1 and showed a substantial increase in Cds1 expression that did not resemble the Western blot data[42]. Similarly in this thesis using the Ab:Cds1 antibody, I identified the same p55 protein whose expression did not correlate with the mRNA results (Figures 6.3-5).

Another study using subcellular fractions of the human epidermoid carcinoma cell line A431 compared the Cds activity with the expression of the same p55 protein detected by Ab:Cds1 in Western blot and immunofluorescence experiments to demonstrate the co-localisation of Cds1 with calnexin and the IP3 receptor in the ER[119]. Using a similar assay in this study, Cds activity in rat samples also correlated with the expression of the p55 protein identified by Ab:Cds1, and the immunoreactity co-localise with ER markers but it was enriched in mitochondrial fractions (Figure 6.8 and Figure 6.10). Mitochondrial Cds activity was also increased significantly in myocardial tissue with maturity of SHHF rats, while the activity in the microsomal fraction remained unaltered.[93] However, the characterisation of the antibody showed that the p55 protein detected was unlikely to be Cds1 (Section 6.3.4).

9.1.3: Endogenous RdgBβ expression is regulated by development and maturity in rat heart.

Previously, RdgBβ transcripts were found expressed in human and mouse heart[39,104] and protein expression was described in fractionated rat heart cytosol.[41] This thesis described the endogenous mRNA and protein expression of RdgBβ in rat heart and H9c2 cells differentiated with media supplemented with 1% FCS and 1μM retinoic acid for a minimum of 8 days (Figure 5.6), and isolated neonatal rat cardiomyocytes (Figure 5.9). In addition, the protein expression of RdgBβ was found to be stronger in the adult compared to neonatal rat heart lysates (Figure 5.8). Contrary to the ubiquitous presence of PITPα and PITPβ, this particular expression of RdgBβ in the heart suggests a specific function related to development and maturity of cardiomyocytes. Considering that RdgBβ mRNA downregulation led to cellular hypertrophy (Figure 8.3), the cardiac function of RdgBβ is likely associated with physiological hypertrophy due to cell growth and development. Therefore the null hypothesis was rejected.

H9c2 cells differentiation also showed an increase in mitochondrial biogenesis (Figure 6.3 and Figure 6.4). Since the cellular localisation study showed that RdgBβ is mainly cytosolic, but some immunoreactivity was also observed in rat heart and brain microsomes (Figure 5.10 and Figure 5.11), it is possible that the physiological function of RdgBβ is related to its ability to connect membranes and lipids. For instance, RdgBβ could facilitate PA transport into the mitochondria in tissues such as the heart and the brain which present great quantities of mitochondria. In this study RdgBβ was unable to directly influence Cds activity in rat heart (Figure 8.2) and it was not affected by AVP stimulation in H9c2 cells (Figure 7.2).

9.1.4: Cds1 expression is regulated by vasopressin stimulation of H9c2 cells.

Previously, the presence of Cds1 in the heart has shown diverse results. Northern blot studies have shown no Cds1 expression,[75] while another study indicated the presence of Cds-1 mRNA in human heart.[51] Cds1 was also reported as a direct target of the transcriptional factor PGC-1 also suggesting that it plays a role in mitochondrial metabolism and membrane structure. That study showed a correlation between decreased Cds1 gene expression and reduced CL levels in adult rats.[110] In this thesis it was shown that Cds1 mRNA expression was unaltered by H9c2 cells differentiation (Figure 6.5) and it was possibly a minor contributor to the total Cds activity measured in rat heart samples (Figure 8.1). On the other hand, this study favours the presence of Cds1 in rat heart by showing a significant increase of Cds1 mRNA expression after AVP stimulation of H9c2 cells while Cds2 remained unaltered (Figure 7.3). It is known that AVP stimulates phospholipase C signalling therefore Cds1 might be associated with PIP_2 production in the heart. In fact there are some studies that have reported the importance of Cds in controlling the activity of the PI cycle in signal transduction systems. For instance, phototransduction in *Drosophila* is mediated through PLC signalling, the only isoform of Cds (CdsA) plays a regulatory role by providing PIP_2 to the system. Flies expressing an inactive mutant form of CdsA appeared to be similar to wild type flies when grown in the dark, however mutant flies developed retinal degeneration when exposed to light that could be rescued by CdsA expression.[124] Similarly the PITP domain of RdgB was able to rescue the defective light response of RdgB mutants.[125]

Furthermore, a recent study showed the links between CdsA, PI metabolism, and the insulin pathway activity in order to control cell growth and neutral lipid storage by diverting PA from PI synthesis to TG synthesis. Interestingly, the role of CdsA in fat cell growth was only revealed under conditions in which growth was mildly compromised.[72] This observation suggested that the CDP-DAG–dependent route of phospholipid biosynthesis could be vital only in specific physiological scenarios, such as nutrient starvation, mating, or germination as described in cycling fission yeast (*S. Japonicus*). Cds mutant fission yeast did not stop cell growth provided that the mutant cells were supplemented with choline or ethanolamine indicating that the cells were able to switch to the Kennedy pathway.[49]

PIP_2 is also the biochemical target for the vascular endothelial growth factor A (VEGFA) signalling to generate further messengers, including PIP_3, IP_3, and DAG[64]. A recent report suggested that the angiogenesis defect observed in Cds-deficient zebrafish embryos was caused by a failure to fully restore the phosphoinositides by VEGFA. In the same study, transfection of Cds1 or Cds2 siRNAs into HUVECs resulted in significant decreases in endothelial cell invasion.[87]

Finally, PIP_2 signalling regulates actin filament dynamics leading to myocyte cell growth.[68] Since Cds 1 levels were found to regulate the rate of the PI cycle[75] and Cds1 siRNA transfection of differentiated H9c2 cells affected their morphology (Figure 8.3), it is plausible that the primary function of Cds1 in the heart is to regulate and promote actin formation within the cell via PIP_2 production.

9.2: Study Limitations and future work.

The observations of the PA transfer capability of RdgB proteins and the mutational analysis in Chapter 3 relied on the assumption that the PITP domain of RdgB proteins resembles the structure of PITPα because there are not crystal structures reported for any RdgB proteins to date. In addition, the study was performed in Dm-RdgBα recombinants since the attempts to purify RdgBβ mutants were ineffective. Future biochemical studies may optimise the purification of RdgBβ mutants, complete the analysis of the amino acids that are in contact with the phosphate moiety of PI (T113 and K202), or consider the possibility of testing the double basic amino acid sequence (K28K29) and surrounding positively charged residues of RdgB proteins as described in Section 3.5.. However, deciphering the tri-dimensional structure of RdgB proteins binding PA will ultimately allow a more comprehensive study into the PA transfer capability of Class I PITPs.

Ab:Rb59 outperformed all other antibodies characterised in this thesis and was validated for the effective detection of RdgBβ by immunoblotting of recombinant and overexpressed proteins in Cos7 and H9c2 cells, as well as in rat heart cells and tissue samples (Chapter 4). Unfortunately, the low availability of Ab:Rb59 limited greatly the scope of experiments that can be conducted using this antibody. In addition to Ab:Rb59, Ab:101 was found to be effective at identifying recombinant and over-expressed RdgBβ, but it also detected additional cross reactive bands (Figure 4.2.A). Affinity purification enhanced the sensitivity of the antibody Ab:101 to the recombinant protein (Figure 4.3.A), but the specificity to the endogenous protein was not improved (Figure 4.5.B). Therefore the need to obtain sufficient quantities of an antibody as effective as Ab:Rb59 still remains.

The dependency on antibodies for protein detection in biomedical research raises concern for future studies, which may incur into extensive use of time and resources in order to validate the antibody only to discover that the investigation is not viable. A novel alternative to the use of polyclonal or monoclonal antibodies is the chemiluminescent quantification of protein expression. This method consists in inserting the gene of the protein of interest into the multiple cloning site of the mammalian expression vector capable of producing a chemiluminescent signal via enzyme fragment complementation that can be detected by spectrophotometry.[32] Another approach is the production of recombinant antibodies.[10] The production and stable expression of these recombinant antibodies has been developed in several hosts, however the procedure also requires extensive experimentation.[38]

Cds activity increased after differentiation (Figure 6.6) and when differentiated H9c2 cells and adult heart tissue were fractionated, Cds activity was constantly higher in the mitochondrial fractions, rather than in microsomes or mitochondrial associated membranes as expected (Figure 6.8 and 6.10). However, the antibody mitofusin2 is a mitochondrial protein rather than MAM marker protein and antibodies such the sigma1 receptor or ACSL4 were not investigated in these experiments. In addition, the Cds activity assay used here was not able to distinguish between Cds1, Cds2 or Tamm41 contribution towards the CDP-DAG synthesis measured. Furthermore, the study into the protein expression of Cds1 was confounded by the extensive characterisation of the antibody used. There is still the possibility that the antibody used here is species-dependent which was not tested. Moreover, additional controls for siRNA experiments such as endogenous positive and mock controls were not performed. These

experiments will conclude whether Ab:Cds1 is an effective antibody for immunoblotting of rat samples.

The observations of this study raise interesting questions which could be subject of future studies. For instance, is Tamm41 the mitochondrial Cds protein in the mammalian heart? And, what is the identity of this 55kDa protein? The characteristics of this unknown protein include its significant upregulation by H9c2 cells differentiation (Figure 6.3 and Figure 6.4), its enrichment in membrane mitochondrial fractions and co-localisation with cellular fractions with high Cds activity in human[119] and rat samples (Figure 6.8 and Figure 6.10). Do Cds1 or RdgBβ affect phosphoinositide signalling? Another line of enquiry may explore whether RdgBβ is somehow required for mitochondrial biogenesis or Cardiolipin synthesis during differentiation of H9c2 cells.

References

1. Ahuja,P., Wanagat,J., Wang,Z., Wang,Y., Liem,D.A., Ping,P., Antoshechkin,I.A., Margulies,K.B., & Maclellan,W.R. Divergent mitochondrial biogenesis responses in human cardiomyopathy. *Circulation* **127**, 1957-1967 (2013).

2. Akbari,M.F., Boer,J.M., Lange-Turenhout,E.A., Pieters,R., & den Boer,M.L. Altered expression of miR-24, miR-126 and miR-365 does not affect viability of childhood TCF3-rearranged leukemia cells. *Leukemia* **28**, 1008-1014 (2014).

3. Alb,J.G., Jr., Phillips,S.E., Rostand,K., Cui,X., Pinxteren,J., Cotlin,L., Manning,T.G.S., York,J.D., Sontheimer, J.F, Collawn,J.F., & Bankaitis,V.A. Genetic ablation of phosphatidylinositol transfer protein function in murine embryonic stem cells. *Mol. Biol. Cell* **13**, 739-754 (2002).

4. Allen-Baume,V., Segui,B., & Cockcroft,S. Current thoughts on the phosphatidylinositol transfer protein family. *FEBS Lett.* **531**, 74-80 (2002).

5. Andresen,B.T., Rizzo,M.A., Shome,K., & Romero,G. The role of phosphatidic acid in the regulation of the Ras/MEK/Erk signaling cascade. *FEBS Lett.* **531**, 65-68 (2002).

6. Babu,M.M., van der,L.R., de Groot,N.S., & Gsponer,J. Intrinsically disordered proteins: regulation and disease. *Curr. Opin. Struct. Biol* **21**, 432-440 (2011).

7. Baker,M. Reproducibility crisis: Blame it on the antibodies. *Nature* **521**, 274-276 (2015).

8. Balla,T. Phosphoinositides: tiny lipids with giant impact on cell regulation. *Physiol Rev.* **93**, 1019-1137 (2013).

9. Bordeaux,J., Welsh,A., Agarwal,S., Killiam,E., Baquero,M., Hanna,J., Anagnostou,V., & Rimm,D. Antibody validation. *Biotechniques* **48**, 197-209 (2010).

10. Bradbury,A. & Pluckthun,A. Reproducibility: Standardize antibodies used in research. *Nature* **518**, 27-29 (2015).

11. Branco,A.F., Pereira,S.P., Gonzalez,S., Gusev,O., Rizvanov,A.A., & Oliveira,P.J. Gene Expression Profiling of H9c2 Myoblast Differentiation towards a Cardiac-Like Phenotype. *PLoS. ONE.* **10**, e0129303 (2015).

12. Branco,A.F., Sampaio,S.F., Moreira,A.C., Holy,J., Wallace,K.B., Baldeiras,I., Oliveira,P.J., & Sardao,V.A. Differentiation-dependent doxorubicin toxicity on H9c2 cardiomyoblasts. *Cardiovasc. Toxicol.* **12**, 326-340 (2012).

13. Branco,A.F., Sampaio,S.F., Wieckowski,M.R., Sardao,V.A., & Oliveira,P.J. Mitochondrial disruption occurs downstream from beta-adrenergic overactivation by isoproterenol in differentiated, but not undifferentiated H9c2 cardiomyoblasts: differential activation of stress and survival pathways. *Int. J. Biochem. Cell Biol.* **45**, 2379-2391 (2013).

14. Brostrom,M.A., Reilly,B.A., Wilson,F.J., & Brostrom,C.O. Vasopressin-induced hypertrophy in H9c2 heart-derived myocytes. *Int. J Biochem. Cell Biol.* **32**, 993-1006 (2000).

15. Carvou,N., Holic,R., Li,M., Futter,C., Skippen,A., & Cockcroft,S. Phosphatidylinositol- and phosphatidylcholine- transfer activity of PITPβ is essential for COP1-mediated retrograde transport from the Golgi to the endoplasmic reticulum. *J Cell Sci.* **123**, 1262-1273 (2010).

16. Cedars,A., Jenkins,C.M., Mancuso,D.J., & Gross,R.W. Calcium-independent phospholipases in the heart: mediators of cellular signaling, bioenergetics, and ischemia-induced electrophysiologic dysfunction. *J. Cardiovasc. Pharmacol.* **53**, 277-289 (2009).

17. Chang,J.T., Milligan,S., Li,Y., Chew,C.E., Wiggs,J., Copeland,N.G., Jenkins,N.A., Campochiaro,P.A., Hyde,D.R., & Zack,D.J. Mammalian

homolog of D*rososphila retinal degeneration B* rescues the mutant fly phenotype. *J. Neurosci.* **17**, 5881-5890 (1997).

18. Cocco,L., Follo,M.Y., Manzoli,L., & Suh,P.G. Phosphoinositide-specific phospholipase C in health and disease. *J. Lipid Res.* **56**, 1853-1860 (2015).

19. Cockcroft,S. Trafficking of phosphatidylinositol by phosphatidylinositol transfer proteins. *Biochem. Soc. Symp.* **74**, 259-271 (2007).

20. Cockcroft,S. Measurement of phosphatidylinositol and phosphatidylcholine binding and transfer activity of the lipid transport protein PITP. *Methods Mol Biol* **462**, 363-377 (2009).

21. Cockcroft,S. & Garner,K. Function of the phosphatidylinositol transfer protein gene family: is phosphatidylinositol transfer the mechanism of action? *Crit. Rev. Biochem. Mol. Biol.* **46**, 89-117 (2011).

22. Cockcroft,S. & Garner,K. 14-3-3 protein and ATRAP bind to the soluble class IIB phosphatidylinositol transfer protein RdgBbeta at distinct sites. *Biochem. Soc. Trans.* **40**, 451-456 (2012).

23. Cockcroft,S. & Garner,K. Potential role for phosphatidylinositol transfer protein (PITP) family in lipid transfer during phospholipase C signalling. *Adv. Biol. Regul.* **53**, 280-291 (2013).

24. Cockcroft,S., Garner,K., Yadav,S., Gomez-Espinoza,E., & Raghu,P. RdgBalpha reciprocally transfers PA and PI at ER-PM contact sites to maintain PI(4,5)P2 homoeostasis during phospholipase C signalling in Drosophila photoreceptors. *Biochem. Soc. Trans.* **44**, 286-292 (2016).

25. Comelli,M., Domenis,R., Bisetto,E., Contin,M., Marchini,M., Ortolani,F., Tomasetig,L., & Mavelli,I. Cardiac differentiation promotes mitochondria development and ameliorates oxidative capacity in H9c2 cardiomyoblasts. *Mitochondrion.* **11**, 315-326 (2011).

26. Connerth,M., Tatsuta,T., Haag,M., Klecker,T., Westermann,B., & Langer,T. Intramitochondrial transport of phosphatidic acid in yeast by a lipid transfer protein. *Science* **338**, 815-818 (2012).

27. Cunningham,E., Thomas,G.M.H., Ball,A., Hiles,I., & Cockcroft,S. Phosphatidylinositol transfer protein dictates the rate of inositol trisphosphate production by promoting the synthesis of PIP$_2$. *Current Biol.* **5**, 775-783 (1995).

28. D'Souza,K. & Epand,R.M. The phosphatidylinositol synthase-catalyzed formation of phosphatidylinositol does not exhibit acyl chain specificity. *Biochemistry* **54**, 1151-1153 (2015).

29. D'Souza,K., Kim,Y.J., Balla,T., & Epand,R.M. Distinct Properties of the Two Isoforms of CDP-Diacylglycerol Synthase. *Biochemistry* **53**, 7358-7367 (2014).

30. de Brito,O.M. & Scorrano,L. Mitofusin 2 tethers endoplasmic reticulum to mitochondria. *Nature* **456**, 605-610 (2008).

31. Dhalla,N.S., Xu,Y.J., Sheu,S.S., Tappia,P.S., & Panagia,V. Phosphatidic acid: a potential signal transducer for cardiac hypertrophy. *J Mol. Cell Cardiol.* **29**, 2865-2871 (1997).

32. Eglen,R.M. & Singh,R. Beta galactosidase enzyme fragment complementation as a novel technology for high throughput screening. *Comb. Chem. High Throughput. Screen.* **6**, 381-387 (2003).

33. Epand,R.M. Features of the Phosphatidylinositol Cycle and its Role in Signal Transduction. *J. Membr. Biol.* (2016).

34. Fagone,P. & Jackowski,S. Membrane phospholipid synthesis and endoplasmic reticulum function. *J Lipid Res.* **50 Suppl**, S311-S316 (2009).

35. Filipeanu,C.M., Zhou,F., & Wu,G. Analysis of Rab1 function in cardiomyocyte growth. *Methods Enzymol.* **438**, 217-226 (2008).

36. Foster,D.A. Regulation of mTOR by phosphatidic acid? *Cancer Res.* **67**, 1-4 (2007).

37. Foster,D.A., Salloum,D., Menon,D., & Frias,M.A. Phospholipase D and the maintenance of phosphatidic acid levels for regulation of mammalian target of rapamycin (mTOR). *J. Biol. Chem.* **289**, 22583-22588 (2014).

38. Frenzel,A., Hust,M., & Schirrmann,T. Expression of recombinant antibodies. *Front Immunol.* **4**, 217 (2013).

39. Fullwood,Y., dos Santos,M., & Hsuan,J.J. Cloning and characterization of a novel human phosphatidylinositol transfer protein, rgdBβ. *J. Biol. Chem.* **274**, 31553-31558 (1999).

40. Garner,K., Hunt,A.N., Koster,G., Somerharju,P., Grover,E., Li,M., Raghu,P., Holic,R., & Cockcroft,S. Phosphatidylinositol transfer protein, Cytoplasmic 1 (PITPNC1) binds and transfers phosphatidic acid. *J Biol. Chem.* **287**, 32263-32276 (2012).

41. Garner,K., Li,M., Ugwuanya,N., & Cockcroft,S. The phosphatidylinositol transfer protein, RdgBβ binds 14-3-3 via its unstructured C-terminus, whereas its lipid binding domain interacts with the integral membrane protein, ATRAP (Angiotensin II Type I receptor-associated protein). *Biochem. J.* **439**, 97-111 (2011).

42. Gemmill,R.M., Roche,J., Potiron,V.A., Nasarre,P., Mitas,M., Coldren,C.D., Helfrich,B.A., Garrett-Mayer,E., Bunn,P.A., & Drabkin,H.A. ZEB1-responsive genes in non-small cell lung cancer. *Cancer Lett.* **300**, 66-78 (2011).

43. Giusti,L., Gargini,C., Ceccarelli,F., Bacci,M., Italiani,P., & Mazzoni,M.R. Modulation of endothelin-A receptor, Galpha subunit, and RGS2 expression during H9c2 cardiomyoblast differentiation. *J. Recept. Signal. Transduct. Res.* **24**, 297-317 (2004).

44. Gresset,A., Sondek,J., & Harden,T.K. The phospholipase C isozymes and their regulation. *Subcell. Biochem.* **58**, 61-94 (2012).

45. Halberg,N., Sengelaub,C.A., Navrazhina,K., Molina,H., Uryu,K., & Tavazoie,S.F. PITPNC1 Recruits RAB1B to the Golgi Network to Drive Malignant Secretion. *Cancer Cell* **29**, 339-353 (2016).

46. Halford,S., Dulai,K.S., Daw,S.C., Fitzgibbon,J., & Hunt,D.M. Isolation and chromosomal localization of two human CDP-diacylglycerol synthase (CDS) genes. *Genomics* **54**, 140-144 (1998).

47. Hamilton,B.A., Smith,D.J., Mueller,K.L., Kerrebrock,A.W., Bronson,R.T., Berkel,V.v., Daly,M.J., Kroglyak,L., Reeve,M.P., Nernhauser,J.L., Hawkins,T.L., Rubin,E.M., & Lander,E.S. The *vibrator* mutation causes neurogeneration via reduced expression of PITPα: Positional complementation cloning and extragenic suppression. *Neuron* **18**, 711-722 (1997).

48. Hara,S., Swigart,P., Jones,D., & Cockcroft,S. The first 5 amino acids of the carboxy terminus of phosphatidylinositol transfer protein α (PITPα) play a critical role in inositol lipid signaling: transfer activity of PITP is essential but not sufficient for restoration of phospholipase C signaling. *J. Biol. Chem.* **272**, 14909-14913 (1997).

49. He,Y., Yam,C., Pomraning,K., Chin,J.S., Yew,J.Y., Freitag,M., & Oliferenko,S. Increase in cellular triacylglycerol content and emergence of large ER-associated lipid droplets in the absence of CDP-DG synthase function. *Mol. Biol. Cell* **25**, 4083-4095 (2014).

50. Heacock,A.M. & Agranoff,B.W. CDP-diacylglycerol synthase from mammalian tissues. *Biochim. Biophys. Acta* **1348**, 166-172 (1997).

51. Heacock,A.M., Uhler,M.D., & Agranoff,B.W. Cloning of CDP-diacylglycerol synthase from a human neuronal cell line. *J Neurochem.* **67**, 2200-2203 (1996).

52. Hermansson,M., Hokynar,K., & Somerharju,P. Mechanisms of glycerophospholipid homeostasis in mammalian cells. *Prog. Lipid Res.* **50**, 240-257 (2011).

53. Hescheler,J., Meyer,R., Plant,S., Krautwurst,D., Rosenthal,W., & Schultz,G. Morphological, biochemical, and electrophysiological characterization of a clonal cell (H9c2) line from rat heart. *Circ. Res.* **69**, 1476-1486 (1991).

54. Hom,J. & Sheu,S.S. Morphological dynamics of mitochondria--a special emphasis on cardiac muscle cells. *J Mol. Cell Cardiol.* **46**, 811-820 (2009).

55. Horvath,S.E. & Daum,G. Lipids of mitochondria. *Prog. Lipid Res.* **52**, 590-614 (2013).

56. Hunt,A.N., Skippen,A., Koster,G., Postle,A.D., & Cockcroft,S. Acyl chain-based molecular selectivity for HL60 cellular phosphatidylinositol and of phosphatidylcholine by phosphatidylinositol transfer protein α. *Biochim Biophys Acta* **1686**, 50-60 (2004).

57. Icho,T., Sparrow,C.P., & Raetz,C.R. Molecular cloning and sequencing of the gene for CDP-diglyceride synthetase of Escherichia coli. *J Biol. Chem.* **260**, 12078-12083 (1985).

58. Inglis-Broadgate,S.L., Ocaka,L., Banerjee,R., Gaasenbeek,M., Chapple,J.P., Cheetham,M.E., Clark,B.J., Hunt,D.M., & Halford,S. Isolation and characterization of murine Cds (CDP-diacylglycerol synthase) 1 and 2. *Gene* **356**, 19-31 (2005).

59. Jenkins,C.M., Cedars,A., & Gross,R.W. Eicosanoid signalling pathways in the heart. *Cardiovasc. Res.* **82**, 240-249 (2009).

60. Jiang,Y.J., Lu,B., Xu,F.Y., Gartshore,J., Taylor,W.A., Halayko,A.J., Gonzalez,F.J., Takasaki,J., Choy,P.C., & Hatch,G.M. Stimulation of cardiac cardiolipin biosynthesis by PPARalpha activation. *J Lipid Res.* **45**, 244-252 (2004).

61. Kim,S., Kedan,A., Marom,M., Gavert,N., Keinan,O., Selitrennik,M., Laufman,O., & Lev,S. The phosphatidylinositol-transfer protein Nir2 binds phosphatidic acid and positively regulates phosphoinositide signalling. *EMBO Rep.* **14**, 891-899 (2013).

62. Kim,Y.J., Guzman-Hernandez,M.L., & Balla,T. A Highly Dynamic ER-Derived Phosphatidylinositol-Synthesizing Organelle Supplies Phosphoinositides to Cellular Membranes. *Dev. Cell* **21**, 813-824 (2011).

63. Kimes,B.W. & Brandt,B.L. Properties of a clonal muscle cell line from rat heart. *Exp. Cell Res.* **98**, 367-381 (1976).

64. Koch,S. & Claesson-Welsh,L. Signal transduction by vascular endothelial growth factor receptors. *Cold Spring Harb. Perspect. Med.* **2**, a006502 (2012).

65. Konorev,E.A., Vanamala,S., & Kalyanaraman,B. Differences in doxorubicin-induced apoptotic signaling in adult and immature cardiomyocytes. *Free Radic. Biol. Med.* **45**, 1723-1728 (2008).

66. Kooijman,E.E., Tieleman,D.P., Testerink,C., Munnik,T., Rijkers,D.T., Burger,K.N., & de Kruijff,B. An electrostatic/hydrogen bond switch as the basis for the specific interaction of phosphatidic acid with proteins. *J. Biol Chem.* **282**, 11356-11364 (2007).

67. Kuznetsov,A.V., Javadov,S., Sickinger,S., Frotschnig,S., & Grimm,M. H9c2 and HL-1 cells demonstrate distinct features of energy metabolism, mitochondrial function and sensitivity to hypoxia-reoxygenation. *Biochim. Biophys. Acta* **1853**, 276-284 (2015).

68. Lai,L., Wang,M., Martin,O.J., Leone,T.C., Vega,R.B., Han,X., & Kelly,D.P. A role for peroxisome proliferator-activated receptor gamma coactivator 1 (PGC-1) in the regulation of cardiac mitochondrial phospholipid biosynthesis. *J Biol. Chem.* **289**, 2250-2259 (2014).

69. Lehman,J.J., Barger,P.M., Kovacs,A., Saffitz,J.E., Medeiros,D.M., & Kelly,D.P. Peroxisome proliferator-activated receptor gamma coactivator-1 promotes cardiac mitochondrial biogenesis. *J Clin. Invest* **106**, 847-856 (2000).

70. Liu,S.Y., Tappia,P.S., Dai,J., Williams,S.A., & Panagia,V. Phospholipase A2-mediated activation of phospholipase D in rat heart sarcolemma. *J Mol. Cell Cardiol.* **30**, 1203-1214 (1998).

71. Liu,X., Yin,Y., Wu,J., & Liu,Z. Structure and mechanism of an intramembrane liponucleotide synthetase central for phospholipid biosynthesis. *Nat. Commun.* **5**, 4244 (2014).

72. Liu,Y., Wang,W., Shui,G., & Huang,X. CDP-diacylglycerol synthetase coordinates cell growth and fat storage through phosphatidylinositol metabolism and the insulin pathway. *PLoS. Genet.* **10**, e1004172 (2014).

73. Livak,K.J. & Schmittgen,T.D. Analysis of relative gene expression data using real-time quantitative PCR and the 2(-Delta Delta C(T)) Method. *Methods* **25**, 402-408 (2001).

74. Lydikis,A., Jackson,P.D., Rock,C.O., & Jackowski,S. The role of CDP-diacylglycerol synthase and phosphatidylinositol synthase activity levels in the regulation of cellular phosphatidylinositol content. *J. Biol. Chem.* **272**, 33402-33409 (1997).

75. Lykidis,A. Comparative genomics and evolution of eukaryotic phospholipid biosynthesis. *Prog. Lipid Res.* **46**, 171-199 (2007).

76. Marshall,A.K., Barrett,O.P., Cullingford,T.E., Shanmugasundram,A., Sugden,P.H., & Clerk,A. ERK1/2 signaling dominates over RhoA signaling in regulating early changes in RNA expression induced by endothelin-1 in neonatal rat cardiomyocytes. *PLoS. ONE.* **5**, e10027 (2010).

77. McKee,E.E., Grier,B.L., Thompson,G.S., & McCourt,J.D. Isolation and incubation conditions to study heart mitochondrial protein synthesis. *Am. J. Physiol* **258**, E492-E502 (1990).

78. Mehta PK & Griendling KK. Angiotensin II cell signaling: physiological and pathological effects in the cardiovascular system. *Am. J Physiol Cell Physiol* **292**, C82-C97 (2007).

79. Mejia,E.M., Nguyen,H., & Hatch,G.M. Mammalian cardiolipin biosynthesis. *Chem. Phys. Lipids* **179**, 11-16 (2014).

80. Menard,C., Pupier,S., Mornet,D., Kitzmann,M., Nargeot,J., & Lory,P. Modulation of L-type calcium channel expression during retinoic acid-induced differentiation of H9C2 cardiac cells. *J Biol. Chem.* **274**, 29063-29070 (1999).

81. Mok,A.Y., McDougall,G.E., & McMurray,W.C. CDP-diacylglycerol synthesis in rat liver mitochondria. *FEBS Lett.* **312**, 236-240 (1992).

82. Morgan,C.P., Skippen,A., Segui,B., Ball,A., Allen-Baume,V., Larijani,B., Murray-Rust,J., McDonald,N., Sapkota,G., Morrice,N.A., & Cockcroft,S. Phosphorylation of a distinct structural form of phosphatidylinositol transfer protein α at Ser^{166} by protein kinase C disrupts receptor-mediated phospholipase C signalling by inhibiting delivery of phosphatidylinositol to membranes. *J Biol. Chem.* **279**, 47159-47171 (2004).

83. Nelson,R.K. & Frohman,M.A. Physiological and Pathophysiological roles for Phospholipase D. *J Lipid Res.* (2015).

84. Novak,F., Kolar,F., Hamplova,B., Mrnka,L., Pelouch,V., Ostadal,B., & Novakova,O. Myocardial phospholipid remodeling under different types of load imposed during early postnatal development. *Physiol Res.* **58 Suppl 2**, S13-S32 (2009).

85. Ong,S.B. & Hausenloy,D.J. Mitochondrial morphology and cardiovascular disease. *Cardiovasc. Res.* **88**, 16-29 (2010).

86. Oppermann,M., Gess,B., Schweda,F., & Castrop,H. Atrap deficiency increases arterial blood pressure and plasma volume. *J Am. Soc. Nephrol.* **21**, 468-477 (2010).

87. Pan,W., Pham,V.N., Stratman,A.N., Castranova,D., Kamei,M., Kidd,K.R., Lo,B.D., Shaw,K.M., Torres-Vazquez,J., Mikelis,C.M., Gutkind,J.S., Davis,G.E., & Weinstein,B.M. CDP-diacylglycerol synthase-controlled

phosphoinositide availability limits VEGFA signaling and vascular morphogenesis. *Blood* **120**, 489-498 (2012).

88. Pereira,S.L., Ramalho-Santos,J., Branco,A.F., Sardao,V.A., Oliveira,P.J., & Carvalho,R.A. Metabolic remodeling during H9c2 myoblast differentiation: relevance for in vitro toxicity studies. *Cardiovasc. Toxicol.* **11**, 180-190 (2011).

89. Peter,A.K., Bjerke,M.A., & Leinwand,L.A. Biology of the cardiac myocyte in heart disease. *Mol. Biol. Cell* **27**, 2149-2160 (2016).

90. Png,K.J., Halberg,N., Yoshida,M., & Tavazoie,S.F. A microRNA regulon that mediates endothelial recruitment and metastasis by cancer cells. *Nature* **481**, 190-194 (2012).

91. Potting,C., Wilmes,C., Engmann,T., Osman,C., & Langer,T. Regulation of mitochondrial phospholipids by Ups1/PRELI-like proteins depends on proteolysis and Mdm35. *EMBO J* **29**, 2888-2898 (2010).

92. Rechsteiner,M. & Rogers,S.W. PEST sequences and regulation by proteolysis. *Trends Biochem. Sci.* **21**, 267-271 (1996).

93. Saini-Chohan,H.K., Holmes,M.G., Chicco,A.J., Taylor,W.A., Moore,R.L., McCune,S.A., Hickson-Bick,D.L., Hatch,G.M., & Sparagna,G.C. Cardiolipin biosynthesis and remodeling enzymes are altered during development of heart failure. *J Lipid Res.* **50**, 1600-1608 (2009).

94. Samak,M., Fatullayev,J., Sabashnikov,A., Zeriouh,M., Schmack,B., Farag,M., Popov,A.F., Dohmen,P.M., Choi,Y.H., Wahlers,T., & Weymann,A. Cardiac Hypertrophy: An Introduction to Molecular and Cellular Basis. *Med. Sci. Monit. Basic Res.* **22**, 75-79 (2016).

95. Santy,L.C., Frank,S.R., & Casanova,J.E. Expression and analysis of ARNO and ARNO mutants and their effects on ADP-ribosylation factor (ARF)-mediated actin cytoskeletal rearrangements. *Methods Enzymol.* **329**, 256-264 (2001).

96. Schouten,A., Agianian,B., Westerman,J., Kroon,J., Wirtz,K.W., & Gros,P. Structure of apo-phosphatidylinositol transfer protein alpha provides insight into membrane association. *EMBO J* **21**, 2117-2121 (2002).

97. Segui,B., Allen-Baume,V., & Cockcroft,S. Phosphatidylinositol transfer protein-beta displays minimal sphingomyelin transfer activity and is not required for biosynthesis and trafficking of sphingomyelin. *Biochem. J.* **366**, 23-34 (2002).

98. Shadan,S., Holic,R., Carvou,N., Ee,P., Li,M., Murray-Rust,J., & Cockcroft,S. Dynamics of lipid transfer by phosphatidylinositol transfer proteins in cells. *Traffic* **9**, 1743-1756 (2008).

99. Shen,H., Heacock,P.N., Clancey,C.J., & Dowhan,W. The CDS1 gene encoding CDP-diacylglycerol synthase in Saccharomyces cerevisiae is essential for cell growth. *J Biol. Chem.* **271**, 789-795 (1996).

100. Shen,Z., Ye,C., McCain,K., & Greenberg,M.L. The Role of Cardiolipin in Cardiovascular Health. *Biomed. Res. Int.* **2015**, 891707 (2015).

101. Shin,J.J. & Loewen,C.J. Putting the pH into phosphatidic acid signaling. *BMC. Biol.* **9**, 85 (2011).

102. Sonenberg,N. & Hinnebusch,A.G. Regulation of translation initiation in eukaryotes: mechanisms and biological targets. *Cell* **136**, 731-745 (2009).

103. Swigart,P., Insall,R.H., Wilkins,A., & Cockcroft,S. Purification and cloning of phosphatidylinositol transfer proteins from *Dictyostelium discoideum*: Homologues of both mammalian PITPs and *S. cerevisiae* Sec14p are found in the same cell. *Biochem. J.* **347**, 837-843 (2000).

104. Takano,N., Owada,Y., Suzuki,R., Sakagami,H., Shimosegawa,T., & Kondo,H. Cloning and characterization of a novel variant (mM-rdgBbeta1) of mouse M-rdgBs, mammalian homologs of Drosophila retinal degeneration B gene proteins, and its mRNA localization in mouse brain in comparison with other M-rdgBs. *J. Neurochem.* **84**, 829-839 (2003).

105. Takeuchi,K. & Reue,K. Biochemistry, physiology, and genetics of GPAT, AGPAT, and lipin enzymes in triglyceride synthesis. *Am. J. Physiol Endocrinol. Metab* **296**, E1195-E1209 (2009).

106. Tamura,Y., Harada,Y., Nishikawa,S.I., Yamano,K., Kamiya,M., Shiota,T., Kuroda,T., Kuge,O., Sesaki,H., Imai,K., Tomii,K., & Endo,T. Tam41 Is a CDP-Diacylglycerol Synthase Required for Cardiolipin Biosynthesis in Mitochondria. *Cell Metab* **17**, 1-10 (2013).

107. Tanaka,Y., Tamura,K., Koide,Y., Sakai,M., Tsurumi,Y., Noda,Y., Umemura,M., Ishigami,T., Uchino,K., Kimura,K., Horiuchi,M., & Umemura,S. The novel angiotensin II type 1 receptor (AT1R)-associated protein ATRAP downregulates AT1R and ameliorates cardiomyocyte hypertrophy. *FEBS Lett.* **579**, 1579-1586 (2005).

108. Thomas,G.M.H., Cunningham,E., & Cockcroft,S. Purification of phosphatidylinositol transfer protein from brain cytosol for reconstituting G-protein-regulated phosphoinositide-specific phospholipase C-β isozymes. *Methods in Enzymol.* **238**, 168-181 (1994).

109. Tilley,S.J., Skippen,A., Murray-Rust,J., Swigart,P., Stewart,A., Morgan,C.P., Cockcroft,S., & McDonald,N.Q. Structure-function analysis of human phosphatidylinositol transfer protein alpha bound to phosphatidylinositol. *Structure* **12**, 317-326 (2004).

110. Tsai,C.F., Wang,Y.T., Chen,Y.R., Lai,C.Y., Lin,P.Y., Pan,K.T., Chen,J.Y., Khoo,K.H., & Chen,Y.J. Immobilized metal affinity chromatography revisited: pH/acid control toward high selectivity in phosphoproteomics. *J Proteome. Res.* **7**, 4058-4069 (2008).

111. Vance,J.E. MAM (mitochondria-associated membranes) in mammalian cells: lipids and beyond. *Biochim. Biophys. Acta* **1841**, 595-609 (2014).

112. Vance,J.E. Phospholipid synthesis and transport in Mammalian cells. *Traffic.* **16**, 1-18 (2015).

113. Vasilevsky,N.A., Brush,M.H., Paddock,H., Ponting,L., Tripathy,S.J., Larocca,G.M., & Haendel,M.A. On the reproducibility of science: unique identification of research resources in the biomedical literature. *PeerJ.* **1**, e148 (2013).

114. Vega,R.B., Horton,J.L., & Kelly,D.P. Maintaining ancient organelles: mitochondrial biogenesis and maturation. *Circ. Res.* **116**, 1820-1834 (2015).

115. Vihtelic,T.S., Goebl,M., Milligan,S., O'Tousa,S.E., & Hyde,D.R. Localization of Drosophila retinal degeneration B, a membrane- associated phosphatidylinositol transfer protein. *J. Cell Biol.* **122**, 1013-1022 (1993).

116. Wang,X., Devaiah,S.P., Zhang,W., & Welti,R. Signaling functions of phosphatidic acid. *Prog. Lipid Res.* **45**, 250-278 (2006).

117. Watanabe,Y., Tamura,Y., Kawano,S., & Endo,T. Structural and mechanistic insights into phospholipid transfer by Ups1-Mdm35 in mitochondria. *Nat. Commun.* **6**, 7922 (2015).

118. Watkins,S.J., Borthwick,G.M., & Arthur,H.M. The H9C2 cell line and primary neonatal cardiomyocyte cells show similar hypertrophic responses in vitro. *In Vitro Cell Dev. Biol. Anim* **47**, 125-131 (2011).

119. Waugh,M.G., Minogue,S., Clayton,E.L., & Hsuan,J.J. CDP-diacylglycerol phospholipid synthesis in detergent-soluble, non-raft, membrane microdomains of the endoplasmic reticulum. *J Lipid Res.* **52**, 2148-2158 (2011).

120. Weller,M.G. Quality Issues of Research Antibodies. *Anal. Chem. Insights.* **11**, 21-27 (2016).

121. Wieckowski,M.R., Giorgi,C., Lebiedzinska,M., Duszynski,J., & Pinton,P. Isolation of mitochondria-associated membranes and mitochondria from animal tissues and cells. *Nat. Protoc.* **4**, 1582-1590 (2009).

122. Wirtz,K.W., Schouten,A., & Gros,P. Phosphatidylinositol transfer proteins: from closed for transport to open for exchange. *Adv. Enzyme Regul.* **46**, 301-311 (2006).

123. Woodcock,E.A., Kistler,P.M., & Ju,Y.K. Phosphoinositide signalling and cardiac arrhythmias. *Cardiovasc. Res.* **82**, 286-295 (2009).

124. Wu,L., Niemeyer,B., Colley,N., Socolich,M., & Zuker,C.S. Regulation of PLC-mediated signalling *in vivo* by CDP-diacylglycerol synthase. *Nature* **373**, 216-222 (1995).

125. Yadav,S., Garner,K., Georgiev,P., Li,M., Espinosa,E.G., Panda,A., Mathre,S., Okkenhaug,H., Cockcroft,S., & Raghu,P. RDGBα, A PI-PA transfer protein regulates G-protein coupled PtdIns(4,5)P2 signalling during Drosophila phototransduction. *J. Cell Sci.* **128**, 3330-3344 (2015).

126. Yamashita,A., Hayashi,Y., Matsumoto,N., Nemoto-Sasaki,Y., Oka,S., Tanikawa,T., & Sugiura,T. Glycerophosphate/Acylglycerophosphate acyltransferases. *Biology. (Basel)* **3**, 801-830 (2014).

127. Ye,C., Shen,Z., & Greenberg,M.L. Cardiolipin remodeling: a regulatory hub for modulating cardiolipin metabolism and function. *J. Bioenerg. Biomembr.* **48**, 113-123 (2016).

128. Yi,M., Weaver,D., Eisner,V., Varnai,P., Hunyady,L., Ma,J., Csordas,G., & Hajnoczky,G. Switch from ER-mitochondrial to SR-mitochondrial calcium coupling during muscle differentiation. *Cell Calcium* **52**, 355-365 (2012).

129. Yoder,M.D., Thomas,L.M., Tremblay,J.M., Oliver,R.L., Yarbrough,L.R., & Helmkamp,G.M., Jr. Structure of a multifunctional protein. Mammalian phosphatidylinositol transfer protein complexed with phosphatidylcholine. *J Biol Chem.* **276**, 9246-9252 (2001).

130. Young,B.P., Shin,J.J., Orij,R., Chao,J.T., Li,S.C., Guan,X.L., Khong,A., Jan,E., Wenk,M.R., Prinz,W.A., Smits,G.J., & Loewen,C.J. Phosphatidic acid is a pH biosensor that links membrane biogenesis to metabolism. *Science* **329**, 1085-1088 (2010).

131. Yu,C.H., Panagia,V., Tappia,P.S., Liu,S.Y., Takeda,N., & Dhalla,N.S. Alterations of sarcolemmal phospholipase D and phosphatidate phosphohydrolase in congestive heart failure. *Biochim Biophys Acta* **1584**, 65-72 (2002).

132. Zhu,W., Tilley,D.G., Myers,V.D., Coleman,R.C., & Feldman,A.M. Arginine vasopressin enhances cell survival via a G protein-coupled receptor kinase 2/beta-arrestin1/extracellular-regulated kinase 1/2-dependent pathway in H9c2 cells. *Mol. Pharmacol.* **84**, 227-235 (2013).